Universidade de Aveiro
2015

Departamento de Química

Nuno Ricardo de Oliveira Jordão

Estudo do proteoma de superfície celular para análise de mutações de DJ-1 associadas à doença de Parkinson

Study of the cell surface proteome for the analysis of Parkinson's disease associated DJ-1 mutations

Universidade de Aveiro
2015

Departamento de Química

Nuno Ricardo de Oliveira Jordão

Estudo do proteoma de superfície celular para análise de mutações de DJ-1 associadas à doença de Parkinson

Study of the cell surface proteome for the analysis of Parkinson's disease associated DJ-1 mutations

Dissertação apresentada à Universidade de Aveiro para cumprimento dos requisitos necessários à obtenção do grau de Mestre em Biotecnologia, ramo de Biotecnologia Molecular, realizada sob a orientação científica do Doutor Bruno Manadas, Investigador Principal da Unidade de LSMS (Life Sciences Mass Spectrometry) do Centro de Neurociências da Universidade de Coimbra, e do Doutor Rui Vitorino, Investigador Auxiliar do Departamento de Química da Universidade de Aveiro.

Financiado por Fundos FEDER através do Programa Operacional Factores de Competitividade – COMPETE e por Fundos Nacionais através da FCT – Fundação para a Ciência e a Tecnologia no âmbito do projecto UID/NEU/04539/2013

o júri

presidente

Doutora Luísa Alexandra Seuanes Serafim Martins Leal
Professora auxiliar do Departamento de Química da Universidade de Aveiro

Doutora Paula Cristina Veríssimo Pires
Professora Auxiliar do Departamento de Ciências da Vida da Faculdade de Ciências e Tecnologias da Universidade de Coimbra

Doutor Bruno José Fernandes Oliveira Manadas
Investigador auxiliar do Centro de Neurociências e Biologia Celular da Universidade de Coimbra

agradecimentos

Acho que devo começar na casa da tese. Sendo a parte mais essencial para a concretização do meu trabalho, quero em primeiro lugar agradecer ao Doutor Bruno Manadas por me acolher no CNC-Biotech, orientar no mais sincero sentido da palavra, e por sequer permitir a existência do projecto do qual pude contribuir. Sempre simpático, paciente e prestável para qualquer aflição ou dúvida no trabalho (e até para me arranjar o computador), com um notável sentido crítico, conhecimento profundo e contagiante bom humor. Ao Doutor Mário Grãos, do também tenho de agradecer não apenas pela cedência do seu laboratório para a cultura de células mas também por todos os conselhos dados ao longo do ano e empenhada ajuda relativamente a todo o tipo de questões e pedidos. Também não devo esquecer do Doutor Rui Vitorino, que apesar de não ter acompanhado tanto o meu trabalho pela distância geográfica sempre manifestou tacto e preocupação pela minha tese, tanto a nível de resultados como de satisfação pelo trabalho feito, e demonstrou ser um óptimo elo de ligação entre Cantanhede e a Universidade de Aveiro.

Mas se devo agradecer a alguém pela disponibilidade imediata e ensinamento (não só do trabalho realizado mas também da profissão a realizar), destacar-se-ão a Matilde Melo e a Sandra Anjo. Tenho a agradecer à Matilde pela paciência demonstrada em ensinar tudo e mais alguma coisa e enorme prestabilidade no início da tese. À Sandra, pela ajuda constante na segunda metade do projecto, sempre lá para me ajudar nos procedimentos e nos raciocínios. Também tenho a agradecer à Cátia Santa pelo auxílio prestado em várias partes do projecto, e constante sentido de ajuda. Também há que agradecer à Andreia e à Andrea, as minhas comparsas de bancada que me acompanharam na realização do projecto e deram um pouco mais de discussão, descontracção e diversão ao meu trabalho. Também não posso deixar de referir e deixar um agradecimento à Joana e à Margarida pelos momentos de apoio, diversão e regabofe; à Vera pela espectacularidade de pessoa que é, que se resume em muita calma, delicadeza e e afabilidade; à Mariana e Karolina pela simpatia e também sempre com aquela ajuda pronta para dar mesmo sem pedir. Não esquecer as raparigas do laboratório do Mário Grãos, Heloísa, Daniela, Margarida, Tânia e Inês, que sempre me fizeram companhia enquanto estava para os lados da “solitária”, e deram mais diversão e ajuda que o que poderia pedir. E, claro, não posso esquecer os meus camaradas de pelotão, a Carolina, o Diogo e a Vanessa, de quem pude contar com todo o tipo de galhofadas, companheirismo e apoio nesta epopeia.

Agora numa casa mais pessoal. Não quero, não consigo, nomear amigos. Cresceram comigo e me fizeram crescer em Leiria, viveram comigo esta meia década emancipatória em Aveiro, outros tantos doutros lugares, que me deram chão e o céu. Ao GrETUA, a minha segunda casa na minha segunda cidade. Sangue do meu sangue, minha Mãe Coragem, a pessoa que mais admiro, uma frase não chega para retribuir o calor, a lição, o sustento, a razão de eu estar onde estou e ser como sou. O meu melhor é o melhor que lhe posso tentar dar. À minha irmã, também tenho a agradecer pela ajuda e desinteressada semi-providência desde o meu primeiro dia.

A todos, devo tudo. Por fim, e refraseando um mantra de Jerusalém: se me esquecer de ti, Aveiro, que me seque a mão direita.

palavras-chave

doença de Parkinson, DJ-1, mutação M26I, mutação E163K, produção de proteína, SH-SY5Y, stress oxidativo, biotinilação, pull-down, LC-MS/MS, SWATH MS

resumo

A doença de Parkinson é uma doença neurodegenerativa caracterizada por uma neurodegeneração selectiva e depleção de dopamina, e apesar de grande parte dos casos terem origem esporádica diversas mutações monogénicas têm sido associadas ao desenvolvimento de um fenótipo parkinsoniano. A proteína DJ-1 é de particular interesse, dado o seu papel neuroprotector contra stress oxidativo e disfunção mitocondrial, e a identificação de mutações correlacionadas a doença de Parkinson precoce.

Neste estudo, foram produzidas duas mutações patológicas da proteína DJ-1, M26I e E163K. Uma análise SDS-PAGE e LC-MS/MS comprovou uma produção e purificação adequada das mutações, e SEC-HPLC assegurou a preservação estrutural das mutações de DJ-1 como homodímeros, uma característica chave de DJ-1 fundamental para a sua actividade biológica. Por outro lado, estudos de viabilidade de SH-SY5Y indicaram que, apesar do papel protector da forma nativa contra stress oxidativo, as mutações M26I e E163K demonstraram uma reduzida capacidade neuroprotectiva.

Para melhor compreender os motivos desta disfunção biológica, foi desenvolvido um protocolo para marcação das proteínas de superfície celular com Sulfo-NHS-LC-biotina e pull-down com avidina para enriquecimento e subsequente análise MS. Vários ensaios como *western blotting*, LC-MS/MS e microscopia confocal confirmaram a adequação do protocolo sugerido. Quando aplicado para uma análise de variações proteómicas relacionadas com stress oxidativo, em fracções enriquecidas provenientes da biotinilação de SH-SY5Y e pull-down da parte membranar do extracto celular, permitiu a identificação de várias proteínas de interesse, nomeadamente quatro proteínas com diferença significativa resultante da indução de stress oxidativo. Também foi realizado um pull-down com a totalidade extracto celular, que resultou em dados não conclusivos relativamente ao uso de ultracentrifugação antes do pull-down.

Não obstante, este estudo correspondeu à primeira análise da superfície celular de SH-SY5Y realizada num contexto da doença de Parkinson, que poderá ser usada no futuro para estudar alterações no proteoma de superfície celular em ambiente de stress oxidativo e de adição da proteína DJ-1, na forma nativa e mutante, de forma a fornecer novas pistas referentes ao seu *intake* e modulação da sinalização em ambiente oxidativo, e em suma contribuindo para uma nova perspectica sobre os mecanismos protectores ou despoletadores da doença de Parkinson.

keywords

Parkinson's disease, DJ-1, M26 mutation, E163K mutation, protein production, SH-SY5Y, oxidative stress, biotinylation, avidin pull-down, LC-MS/MS, SWATH MS

abstract

Parkinson's disease (PD) is a neurodegenerative disease, characterized with selective neurodegeneration and dopamine depletion. Despite most cases appear to have sporadic origin, it has been associated various monogenic mutations to the onset of a parkinsonian phenotype. DJ-1 protein is of particular interest given its neuroprotective role against oxidative stress and mitochondria impairment, and the identification of several mutations correlated with early onset PD.

For this study, it were then produced two pathological mutations of DJ-1, M26I and E163K. SDS-PAGE and LC-MS/MS analysis confirmed the adequate production and purification of the both mutant proteins, and SEC-HPLC secured the structural perseverance of the mutations as homodimers, a key feature of DJ-1 essential for its biological activity. On the other hand, SH-SY5Y viability assays indicated that despite the native form protective role against oxidative stress, M26I and E163K mutations showed a compromised neuroprotective capacity.

To better understand the reasons for this biological impairment, it was developed a protocol for cell surface proteins labelling with Sulfo-NHS-LC-biotin and avidin pull-down for enrichment and downstream MS analysis. Assays such as western blotting, LC-MS/MS and confocal microscopy confirmed the adequacy of the proposed procedure. When applied for the analysis of proteome variations related to oxidative stress, in enriched fractions from SH-SY5Y biotinylation and avidin pull-down of crude membrane sub cellular part, it allowed the identification of several proteins of interest, namely four proteins with significant difference caused by oxidative stress induction, and of other proteins of interest. It was also performed the direct pull-down of whole protein extract, offering inconclusive results regarding the preferential use of ultracentrifugation before pull-down.

Nevertheless, it was the first time that SH-SY5Y cell surface was analysed in a PD context, and it could be used in the future to study cell surface proteome alterations modulated by oxidative stress and extracellular presence of native or mutant DJ-1, providing new insights regarding its intake and signalling modulation in pathological conditions, and hence contributing for a new perspective over preventive or eliciting mechanisms associated to the onset of Parkinson's disease.

Table of contents

List of abbreviations

%CV | coefficient variation

ε | molar extinction coefficient

AC | affinity chromatography

ACN | acetonitrile

Akt | protein kinase B

ASK1 | apoptosis signal-regulating kinase 1

Bax | Bcl-2-associated X protein

Bcl-xL | Bcl-2-like protein, isoform L

BPE | B-phycoeryhtrin

BSA | bovine serum albumin

C- | negative control

C106-SO_2^- | 106-cysteine sulfinate

C106-SO_3^- | 106-cysteine sulfonate

D-PBS | Dulbecco's phosphate-buffered saline

DAQ | dopamine derived quinone

DAT | dopamine transporter

Daxx | Death domain-associated protein 6

DDA | data dependent acquisition

DMF | dimethylformamide

DMSO | dimethyl sulfoxide

DNA | desoxirribonucleic acid

DTT | dithiothreitol

E. coli **|** *Escherichia coli*

E163K **|** 163-residue glutamic acid to lysine mutation

EDTA **|** ethylenediaminetetraacetic acid

EOPD **|** early-onset Parkinson's disease

ESI **|** electrospray ionization

FA **|** formic acid

FBS **|** fetal bovine sérum

FDR **|** false discovery rate

GABA **|** gamma-aminobutyric acid

GC **|** guanine and cytosine

GFP **|** green fluorescent protein

GO **|** gene ontology

GOrilla **|** gene ontology enrichment analysis and visualization tool

GPi **|** *globus pallidus internus*

GRAVY **|** grand average of hydropahty

GTP **|** guanosine triphosphate

H_2O_2 **|** hydrogen peroxide

HABA **|** 4'-hydroxyazobenzene-2-carboxylic acid

His **|** hexahistidine

HPLC **|** high performance liquid chromatography

Hsp-70 **|** Heat shock protein 70 kDa

ICAT **|** isotope-coded affinity tag

ID **|** identification

IDA **|** information dependent acquisition

Igepal **|** octylphenoxypolyethoxyethanol

iTRAQ **|** isobaric tag for relative and absolute quantitation

IP **|** immunoprecipitation

IPTG **|** isopropyl-β-D-thiogalactopyranoside

IS | internal standard

JOPD | juvenile-onset Parkinson's disease

Ka | association constant

K_{av} | partition coefficient

l-dopa | levodopa

L-B | Luria-Bertani medium

LB | Lewy bodies

LC | liquid chromatography

LC-MS/MS | liquid chromatography coupled to tandem mass spectrometry

LRRK2 | leucine-rich repeat kinase 2

m/z | mass to charge ratio

M26I | 26-residue methionine to interleucine mutation

MALDI | matrix assisted laser desorption and ionization

MALE | maltose-binding periplasmic protein

MEM | minimal essential medium

MM | molecular marker

MMTS | methyl methanethiosulfonate

MS | mass spectrometry

MS1 | precursor ion spectra

MS2 | fragment ion spectra

MS/MS | tandem mass spectrometry

mRNA | messenger RNA

MPTP | 1-methyl-4-phenyl-1,2,3,6-tetrahydropyridine

MW | molecular weight

MWCO | molecular weight cut-off

NHS | N-hydroxysuccinimide

Nrf2 | nuclear factor erythroid 2-related factor

NSAIDs | non-steroidal anti-inflammatory drugs

ORF | open reading frame

PAGE | polyacrylamide gel electrophoresis

PBS | phosphate-buffered saline

PBS+G | PBS with 5% glycerol

PBS-T | phosphate-buffered saline with 0.1% Tween-20

PCD | programmed cell death

PCR | polymerase chain reaction

PD | Parkinson's disease

pDNA | plasmid DNA

PFA | paraformaldehyde

Pfpl | pore forming protein-like

pKa | logarithmic acidity constant

PIASx-α | E3 SUMO-protein ligase PIAS2, isoform α

PI3K | Phosphoinositide 3-kinase

PINK1 | PTEN induced putative kinase

PMT | photomultiplication

PON2 | paraoxonase-2

PP | ProteinPilot software

PS | Parkinson's syndrome

PTEN | phosphate and tensin homolog

PVDF | polyvinylidene fluoride

q-TOF | quadrupole time-of-flight system

R^2 | coefficient of determination

REM | rapid eye movement

RING | really interesting new gene finger domain

RIPA | radioimmunoprecipitation assay

RNA | ribonucleic acid

ROS | reactive oxygen species

SAPE | streptavidin B-phycoerythrin conjugate

SEC | size exclusion chromatography

SDS | sodium dodecyl sulfate

SILAC | stable isotope labelling by amino acids in cell culture

SNc | *substancia nigra pars compacta*

SNCA | *synuclein alpha*

SNr | *substancia nigra pars reticulata*

SOD3 | superoxide dismutase 3

SRM | selected reaction monitoring

STRING | search tool for the retrieval of interacting genes

SWATH | sequential window acquisition of all theoretical fragment ion spectra

TAP | tandem affinity purification

TBS | Tris-buffered saline

TCA | trichloroacetic acid

TCEP | tris(2-carboxyethyl)phosphine

TEAB | triethylammonium bicarbonate buffer

TEV | tobacco etch virus

TH | tyrosine hydroxylase

TMHMM | transmembrane prediction with hidden Markov models

Tween 20 | polyoxyethylene (20) sorbitan monolaurate

VN | ventrolateral nucleus

UPS | ureide permease

WT | wild-type

XIC | extracted ion chromatogram

YOPD | young-onset Parkinson's disease

1. Introduction

1.1. Parkinson's disease

Parkinson's disease (PD) was first described on the 1817 monograph *An Essay on the Shaking Palsy*, by James Parkinson, as a disorder of "involuntary tremulous motion with lessened muscular power" [1]. Since then, it has been profusely studied and nowadays is considered a complex and idiopathic pathology that results in the selective neuron degeneration, decrease of dopamine levels and consequent display of various motor disorders. Frequency and intensity of PD symptoms usually increase with its progression, and ultimately result in severe disability and decrease of quality of life [2].

Late studies have demonstrated the disease complexity, and nowadays a broader meaning to the pathology is established, with PD being a distinct form of parkinsonism, Parkinson's syndrome (PS). Parkinsonism regards any disease that includes striatal dopamine deficiency or striatal damage, generally characterized by tremor at rest, rigidity, slowness or absence of voluntary movement, and postural instability. PD is the most common cause of parkinsonism, accounting for about 80% of cases, but there are other forms that differ in symptoms onset, pathology and treatment response [3].

Median age of onset of PD is about 60 years, but 5 to 10% of cases develop before reaching 50 years of age, in cases designated as early onset PD (EOPD). These cases usually have genetic causes, while late onset is more common in sporadic PD. EOPD can be divided in juvenile onset PD (JOPD), with onset before 20 years old, and young onset PD (YOPD) occurred between 20 and 40 years of age, all with particular clinical phenotype [2], [4].

Nowadays, PD is the second most common neurodegenerative disorder, after Alzheimer's disease. Since it is an age-related illness, and considering the demographic

trend of an increasingly older population, it is expected an increment of PD's prevalence and health care burden inherent to the disease [5].

1.1.1. Diagnosis and treatment of PD

Parkinson's disease is initially noticed with a gradual and asymmetrical onset of motor symptoms such as impairment of dexterity and flexing of arms, dragging of one foot, fatigue or stiffness, usually overlooked and undiagnosed for 2 to 3 years.

A standard diagnosis of the pathology should always detect development of bradykinesia, since PD is the most common cause for the symptom. In a late phase of the disease, it is also displayed a rigid and expressionless face, drooling, monotonous and slurred speech, flexed posture, severe pill rolling tremor of hands, visual hallucination, and an ultimate disability for performance of ordinary tasks [6]. PD has also high prevalence of several non-motor symptoms, such as depression, anxiety or apathy, cognitive impairment, hyposmia, psychotic and sleep disorders, constipation, incontinence, among others. These increase in intensity and quantity in late progress of the disease [7], [8]. It has been observed that 12% of non-demented PD patients lack in non-motor symptoms display, while 25% manifest four or more non-motor symptoms. Furthermore, 24 to 31% of PD patients have dementia, which corresponds to 3-4% of this pathology in the whole population [9].

Disease development may last up to 20 years [7], but mean duration between diagnosis and death is 15 years and studies suggest a mortality rate up to a 2-fold increase. Pneumonia is the most common cause of death among PD patients [6].

The inexistence of a standard diagnostic test or marker for PD, given its obscure pathology, and variable clinical criteria leads to some uncertainty regarding its detection and distinction from other parkinsonian forms: about 24% of PD patients are wrongfully diagnosed [10], being specially common in early stages of the disease [2], and several non-motor symptoms are overlooked in 40% to 81% of patients [11]. Asymmetric symptom onset, response to levodopa and a long term follow-up of patients are the most important features that provide accurate diagnosis and

discrimination of PD from other forms [2], [12]. A definite diagnosis can only be confirmed with autopsy, with studies noting between 76 to 87% post-mortem confirmation of the clinical PD diagnosis [12].

In addition, Parkinson's disease is not reversible, since there is no form to halt or retard dopaminergic neuron degeneration, a hallmark for the disease [3]. Nevertheless, there are several forms of medication that treat PD symptoms and improve quality of life and functional capacity of the patient. Levodopa (l-dopa) is the most common treatment. Patient response is variable, with 20 to 70% of motor onset inhibition, but some patients develop early adverse reaction and little response to the drug. Also, treatment-related complications occur after 5 to 7 years, nulling any long-time benefits [7]. Alternatives to l-dopa include non-ergoline dopamine antagonists, used as primary treatment in PD patients under 55 years, and type B monoamine oxidase inhibitors [6].

1.1.2. Pathophysiology of PD

The pathological hallmark of PD is a selective loss of dopaminergic and neuromelanin-containing neurons in the *substancia nigra pars compacta* (SNc), though it also occurs in other brain regions [13]. The disease is subsequently marked with a decrease of dopamine concentration in the striatum [14]. The pattern of SNc loss also parallels mRNA expression decrease of the dopamine transporter (DAT) in SNc neurons [15].

Motor manifestations begin typically when dopamine concentration falls below 60-70% in the contralateral striatum, and 60% of SNc dopaminergic neurons have been lost [3]. This is confirmed with l-dopa administration, a precursor of dopamine metabolism able to replenish striatal dopamine levels and alleviate PD symptoms [16].

1.1.2.1. Dopaminergic neuron degeneration

Whichever factor provokes neurodegeneration, studies of toxic PD models and functions of genes implicated in PD suggest two major hypothesis regarding its pathogenesis. The first hypothesis affirms that misfolding and aggregation of proteins;

a second one proposes the key event is mitochondrial dysfunction related with oxidative stress, including the formation of toxic oxidized dopamine species. Some studies also show increased levels of apoptosis markers in PD dopaminergic neurons, like Bax, Bcl-xL, caspase-3, caspase-8 and caspase-9, but is still to be assessed whether there is an abnormal regulation of programmed cell death (PCD) or an accurate response for already damaged cells [3].

1.1.2.1.1. Protein aggregation

In Parkinson's disease, nerve loss is accompanied by the appearance of different intraneural inclusions on the surviving neurons, called Lewy bodies (LB) and Lewy neurites. Lewy bodies are mainly a spherical inclusion bodies of 8 to 30 μm, composed of filaments with 7 to 20 nm width and dense granular material and vesicular structures [6]. Lewy bodies can be found in an average of 3.6% of *substancia nigra* neurons, regardless of PD's progression [17]. Lewy neurites are similar to Lewy bodies, but with a less smooth surface and elongated club-shaped or serpentine structures [18].

The main component of Lewy structures is a post-translationally modified and aggregated form of proteins such as α-synuclein, parkin and ubiquitin. Histological staining with α-synuclein or ubiquitin antibodies has become the standard method for PD diagnosis [3]. Analysis of the brain of non-PD patients found LB in 4% of individuals over 60 years and 13% over 90 years, attributed to a presymptomatic disease onset [19].

The role of LB formation in neuronal cell death is controversial, with regard of a possible cytoprotective role for the Lewy bodies, since most part of apoptotic neurons do not have LB. Also, mice exposed to paraquat showed degeneration of some nigrostriatal neurons and formation of Lewy structures, but these were the most protected from neurodegeneration. Regardless of Lewy structures toxic or protective function, the accumulation of misfolded proteins is a key event in PD degeneration [20].

Several environmental and genetic-related pathogenic factors are thought to cause neurodegeneration through induction of toxic protein conformations or interference with processes that correct misfolded proteins. One of the triggers for this

dysfunction may be oxidative stress and reactive oxygen species (ROS) damage, since it has been observed enhanced misfolding and aggregation after α-synuclein suffers oxidative damage [21].

Cells usually respond to protein misfolding with activation of chaperones; if not properly refolded, they are targeted with poliubiquitination for proteasomal degradation, in the ubiquitin-protease pathway. There is an age-related decline of chaperone and proteasome activity, and subsequent misfolded protein handling, that favors protein accumulation in Parkinson's disease [22].

1.1.2.1.2. Oxidative stress and mitochondria dysfunction

Consideration of the mitochondria role on PD pathogenesis began with studies *in vivo* of 1-methyl-4-phenyl-1,2,3,6-tetrahydropyridine (MPTP), where it was found a blockage on the mitochondrial electron transporter chain by inhibition of complex I, leading to oxidative stress and energy imbalance in affected neurons. Later it was confirmed the formation of complex I abnormalities and reduced function of mitochondria in PD patients [23], which could be resultant of mutant mitochondrial DNA inheritance or systemic induction. Overall, the data support the existence of mitochondrial mutations in PD, but these are yet to be identified [24].

Mitochondria activity and dopamine metabolism produces ROS, and dopamine is also capable of self-oxidation [3]. Inhibition of complex I increases production of oxidizing species, which damages several biomolecules and affects the complex I itself, causing a snowball effect of increased mitochondria dysfunction [25], [26].

The increase of ROS and mitochondria failure could have several effects, such as an increase of protein misfolding and activity of ubiquitin-proteasome system, or the disruption of dopamine vesicular storage and damaging of cytosolic components by dopamine-mediated reactions. But there is no primary linkage of abnormal oxidative phosphorylation on the mitochondria, or ROS generation, with PD development [3].

1.1.2.2. Effects of dopamine imbalance

The classical pathophysiological model for PD discusses the impairment of a looping pathway belonged to the motor circuit, between the cortex and several regions of the basal ganglia [27]. SNc neurons project dopamine mainly to the putamen, with a role of modulation of gamma-aminobutyric acid related (GABAergic) pathways, with enhancing of the direct circuit and inhibition of the indirect circuit. Dopamine reduces firing of *globus pallidus internus* (GPi) and *substancia nigra pars reticulata* (SNr), and facilitates glutamatergic output to cortical motor areas. In PD development, dopamine deficit leads to increased activity of the indirect circuit, with decrease of direct circuit. This leads to an increased GABAergic firing of GPi and SNr, inhibition of the ventrolateral nucleus (VN) of the thalamus and consequent reduced glutamatergic activation of cortical and brainstem motor regions. In consequence, there is a glutamatergic imbalance, since the glutamate signal transmitted onto the putamen is not returned to cortical areas of the motor circuit, which eventually results in stiffness, motor difficulties and slowed reactions [28].

It is now known that the dopaminergic system can affect several basal ganglia structures besides the putamen, as well as cortical areas of limbic and associative circuits. Neurodegeneration and LB formation can also be found in such areas, which could explain the onset of non-motor symptoms and the wide clinical range of PD patients. Also, there are other dopaminergic neurotransmitters, besides dopamine, of which the deficit effect remains mostly unknown [27].

1.1.3. Etiology of PD

The main obstacle to the development of neuroprotective drugs is the lack of total knowledge of specific molecular events that provoke neurodegeneration. PD was initially considered to be caused mainly by environmental factors, and the finding of the MPTP model was crucial for research of PD's pathology. Interest of scientific

community has risen with the discovery of several monogenetic mutations that cause inherited PD, though 90% to 95% of cases still appear to be sporadic [3], [29].

Nowadays, Parkinson's disease is considered multifactorial, and pathogenic mechanisms in sporadic PD, albeit not well understood, are caused by an interaction of variable environmental exposure and susceptibility genes [2], [7].

1.1.3.1. Age, gender and ethnicity

Ageing is the major risk factor, with 10% or less of patients being diagnosed under 45 years of age [6], [30]. In Europe, Parkinson's disease has a prevalence rate of 108 to 257 / 100,000 and incidence rate of 11 to 19 / 100,000 per year. These rates rise steeply in individuals over 60 years, with prevalence of 1280 to 1500/100,000, incidence of 346 / 100,000 [31]. Prevalence may reach 1 to 3% of individuals above 80 years of age [32].

PD studies focused on its relation with race or ethnicity are not consensual or sufficient [30], and it is unlikely to be a post-industrial condition [33]. Furthermore, some studies suggest a 1.5 to 2-fold increase of PD risk among men, while other studies found no difference between genders [30], [34]. The hypothesis can be explained with estrogen's neuroprotective effect, but its role on PD is largely disputed [2], [35].

1.1.3.2. Environmental factors

Although PD is generally considered from sporadic origin, few environmental causes or triggers have been confirmed. The few factors with sufficient evidence and consensus are tobacco and coffee consumption, with a protective role over PD risk [36].

The study over PD's aetiology gained weight when it was discovered that human administration of MPTP, similar to paraquat herbicide, lead to development of chronic PD symptoms and degeneration of dopaminergic neurons [37]. Later it was also found the effect of MPTP, the herbicide paraquat, and the pesticide rotenone over the selective inhibition of complex-I, fibrillar accumulation in nigral neurons and dopamine

depletion [38]. Due to PD onset similarity upon MPTP intake, this compound has been the most used animal model for the study of the disease [3].

Since then, several epidemiological and clinical studies have been performed that associate pesticides exposure with PD, being reported a 1 to 4-fold increase of risk [36], [39]. It has been also denoted an association between increased risk of PD and rural living, well water use, farming activity, occupational exposure to metals or industry components, but with no consent [36]. Many believe in interactions between pesticides use and rural living, farming and well water use, of unknown mechanisms [40].

Various groups of food and nutrients have also been studied as potential causes of PD, but overall they do not seem to play a major role in its pathology. Intake of antioxidants, like vitamin A, C, E and beta carotene, slightly decrease PD risk, resulted from a presumed protective role in oxidative stress conditions. Dairy products are associated with increased PD risk, more latent in men for unknown motives [2], [36].

Regarding caffeine consumption, epidemiological and pre-clinical data conclude that caffeine can influence or prevent the onset of PD patients. Coffee drinkers appear to have 30% to 60% reduced risk of PD onset [41], [42]. Caffeine is an adenosine antagonist, and has been shown its inhibitory effect over MPTP toxicity in mice, by downregulation of adenosine A_{2A} receptors [43]. Additionally, it has been noted a slight reduction of PD risk with consumption of tea and alcohol [36], [42].

There is also an inverse association between tobacco consumption and risk of PD, with some suggesting that non-smokers are more than twice as likely to develop the pathology [2], [41]. Nicotine could influence stimulation of dopamine release, upregulate nicotinic receptors and signalling cascades, or act against neuronal damage by inhibition of monoamine oxidase B [44]. Still, studies demonstrating nicotine protective pathways and clinical trials for nicotine based treatment remain having inconclusive results [45].

Previous clinical conditions may also contribute to PD onset. Patients appear to have inflammatory markers in the brain, but it is unknown whether it's a cause or effect of neurodegeneration [16], [46]. Prospective studies already noted a modest decrease

of PD risk with use of nonsteroidal anti-inflammatory drugs (NSAIDs) [47] and induction of an inflammatory response using MPTP model [48]. Several pathologies have also been associated with an increased risk for future development of PD, such as head trauma, olfactory dysfunction, REM sleep behavior disorder, history of mental illness (depression, anxiety, dementia), influenza or other viral infections, diabetes, and vascular diseases, but with lack of concluding evidence that distinguish a causative relation from a correlation of etiologic factors. On the other hand, gout is able to decrease PD risk by 30%, since the highly concentrated uric acid has antioxidant and ROS scavenging properties, and there is consistent evidence for a lower overall cancer risk among PD cases, but increased risk of melanoma [36].

1.1.3.3. Genetic factors

Although most cases of PD are idiopathic, there are seldom familial cases of parkinsonism that appear to follow dominant or recessive inheritance patterns that can be traced to single mutations [49]. The genetic component of PD was firstly found with the discovery of mutations in the gene expressing α-synuclein that can directly cause Parkinson's disease. Since then, it has been identified several genes linked to PD, with loci identified as PARK, which allowed the development of a novel PD research paradigma and new theories for pathological degeneration.

As of today, it was confirmed the existence of 12 confirmed genes implicated in monogenic parkinsonism (Table 1.1), and also other PARK loci identified in genome-wide approaches but with no attributed proteins [50]. Although follow-up studies are inconsistent and inconclusive, there is ample evidence of PD causation with five genes: *SNCA*, *Parkin*, *PINK*, *DJ-1* and *LRRK2*. Overall, they account for a total of more than 500 DNA variants associated with PD, including about 82% single mutations and 18% copy number variations [51].

Table 1.1 – Genes implicated in monogenic parkinsonism, confirmed with genome-wide linkage and PD modelling [29], [50].

Locus	Gene (protein)	Mode of autossomal inheritance	Protein function	Clinical display	Age of onset
PARK1/ PARK4	*SNCA* (α-synuclein)	dominant	Unknown synaptic function	PD with or without dementia, parkinsonism, diffuse LB disease	early to late onset
PARK2	*parkin*	recessive	E3 ubiquitin ligase	parkinsonism	early onset
PARK5	*UCLH1*	dominant	Upiquitin ligase and hydrolase	PD	early onset
PARK6	*PINK1*	recessive	Mitochondrial Ser-Thr kinase	parkinsonism	early onset
PARK7	*DJ-1*	recessive	Probable oxidative stress response	parkinsonism	juvenile and early onset
PARK8	*LRRK2* (dardarin)	dominant	Unknown protein kinase	PD	late onset
PARK9	*ATP13A2*	recessive	Lysosomal membrane transporter	atypical parkinsonism	juvenile onset
PARK14	*PLA2G6*	recessive	Phospholipase	atypical parkinsonism	juvenile onset
PARK15	*FBXO7*	recessive	F-box protein of ubiquitin-ligase complex	atypical parkinsonism	juvenile onset

Also, 20 common variants have been identified as capable of PD modulation. Given the small fraction of genetic representativity in the disease burden, it is very likely the existence of several other genetic determinants.

Furthermore, there are some candidate genes for PD etiology, mainly through exome sequencing, such as *GBA*, *DNAJC6*, or *SYNJ1* [50].

There are some differences between clinical features of sporadic and inherited forms of PD, the most striking being a general early onset on inherited forms of PD, and occasional absence of Lewy structures. Still, there are sufficient similarities between them to enable an insight of common PD pathogenesis, as is also observed an interference of PD-related genes in sporadic cases of the disease [3], [29].

1.1.3.3.1. SNCA

Mutations in the *SNCA* gene were the first identified, in a large PD kindred with autosomal dominant and early onset parkinsonism [52]. This gene has two loci, hence the attribution of PARK1 and PARK4 to the gene [29]. Several mutations were attributed to the development of inherited PD (Figure 1.1), such as various substitutions, and duplications or triplications of the gene. Age onset decreases and symptomatic severity increases with the number of copies of the *SNCA* locus [53]. It has been also postulated an increase of sporadic PD risk with a variant in *SNCA* promoter [54].

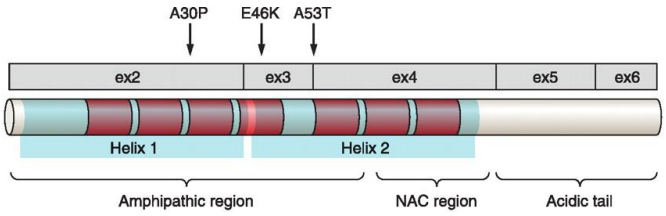

Figure 1.1 – Schematic representation of α-synuclein, with missense mutations above the protein exon organization. In red, localization of KTKEGV motifs. Besides missense mutations, there are genomic duplications or triplications of several sizes [55].

The resultant α-synuclein protein is relatively small, with 140 residues, an N-terminal α-helix and acidic C-terminal regions, and has a hydrophobic central component. It is expressed ubiquitously in the brain, in glia and neurons, and concentrated in cytoplasmic regions of presynaptic terminals [56].

Various functions have been attributed to α-synuclein, such as the regulation of vesicle dynamics in the presynaptic membrane, maintenance neuronal plasticity, or protection of nerve terminals from injuries [29]. Studies in *SNCA* knock-out mice found wide range of effects, including synaptic deficits, decrease of number of vesicles in presynaptic milieu, interference in lipid-mediated signalling cascade and vesicle trafficking, phospholipid depletion in mitochondrial membrane and impairment of complex II and III activity in the respiratory chain [57], [58].

It is strongly suggested an accumulation of α-synuclein as an early step for the pathogenesis of sporadic and inherited PD, which leads to the aggregation of the

protein in Lewy bodies or neurites. In inherited forms of the disease, protein overexpression or dysfunction, particularly self-assembly or impairment of phosphorylation, can exacerbate formation of insoluble aggregates [19], [29].

Specific degeneration of dopaminergic neurons could be due to an antagonism between α-synuclein and dopamine, since the protein neurotoxicity can be mediated by endogenous dopamine production, and it has been demonstrated the apoptosis of dopaminergic neurons with overexpression of α-synuclein, either wild-type or mutant, increased in oxidative stress conditions [59].

1.1.3.3.2. LRRK2

Leucine-rich repeat kinase 2 (*LRRK2*), also designated as PARK8, is predicted to encode a large 285 kDa protein, called dardarin. It has multiple domains, belonging to the Ras GTPase superfamily. *LRRK2* has N-terminal leucine-rich repeats and C-terminal with WD40 repeats, both likely to mediate protein-protein interactions [29].

Several missense mutations have been identified in *LRRK2*, in families with autosomal dominant late-onset PD, with some of the mutations in the kinase domain (Figure 1.2). Each mutation has a characteristic onset of parkinsonism, and it was reported an increased penetrance of some mutations in particular populations [60]. The most common *LRRK2* substitution is G2019S, with an onset similar to PD and prevalence of about 4% of familial and 1.5% of sporadic PD, but incidence increases between North African Arabs where it reaches 37% inherited and 41% sporadic PD [61].

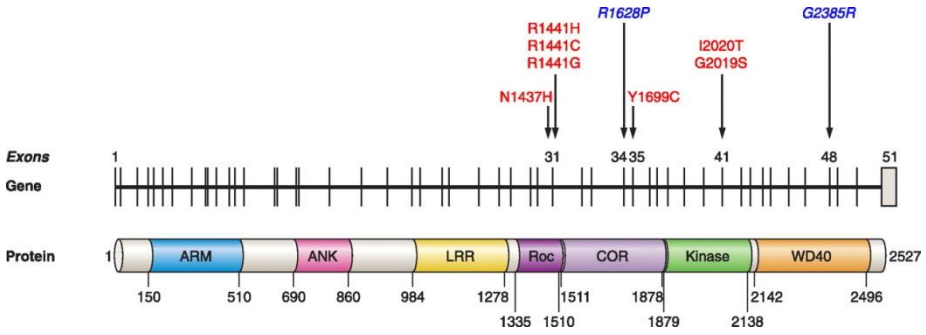

Figure 1.2 – Schematic representation of the *LRRK2* gene and protein with colored domains. Above the protein organization, missense pathogenic mutations in red, Asian-specific risk factors in blue [55].

LRRK2 mutations can have several effects, such as appearance of α-synuclein, tau or ubiquitin inclusions, or enhanced kinase activity. Intracellular localization and function of the protein is unclear, but studies remark the protein expression in the SNc, localization in the cytoplasm and also presence in Lewy structures of sporadic PD [62], [63].

1.1.3.3.3. Parkin

Parkin is a 465 residue protein, localized in PARK2, with ubiquitin-like N-terminal and two RING domains characteristic of E3 ubiquitin ligase. Parkin is able to signal substrate for ubiquitin proteasome system (UPS) degradation, presenting E3-like behavior by binding with E2 ubiquitin-conjugating enzyme. There are several suggested substrates for *parkin* targeting, with some implicated in PD such as dopamine transporter, transcription factors or glycosylated α-synuclein, and its accumulation results in selective dopaminergic toxicity for some substrates [29], [64].

Mutations in *parkin* gene (Figure 1.3) are the most frequent cause of early onset recessive parkinsonism, present in about half of the individuals with recessive familial onset before 45 years and 77% of juvenile sporadic cases before 20 years of age [65]. It has been reported missense and nonsense mutations, deletions and rearrangements of the gene, and resulted in a pathology of early onset, slow progression and L-dopa response, loss of dopaminergic neurons without LB formation, and possible formation of α-synuclein and ubiquitin inclusions. In addition, *parkin* mutation-enabled inactivation leads to reduction of UPS degradation [60], [66].

Parkin knock-out mice display little decrease of dopaminergic neuron survival [67], but show reduced level of mitochondrial proteins involved in oxidative phosphorylation[68]. The protein can be localized in the mitochondrial matrix, where it enhances the activity and proliferation of the organelle, and the overexpression of the protein resulted in prevention of mitochondrial swelling and apoptosis [69]. *Parkin* dysfunction can also participate in sporadic PD, since oxidative stress, dopamine and S-nitrosylation can lead to modification and inactivation of the protein. Increased

insoluble protein levels were found in brains of PD patients, which could result in reduction of its protective role in the proteasome [70].

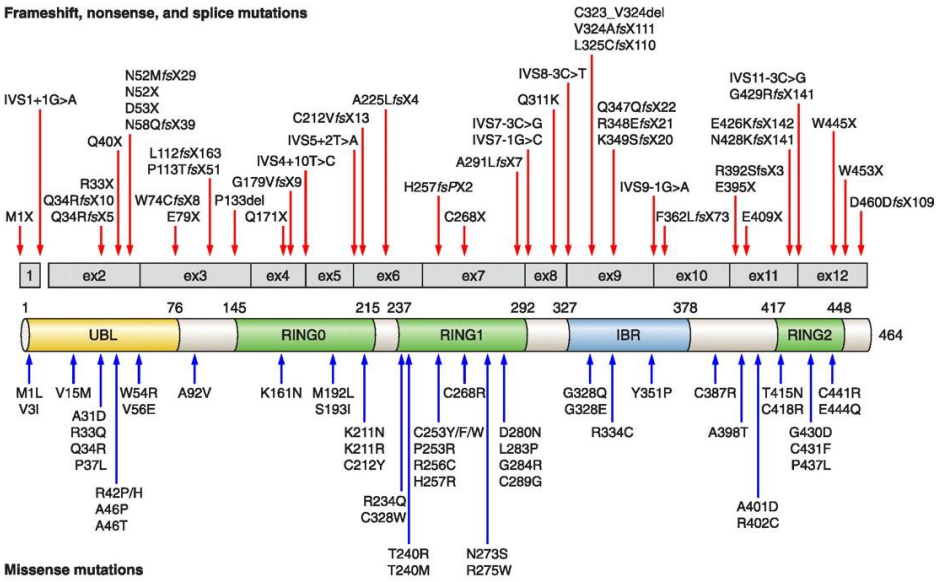

Figure 1.3 – Schematic representation of pathogenic frameshift mutations, above the transcript. Protein organization with coloured domains, and missense mutations below. Not mentioned: exon deletions, duplications or triplications causative of PD [55].

1.1.3.3.4. PINK1

PTEN-induced kinase 1 (PINK1) is a highly conserved 581 residue protein, present in PARK6 locus, ubiquitously expressed in the brain. It has low solubility, and constitutes 10% of LB in sporadic PD [71]. Homozygous or compound heterozygous mutations in the coding gene are related with onset of a various phenotype and age of onset, and PINK1 mutations (Figure 1.4) are attributed to 10% of autosomal recessive juvenile parkinsonism [72].

PINK1 protein has an N-terminal targeting motif, for localization of the protein to the mitochondrial membrane, and a catalytic serine-threonine kinase domain, with in vitro autophosphorilation activity. Overexpression of PINK1 is associated with prevention of mitochondrial depolarization and apoptosis, with kinase activity required for the protective role [73]. Studies with *PINK1* knock-out *Drosophila melanogaster*

notice dopaminergic neurodegeneration, increased sensitivity to stress agents, and enlargement and fragmentation of the mitochondrial cristae. Also, *parkin* appears to have similar phenotype in equal conditions and is capable of rescuing mitochondrial dysfunction caused by *PINK1* deficiency, but *PINK1* was unable to restore a *parkin* deficit, which indicates that both proteins are on the same mitochondrial pathway, with *parkin* being downstream of *PINK1* [74].

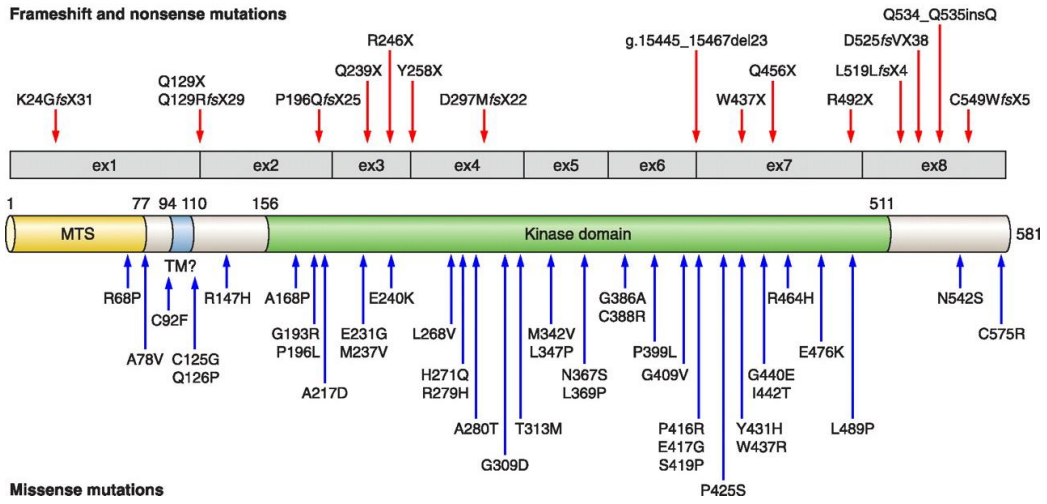

Figure 1.4 – Representation of PINK1, with frameshift and nonsense mutations above protein transcript. Protein organization, with coloured domains, and missense mutations below [55].

1.1.3.3.5. PARK7/DJ-1

DJ-1 was firstly described as an oncogene [75]. Later, the protein was associated with familial PD, with mapping of DJ-1 mutations from a kindred with an autosomal recessively inherited form of parkinsonism of early onset [76]. Autossomal recessive EOPD can be caused by DJ-1 mutations, though generally they are very rare and with a complex etiology and parkinsonian display [60]. It is estimated to account for 1 to 2% of early-onset cases, and the average of onset is at about 30 years of age, but in some cases the onset could occur up to 70 years [50].

The gene is localized in PARK7 and is expressed in increased levels in the brain. The protein is largely cytoplasmic, but can also be found in the nucleus, mitochondria

and extracellular space [77]. Though the key function of the protein is not clear, it was reported a translocation of the protein to the mitochondria as an oxidative stress response, reducing toxic cell damage, and is also believed to bind to RNA and help on its transportation to the mitochondria [78], [79].

The protein is thought to protect neurons from oxidative stress by acting as a redox-dependent chaperone. It has several self-oxidizing residues, particularly 106-cysteine (C106), but extensive oxidation can inactivate DJ-1, which has been identified in the brain of idiopathic PD patients [80]. Some pathogenic missense mutations (Figure 1.5) prevent DJ-1 dimerization, the most notorious being L166P, or result in structural changes that lead to impairment and degradation of the protein [81].

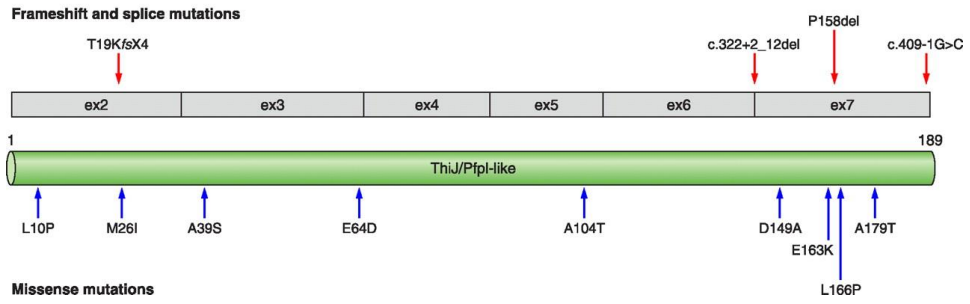

Figure 1.5 – Schematic representation of DJ-1 transcript organization and protein, composed of one domain. Missense mutations below the protein. Frameshift and splice mutations, and exon rearrangements, above transcript. Not mentioned gene exon deletions and duplications [55].

Taking in account phenotype similarity of homozygous null allele carriers, joined with common protection of the mitochondria, recent studies suggest that DJ-1, *parkin* and *PINK1* could participate in mitochondrial signalling cascades that run in parallel or convergent pathways of *parkin* and *PINK1*, but there is absence of evidenced DJ-1 direct relation with *parkin* or *PINK1* [82].

1.1.3.4. PD etiology and pathology overview

Current therapies for PD rely on dopamine replacement in the striatum and improve symptoms, but do not prevent progression of degeneration. The most vital question remains to be whether there is a common pathway for environmental and mendelian forms of PD. Despite multiple idiopathy, the pathogenesis of the disease seems to converge on common mechanisms, all of which interlinked, that could be corrected for prevention of PD development. Possible targets would be prevention of α-synuclein toxicity, antioxidant treatment or reversing of mitochondria dysfunction. If the convergence for all possible causes happens early in PD-originating pathways, it is possible to develop a preventive drug for any form of PD; if there is late convergence, or no convergence at all, it is needed a therapy design according to each case [83].

These questions could be resolved with the development of more *in vitro* neuronal models for characterization of pathogenic mechanisms and interactions occurred with several identified causes of PD, and complementary generation of *in vivo* models that could replicate the several pathologies that are observed in human PD [29].

1.2. DJ-1

The gene PARK7 expresses DJ-1, a small protein of 189 residues and about 22 kDa (Figure 1.6.A), highly conserved and ubiquitous to all biological kingdoms [84]. The gene itself contains 8 exons, the first being alternatively spliced in 1A and 1B exons, and exon 2 to 7 comprises the open reading frame (ORF) that encodes the protein [85]. Considering protein domain homology, DJ-1 is assigned to the ThiJ/Pfpl superfamily [86].

DJ-1 is expressed throughout the human body, with unknown tissue-specific functional mechanisms. Regarding cell distribution, DJ-1 is very dynamic, with translocation of the protein to the mitochondria or nucleus for specific roles as regulation of transcription, signal transduction or maintenance [87]. The protein has

also been associated with negative mediation of RNA binding, enhancing of male rodent fertility, androgen receptor regulation, among others [88].

Considering the structure and protein homology research, in addition to *in vitro* and *in vivo* assays, it is concluded that DJ-1 is a pleiotropic protein, with diverse and condition-dependent biochemical activities. Though the main attribution is protection against oxidative insults, other DJ-1 roles include maintenance of mitochondria and enhancing of cell survival in conditions of apoptosis stimulation [49], [88].

There is a consensus regarding DJ-1 dimerization of DJ-1 and 106-cysteine oxidation as culprits of DJ-1 protective activity, which affects multiple response pathways against oxidative and mitochondrial stress conditions. But specific DJ-1 mechanisms and protein interactions are largely unknown, for which is required more characterization studies of wild-type and mutant forms to verify the nature of several functions and to clarify DJ-1 activity pathways [88].

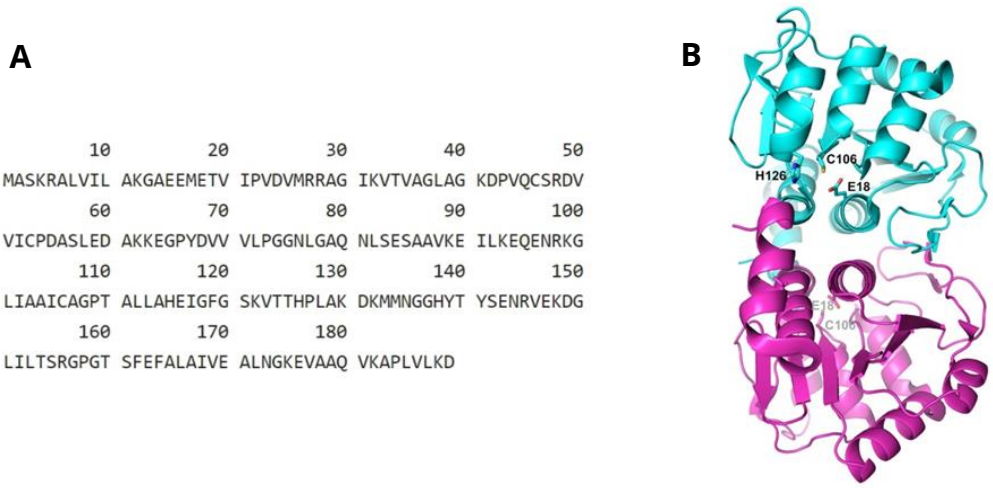

Figure 1.6 – Representation of DJ-1 structure: (A) Primary structure of human DJ-1, obtained from Protein Data Bank (1P5F). (B) Crystal structure of human DJ-1 protein, as the active homodimer. Two subunits are colored in cyan and magenta. Residues of the catalytic triad (E18, C106, H126) shown in sticks.

1.2.1. Structure and function

The three-dimensional structure for the protein DJ-1 has been determined in various conditions, highlighting a flavodoxin-like secondary fold and a compact

globular domain (Figure 1.6B). Human DJ-1 monomer consists in six-strand parallel β-sheet, sandwiched by α-helical arrangements [89]. In crystal and in solution, DJ-1 protein is present in the homodimeric form, seen as essential for protein activity. Crystallization analysis also highlighted the residue 106-cysteine (C106), identified as the most sensitive to oxidation in DJ-1. Structural homologs also present similar oxidation of the equivalent cysteine residue, suggesting that cysteine oxidation is a conserved feature of DJ-1 superfamily, though it has not been found any direct causative link between C106 oxidation and DJ-1 protection [88].

Furthermore, it has been noted the homology of DJ-1 to several bacterial protein domains, such as cysteine protease Pfpl and other proteases, unknown catalase, ThiJ involved in thiamine biosynthesis or redox-sensitive chaperone YajL. It is also noticed an α-helix at the C-terminal region, which could block putative catalytic site of DJ-1 that regulates protein activity [84], [89]–[91].

The relevance of the dimer for DJ-1 activity was confirmed with *in vitro* assays with L166P missense mutation. The mutation occurs near the catalytic triad and dimer interface, and was already reported its parkinsonian phenotype. The mutant protein presents poor folding, with disruption of the C-terminal region and the dimeric form, and extinction of protein activity via degradation pathways [89], [91]. Despite the knowledge of several others missense mutations, L166P is the one with most profound structural defects, but research suggests a slight structural alteration to the protein is enough to result in loss of function [88]. Some pathogenic DJ-1 missense mutations exacerbate destabilization of the highly oxidized protein form, and lead to loss of function in conditions where DJ-1 would still confer protection [86], [92].

Also, DJ-1 knock-out in *D. melanogaster* shows increased sensitivity to oxidative stress, and overexpression of phosphoinoisitide-3 kinase and protein kinase B (PI3K-AKT) pathway products, attributed to apoptosis blockage and oncogenesis [93].

1.2.2. C106 and regulation of oxidative stress

All functional activity assigned to DJ-1 seems to rely on C106 reactivity, and several homologies have been made to the single-domain protein, which makes difficult to attribute specific biochemical activity. But several studies foresee an overall role for DJ-1 as a cellular redox sensor, with altered activity in oxidative stress conditions [90].

C106 is located at the bottom of a surface grove of DJ-1, in a sharp turn between a β-strand and α-helix commonly designated as nucleophile elbow. It belongs to the active site designated as catalytic triad, consisting of Glu18, Cys106 and His126 residues. Two oxidized forms of the residue have been identified, C106 sulfinate (C106-SO_2^-) and sulfonate (C106-SO_3^-). The oxidation is stabilized with hydrogen bonds to E18, but also G75 and A107. These help on the ionization of C106 thiol side chain and its pKa decrease, to about 5.4, prone to oxidation. Despite subsequent changes in DJ-1 activity, C106 oxidation doesn't alter the structure of the protein. [84], [86], [88].

Currently it is considered that C106 oxidation is the main responsible for DJ-1 cytoprotection against oxidative insults [78], which was confirmed with several studies. Engineered C106DD and C106EE mutants mimic the design of oxidized forms of C106, and indicates that oxidation of cysteine residue is relevant to protein function or activation [94]. But C106D mutation, that mimics C106-SO_2^- electrostatic properties but has different planar geometry, shows an abrogated activity for DJ-1 [78]. Furthermore, E18 mutations that allow C106-SO_2^- formation are cytoprotective, while oxidation-impeditive mutations are not [95], and substitution of C106 to alanine, serine or aspartic acid eliminates DJ-1 capacity to protect cells from oxidative insults [88].

It still remains to be fully answered which form of C106 is the most beneficial for neuroprotection. The data largely suggest a protective role for C106-SO_2^-, giving ability for mitochondria translocation, chaperone activity or apoptosis signal-regulating kinase 1 (ASK1) inhibition [78].

The reduced form of DJ-1 is able to scavenge ROS, and also bind to mRNA. Conditions of extremely oxidative stress could lead to C106-SO_3^- formation and

oxidation of other cysteine and methionine residues, associated with protein aggregation, loss of structure and possible apoptosis potentiation. This associates with ageing, cancer or neurodegeneration, and it has been detected extensive cysteine and methionine oxidation in brain tissue of PD patients [86], [88]. Oxidant impairment of DJ-1 can be exacerbated with pathogenic M26I mutation, suggesting a link between excessive cysteine and methionine mutation in DJ-1 and parkinsonism [78]. Other cysteine residues, on the 46 and 53 position of DJ-1 sequence, could be alternate redox centers to regulate DJ-1 oxidation and activation, though C103 is the most important residue and the best conserved in DJ-1 family [92], [96].

The oxidation of C106 and other residues requires ROS consumption, so the protein was proposed as being an ROS scavenger. DJ-1 is able to use and eliminate hydrogen peroxide in *in vitro* conditions, and DJ-1 knock-out mice demonstrate accumulated mitochondrial hydrogen peroxide and diminished mitochondrial function. But giving the lack of ability to reverse its oxidized form, for multiple ROS processing, it is thought that DJ-1 burden on overall ROS elimination is not significant [88], [94].

In addition, dopamine-derived quinones (DAQ) can be produced endogenously in oxidative conditions and have been attributed to dopaminergic degeneration [97], [98]. DAQ with protein adduct formation showed ability to covalently modify cysteine residues, particularly C106, and impair functional activity of DJ-1, suggesting that the protein could be a useful response to oxidized dopamine insults [99].

1.2.3. Mitochondrial maintenance

Mitochondria are the main source for endogenous ROS, and several studies relate DJ-1 to promotion of adequate function of mitochondria, including defence against complex I inhibition. Mitochondrial dysfunction is a key factor of parkinsonism pathophysiology, and oxidative stress may be related, since it can be a cause or an effect of mitochondrial damage [48], [88]. A series of studies point out that oxidative conditions enhance the translocation of DJ-1 towards the mitochondria. The protein

can be found on the outer mitochondrial membrane, intermembrane space and matrix of neuron mitochondria [77], [78], [95].

DJ-1 knock-out mice display fibroblasts with shorter and more fragmented mitochondria, and rescue of mitochondrial integrity was only achieved with DJ-1 forms capable of C106 oxidation [95]. Also, manipulated enhancing of DJ-1 translocation results in enhanced protection in neuroblastoma cells. Furthermore, C106 oxidation also appears to facilitate this relocation, but C106S mutation shows some of the protein associated with the mitochondria, indicating that oxidation may not be the single factor for DJ-1 translocation to the mitochondria[88].

Nevertheless, there are solid evidences that DJ-1 is capable of localizing to the mitochondria in oxidative stress conditions, protecting it from any resultant damage [78].

1.2.4. Other protective functions

Homology with YajL protein and other chaperones of DJ-1 superfamily, coupled with *in vitro* and *in vivo* studies, indicate that DJ-1 has chaperone activity, particularly to prevent the fibrillation of α-synuclein in oxidized conditions. This is only evident with oxidation of C106 to C106-SO_2^-, seen as a key feature for redox-sensitive chaperone activity [80]. DJ-1 chaperone activity can be inhibited in reducing conditions, and not only C106 mutations in DJ-1 hamper chaperone activity, but also C47 and C53 residues. These results confirm a possible induced chaperone activity of DJ-1, after redox alterations in the cytoplasm and the protein, and this function is capable of α-synuclein aggregation suppression and ROS protection [80], [100]. But in vivo studies have presented conflicting results regarding chaperone ability to reduce α-synuclein toxicity. In dopaminergic cells, it is thought that DJ-1 can protect against α-synuclein toxicity through a Hsp-70 chaperone dependent pathway [88].

Glyoxal are small and cytotoxic oxaldeides, resulted from glucose oxidation. It was shown that DJ-1 also has glyoxalase activity, and the presence of the protein in dopaminergic SH-SY5Y cells protect them from glyoxal administration. Also, mutations

in the catalytic cysteine and glutamic acid nulls protein activity, confirming active DJ-1 protective role with scavenging of reactive carbonyl species [101].

Despite high similarity of DJ-1 to PfpI/PH1704 proteases, DJ-1 appears to have little or no protease activity. This could be explained with DJ-1 distorted catalytic triad, in comparison to the PfpI, and the C-terminal helix covers and prevents the putative site [89], [102]. Upon the removal of the C-terminal α-helix, DJ-1 acquired cysteine protease activity, having a catalytic diad of C106 and H126, and also enhanced protection from oxidative stress-induced apoptosis. Moreover, endogenous DJ-1 in dopaminergic neurons also appears to be capable of C-terminal cleavage in response of mild oxidative conditions, supporting the hypothesis of protease activity against oxidative stress [103].

1.2.5. DJ-1 interaction and modulation

The first DJ-1 identified interactor was the androgen receptor-interacting protein 3, known as a protein inhibitor of activated signal transducers and activator of transcription (PIASx-α) [104]. DJ-1 additionally demonstrates a role on RNA binding and regulation. Recently it was found a preferred interaction between DJ-1 and GC rich sequences in mRNA transcripts that translate to proteins of PTEN/Akt kinase pathway, ROS detoxification and mitochondrial function, and this mechanism could explain DJ-1 pleiotropy. But DJ-1 oxidation can compromise its mRNA binding activity [79], [105].

Furthermore, DJ-1 is capable of transcriptional upregulation of antioxidative genes, such as glutamate cysteine ligase or superoxide dismutase 3 (SOD3), and cell specificity could pass through the regulation of particular antioxidants. Also, DJ-1 was reported to interact and stabilize nuclear factor erythroid 2-related factor 2 (Nrf2), identified as an transcriptional master regulator for antioxidant response [87].

DJ-1 can also bind to proteins such as Cezanne, Bcl-xL, and proteins related to androgen receptor function. These probably mediated through covalent bonds between the ligand and C106. Furthermore, it has been demonstrated the interaction of DJ-1 with apoptosis-related proteins, such as Daxx and inhibition of ASK1 and p53. It is

known that C106 oxidation is needed for this interaction, which results in apoptosis cascade interruption and cell survival enhancement. Still, specific mechanisms for its broad interaction are not fully understood [90].

DJ-1 is highly expressed in neurons of all regions of the brain, but in the *substancia nigra* it can be found equally on neurons and non-neuronal cells such as astrocytes, highlighting a distinct role of the protein on this region. The expression of DJ-1 in astrocytes could be for protection of surrounding neurons against pathological conditions, which was already shown with overexpression of DJ-1 in astrocytes, which resulted in enhancement of neuroprotective capacity against rotenone. Cellular redox homeostasis relies on glutathione, and DJ-1 enhances the transcription and activity of glutathione cysteine ligase. Glutathione secretion is particularly important in astrocytes, for neuron protection, and DJ-1 can help on the expression of these protective factors [88].

Overall, despite an extended structural and homology data, and multiple in vitro and in vivo assays, biochemical function remains to be fully addressed due to insufficient or inconclusive data [90].

1.2.6. Pathologic significance of mutant DJ-1

Pathogenic DJ-1 mutations are accountable for the onset of several cases of parkinsonism, though it represents a low number within early-onset PD. However, despite low mutation frequency, it is the second most common known genetic cause of PD, and an increasing number of mutations causing the disease have been found. Given the high variability in coding and noncoding sequence of the gene, the number of DJ-1 monogenic forms of PD could increase [106].

Patients with a pathogenic mutation of DJ-1 usually develop resting and postural tremor, asymmetric onset and slow progression of symptoms, but symptoms may vary with respective mutation. For example, patients with L166P mutation had psychotic episodes, patients with M26I mutation were affected with anxiety and patients with E163K mutation developed dementia and motor neurodegeneration.

Several DJ-1 mutations have been directly related to parkinsonian onset (Table 1.2). Besides mutations of the coding sequence, there are studies that indicate a potential pathogenic role for DJ-1 promoter and non-translated mRNA, that can affect expression and activity induction of DJ-1 [87].

Table 1.2 - Identified genetic variants of DJ-1, related to Parkinson's disease [87].

mutation	population	inheritance	effect
L166P	Italian	homozygous	protein instability
14-kb deletion	Dutch	homozygous	protein loss
M26I	Ashkenazi Jewish	homozygous	decreased stability
D149A	Afro Caribbean	heterozygous	unknown
IVS6-1G-C	Hispanic	heterozygous	altered transcript
c.56delC	Hispanic	heterozygous	frameshift
c.57G→A	-	-	unknown
g.168_185del	Global	both	polymorphism
A104T	Latino	heterozygous	unknown
Ex5-7del	Northern Italian	heterozygous	altered transcript
IVS5+2-12del	Russian	heterozygous	altered transcript
R98Q	Global	heterozygous	polymorphism
E64D	Turkish	homozygous	unknown
E163K	Italian	compound	altered activity
g.168_185dup	-	-	unknown
P158del	Dutch	homozygous	unknown
A179T	Dutch	homozygous	unknown
Ex1-5dup	Dutch	homozygous	unknown

There are no autopsy studies of PD patients with pathogenic forms of DJ-1, but *antemortem* imaging notices changes in brain of these patients and severe dopamine depletion resultant from DJ-1 mutations [107].

In the human brain, DJ-1 is moderately expressed in neurons and astrocytes, and in sporadic PD it was found to be increased in astrocytes of PD patients, though it did not appear accumulated in Lewy bodies [108].

DJ-1 was firstly proposed for a protective role in the oxidative stress response [84], which was later demonstrated in DJ-1 deficient cells where a decreased survival was stated, including enlarged sensitivity to oxidative stress and proteasomal inhibition [102]. The activation of the protective mechanism requires the DJ-1 signaling by

oxidation of the active site C106 to cystein-sulfinic acid and consequent translocation to the mitochondria [78], [95]. Pathogenic mutations of DJ-1 lead to an alteration of mitochondrial dynamics and morphology, increase of ROS mitochondrial production, enhance of autophagic activity promoted by *parkin* and *PINK1*, and accumulation of apoptosis markers [109]. Also, while the wild-type form of DJ-1, PARK1 and *parkin* can correct mitochondrial fragmentation caused by α-synuclein overexpression, this correction is not possible with dysfunctional mutants [110].

DJ-1 deficiency can be compensated with *parkin* or *PINK1* overexpression, suggesting that DJ-1 pathway works in parallel to the *parkin/PINK1* pathway for mitochondrial maintenance [109], [111]. However, DJ-1 could have a more important role for an immediate feedback to ROS generation, since in oxidative stress the protein is able to downregulate *parkin* recruitment to depolarized mitochondria, which is dependent of *PINK1* [112]. This crosslinked interaction could be mediated through outer membrane mitochondrial proteins involved in fusion and fission or motility regulation [90].

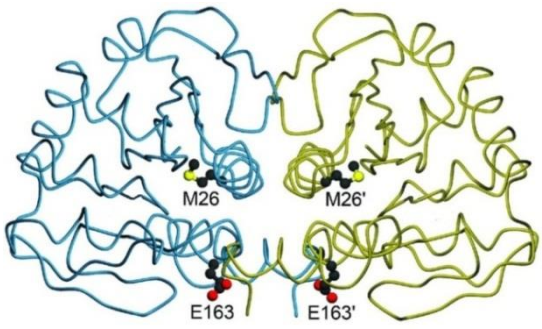

Figure 1.7 – Location of the two residues of M26I and E163K pathogenic mutations, in each monomer of the DJ-1 dimer. Each monomer is coloured in blue and green.

1.2.6.1. M26I

The missense substitution of 26-methionine residue to isoleucine (M26I) was first identified in an Ashkenazi Jewish patient diagnosed with early-onset PD [87]. M26 is located in the α-helix A, near its C-terminal end. When the protein acquires its dimeric

form, the substitution is located on its core (Figure 1.7). This residue is highly conserved in the protein sequence, so it is predicted that this substitution, though conservative, could be relevant for structural and functional changes in DJ-1 [86].

The stability of the quaternary structure of M26I is somewhat disputed. Though *in vitro* studies concluded the mutant exists at low levels and stability and has enhanced propensity to form oligomers, other studies note an ability of M26I to fold similarly to wild-type DJ-1, and is not subjected to proteasomal degradation [113]. Circular dichroism analysis indicates that the secondary structural content of DJ-1 in solution seems unaffected in M26I in comparison to the wild-type form, with about 35% α-helix, 18% β-sheet and 47% coil, turn or others. Furthermore, M26I shows a modest decrease of thermal stabilization, decrease of expression levels, and increased turnover rate, though not as intense as the functional disruptive L166P mutation [86], [92], [113].

Although M26I is near the dimer interface, it isn't responsible for intermolecular bonds between monomers that constitute and stabilize the homodimer. But the substitution results in displacement of I31, creation of a small cavity in the hydrophobic core and loss of optimal packing in the interior of the protein. The creation of the cavity could contribute to greater conformational flexibility and may be the cause for the slight thermal destabilization of M26I [86].

Regarding the mitochondrial role, it was shown that M26I is also present in the mitochondria, but relocation from cytoplasm to this organelle in oxidative stress conditions is more significant for the wild-type form [113].

An increase of M26I stability was achieved with the introduction of a dysulfide bridge between 51-valine and 53-cysteine, which resulted in rescue of DJ-1 thermal stability, improving of ROS scavenging activity and blocking of α-synuclein aggregation through chaperone-like function [114]. Furthermore, M26I can form heterodimers with WT DJ-1, which stabilizes the mutant form and could explain the absence of onset in heterozygous individuals. These results suggest that the main pathology for M26I mutation in DJ-1 is a decreased stability of the protein structure and subsequent impairment of function, despite resulting from a minor structural defect [88], [92].

1.2.6.2. E163K

This mutation was firstly described in a southern Italian family, that manifested early onset parkinsonism with dementia and motor degeneration with onset similar to amyotrophic lateral sclerosis. These individuals carried the homozygous missense E163K substitution in exon 7 of DJ-1, and also a homozygous duplication of the pro-motor region, but relevance of each mutation in this kind of onset is debatable [115].

The substitution of 163-glutamic acid to lysine (E163K) is a missense and nonconservative mutation, with a change from negative to positive residue, that occurs in a conserved residue of the structurally essential helix G [87] and is located near the dimer interface (Figure 17). A particular feature of the 163-glutamic acid residue is the formation of a salt bridge between its carboxylate side chain and guanidinium side chain of 145-arginine, located in the turn of β-strands 8 and 9. The latter residue is also responsible to anchor the C-terminus of the opposite monomer, through hydrogen bonding. The high degree of conservation of these two residues, in DJ-1 homologues, highlights the importance of this interaction. E163K substitution results in the disruption of the salt bridge, increased mobility of 145-arginine, weakening of the network of hydrogen bonds across the dimeric interface, and eventual decline of DJ-1 quaternary structure. E163K mutant protein has a decreased thermal stability, more significant than the M26I mutant, but E163K mutant maintains overall secondary structure and dimerization capacity in relation to wild type DJ-1 and M26I [86].

Under normal conditions E163K doesn’t feature any significant behaviour, but under oxidative stress conditions the protein doesn’t appear to be relocated to the mitochondria. This could be due to the charge exchange of 163 residue and slight structural changes, which could prevent the protein from interacting with other proteins responsible for the intracellular distribution of DJ-1. As a result, and unlike other mutations, E163K shows impaired response capacity towards oxidative insults, while maintaining protection against proteasome inhibition and mitochondrial damage [116].

1.3. Proteomics

The assessment of gene, protein or metabolite profiles is insufficient to provide complete descriptions of complex biological problems - genome has a static nature, and proteome or metabolome profiles vary with several intra and extracellular factors [117]. Given recent advances in instrumental techniques and bioinformatics tools, it has been established a new field of study: systems biology, focusing on a holistic elucidation of biologic systems and a systematic analysis of its complex interactions and dynamics [118]. This includes expression proteomics, which studies changes in protein expression under different conditions, and functional proteomics, that intends to understand protein function and its role on the cell [119]. This field has become a very useful tool for the correlation of cell behaviour responses, as feedback of changes in the cellular environment, with alterations regarding protein expression or post-translational modifications [120]. Proteomics can provide a thorough analysis by resolving the expressed protein profiles in various conditions, using gel electrophoresis related techniques, or more recently the identification and quantification of proteins via mass spectrometry (MS) analysis, which has become proteomics' most important toll [121], [122].

1.3.1. MS analysis

Proteomic analysis reached a turning point with the use of MS for protein identification, and has become a key step for characterization of large protein complexes, being typically performed after any type of tag-based affinity procedure when is desired a particular subset of proteins [117].

MS analysis consists on the measurement of mass to charge ratios (m/z) of gas-phase ionized analytes, with high speed, sensitivity and range. The mass spectrometer is constituted by: ion source, where the sample analytes are ionized and converted to a gaseous phase; a mass analyser separates the ions according to their

m/z value; a detector counts the number of ions of each m/z; software is needed for data processing and development of the mass spectra [123].

The analysis of proteins with MS analysis began with the development of soft ionization techniques, such as matrix-assisted laser desorption ionization (MALDI) or electrospray ionization (ESI). MALDI MS is often used for a protein identification of simple peptide mixtures, where the sample is sublimated and ionized from a crystalline matrix. But for analysis of complex mixtures, it is preferable the usage of ESI MS: peptides are ionized from a solution to the gaseous phase, and this allows an upstream coupling of liquid-separation techniques, such as liquid chromatography (LC) or capillarity electrophoresis, useful for peptide mixture fractionation before its input on the mass spectrometer [119].

Furthermore, ESI coupled with LC can be used within tandem mass spectrometry (LC-MS/MS), for identification and characterisation of the protein constituents of the sample: after the ion detection in the first MS unit, ions are selected according to m/z values and fragmented for a second MS run. Through comparison of the MS/MS spectra against *in silico* measurements of all proteins contained in a database, such as Mascot, it is possible the identification of each peptide fragment according to mass and sequence, and subsequent protein identification in complex mixtures [118]. LC-MS/MS can also be used for relative quantification of each protein, which could be relevant for the discovery of condition-dependent dynamics in proteomic studies.

The most widely MS method used for tandem mass spectrometry is known as shotgun, or discovery, proteomics, operated in a data, or information, dependent acquisition mode (DDA) where it is generated the fragment ion spectra (MS2) of selected m/z windows of precursor ions spectra (MS1), for the identification of proteins. This is widely used for the identification of large array of proteins in complex samples, but has some disadvantages: quantification limitations due to irreproducibility; under-sampling; long instrument cycle-times, dependent of sampling speed; the overlooking of the major part of proteins in complex samples [124]–[126]. There is another approach, named targeted proteomics, that operates on a selected reaction monitoring (SRM) mode, where it is surveyed for the identification and quantification of a limited

set of proteins, selected before the MS sample run: it is more useful for biomarker research and systems biology, given its reproducibility and accuracy, but is very limited to the number of analysed proteins for each acquisition. But there has been efforts to develop new strategies that do not require the pre-selection of protein lists or precursor ions for the MS2 acquisition, designated as data-independent acquisition (DIA), where MS/MS scans are made systematically and independent of previous information and it is able of acquiring a single dataset very useful for the identification and label-free quantification of a large set of proteins [124], [127]. It was lately developed a new approach of DIA acquisition with an optimized strategy for the reading of the fragment ion spectra, consisting on the sequential window acquisition of all theoretical fragment-ion (SWATH-MS). It consists in systematic MS1 scans over intervals of retention time intervals of the LC, and then fragment ion spectra of consecutively collected isolation windows from the precursor ion spectra, of usually 25Da width, are acquired creating a complex map of fragment ions. It requires only the selection of a spectral library of proteins, which can be used one created from IDA acquisition; this is only used run of DIA-acquired samples, and before SWATH processing of obtained data, which allows a correction or update of the SWATH analysis of the sample [124]. There has already been studies reporting an efficient proteomic analysis based on the protein identification with IDA acquisition and quantification with SWATH analysis, since both approaches can be used in the same type of mass spectrometer based on a hybrid quadrupole time-of-flight (Q-ToF) system, which are able of providing fast acquisition speed, high resolution and sensitivity and excellent mass accuracy [126], [128]–[130].

It is worth noting that besides label-free methods to compare identical peptides between samples, allowing the identification and quantification of proteins, there are other strategies for quantitative proteomics based on the peptide labelling with stable isotopes, using approaches such as SILAC, ICAT or iTRAQ [117], [131].

Any of these strategies, label or label-free, used for identification or for absolute or relative quantification of proteomes, can be valuable for the research of numerous pathological conditions, particularly neurodegenerative diseases, giving the fact that its

development is inherently associated with several protein-related changes at a cytological level. The determination of key modifications in certain subcellular compartments, specific brain regions or neuron types, as well in the presence of specific conditions, could give important information regarding the changes in protein expression and regulation that trigger such diseases [132].

1.3.2. Cell surface enrichment

The plasma membrane is a sub-cellular compartment of great interest, since it contains cell surface proteins (integral to the plasma membrane or peripheral proteins on the extracellular side) that could be widely studied namely for disease research [133], [134]. These are responsible for the mediation of numerous cell processes and responses, including intercellular communication, external stimuli response, vesicle trafficking (including secretion and endocytosis), ion and low molecular weight compounds transport, protein translocation particularly it contains receptors and cascade signalling mediators, capable of regulating processes such as transcription and translation, metabolism, differentiation, apoptosis, or cell survival [120], [135], [136]

The composition of the cell surface proteome can be significantly altered during disease progression, so it is to consider an identification of biomarkers that could be used as targets to correct stimuli and signal cascade associated with pathogenesis [136]. It has been previously noted cell surface proteins alterations and pathways associated to several key cell features or responses, such as apoptosis induction and immune response stimuli, cell growth and tumour development, among others [133]. The profiling of cell surface proteins in disease conditions, and relative quantification for expression variation analysis, can provide the identification of key membrane mediators of cell feedback, that can be used as targets for molecular diagnosis and drug-based therapeutics [133]. This could be an useful approach for expression proteomics, resourcing to the identification of proteins correlating with changes of cellular behavior as a result of environmental or intrinsic changes [120].

The analysis of whole-cell lysates for the study of medium or low abundant cell surface proteins would be very difficult: the preparation of high concentrated subcellular fractions of cell surface proteins, with low contamination of organelles and cytosolic compounds, becomes an essential step for the specific study of plasma membrane associated proteins [120]. There are some tools able of obtaining an enrichment of the plasma membrane and cell surface, usually for a downstream analysis based on gel electrophoresis or mass spectrometry: two-phase partition or ultracentrifugation for extraction of membrane protein fraction [136]; centrifugal collection of membrane fraction [135]; use of silica and nanoparticles [137], [138]; cell shaving [136]; the use of global cell surface protein biotinylation, coupled with avidin based enrichment of biotinylated proteins [120], [133], [139].

The major drawbacks for the study of cell surface proteins are their low abundance in cellular extracts and hydrophobic nature (leading to poor solubility and existence of less trypsin cleavage sites), and inefficiency over protein cytosolic and other membrane proteins removal [134], [135]. Of all the described, cell surface biotinylation coupled with MS analysis has turned into the most often used approach for the cell surface *in vivo* and *in vitro* proteome research, in a pathological context, due to its low contaminant abundance and specific labelling of cell surface proteins, if using a membrane-impermeable derivative of biotin and a protocol that maintains cell integrity [134], [140].

1.3.2.1. Biotinylation-avidin based MS studies

Biotin, also designated as vitamin H, is a small molecule though capable of a strong interaction with the egg white protein avidin. This protein is assembled in a tetrameric form, with each monomer consisting of a rigid eight-stranded β-barrel, very similar to the bacterial related streptavidin. Hydrophobic interactions are responsible for the tight binding of one biotin molecule at the core of the avidin monomer, which has the highest affinity found in nature the interaction between a ligand and a protein, with $K_a \approx 10^{15}\ M^{-1}$ [141]. This was widely converted into a valuable commodity as a

versatile affinity-based tool for biochemical and biomedical research, usually requiring the biotinylation of biomolecules, such as DNA, antibodies or proteins: biotinylated compounds can be detected using avidin, or streptavidin, conjugated with fluorophores, chromophores or related enzymes; they can also be captured from a complex mixture using avidin or streptavidin-coated solid supports such as resins, magnetic beads, or microtiter plates [139].

Regarding an MS study approach, this has been used for the analysis of cell subpopulations through covalent binding of biotin-containing tags, and capture of biotinylated proteins with avidin or homologues conjugated with chromatography matrices, for downstream protein identification with MS analysis. There are several derivatives of biotin, for multiple uses: use of biotin conjugated with a succinimide ester for labelling of cell surface proteins; elaboration of genetic strategies for labelling of specific intracellular organelles; detection of newly synthesized proteins; among several other possible strategies [139], [142].

Proteins can be labelled on several sites of the protein: biotin is most commonly conjugated with a succinimide ester, N-hydroxysuccinimide (NHS), which binds covalently to primary amines, present in the side chain of lysine residues and N-terminal side of proteins. This has the advantage of the numerous presence of lysine residues in proteins, and their presence in accessible positions of the protein. There are other possible biotin conjugates that react with different protein groups or give the compound different features. Lately was added a long chain between the NHS and biotin group, forming NHS-LC-biotin, to reduce steric hindrance and increase availability of biotin to avidin based resin, improving their interaction and capture of biotinylated proteins. Furthermore, the labelling of cell surface proteins implies no membrane permeability of the biotin compound used, possible with water-soluble analogues: Sulfo-NHS-LC-biotin is soluble in water, not needing the use of organic solvents such as dimethylformamide (DMF) or dimethyl sulfoxide (DMSO), and the added hydrophilic group does not allow the biotin diffusion through the plasma membrane, making it the most popular choice for the labelling of cell surface proteins [139].

One of the main problems regarding the biotinylation of proteins is its elution from the avidin-based resins, given the high affinity between biotin and avidin. Usually it is required the use of denaturant conditions for the release of biotinylated proteins captured in avidin pull-down. There are some alternatives that can be used to permit the use of non-denaturant conditions: biotin compounds with pH or temperature dependent avidin binding; cleavable biotin compounds for the downstream release of the captured proteins from the avidin matrix; use of monomeric avidin, instead of the tetrameric form, with lower affinity to biotin [133], [139], [143].

1.3.3. *In vitro* proteome analysis of DJ-1

Like neurotoxin based models have been very important for the elucidation of culprits of PD pathology, studies based on the manipulation of PD genes should be valuable for the creation of new research models, characterization of PD related proteins and clarification of cellular mechanisms that trigger the development of the disease [3].

The SH-SY5Y neuroblastoma cell line has become a common *in vitro* model of dopaminergic neurons, suitable for PD research, since they have many characteristics of these neurons, including: expression of dopamine-β-hydroxylase and dopamine transporter (DA) [144]; decreased viability in oxidative conditions, after addition of hydrogen peroxide or dopaminergic neurotoxins such as 1-methyl-4-phenylpiridium (a toxic metabolite of MPTP) and 6-hydroxydopamine [145].

DJ-1 is expressed in neurons and astrocytes, and it has been demonstrated its uptake in dopaminergic neurons. Given DJ-1 role against oxidative stress, the protein is able to prevent ROS production and cell death in SH-SY5Y culture and in SNc of the brain of rats [146]. DJ-1 is overexpressed in astrocytes, in an attempt to protect themselves and surrounding neurons against oxidative insults, and DJ-1 knock-off reduces astrocyte-mediated protection [147]. Furthermore, PD causative mutations of DJ-1 are able to abrogate protective activity of the protein in cell culture and animal models [145], [146].

Various individual mechanisms associated with DJ-1 protection are already known, but there is not a profound analysis regarding DJ-1 neuron uptake and dynamic interaction with membrane proteins, or any variations in pathological conditions. It has already been found interactions between DJ-1 and some proteins found on the membrane: paraoxonase-2 (PON2), an interacting target of DJ-1, is found on the cytoplasm and all membranous structures and has an antioxidant role; DJ-1 positively interacts with tyrosine hydroxylase (TH), which can be found in the plasma membrane and is responsible for dopamine synthesis and synaptic vesicle packing [148]–[150].

In addition, it has been already made a proteomic analysis of the cell surface proteome of SH-SY5Y cells, with subcellular protein extract being obtained using affinity purification with biotinylation of cell surface proteins and avidin chromatography, followed with MS analysis [151], [152], though not in a PD context. This approach could be used for the study of a cell surface dynamic proteome regarding DJ-1 activity and mutant-enabled dysfunction associated with PD development, using an *in vitro* model of oxidative stress.

2. Objectives

Despite extensive research, Parkinson's disease still has an idiopathic pathology, but lately several genes where monogenic mutations are able to develop parkinsonian phenotype have been identified, including *PARK7*/*DJ-1*. Several DJ-1 mutations attributed to cases of PD development, including M26I and E163K missense mutations. DJ-1 has a pleiotropic role preventing neuronal degeneration, particularly against oxidative stress and mitochondrial damage. But key function and protective mechanisms of DJ-1, in addition with the effects of activity impairment responsible for PD development, remain to be fully assessed.

With this line of thought, the aim of this study was the characterization of the membrane protein dynamics under oxidative stress conditions – including direct interactomic analysis between the various DJ-1 forms and cell surface proteins, and proteome analysis after additional stimulation of culture with extracellular addition wild-type and M26I and E163K mutant forms of DJ-1. This could help on the clarification of the effects of oxidative stress and DJ-1 mutation over the protein constitution in the membrane, and elucidation of interactions responsible for DJ-1 intake in neurons or activation of neuroprotective signalling pathways, which could provide new data regarding DJ-1 dysfunction and associated PD development.

In order to accomplish these goals, the following tasks were proposed: i) production of M26I and E163K mutant forms of DJ-1, recombined with a poli-histidine tag for affinity purification, followed by its structural and biological characterization; ii) delineation of a procedure for enrichment of cell surface proteins from SH-SY5Y culture, an established *in vitro* model for PD studies, through biotin labelling and avidin pull-down purification; iii) LC-MS/MS characterization of cell surface protein profiles of the *in vitro* model subjected to PD related conditions, particularly oxidative stress and additional intake of the wild-type and mutant forms of DJ-1.

3. Methods

3.1. Polyacrylamide gel protein separation

Protein samples were prepared through addition of Laemmli Sample Buffer (SB) (Bio-Rad) for a final concentration of 32.9 mM Tris-HCl, pH 6.8, 1.05% SDS, 26.3% (w/v) glycerol, 0.005% bromophenol blue and 5 minutes incubation of samples at 95ºC without agitation, in a Thermomixer (Eppendorf), for protein denaturation. After cooling at room temperature, 4 µL of bis-acrilamide (acrylamide/bis solution, 37.5:1) were added per 30µL of sample to promote cysteine alkylation.

After sample preparation, samples intended for MS analysis were separated through gel electrophoresis, using a Mini-PROTEAN TGX precast 4-20% SDS-polyacrylamide gel (Bio-rad) and a Mini-PROTEAN Tetra Electrophoresis System (Bio-Rad), proceeded with colloidal coomassie staining. In biological analysis of biotinylated cell surface proteins, proteins were separated in 15 min of 150 V, until run front reached a third of the gel length; in other assays was used 120 V, until sample front reached the bottom of the gel.

Samples intended for a staining or western blot approach were loaded on a self-prepared 12.5% polyacrylamide gel; proteins were separated using a Mini-PROTEAN Tetra Electrophoresis System (Bio-rad) and stained through colloidal coomasie or silver staining methods.

3.1.1. Colloidal coomassie staining

After electrophoresis separation, gel was washed with distilled water and immersed in staining solution [10% (v/v) of 85% phosphoric acid solution, 10% (w/v)

ammonium sulphate, 20% (v/v) methanol], and filtered powder of Coomasie Brilliant Blue G-250 (Bio-Rad) where then added, allowing the formation of colloidal particles for subsequent staining of proteins, and left incubating overnight with agitation. Gel was then washed several times with distilled water until the distinct discernment of protein bands, and was left in distilled water until downstream processing.

3.1.2. Silver staining

After electrophoresis separation and washing of gel with distilled water, it was immersed in fixation solution [25% (v/v) methanol, 5% (v/v) acetic acid] for 30 minutes, then dehydrated with gel incubation in two alcoholic solutions [50% and 30% (v/v) ethanol, respectively], for 10 minutes each; afterwards, gel was subjected to a 0.2 g/L sodium thiosulfate solution, for 1 minute, followed with 3 washes with deionized water and then immersion of gel in a 2 g/L silver nitrate solution for 20 minutes; later, it was exchanged to a developing solution [0.7 mL/L of 37% formaldehyde solution, 30 g/L of anhydrous sodium carbonate, 10 mg/L of sodium thiosulfate]; once it was reached the desired level of protein staining, the reaction was terminated with a 1 minute incubation with a stop solution [50 g/L Tris, 2.5% (v/v) acetic acid solution]. All steps were performed with agitation. Gel was left immersed in distilled water until further use.

3.2. MS analysis

3.2.1. Protein digestion

3.2.1.1. In-gel digestion and peptide extraction

After gel electrophoresis and Coomassie Blue staining of separated proteins, described in section 3.1, the gel lanes were sliced into small pieces under a flow chamber and distributed in several LoBind tubes (Eppendorf) according to gel lane

sections, where they were left immersed with 1 mL of deionized water to prevent gel dehydration. In all experiments, except MS identification of DJ-1 mutant and contaminants, gel lanes were cut in three transversal sections and digested separately. Deionized water of each tube was switched to 1 mL of destaining solution [50mM ammonium bicarbonate, 30% acetonitrile (ACN)] and microcentrifuge tubes were incubated for 15 minutes in a thermomixer (Comfort, Eppendorf), under 25ºC and 850 rpm. The destaining solution of each tube was replaced with 1 mL of deionized water, then incubated in thermomixer for 10 minutes, under 25ºC and 850 rpm. These two steps allow the release of Coomassie Blue from the gel pieces - if gel pieces still appeared blue, the incubation with 1 mL destaining solution was repeated, then deionized water; when gel pieces were colourless, water was discarded and gel pieces were dehydrated in a Concentrator Plus (Eppendorf), at 60ºC, until gel pieces were white and fully dried.

After gel drying, the trypsin solution as added to each tube (10 µg/mL in 10 mM ammonium bicarbonate solution), enough to fully cover gel pieces (approximately 100 µL), and were left incubating overnight, in the dark and at room temperature, to allow an extensive hydrolysis of the proteins retained in the gel pieces. After about 16 hours of trypsin incubation, liquid phase was collected to a new Lobind tube; peptides retained in gel pieces were extracted with the sequential addition of 100 µL of three ACN solutions [30%, 50%, and 98% (v/v) of acetonitrile, all in 1% (v/v) formic acid (FA)] to each gel containing tube, Thermomixer incubation for 15 minutes, at 25ºC and 1050 rpm, and collection of each solution to the same new microcentrifuge tube. Peptide containing solutions were then subjected to the Concentrator Plus at 60ºC, until all solvent has evaporated. Dried peptides were ressuspended with 22 µL of mobile phase A solution [2% (v/v) ACN, 0.1% (v/v) FA], sonicated on a VCX750W Vibra-Cell sonicator (Sonics) with a cup-horn, set to 1 minute, 1 second on-off cycles and 20% amplitude). After a brief vortex and spin, peptide solution was collected to a new microcentrifuge tube.

3.2.1.2. Liquid digestion

Without passing through gel electrophoresis protein separation, approximately 50 µg of protein samples were put onto an LoBind microcentrifuge tube and added a 0.5M solution of triethylammonium bicarbonate buffer (TEAB) for a final volume of 45 µL, then added 4 µL of a 50 mM solution of tris(2-carboxyethyl)phosphine (TCEP). After a brief vortex and spin following each addition, samples were sonicated on a 750 W
Vibra-Cell with a cup-horn (1 minute, 1 second on on-off cycles, 20% amplitude), then was added 2 µL of a 200 mM solution of methyl methanethiosulfonate (MMTS) and samples were incubated for 10minutes at room temperature. Afterwards was added 0.5 M TEAB in order to have a final volume of 100 µL after addition of digestion enzyme. For protein digestion, was added 1 µg of trypsin, or 1 µg of trypsin and 1 µg of chymotrypsin. Samples were mixed for 1 minute and 600 rpm at the Thermomixer, the left incubating for 16 hours at 37°C without agitation. For digestion termination 2 µL of 100% FA were added, and samples were evaporated on the Concentrator Plus.

3.2.2. Peptide preparation for MS

After digestion of proteins, described in section 3.2.1, resulting peptides were desalted using C18 Bond Elut OMIX pipette tips (Agilent Technology): tips were hydrated with 200 µL of 50% ACN and equilibrated with 300 µL of mobile phase A solution; peptide solution was loaded onto the columns and eluted, with this step being repeated four more times; column was washed with more 100 µL of mobile phase A solution; finally, desalted peptides were eluted to a new LoBind tube using four times 100 µL of a solution with 70% ACN and 0.1% formic acid. The eluate was then concentrated on the Concentrator Plus at 60°C, for solvent evaporation, and dried peptides were ressuspended in 20 µL of mobile phase A solution, sonicated on a 750 W Vibra-Cell with a cup-horn (2 minutes, 1 second on-off cycles, 20% amplitude) and centrifuged in a MiniSpin (Eppendorf) for 5 minutes at 14,100×g. Supernatant was

transferred to an LC vial, for subsequent LC-MS/MS analysis or storage at 4ºC until its analysis in the mass spectrometer.

3.2.3. LC-MS/MS analysis

After sample preparation, described at section 3.2, peptides were separated by liquid chromatography, using a NanoLC Ultra 2D system (Eksigent) on a ChromXP C18 reverse phase column (300 µm ID, 15 cm length, 3 µm particles, 120 Å pore size) (Eksigent), at 5 µL/min. These were then eluted into the mass spectrometer with 0.1% FA and an ACN gradient (5 to 35% in liquid digestion samples, 2 to 35% for in-gel digested samples), for 24 minutes, using an ESI DuoSpray source (ABSciex), for sample loading to the mass spectrometer (Triple TOF 5600 System).

Regarding the analysis of stock WT, M26I and E163K for contaminant identification, samples were only subjected to IDA acquisition; in all others, they were run in IDA and SWATH acquisition mode.

3.2.3.1. IDA acquisition for protein identification

The mass spectrometer, operated with Analyst TF software (v 1.6, AB Sciex) was programmed for an IDA scanning of the full spectra (350 to 1250 m/z, for 250 ms), followed with 20 MS/MS scans (100-1500 m/z, 100 ms each). After selection of candidate ions with multiple charged ions (between +2 and +5), from MS1, they were isolated for MS2 fragmentation. One additional MS/MS spectra was performed before adding those ions to the exclusion list, for 15 seconds.

Protein identification was performed using Protein Pilot software (v 5.0, AB Sciex), with Mascot search using different parameters for each performed assay. Data processing and exclusion was based on an independent False Discovery Rate (FDR) analysis, using 5% critical FDR as the target-decoy for the threshold definition of unused score and individual confidence threshold. In the MS analysis of stock WT, M26I and E163K, it was excluded proteins with less than three peptide hits.

3.2.3.2. SWATH acquisition for protein quantification

For SWATH acquisition of samples, mass spectrometer was operated in a looped product ion mode and tuned to allow a quadrupole mass selection of 25 m/z. Each cycle consisted on the sequential SWATH MS/MS acquisition of overlapping windows through a crescent range of 350 to 1100 m/z of the precursor ion spectra. Windows were selected with an isolation width of 26 m/z, for a 1 m/z window overlap, and was acquired a SWATH MS/MS spectra of 100-1500 m/z for 100 ms from each. In the beginning of each cycle, one 50 ms survey scan covering the queried precursor ion range of 350-1100 m/z was acquired, adding up to a cycle time of 3.25 seconds.

The library of peptide precursor masses and fragment ions to be considered for SWATH data processing was previously constructed, using ProteinPilot data resulted from the combination of IDA MS files of the same or related samples, obtained as described in section 3.3.3.2. Library peptides were selected for SWATH analysis using Peak View software (v. 2.1, AB Sciex) and the following initial criteria: ranking of unique peptides by the intensity of the precursor ions described in the library; exclusion of biological modifications and isoforms. SWATH quantitation of proteins was performed using up to 15 peptides from each protein and the proteins with under 5% local FDR in the used library. After it was performed matching of the IDA and SWATH spectra, for retrieving of quantitative information, fragment ions were scored based on retention time, peak width overlap, peak intensity ratio, correct isotopic state, m/z error and MS/MS score. Peak group score, attributed to each peptide, was constructed from the integration and combination of fragment ion scores, with selection of the best scoring peak group. Peak group confidence was based on a FDR target-decoy approach analysis, with selection of 1% FDR for all quantitations. Peptides meeting the threshold in all runs were kept, respective target fragment ions were extracted using an extracted-ion chromatogram (XIC) window of 5 min. After retention time adjustment and processing of SWATH data, protein levels were obtained with the sum of the score of the respective peptides. Protein levels were normalized to total score within each sample, or normalization to internal standard consisting of a mixture of green

fluorescent protein (GFP) and maltose-binding periplasmic protein (MALE), added in equal quantities to each sample before electrophoresis protein separation.

3.3. DJ-1 mutants production

3.3.1. Mutant constructs recombination and culture

The plasmid constructs (DJ-1_M26I_pSKB-3; DJ-1_E163K_pSKB-3) were kindly provided by Lúcia Sabala and Liliana Loureiro, produced during their master thesis of previous years and stored at -20ºC. It was transferred 1 µL of pDNA of each DJ-1 mutation onto a 100 µL aliquot of competent *E. coli* BL21star (DE3) strain and left on ice for 30 minutes, then placed in water bath at 42ºC, for 1 minute, and finally put back on ice. Transformed *E. coli* was then inoculated onto a Luria Bertani (L-B) agar plate supplemented with 50 µg/mL kanamycin, left incubating overnight at 37ºC. In the end, the plate was put at 4ºC, to inhibit culture growth, and after approximately 6 hours was picked one or two kanamycin-resistant colonies from agar plate, which were used to inoculate 70 mL of liquid L-B medium supplemented with 50 µg/mL kanamycin, left incubating overnight at 37ºC and 170 rpm agitation. For the liquid culture scale-up, 50 mL of liquid culture was transferred to 2 L of liquid L-B supplemented with 50 µg/mL kanamycin (2×25 mL onto 2×1 L cultures), left in incubator at 37ºC and 155 rpm agitation for culture growth. After 1 hour, the optical density at 600 nm for one of the two cultures was monitored, and culture temperature was lowered to 18ºC when optical density was above 0.5. One hour after temperature decrease, liquid medium was supplemented with isopropyl-β-D-thiogalactopyranoside (IPTG) for a final concentration of 1 mM, for induction of mutant DJ-1 expression that was left overnight for approximately 16 hours, at 18ºC and 155 rpm.

3.3.2. Mutant DJ-1 purification

After IPTG-induction based production of the DJ-1 mutants, M26I and E163K, cultures were centrifuged for 30 minutes, at 4ºC and 4000×g, supernatant was discarded and cellular pellet was ressuspended in 60 mL of buffer A (composed with 20 mM sodium phosphate, 500 mM NaCl and 20 mM imidazole, pH 7.4), to be later lysed through 3 passages at a high pressure homogeneizer EmulsiFlex-C3 (AVESTIN), at about 1000 bar. Cell lysate was later subjected to centrifugation, under 30 minutes, 4ºC and 4,000×g; the supernatant (clarified protein extract) was collected for its subjection to two consecutive chromatographies for the purification of M26I or E163K DJ-1 proteins.

3.3.2.1. HisTrap affinity chromatography

Clarified protein extract was loaded onto a 5 mL HisTrap HP column (GE Healthcare), using a peristaltic pump, EP-1 Econo Pump (Bio-Rad) previously washed with 25 mL of deionized water followed by the same volume of buffer A. The column is used for an immobilized metal ion affinity chromatography and contains Ni sepharose, which preferentially retains histidine-tagged proteins, such as the produced recombined Dj-1 mutations. After column loading, HisTrap column was assembled onto a low-pressure chromatography system, BioLogic LP (Bio-Rad), after it was purged with buffer B (20 mM sodium phosphate, 500 mM NaCl and 500 mM imidazole, pH 7.4) then buffer A. HisTrap column was thoroughly washed with buffer A, and as soon as optical density at 280 nm was stable was initiated a step gradient chromatography, with flow of 5 mL/min, increasing concentration of imidazole (50, 100, 300 and finally 500mM) through automated mixtures of buffer A and buffer B, and collection of fractions of variable volume during the optical density peaks at the beginning of each imidazole concentration step. Fractions that predictively contained DJ-1 mutants, collected at the beginning of the 300 mM step (and where was registered the highest chromatographic peak), were combined and selected for a second chromatography.

3.3.2.2. Superdex 200 size-exclusion chromatography

For the purification of the dimeric form of the DJ-1 mutants was used a HiLoad 26/600 Superdex 200 prep grade column (GE Healthcare), assembled to a low-pressure chromatography system. This column allows the performance of a size-exclusion chromatography, due to its cross-linked agarose and dextran matrix. After column and loop washing with phosphate-buffered saline (PBS) (8 mM K_2HPO_4, 2 mM $NaH_2PO_4 \cdot H_2O$, 150 mM NaCl), DJ-1 mutant-containing sample was injected onto loop, and after column equilibration sample was injected onto the column and eluted with PBS, a flow rate of 3 mL/min and collection of fractions of about 10 mL. The fractions containing the highest chromatographic peak were selected, predicted to occur after the elution of DJ-1 mutant aggregate and before the elution of its monomeric form.

3.3.3. Mutants DJ-1 concentration and storage

Fractions containing the dimeric form of the DJ-1 mutants were concentrated using a 10 kDa molecular weight cut-off (MWCO) centrifugal concentrator (Millipore) and several cycles of 3220×g centrifugations; during the concentration process, protein concentration was analyzed through absorbance measurement at 280n m, using a Nanodrop ND-1000 Spectrophotometer (Thermo FisherScientific) and considering the extinction coefficient predicted for DJ-1, $\varepsilon = 3.4\ (\mu g/\mu L)^{-1}\ cm^{-1}$. Protein concentration was terminated when was reached about 2 µg/µL, and M26I and E163K DJ-1 mutations were stored in PBS or in PBS with 5% glycerol, at -80ºC, until further use.

3.4. DJ-1 mutants characterization

3.4.1. 2-D Quant Kit

It was used the 2-D Quant Kit (GE Healthcare) for an accurate quantification of concentration of the quantified stock solutions of the DJ-1 mutants. Several standard

solutions were prepared between 0 and 60 µg of bovine serum albumin (BSA) in microcentrifuge tubes, from a 2 g/mL stock solution provided in the kit (as are all further mentioned solutions), and approximately 30 µg of wild-type (WT), M26I and E163K stock solutions in PBS and in PBS with 5% glycerol (calculated from Nanodrop measurement for DJ-1 mutants, and concentration provided by Matilde Melo for WT DJ-1) were used. To each standard and sample 500 µL of precipitant were added, followed with brief vortex and spin, then 500 µL of Co-precipitant were added to each, later subjected to brief vortex and centrifugation at the MiniSpin, at 14,100×g, for 5 minutes. After discarding the supernatant, 100µL of Copper Solution and 400µL of deionized water were added, and each microcentrifuge tube was subjected to a 30 second vortex and a brief spin. Lastly, 1 mL of Working Color Reagent was added to each standard and sample (previously prepared through a mixture of 1 part Color Reagent B and 100 parts of Color Reagent A), and incubated for 15 minutes at room temperature. After pipetting 200 µL of each standard and sample to a multi-well 96 plate, 480nm absorbance of each well was read using a Microplate Spectrophotometer (PowerWave XS, BioTek). Optical density is inversely related to protein mass, which was used to construct the calibration curve from the standard solutions, then interpolated protein concentrations of the DJ-1 stock solutions.

3.4.2. SEC-HPLC

Size-exclusion high performance liquid chromatography (SEC-HPLC) was performed for the quantification of the molecular weight (MW) of the quaternary structure of stock DJ-1 mutants produced, to confirm its dimeric form, comparing its elution volume with the one of standard solutions with known MW. Proteins for the production of standard solutions were included on the Gel Filtration Calibration Kit - Low Molecular Weight (GE Healthcare): Blue Dextran 200 (MW = 2000 kDa, for quantification of dead volume); aprotinin (MW = 6.5 kDa); ribonuclease A (MW = 13.7 kDa); carbonic anhydrase (MW = 29.0 kDa); ovalbumin (MW = 43.0 kDa); conalbumin (MW = 75.0 kDa). It was prepared 3 mg/mL solutions in PBS for all standard proteins,

except 4 mg/mL in PBS for ovalbumin, 3 mg/mL in deionized water for carbonic anhydrase and 1 mg/mL in deionized water for blue dextran. DJ-1 mutant and wild-type samples were diluted to 1 mg/mL in PBS. Standard and sample solutions were filtrated three times using C18 resin Ziptips (Merck Millipore), and collected onto HPLC vials. For the HPLC run a Superdex 200 5/150 GL column (GE Healthcare) was used assembled onto the HPLC system Prominence Shimadzu (Shimadzu Scientific Instruments). After system equilibration with PBS, it was injected to the column 13 µL of standard and 40 µL of sample solutions and proteins were sequentially eluted using PBS buffer, at a flow rate of 0.3 mL/min. Chromatograms of 220 nm absorbance were later analysed and collected using LC Solution Software (Shimadzu Scientific Instruments), with which was registered peak retention times for the construction of the calibration curve and interpolation of quaternary MW of DJ-1 WT, M26I and E163K.

3.4.3. MS identification of mutants and wild-type DJ-1, and stock contaminants

It was used 15 µg of each stock solution protein stored in PBS and 5% glycerol, of produced M26I and E163K DJ-1 and previously produced WT DJ-1, for SDS-PAGE protein separation and in-gel digestion of samples, as described in sections 3.1 and 3.2. Each gel lane was divided in four sections that were separately subjected for LC-MS/MS for better discrimination of protein contaminants: the upper and lower lane section (1 and 4, respectively) were processed together, having seldom visible contaminants after coomassie staining; sector 2 included some visible contaminants of molecular weight between 20 and 75; section 3 included the most visible band, attributed to DJ-1. After digestion, samples were prepared and run in MS analysis using IDA acquisition for all samples. ProteinPilot parameters were set as: instrument TripleTOF 5600; acrylamide as cysteine alkylating reagent; digestion with trypsin; gel-based ID; thorough ID search effort; detection threshold of 0.05 Unused ProtScore (10% confidence score); separated processing with SwissProt database with all proteins, dated from September 2014 (designated protein database), or the same SwissProt database with all proteins and

added FASTA entries of hexahistidine tagged wild-type and natural or synthetic mutant forms of DJ-1 (designated mutant database). Protein identification was based on an independent False Rate Discovery analysis (FDR) analysis, using the target-decoy approach, with selection of proteins with Unused ProtScore and peptides with ProteinPilot Confidence above the local 5% FDR threshold, and exclusion of proteins with less than three peptides with confidence above 95%.

3.5. Biotinylation assays

3.5.1. Wild-type DJ-1 biotinylation

Fifteen micrograms of recombinant wild-type DJ-1, stored in PBS with 5% glycerol, were diluted in 50 µL of PBS, added 600 µL of PBS buffer with 3.5 mM of EZ-Link Sulfo-NHS-LC-biotin (Life Technologies), and left incubating for 2 hours at 4ºC, in a rotating mixer. Afterwards 600 µL of 1.728 M Tris-HCl buffer were added to quench the remaining biotin, and left incubating for 30 minutes in the same conditions. Solution with biotinylated WT DJ-1 and quenched biotin was concentrated and exchanged solvent to PBS using 5000 MWCO Vivaspin 500 Centrifugal Concentrators (Sartorius), for a final volume of 50 µL.

Twelve and a half microliters of biotinylated DJ-1 solution (biot-DJ1) were stored in -20ºC until further use, for dot blot analysis. The remaining 37.5µL were used for liquid digestion, described in section 3.2.1.1, and MS analysis, using IDA acquisition described in section 3.3.3.1, for modification of ProteinPilot data dictionary and parameter translation files, for the recognition of the modification resulted with protein reaction with Sulfo-NHS-LC-biotin (mass gain of 339.161 Da in lysine and protein N-terminal residues), and subsequent identification of biotinylated proteins directly in ProteinPilot processing of IDA MS data.

3.5.1.1. Dot blot assay

After activation of a Trans-Blot Turbo midi-size LF polyvinylidene fluoride (PVDF) membrane (Bio-Rad), through brief immersion in methanol and wash with deionized water, it was directly added onto membrane the samples correspondent to each condition: 5 µg of biotinylated wild-type DJ-1; 5 µg of non-biotinylated wild-type DJ-1; a negative control without addition of any sample; 1 µL of Bio-Plex streptavidin B-phycoerythrin conjugate (SAPE) (Bio-Rad), diluted from 100 to 10× concentration in Bio-Plex Assay Buffer (Bio-Rad), as positive control. PVDF membrane was then incubated with 5 mL of blocking solution [PBS buffer with 0.1% of Tween-20 (Bio-Rad) (PBS-T) and supplemented with 5% (w/v) of skim milk], in a 15 mL Falcon tube (VWR) covered in tin foil, for 16 hours, at 4ºC and with orbital shaking. Membrane was then washed three times with 5 mL of PBS-T, 5 minutes each with orbital shaker, at room temperature and in the dark. Afterwards membrane was stained with 5 mL of SAPE, freshly prepared and diluted with Assay Buffer to 1× concentration, and incubated 15 minutes at orbital shaker, in room temperature and in the dark. Membrane was finally washed three times with 5mL of Bio-Plex Wash Buffer (Bio-Rad), 5 minutes each and also at orbital shaker, dark and room temperature. Membrane was dried in the dark for 30 minutes and fluorescence was read with the fluorescence scanner Molecular Imager FX (Bio-Rad) and Quantity One software (Bio-Rad), set for usage of a 532 nm excitation laser, 555LP excitation filter and high PMT voltage.

3.5.2. Western blot

SH-SY5Y cells were seeded in 55 cm^2 plates (Corning) at a cell density of 9.375×10^4 cells per cm^2, using a 8 mL cell suspension in culture medium (1:1 mixture of MEM and F-12 with 10% FBS). After 24 hours the culture medium was exchanged to 8 mL stimulation medium (1:1 mixture of MEM and F-12 with 10% FBS). After 48 hours of cell plating, stimulation medium was removed from plates and cells were washed two times with 8mL of PBS buffer. Then 6 mL of 60 µM EZ-Link Sulfo-NHS-LC-biotin were

added, prepared in water or in PBS buffer, and left incubating for 30 minutes at 4ºC. Afterwards 6 mL of Tris-buffered saline (TBS) (50 mM Tris, 150 mM NaCl, pH 7.6) for condition of biotin in PBS, or of 50mM Tris-HCl for biotin in water, were added to the plates and incubated for 10 minutes at 4ºC. The plates' supernatant, containing EZ-Link Sulfo-NHS-LC-biotin and Tris-HCl, was collected and stored at -20ºC, designated as Tris+biotin. Each plate was then scraped two times with 0.5 mL of RIPA buffer (50mM Tris-HCl (pH 7.4), 150mM NaCl, 1% (v/v) Igepal, 0.25% (v/v) Na-deoxycholate, 1mM EDTA) supplemented with 1mM dithiothreitol (DTT) and 10% (v/v) protease inhibitor (Roche), and each protein lysate was collected to a microcentrifuge tube, sonicated on a 750W Vibra-Cell sonicator with a cup-horn (1 minute, 1 second on-off cycles, 40% amplitude), centrifuged for 10 minutes at 20,000×g and 4ºC; supernatant was collected (designated as protein extract) and stored at -20ºC until further use.

Afterwards the avidin pull-down assay was performed, for enrichment of biotinylated proteins. Tris+biotin and protein extract collected from SH-SY5Y biotinylation, with a PBS or aqueous solution. After biotin removal and concentration using centrifugal concentrators Vivaspin 6, for protein extract, and Vivaspin 15 with 10 kDa cut-off (Sartorius), for Tris+biotin solution, concentrated solution of about 1 mL of each was added to a 250 µL slurry containing 50 µL Monomeric Avidin Agarose (Pierce Monomeric Avidin Agarose, Thermo), and incubated overnight, at 4ºC, for about 18h, in a rotating mixer. After Minispin centrifugation at 5 000×g, for 2 minutes, it was collected about 1 mL of supernatant (designated FT1). Remaining resin was washed 5 more times (FT2 to FT6) with PBS, for non-biotinylated protein removal, after at least 5 minute incubation at 4ºC and with same centrifugation procedure. Biotinylated fraction was afterwards collected with 1 hour incubations with two elution buffers, 2 mM D-biotin in PBS (Biotin Buffer, Pierce Monomeric Avidin Agarose kit, Thermo), and 0.1M glycine, pH 2.8 (Regeneration Buffer, Pierce Monomeric Avidin Agarose kit, Thermo), at 4ºC with rotation. It was obtained Bt and Reg fractions, respectively, corresponding to the supernatant collection after centrifugation. Then was added to resin 40 µM of SB 6×, and incubated for 5 minutes at 95º, then stored at -20ºC (SB fraction).

Washing and elution fractions selected for western blotting and silver staining: FT1, FT2, FT4 (also FT6 of protein extract from PBS biotinylation), BT and Reg from all samples subjected to avidin-pull down. Proteins were precipitated with TCA and acetone: addition of 250 µL acid trichloroacetic (TCA) and freezing at -80ºC; after slow thawing, 20 minute centrifugation at 4ºC and 20,000×g and supernatant discard; addition of 100 µL acetone, and store solutions at -20ºC; centrifugation and supernatant removal, with addition of 20 µL PBS; sonication using a 750 W Vibra-Cell (40% amplitude, 2 minutes, 1 second on 1 second off). Samples were then denatured with addition of 4 µL of SB 6× and incubation at 95ºC for 5 minutes.

It was used 12 µL of each FT, BT, Reg and SB fraction for protein separation, using SDS-PAGE, described in section 3.1. Gel proteins were transferred to an activated PVDF membrane, using a Trans-Blot Turbo Transfer System (Bio-Rad) for 45 minutes. PVDF membrane was subjected to SAPE staining of proteins, for detection of biotinylated proteins, using a protocol identic to dot blot, described at section 3.5.1.1.

Another 12 µL of the same fractions were also separated using SDS-PAGE, then subjected to protein silver staining, described in 3.1.2.

3.5.3. Biotin reactivity assay

Different solutions of Sulfo-NHS-LC-biotin were subjected to absorbance measurement at 260 nm, using a Nanodrop ND-1000 Spectrophotometer (Thermo FisherScientific), diluted in order that optical density would be below 1.0 and divided in several 50 µL aliquots, each to be analyzed in different time periods. After absorbance measurement of each aliquot, 5 µL of a 1 M NaOH solution were added, vortexed for 30 seconds and repeated absorbance measurement in less than 1 minute after NaOH addition: an increase of 260nm absorbance demonstrates NHS reactivity. This assay was performed for several EZ-Link Sulfo-NHS-LC-biotin solutions prepared in PBS, freshly prepared or after 20 or 60 days freezing at -80ºC.

3.6. Culture-based assays

3.6.1. SH-SY5Y and HeLa culture

Human cell lines SH-SY5Y (derived from neuroblastoma) and HeLa (derived from cervical cancer) were cultured in a 1:1 mixture of Minimum Essential Media (Gibco) and F-12 Nutrient Mixture (Gibco), supplemented with 10% fetal bovine serum (FBS) (Gibco), 1.25 µg/mL of amphotericin B solution (Invitrogen) and 1% penicillin-streptomycin solution (Cambrex). Cells were kept in a humidified incubator, Shel Lab 3517-2 (Sheldon Manufacturing, Inc.), at 37ºC and in a 95% air / 5% CO_2 atmosphere.

For cell passage, cells were washed with Dulbecco's phosphate buffer saline (D-PBS) (Cambrex) and was then used a 0.05% solution of trypsin-EDTA in PBS (Invitrogen) for cell detachment.

For every cell-based assay, SH-SY5Y cells were seeded at 9.375×10^4 cells per cm^2, and HeLa cells were seeded at 3.5×10^4 cells per cm^2, both with the same incubation conditions as during cell culture.

3.6.2. Viability assays

Fourty eight hours after SH-SY5Y cell plating to 96-well plates (Corning), with each well containing 100 µL of culture medium and cell density described in section 2.6.1, and 24 hours after cell stimuli, it was assessed the number of viable cells using the CellTiter-Glo Luminescent Cell Viability Assay (Promega). After addition of 100 µL of previously prepared CellTiter Reagent to each well, culture plate was covered in tin foil and incubated for 12 minutes, being the first 2 minutes with 300 rpm shaking. Then 150 µL of each well was transferred to a white opaque 96-well plate, and luminescent signal was quantified using a LUMIstar Galaxy automated microplate luminescence reader (BMG Labtech), with selected signal gain of 130. It was used 150 µL of a mixture of 200 µL of culture medium and 100µL of CellTiter-Glo Reagent for quantification of background signal, subtracted to all results.

3.6.2.2. Stimuli for oxidative stress and WT DJ-1 mediated neuroprotection

Twenty four hours after cell plating, culture medium was removed and added culture medium with the same composition (1:1 mixture of MEM and F-12 with 10% FBS), supplemented with 0, 40 or 50 μM of hydrogen peroxide (Sigma-Aldrich) and with 1 μM of His-tagged human DJ-1 in PBS or PBS with 5% glycerol, the corresponding volume of protein vehicle (2.24 μL of PBS or 4.18 μL of PBS with 5% glycerol), 1 μM of his peptide, or absence of protein or vehicle. Wells exchanged to culture medium with no hydrogen peroxide, vehicle or protein addition were used as control condition, for normalization of luminescence values in downstream CellTiter-Glo assay (performed 24 hours later).

3.6.2.2. Stimuli for WT or mutants DJ-1 neuroprotection

Twenty four hours after cell plating, culture medium was removed and added culture medium with the same composition (1:1 mixture of MEM and F-12 with 10% FBS), supplemented with 0, 40 or 50 μM of hydrogen peroxide and with addition of 1 μM of His peptide or 1 μM of His-tagged human wild-type or mutant (M26I or E163K) DJ-1, protein vehicle (5.11 μL of PBS with 5% glycerol) or neither. His peptide and DJ-1 proteins were all stored in PBS + 5% glycerol and previously diluted to 1.8 μg/μL, to be added a volume equal to the protein vehicle condition. Wells exchanged to culture medium with no hydrogen peroxide, vehicle or protein addition were used as control condition, for normalization of luminescence values in downstream CellTiter-Glo assay, performed 48h after cell plating and 24h after cell stimuli.

3.6.3. Medium incubation assay

Twenty four hours after SH-SY5Y cell plating in 96-well plates (MW-96, Corning), with 100 μL of culture medium (1:1 mixture of MEM and F-12 with 10% FBS), medium of

each well was removed and added 200 µL of culture medium (control condition) PBS or deionized water, left incubating for 15 or 30 minutes at room temperature. Afterwards CellTiter-Glo Luminescent Cell Viability Assay was performed, described in section 3.6.2, and with results normalized to luminescence values of control conditions.

A second viability assay was performed, also 48h after SH-SY5Y plating in MW-96 and 24h after culture medium exchange, and after 10min incubation at room temperature, using quenching solutions: Tris-Hcl buffer, 50mM of Tris dissolved in PBS and ph 7.6, or TBS.

A third viability assay was performed, in equal incubation conditions, for a simulation of the biotinylation assay and viability measurement in all collected solutions of the process: culture medium discarded before biotinylation; PBS after 15 min incubation; TBS after 5 min incubation; remaining cells present in well.

3.6.4. Biotin-based histochemistry assays

3.6.4.1. Fluorescence microscopy

HeLa cells were seeded on a 96-well plate, with incubation of 100 µL of cell suspension for each well. Twenty four hours after cell plating, it was removed culture medium and cells were washed two times with 100 µL PBS. For cell biotinylation, it was prepared a 100 µM solution of EZ-Link Sulfo-NHS-LC-biotin in PBS, added 100 µL to each well and left incubating for 30 minutes at room temperature; afterwards was removed biotin solution and cells were washed two times with 100 µL of Tris-HCl buffer. Control condition consisted on a 30 minutes incubation with 100 µL of PBS. Afterwards, cells of both conditions were washed two times with 100 µL of PBS, followed by cell fixation through addition of 100 µL of 4% (w/v) paraformaldehyde (PFA) in PBS and 30 minutes incubation at room temperature. After removal of fixation solution, cells were washed two times with 100 µL of PBS (5 minutes incubation for each wash). It was then added to each well 100 µL of SAPE 1×, diluted in Assay Buffer, and multi-well plate was left incubating covered in tin foil, for 15 minutes and 80 rpm shaking. Lastly, wells were

washed three times with 100 µL of Wash Buffer, 5 minutes for each wash, and cells were left immersed in 100 µL of Assay Buffer for observation at the Axio Observer D1 fluorescence microscope (Zeiss). Two photographs were taken for each replicate of conditions, with 40× magnification, one using bright-field observation and other with rhodamine filter (550/25 bandpass emission filter, 570nm dichroic filter, 605/70 bandpass excitation filter), with settings similar required for excitation and fluorescence emission of SAPE.

3.6.4.2. Confocal microscopy

Before HeLa cell plating, glass coverslips were coated with its assembly on a MW-24 plate (Corning) and incubated overnight with 100 µg/mL of poly-D-histidine (Sigma-Aldrich) in PBS. Afterwards, solution was removed, wells were washed with PBS and plated with HeLa cells, where after 24 hours was performed biotinylation, fixation and SAPE staining identical to the one performed for microscopy fluorescence, with some adaptations: used 250 µL for culture medium incubation and all solutions used in the procedure; 15 minutes incubation with biotin solution; cell washes, for biotin quenching, using TBS buffer. In the end of the process, coverslips were assembled with mounting media and sealed in glass slide, which were stored in 4ºC until further use. Afterwards, cells were observed in LSM 780 confocal microscope (Zeiss), operated with ZEN 2012 software (Zeiss), and photos were taken using Z-stack mode and selected gain of 180, pinhole opening of 90.0 and selection of Smart Setup based on BPE mode (using 488 nm emission laser, and fluorescence reading at approximately 600 nm).

3.7. MS analysis of cell surface biotinylation

3.7.1. MS analysis of trypsin vs. trypsin and chymotrypsin digestion

Samples with 50 µg of proteins, from a membrane-enriched subcellular protein fraction extracted from a mouse cortex, provided by Cátia Santa, were subjected to liquid digestion (described in section 3.2) using 1 µg of trypsin (designated T) or 2 µg of an equimolar mixture of trypsin and chymotrypsin (TC), for downstream MS analysis. Before liquid digestion, it was added 1 µL of internal standard solution, with GFP and MALE.

The MS analysis was performed on IDA and SWATH acquisition modes for four biological replicates of each digestion used. For IDA processing, it was used the following ProteinPilot parameters: instrument TripleTOF 5600; MMTS as cysteine alkylating reagent; digestion with trypsin, or trypsin + chymotrypsin, according to sample; not selected gel-based ID; selected thorough ID search effort; detection threshold of 0.05 Unused ProtScore (10% confidence score); use of modified SwissProt database with all proteins (downloaded at February 2015, attributed species in FASTA entries of GFP and MALE was modified to *Rattus norvegicus*), with search against *R. norvegicus*. Protein identification was based on an independent False Rate Discovery analysis (FDR) analysis, using the target-decoy approach, with selection of proteins with Unused ProtScore and peptides with ProteinPilot Confidence above the local 5% FDR threshold, and inclusion of proteins with at least one peptide with confidence above 95%. SWATH libraries consisted on the correspondent processed IDA acquisition files for each replicate, and SWATH quantitation was performed as previously described.

3.7.2. Experimental avidin pull-down

SH-SY5Y cells were seeded in 141cm^2 plates (Corning), with cell density of 9.375×10^4 cells per cm^2, 16 mL of culture medium (1:1 mixture of MEM and F-12 with 10% FBS) and incubation in conditions described in section 3.6.1. 24 hours later culture

medium was exchanged to stimulation medium; 48h hours after plating, cell biotinylation was performed in conditions similar to the “biotin in water” condition used for western blot, described in section 3.5.2, up to SDS-PAGE protein separation. The protocol used in these experiments had some adaptions: due to larger plate area, it was used 12 mL of biotin and Tris-HCl, and 2×1 mL RIPA buffer, and equal biotinylation conditions; performance of avidin pull-down of protein extract, Tris+biotin solution, and a third avidin pull-down of approximately 100 µg of SH-SY5Y protein extract, not subjected to biotinylation, previously prepared and provided by Sandra Anjo; after the first pull-down of protein extract with biotinylated SH-SY5Y and Tris+biotin solution, it was performed a second pull-down using FT1 fraction of each; used all 24 µL of samples prepared after TCA-acetone precipitation (Bt, Reg and FT fractions), or collected from resin after denaturation (SB fractions), for SDS-PAGE separation of proteins.

After protein separation using SDS-PAGE, it was performed in-gel digestion and MS analysis as described in sections 3.1. and 3.2, for the study of selected fractions collected from pull-down. For IDA acquisition, was selected: Bt, Reg and SB fraction from 1st pull-down of protein extract with biotinylated proteins, and FT1 and Bt fractions from 2nd pull-down; Bt fraction from 1st and 2nd pull-down of Tris+biotin. ProteinPilot processing was set with the following parameters: instrument TripleTOF 5600; acrylamide as cysteine alkylating reagent; digestion with trypsin; gel-based ID; thorough ID search effort; detection threshold of 0.05 Unused ProtScore (10% confidence score); SwissProt database with *Homo sapiens* proteins (dated from May 2015) and added GFP and MALE, with no species-specific search. Protein identification was based on an independent False Rate Discovery analysis (FDR) analysis, using the target-decoy approach, with selection of proteins with Unused ProtScore and peptides with ProteinPilot Confidence above the local 5% FDR threshold, and inclusion of proteins with at least one peptide with confidence above 95%.

For SWATH acquisition, it was selected the same samples used in IDA acquisition, with addition of Bt, Reg and SB fractions of non-biotinylated protein extract. SWATH libraries consisted on the processing of all IDA acquisition files, with parameters and processing as previously described.

3.7.3. SH-SY5Y proteome variation analysis of oxidative stress induction and membrane fraction enrichment

3.7.3.1. Cell plating and stimuli

SH-SY5Y cells were seeded in 141cm^2 plates (Corning), with cell density of 9.375×10^4 cells per cm^2, 16 mL of culture medium (1:1 mixture of MEM and F-12 with 10% FBS) and incubation in conditions described in section 3.6.1. 24 hours later, it was induced oxidative stress with exchange of culture medium to stimulation medium (1:1 mixture of MEM and F-12 with 0.1% FBS) supplemented with 50 μM of hydrogen peroxide. Control conditions consisted on the exchange of culture medium to stimulation medium with no hydrogen peroxide.

3.7.3.2. Cell surface biotinylation and collection of protein extract with total proteins or membrane proteins

Forty eight hours after cell plating, and 24 hours after culture stimuli, 16 mL of culture medium was discarded and cells were washed two times with 16 mL of PBS. Afterwards was added to each plate 10 mL of 100 μM EZ-Link Sulfo-NHS-LC-biotin in PBS, followed with 15 minutes incubation at room temperature. In the end of biotin reaction, biotin solution was collected and plates were washed two times with 10 mL of TBS, for quenching of remaining biotin, and collected after use.

Later, cells in plates intended for direct avidin pull-down (without enrichment of membrane protein fraction) were scraped with 2×1 mL of RIPA buffer supplemented with 1 mM of DTT and 10% (v/v) protease inhibitor, and cell lysate was collected to microcentrifuge tubes. Also, collected biotin and TBS was centrifuged, at 130×g for 2 minutes, supernatant was discarded and cell pellet was transferred to cell lysate. This was subjected to sonication on a 750 W Vibra-Cell with a cup-horn (1 minute, 1 second on-off cycles, 40% amplitude), followed with debris removal with a 10 min centrifugation, at 10,000×g and 4ºC and collection of supernatant (designated as protein extract), stored at -20ºC until further use. Later, collected samples of protein

extract were assembled in 10,000 MWCO Vivaspin 6 tubes and subjected to several cycles of 3,000×g centrifugations at 4ºC, for biotin removal, buffer exchange to PBS and sample concentration to 500 µL.

Regarding cell conditions intended for enrichment of membrane proteins, biotinylation reaction and preparation of protein extract was performed in similar conditions, but was used two times 1 mL of 50 mM Tris-HCl for cell lysis and scraping from plates. After sonication and centrifugation for debris removal, collected protein extract was subjected to ultracentrifugation, at 126,000×g for 1 hour and at 4ºC. Supernatant, containing cytosolic proteins, was discarded and membrane pellet was ressuspended in 500 µL of PBS.

3.7.3.3. Avidin pull-down for enrichment of biotinylated proteins

Before pull-down assays, the total 2mL of Monomeric Avidin resin, originally provided in the Monomeric Avidin Kit inside a chromatography column, was firstly treated with elution of 8 mL of PBS, then 6 mL of Biotin Blocking & Elution Buffer (2mM biotin), 12 mL of Regeneration Buffer (0.1 M glycine) and 8 mL PBS, for blocking of non-reversible avidin binding sites and availability of avidin reversible sites; Monomeric Avidin resin was then removed diluted to a 10 mL slurry with liquid phase composed of PBS with 0.02% (v/v) sodium azide.

After biotinylation and collection of protein extract, this was added to a microcentrifuge tube with 100 µL of Monomeric Avidin resin, diluted in a 500 µL slurry; resin with protein extract was left incubating for 16 hours at 4ºC in a rotating mixer.

After protein extract incubation, non-bound protein was removed with collection of several flow-through fractions (FT1 to FT6): 2 min centrifugation of resin in 10,000×g and 4ºC, supernatant collection (FT fractions, stored in -20ºC), addition of 1 mL PBS and incubation at 4ºC for approximately 5 minutes, in rotating mixer, for collection of next washing faction. Protein concentration was monitored through 280 nm absorbance analysis, using the Nanodrop ND-1000 Spectrophotometer (Thermo FisherScientific), and resin washing was stopped with the collection of the sixth FT fraction, where

absorbance reached the baseline for all assayed fractions. Resins were stored at -20ºC until further use.

For elution of biotin-containing protein, captured in avidin resin of the remaining 150 µL slurry, it was added 1 µL of internal standard solution (GFP and MALE mixture). Later was added 30 µL of SB 6× and samples were denaturated in Thermomixer, at 95ºC, 850 rpm and 5 minutes. After Minispin centrifugation (2 minutes, 14,000×g) it was collected 80 µL of supernatant and subjected to SDS-PAGE protein separation, colloidal coomassie staining, in-gel digestion of peptides and MS analysis, described in sections 3.1 and 3.2. All samples were processed for IDA and SWATH acquisition.

4. Results

As previously mentioned, it is well-established the association of DJ-1 and Parkinson's disease: the protein has an essential role over oxidative stress protection, preventing a viability decrease of neurons, and also several DJ-1 mutations were shown correlated with onset of PD. Since the mechanisms by which the intake of extracellular DJ-1 contributes to neuron protection are largely unknown, as are the mechanisms that could be impaired due to mutations on DJ-1 protein, it is intended the study of the effects of extracellular addition of mutant DJ-1, more specifically M26I and E163K PD associated mutations, over the proteome of the cell surface of SH-SY5Y cell line, in oxidative stress conditions, an often used model for Parkinson's disease.

The concretization of such project requires the accomplishment of two main goals. First, a large production of M26I and E163K DJ-1 protein, for its future usage: the produced protein has then to be undertaken in several assays to confirm the structure and biological role of the produced mutant forms, in comparison with the already produced native form. Secondly, the design of a protocol able to enrich cell surface proteins in SH-SY5Y, for the *in vitro* simulation of oxidative stress and extracellular presence of the wild-type or mutant forms of DJ-1 and MS analysis of any proteome variation.

4.1. Mutant DJ-1 production

Since the availability of several forms of DJ-1 protein is required, the two DJ-1 mutants emphasized on this work were produced, M26I and E163K. The wild-type DJ-1 form used throughout the project was previously produced and kindly provided by Matilde Melo. Plasmid containing M26I and E163K DJ-1 protein expressing sequence

were previously prepared by Lúcia Sabala and Liliana Loureiro, for the production of the DJ-1 mutant forms. These plasmids have several features of interest:

- M26I and E163K point mutations were produced through site-directed mutagenesis of a WT DJ-1 construct (DJ-1_pSKB-3), consisting on its PCR amplification using primers containing the mutation of interest. The presence of the each mutation was later confirmed with Sanger DNA sequencing (unpublished data).

- the used DJ-1_pSKB-3 construct is based on a pSKB-3 plasmid, containing a cloned DJ-1 human gene (optimized for *E. coli* expression) between NdeI and XhoI restriction sites. The plasmid consists on a modified pET-28a plasmid, with thrombin alteration to a tobacco etch virus (TEV) recognition site. The DJ-1 gene is expressed downstream of a hexahistidine (His) expressing sequence and TEV recognition site, for the expression of recombinant DJ-1 with a TEV-cleavable His-tag. The plasmid has a kanamycin resistance gene and also lac repressor and operator genes upstream of construct site, for IPTG-mediated expression induction of the recombinant protein.

4.1.1. Recombinant mutant DJ-1 expression

DJ-1 mutant forms, M26I and E163K, were produced through the application of the respective constructs to an IPTG-inducted expression system: after recombination of plasmids into *E-coli* BL21, and scaled-up culture of the selected bacteria with recombinant plasmids, production of the recombinant mutant forms of DJ-1 was promoted in the mid-log phase of the cell culture.

After cell lysis and removal of debris, expressed recombinant DJ-1 mutants were purified from the protein extracts through affinity chromatography, then a size exclusion chromatography of selected fractions (Figure 4.1 and 4.3). First, after protein extract is passed through an HisTrap column, either M26I or E163K DJ-1 is retained due to its hexahistidine tag and is later eluted using increasing concentrations of imidazole. In both cases the highest chromatography peak, attributed to his-tagged DJ-1, occurred soon after the use of 300 mM imidazole as mobile phase. The elution fractions included on the peak were selected for downstream processing. From M26I mutant purification,

fractions 15 and 16 were selected; regarding E163K, the selected fractions were the 28th and 29th. Since it is of the utmost interest the use of the dimeric form of the protein DJ-1, and M26I and E163K are able of maintaining DJ-1 dimerization, the dimeric form of either DJ-1 mutants was purified by size exclusion chromatography, using a HiLoad 26/600 Superdex 200 prep grade column. In the production of each mutant the fractions with the highest peak were selected, expected to be the dimeric form of DJ-1. It is expected to correspond to the second chromatography peak, since it may occur the previous elution of higher-order oligomeric forms of DJ-1. In M26I the second peak was also the highest - corresponding to fractions 23 to 25 on M26I and fractions 19 to 21; on E163K DJ-1 purification, the first peak was very small, but collected a fraction with similar elution volume than M26I. Protein was then concentrated to about 2 mg/mL, and stored in PBS with 5% glycerol (designated as protein vehicle), at -80ºC, for future use.

Both mutant forms of DJ-1 were efficiently purified as evidenced by SDS-PAGE analysis with Coomassie staining, with analysis of samples collected through the main steps of the production and purification procedure (Figure 4.2 and 4.4). Regarding the production phase, it was observed an increase in the size of a band below 25 kDa, attributed to the DJ-1 monomer, from before to after induction of protein expression. Furthermore, HisTrap loading was seen as efficient, since the flow-through of HisTrap column didn't have the same protein band, but about the same protein quantity regarding other bands. Histrap chromatography analysis shows that the fractions selected for Superdex 200 purification were not the only with DJ-1 correspondent band, comparing them to fractions attributed to other peaks, which could be associated with protein excess or to resin quantity, low interaction or frail competition with imidazole. Nevertheless, in E163K DJ-1 production it is seen a crescent intensity of the DJ-1 band fractions selected for Superdex. On the other hand, Superdex 200 chromatography allowed to obtain a purified solution of either mutant forms, with few bands besides DJ-1 on the fractions selected for storage and on final stock solutions of M26I and E163K.

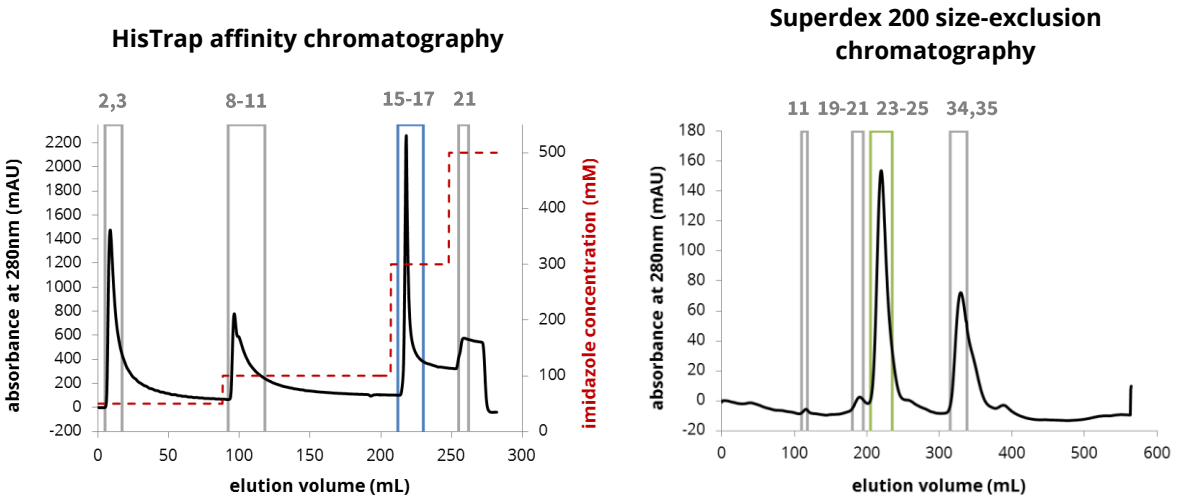

Figure 4.1 – Chromatograms for separation and purification of M26I DJ-1: black line represents chromatograms based on elute absorbance at 280nm, for protein detection; dashed red line represents increasing concentration of imidazole in mobile phase, for elution of histidine-tagged M26I protein; grey squares and numbers correspond to fractions analyzed in SDS-PAGE with coomasie staining; blue box correspond to fractions selected for purification in size-exclusion chromatography; green box corresponds to fractions selected for preparation of M26I DJ-1 stock solutions, in PBS or PBS and 5% glycerol.

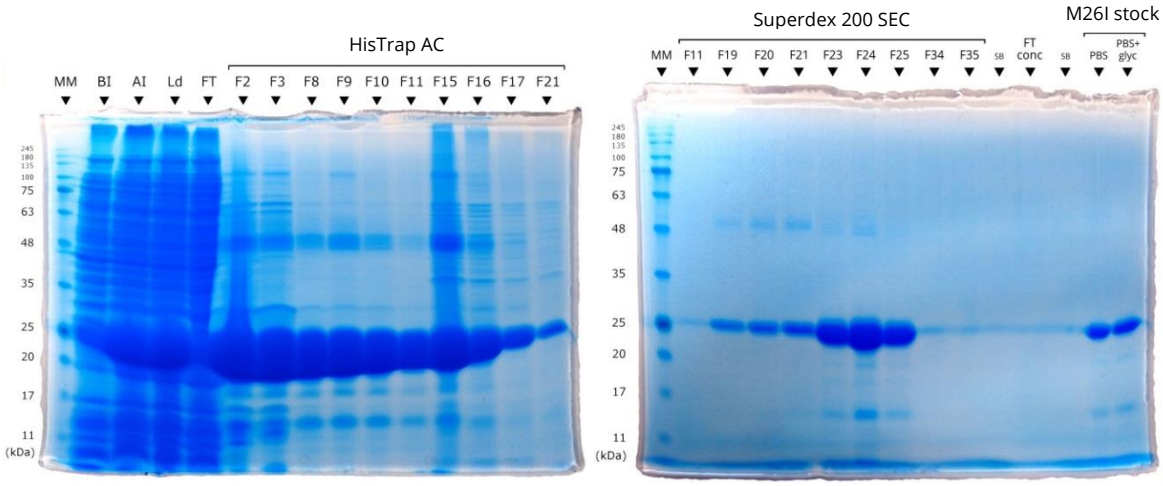

Figure 4.2 – SDS-PAGE analysis with coomassie staining of fractions collected during M26I DJ-1 production and purification. MM = molecular marker; BI = sample collected before induction; AI = after induction; Ld = protein extract loaded to HisTrap column; FT = flow-through from HisTrap elution of protein extract; F[x]= chromatography elution fractions; AC = affinity chromatography; SXC = size-exclusion chromatography; FT conc = flow-through from concentration of purified M26I DJ-1; SB = Sample Buffer; PBS+glyc = PBS with 5% glycerol.

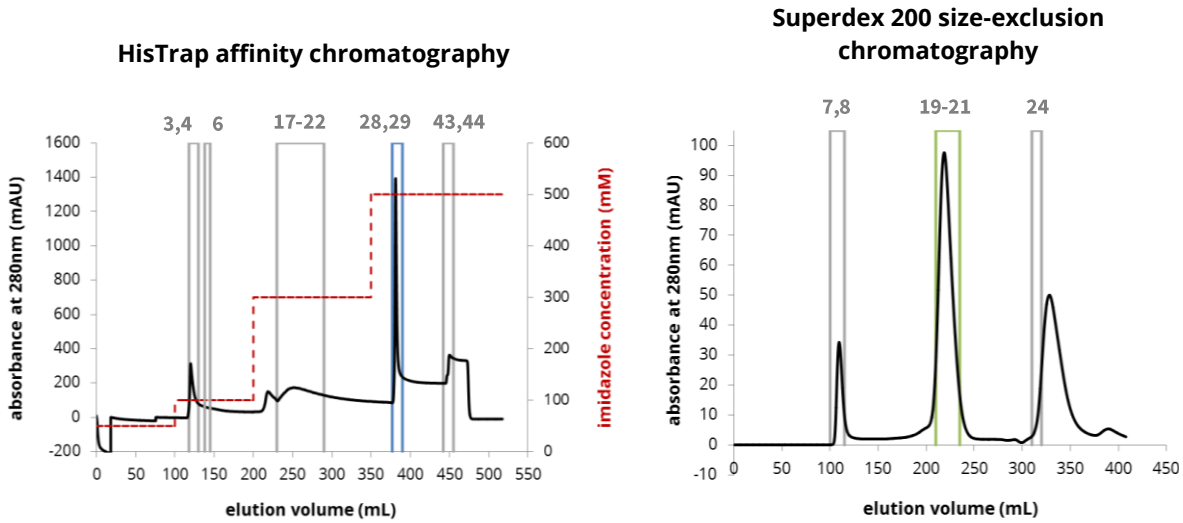

Figure 4.3 – Chromatograms for separation and purification of E163K DJ-1: black line represents chromatograms based on elute absorbance at 280nm, for protein detection; dashed red line represents increasing concentration of imidazole in mobile phase at affinity chromatography; grey squares and numbers correspond to fractions analyzed in SDS-PAGE; blue box correspond to fractions selected for purification in size-exclusion chromatography; green box corresponds to fractions selected for preparation of M26I DJ-1 stock solutions, in PBS or PBS and 5% glycerol.

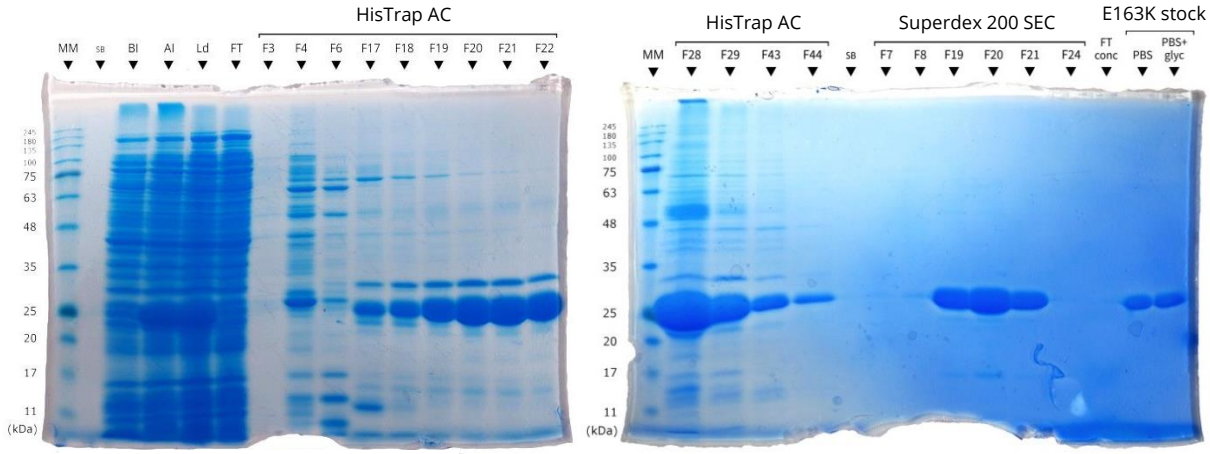

Figure 4.4 – SDS-PAGE analysis with coomasie staining of fractions collected during E163k DJ-1 production and purification. MM = molecular marker; BI = sample collected before induction; AI = after induction; Ld = protein extract loaded to HisTrap column; FT = flow-through from HisTrap elution of protein extract; F[x]= collected chromatography fractions; AC = affinity chromatography; SXC = size-exclusion chromatography; FT conc = flow-through from concentration of purified E163K DJ-1; SB = Sample Buffer; PBS+glyc = PBS with 5% glycerol.

After storage of produced mutant proteins, and coomassie staining of produced stock solutions, with M26I showing some contaminants (Figure 4.2), it was performed a protein silver staining of stock solutions to confirm the presence of contaminants and for a first comparison of WT DJ-1 with the produced protein (Figure 4.5). All protein solutions of native and mutant DJ-1 have similarities, showing the almost predominance of the 20-25 kDa band attributed to DJ-1 and the presence of some contaminants near 12 kDa and 50 kDa, in all stock solutions.

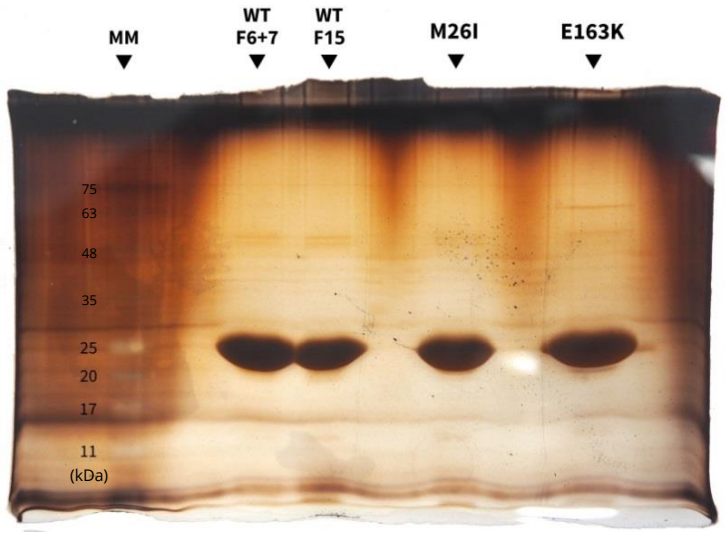

Figure 4.5 – Silver staining of prepared M26I and E163K DJ-1 stock solutions in protein vehicle, and previously produced wild-type DJ-1 stock solutions from fractions 6 and 7 (WT F6+7) or fraction 15 (WT F15), collected on the correspondent Superdex 200 size-exclusion chromatography. MM = molecular marker.

4.1.2. Characterization of wild-type and mutant DJ-1

After concluding the production of the mutant forms of DJ-1, M26I and E163K, the stored protein solutions were subjected to several assays to confirm their adequacy to further studies and compare them to DJ-1 native form, regarding three essential areas: protein identification with MS analysis of the stock solutions; verification of protein dimerization, with determination of the quaternary structure MW; viability assays, to analyze the biological and protective role of DJ-1 and observe the resulting effects of DJ-1 mutant forms on a Parkinson's disease *in vitro* model.

4.1.2.1. DJ-1 and contaminants identification by LC-MS/MS

After observing a high amount of a 20 kDa monomer, attributed to DJ-1, and detecting some contaminants with coomasie and silver gel staining of stock solutions, WT, M26I and E163K DJ-1 were processed for LC-MS/MS. This could confirm DJ-1 production and aid on contaminant identification, to undertake its innocuousness.

The three DJ-1 solutions, WT and mutants M26I and E163K, were separated using gel electrophoresis and prepared for LC-MS/MS analysis, with IDA acquisition, as specified in section 3.4.3. For the identification of a larger yield of proteins besides DJ-1, gel was divided in sections and separately analyzed in MS - section 3 included only the large DJ-1 attributed band. Also, to guarantee not only the identification of the native form of DJ-1 (registered in the Swissprot database used for MS data processing), but also the mutant forms that were produced (not registered), IDA results were processed using two databases: a Protein database, containing all Uniprot annotated proteins, regarding all species; in the other, named Protein+Mutation database, FASTA entries of the recombinant DJ-1 protein sequence were added to Uniprot proteins, including wild-type and several natural or synthetic mutant forms, such as M26I and E163K.

Results are summarized in Table 4.1, and ProteinPilot processing values described with further detail in Supplementary Table 8.2 and 8.3. Graphic representation of sequence coverage of identified DJ-1 in section 3 of three samples and Protein+Mutation database processing is depicted in Supplementary Figure 8.2.

Overall, and excluding the contaminants inherent to MS analysis such as keratin and trypsin, DJ-1 was the most identified protein in all samples, and it was identified several other contaminants of bovine and *E. coli* origins. *E-coli* proteins were expected, being the culture hosting the mutant DJ-1 production, and bovine proteins can be attributed to the L-B medium used. A thorough analysis of protein ID attribution values, after processing of IDA acquisition files, confirmed the presence of WT, M26I and E163K DJ-1 in the respective solutions, with presence of few contaminants and any of them capable of interfering with DJ-1 or *in vitro* activity.

Table 4.1 - DJ-1 and contaminants identification by LC-MS/MS. p = Protein database; pm = modified Protein+Mutation database, with added entries of mutant DJ-1 forms. Color tagging: red = digestion enzyme; dark green = DJ-1 of protein database; light green = identified mutant DJ-1 sequences, added in modified database; orange = keratin proteins; light blue = *E. coli* culture protein contaminants; dark blue = L-B medium contaminants.

	solution	WT						M26I						E163K					
	gel section	1+4		2		3		1+4		2		3		1+4		2		3	
	PP database	p	pm	p	pm	p	pm	p	pm	p	pm	p	pm	p	pm	p	pm	p	pm
accession code	protein name	species																	
sp|P00761|TRYP_PIG	Trypsin	Sus scrofa	X	X	X	X	X	X	X	X	X	X	X	X	X	X	X	X	X	X
sp|Q99497|PARK7_HUMAN	Protein DJ-1	Homo sapiens	X	X	X	X	X		X		X		X		X		X		X	
sp|Q8UW59|PARK7_CHICK	Protein DJ-1	Gallus gallus											X	X						X
D00000|Protein	DJ-1 WT	Homo sapiens						X												
D00001|Protein	DJ-1 M26I	Homo sapiens								X		X		X				X		
D00002|Protein	DJ-1 E163K	Homo sapiens																		X
D00003|Protein	DJ-1 C106A	Homo sapiens						X												
D00004|Protein	DJ-1 C106DD	Homo sapiens						X						X						
sp|Q99497|PARK7_HUMAN; D00004|Protein; D00003|Protein; D00000|Protein	Protein DJ-1; DJ-1 C106DD; DJ-1 C106A; DJ-1 WT	Homo sapiens													X					
sp|P35527|K1C9_HUMAN	Keratin, type I cytoskeletal 9	Homo sapiens	X	X	X	X			X	X					X	X	X	X		
sp|P13645|K1C10_HUMAN	Keratin, type I cytoskeletal 10	Homo sapiens	X	X					X	X					X	X	X	X		
sp|P02533|K1C14_HUMAN	Keratin, type I cytoskeletal 14	Homo sapiens	X	X											X	X				
sp|P08779|K1C16_HUMAN	Keratin, type I cytoskeletal 16	Homo sapiens							X											
sp|P04264|K2C1_HUMAN	Keratin, type II cytoskeletal 1	Homo sapiens	X	X	X	X			X	X	X	X			X	X	X	X		
sp|P35908|K22E_HUMAN	Keratin, type II cytoskeletal 2 epidermal	Homo sapiens	X	X					X	X					X	X				
sp|P13647|K2C5_HUMAN	Keratin, type II cytoskeletal 5	Homo sapiens	X	X																
sp|P0A7W1|RS5_ECOLI	30S ribosomal protein S5	Escherichia coli	X	X					X	X					X	X				
sp|P0A7X3|RS9_ECOLI	30S ribosomal protein S9	Escherichia coli	X							X										
sp|P0A7W1|RS5_ECOLI	30S ribosomal protein S13	Escherichia coli	X	X					X	X					X	X				
sp|P60723|RL4_ECOLI	50S ribosomal protein L4	Escherichia coli	X	X					X						X	X				
sp|P02413|RL15_ECOLI	50S ribosomal protein L15	Escherichia coli	X	X												X				
sp|P0A9A9|FUR_ECOLI	Ferric uptake regulation protein	Escherichia coli	X	X					X	X										
sp|P0ABB0|ATPA_ECOLI	ATP synthase subunit alpha	Escherichia coli															X	X		
sp|P0ACJ8|CRP_ECOLI	cAMP-activated global transcriptional regulator CRP	Escherichia coli						X												
sp|P60712|ACTB_BOVIN	Actin, cytoplasmic 1	Bos taurus	X	X	X							X			X					
sp|Q7ZVI7|ACTB1_DANRE	Actin, cytoplasmic 1	Danio rerio				X														
sp|P41340|ACT3_LIMPO	Actin-3	Limulus polyphemus							X		X									
sp|P29751|ACTB_RABIT	Actin, cytoplasmic 1	Oryctolagus cuniculus								X										
sp|O17320|ACT_CRAGI	Actin	Crassostrea gigas														X	X	X		
sp|P04764|ENOA_RAT	Alpha-enolase	Rattus norvegicus	X	X	X	X														
sp|P02662|CASA1_BOVIN	Alpha-S1-casein	Bos taurus	X	X																
sp|P02663|CASA2_BOVIN	Alpha-S2-casein	Bos taurus							X	X										
sp|P07335|KCRB_RAT	Creatine kinase B-type	Rattus norvegicus			X	X														
sp|O02675|DPYL2_BOVIN	Dihydropyrimidinase-related protein 2	Bos taurus			X	X														
sp|P04797|G3P_RAT	Glyceraldehyde-3-phosphate dehydrogenase	Rattus norvegicus	X	X	X	X														
sp|P19120|HSP7C_BOVIN	Heat shock cognate 71 kDa protein	Bos taurus			X	X														
sp|P01946|HBA_RAT	Hemoglobin subunit alpha-1/2	Rattus norvegicus	X	X	X	X			X	X	X	X								
sp|P02091|HBB1_RAT	Hemoglobin subunit beta-1	Rattus norvegicus			X	X														
sp|P81947|TBA1B_BOVIN	Tubulin alpha-1B chain	Bos taurus				X														
sp|Q2HJ86|TBA1D_BOVIN	Tubulin alpha-1D chain	Bos taurus			X															
sp|P62261|1433E_BOVIN	14-3-3 protein epsilon	Bos taurus				X									X					
sp|P63102|1433Z_RAT	14-3-3 protein zeta/delta	Rattus norvegicus			X															

Comparing results obtained between the two used databases, Protein database and modified Protein+Mutations database (added various DJ-1 mutations, including the ones produced) identified about the same proteins on each sample: the main difference relies on the DJ-1 form attribution given by each database for M26I and E163K DJ-1 samples. Section 1+4 of samples contained the highest amount of contaminants (particularly WT solution), followed with section 2. DJ-1 was identified in all sections , but in section 3 of samples, which contains the presumed DJ-1 band, the sequence coverage was close to 100% (with confidence above 95%) in most samples and was not identified any protein contaminant.

Regarding WT DJ-1, sections 1+4 and 2 had 60 to 70% of sequence coverage of identified DJ-1, and in section 3 (which included the DJ-1 band), sequence coverage was above 95%. In any section of WT DJ-1, the percentage of sequence coverage of DJ-1 decreased when using the mutation database. All samples analyzed from mutant DJ-1 solutions also present these same tendencies.

Regarding M26I DJ-1 samples, when using mutation database it was possible the attribution of the M26I form of DJ-1 in the three sections, and coverage of M26I DJ-1 increased to 100% in section 3. Considering E163K DJ-1 samples, mutation database in sections 1+4 and 2 only attributed other DJ-1 forms besides E163K; nevertheless, in section 3 was attributed the E163K form, with 100% of protein coverage. To note that in sections 1+4 or 2, in among all three forms of DJ-1, the protein was identified using 27-75 identified peptides over 95% confidence, in itself much more than any other protein besides trypsin; in section 3 of all samples, the number increases to 169 to 504 peptides attributed to DJ-1, resulting in a confidence increase of protein coverage.

4.1.2.2. HPLC-SEC analysis of quaternary MW

To verify whether the produced DJ-1 mutants M26I and E163K are capable of maintaining the dimeric form, characteristic of the protein and kept on these mutations, size exclusion chromatography was used to determine the molecular weight of the quaternary structure of mutants and WT DJ-1. Protein solutions were subjected

to elution in a Superdex 200 5/100 GL column, in non-denaturing conditions, and peak retention time was correlated to values registered for protein standards, of known quaternary MW. It was only regarded chromatography peaks of retention time within the standards values.

Using the technique over WT, M26I and E163K DJ-1, using the respective PBS and PBS with 5% glycerol (PBS+G) stock solutions (Figure 4.6 and Table 4.2), it was attributed about 60 kDa to all WT and M26I solutions: giving the low resolution of this technique, the exclusion of ribonuclease as a standard and the fact that other plausible possibilities would be DJ-1 as a monomer or an aggregate, this value was considered as an homodimeric form, expected to register about 40 kDa. Though the technique offered a considerable overestimation of the MW for WT and M26I, for E163K solutions it was determined less a quaternary MW of less than 35 kDa: though is closer to the expected 40 kDa, it's almost half of the value determined for WT and M26I.

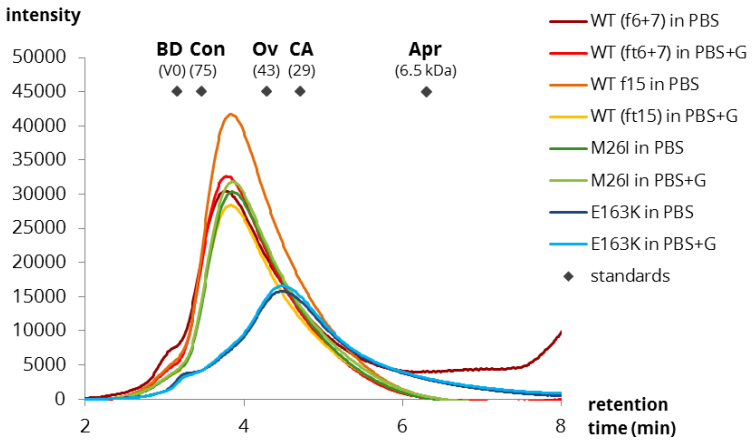

Figure 4.6 - SEC-HPLC chromatogram of WT, M26I and E163K DJ-1 protein stock solutions, and registry of peak retention time of protein standards. Used standards: BD = Blue Dextran 200; Con = conalbumin; Ov = ovalbumin; CA = carbonic anhydrase; Apr = aprotinin. V0 = dead volume. Determined calibration curve: K_{av}= -0.3799 $\log_{10}$(MW) + 1.9143 (R^2 = 0.993).

Table 4.2 – Determination of quaternary molecular weight (MW), from WT, M26I and E163K DJ-1 peak retention times and calibration curve.

samples	MW (Da)
WT (f6+7), PBS	60,470
WT (f6+7), PBS+G	60,203
WT(f15), PBS	60,470
WT (f15), PBS+G	60,203
M26I, PBS	59,198
M26I, PBS+G	58,988
E163K, PBS	34,117
E163K, PBS+G	34,696

The HPLC run of the E163K solutions was then repeated, being compared to E163K DJ-1 previously produced by Lúcia Sabala and which thorough analysis demonstrated its presence in the dimeric form (Figure 4.7 and Table 4.3). SEC-HPLC

denotes that both solutions have protein with the same molecular weight, of about 35 kDa, so it is considered that the produced E163K DJ-1 is in the dimeric form and can be used in further studies, like the WT and M26I forms.

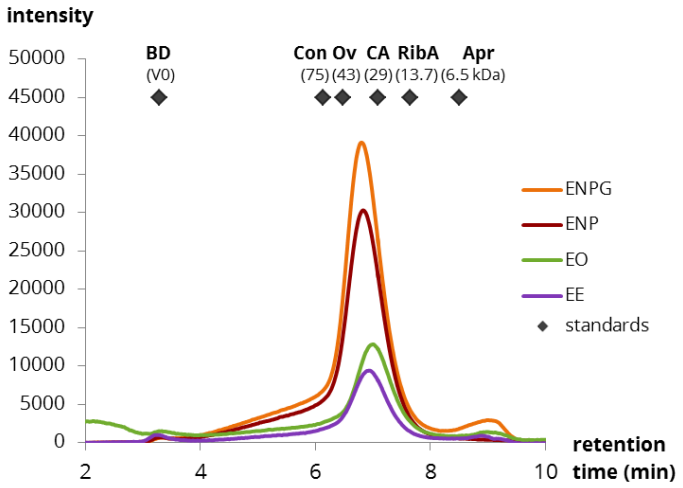

Figure 4.7 - SEC-HPLC chromatogram of E163K DJ-1 protein recently produced compared to previous stock, and registry of peak retention time of protein standards for construction of calibration curve: K_{av}= -0.3332 $\log_{10}$(MW) + 2.0400 (R^2 = 0.991). Used standards equal to Figure 4.6, with addition of ribonuclease A (RibA).

Table 4.3 – Determination of quaternary MW with peak retention times of produced and old stock of E163K, and calibration curve.

samples	MW (Da)
ENP - new E163K DJ-1 stock, stored in PBS	34,692
ENPG - new E163K, stored in PBS+5% glycerol	35,705
EO - old stock of E163K, stored in PBS + 10% glycerol	28,976
EE - old stock (**EO**), concentrated and changed buffer to PBS+5% glycerol	31,108

4.1.3. DJ-1 viability assays for neuroprotection analysis

After LC-MS/MS identification and confirmation of its presence as a homodimer, the produced mutants M26I and E163K can be considered adequate to be analyzed in biological assays, to access any alterations over the functional role of DJ-1 between its native and mutant forms.

When considering the biological role of DJ-1 regarding Parkinson's disease, suppression of oxidative stress is a preponderant feature of the protein in the cellular milieu. Hence, viability assays using *in vitro* cultures in oxidative stress conditions are crucial to study WT DJ-1 protective role and the effects of M26I and E163K impairment on a biological level. The neuroblastoma cell line SH-SY5Y was used for these assays, given its often use in such conditions as a Parkinson's disease model.

The performed viability assay, comparing the native and mutant DJ-1 biological function, is described in section 3.6.2.2.: 24h incubation of SH-S5Y5 cell culture in medium containing 1 μM of WT, M26I or E163K DJ-1 stock solutions (in protein vehicle), or any of these; addition of equal volumes of each protein solution, for annulment of protein vehicle effects over viability; additional assessment of conditions in the absence or presence of 40 or 50 μM of hydrogen peroxide; after 24h incubation with extracellular DJ-1 forms and oxidative stress, it was performed a luciferase-based ATP quantification, correlated with the number of viable cells. It was taken in account only the higher concentration of 50 μM hydrogen peroxide to analyze the oxidative death induction, given the significance of the obtained results (Figure 4.8). Additional viability assay data (40 μM hydrogen peroxide exposition, DJ-1 protein control conditions, and comparison of WT in PBS or PBS with 5% glycerol) can be seen in Supplementary Figure 8.3 and 8.4.

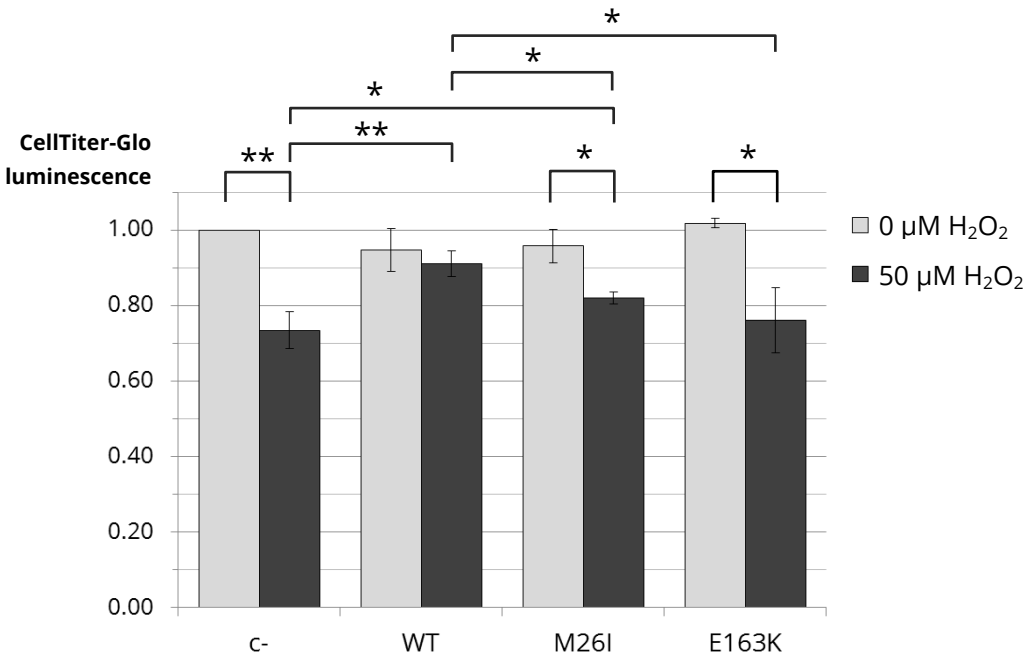

Figure 4.8 – SH-SY5Y cell viability assay, under normal (0 μM H_2O_2) or oxidative stress (50 μM H_2O_2) conditions, and in absence (c-) or presence of different DJ-1 protein forms (WT, M26I, E163K). Values normalized to control condition (c-, 0μM H_2O_2). Negative and positive error bars of each condition corresponding to respective standard deviation (n=3). Above the graphic, indication of condition pairs with significant difference after independent samples t-test analysis: * = p-value under 0.05; ** = p-value under 0.001.

It can be seen a statistically significant decrease of SH-SY5Y viability in the presence of 50 μM hydrogen peroxide, indicating SH-SY5Y vulnerability to oxidative insults. It can also be seen with over 99.9% confidence that, in the presence of oxidative stress, the native form of DJ-1 is able to increase cell viability, maintaining over 90% viability of the cell culture (20% more than in the absence of the protein).

Regarding DJ-1 mutations, it was demonstrated with over 95% confidence a decrease of cell viability in oxidative stress conditions, when considering the addition of either mutant forms of DJ-1 compared to WT. Only with WT DJ-1 addition it is not seen a statistically significant decrease of cell viability, demonstrating the protective effect of DJ-1 in SH-SY5Y cell culture and the increased vulnerability to oxidative stress in the occurrence of mutation in the DJ-1 protein.

Furthermore, in the absence of oxidative stress it is not observed any viability differences between protein conditions. On the other hand, when considering oxidative stress conditions some proteins forms become statistically distinguishable (with 95% confidence): WT DJ-1 offers higher protection than M26I and E163K, showing a cell viability increase of 10% and 15%, respectively; M26I presents significantly lower viability than WT and higher viability than C-, denoting that despite the biological function of DJ-1 is impaired with the M26I mutation, the protein is not totally unable to protect cells from oxidative insults; E163K in oxidative stress conditions was only distinguishable of WT, and has similar results to C-, which could suggest a total loss of oxidative stress protection resulting from this mutation.

Thus, it was found relevant differences of oxidative stress response between WT DJ-1 and negative control, and distinct cell viability between WT, M26I or E163K after hydrogen peroxide addition, confirming the role of DJ-1 over oxidative stress protection in the pathological context of an *in vitro* Parkinson's disease model. The concentration of 50 μM hydrogen peroxide has proven to affect cell viability, so it can be used in further studies to analyze SH-SY5Y cell culture in an oxidative stress condition.

4.2. Biotinylation protocol for MS analysis of cell surface proteome in a PD context

4.2.1. Detection of protein biotinylation

In order to use Sulfo-NHS-LC-biotin for the enrichment of cell surface proteins, it was applied several methods to demonstrate the Sulfo-NHS-LC-biotin impermeability to the plasma membrane and extensive reactivity with proteins, in order to obtain an efficient labelling of cell surface proteins using the proposed biotinylation protocol – for downstream pull-down of biotinylated proteins with avidin resin and an extensive MS identification and quantification of enriched cell surface subcellular proteome.

Streptavidin b-phycoerythrin conjugate (SAPE) is a fluorescence label used for the direct and specific observation of biotinylated product, and was selected for the applied assays: streptavidin, an avidin derivative with similar affinity, is covalent attached to b-phycoerythrin, a phicobiliprotein with excitation between 488 and 561 nm and fluorescence emission at 575 nm when streptavidin interacts with a biotinylated compound. SAPE can be used in several techniques, such as immunoblotting and immunohistochemistry assays – since the use of SAPE in these techniques is generally for the detection of biotinylated antibodies, not the direct detection of biotinylated proteins.

4.2.1.1. Biotinylated proteins blotting assays

As an alternative for comprehensive analysis of enrichment of the cell surface proteins using MS analysis, it was firstly executed adapted immunoblotting and immunohistochemistry procedures to detect biotinylated proteins on the fractions collected during the enrichment process. Its main purpose is the definition of several key steps regarding the procedure efficiency: specificity reaction with cell surface proteins; minimization of biotinylated protein loss through the procedure, and maximization of the MS detection of cell surface proteins. The applied techniques used

SAPE for direct signaling of all biotinylated proteins on the protein fractions collected after avidin pull-down process, without the usually required incubation with antibodies and probe for spectrophotometric detection of specific proteins.

To assure the in-gel and in vivo direct detection of biotinylated proteins, it was firstly performed dot blot assays, which resulted in a noticeable SAPE fluorescence emission and specific interaction and labelling of biotinylated proteins. Detailed results can be found in Supplementary Data 8.4.

After evident success of the dot blot procedure, SAPE could then be used for the direct detection of biotinylated proteins captured in fractions collected after the *in vitro* biotinylation and avidin pull-down procedure, in an adapted western blotting procedure without antibodies incubation, similar to dot blot. For a comprehensive analysis of the proposed procedure, SH-SY5Y cells were plated for two conditions: one where the biotinylating and quenching solutions were prepared in water, another where isotonic buffers were used. After incubation, cells in culture plates were scraped and processed, to obtain protein extract; solutions used for cell biotinylation and biotin quenching was also processed for downstream analysis (designed Tris+biotin), to see the presence of biotinylated protein from detached or lysed cells. After samples incubation with avidin resin, and washing for removal of non-biotinylated proteins, it was consecutively used three different elution methods: resin incubation with biotin solution; incubation with glycine solution; SB addition and *in loco* protein denaturation for elution and collection of proteins retained by avidin resin, expected to correspond to the biotinylated fraction.

Several washing and elution pull-down fractions were selected, further processed and separated for SDS-PAGE for two methods: protein blotting and SAPE staining, for analysis of biotinylated proteins in selected samples, silver staining for observation of the total amount of proteins within the several fractions (Figure 4.9).

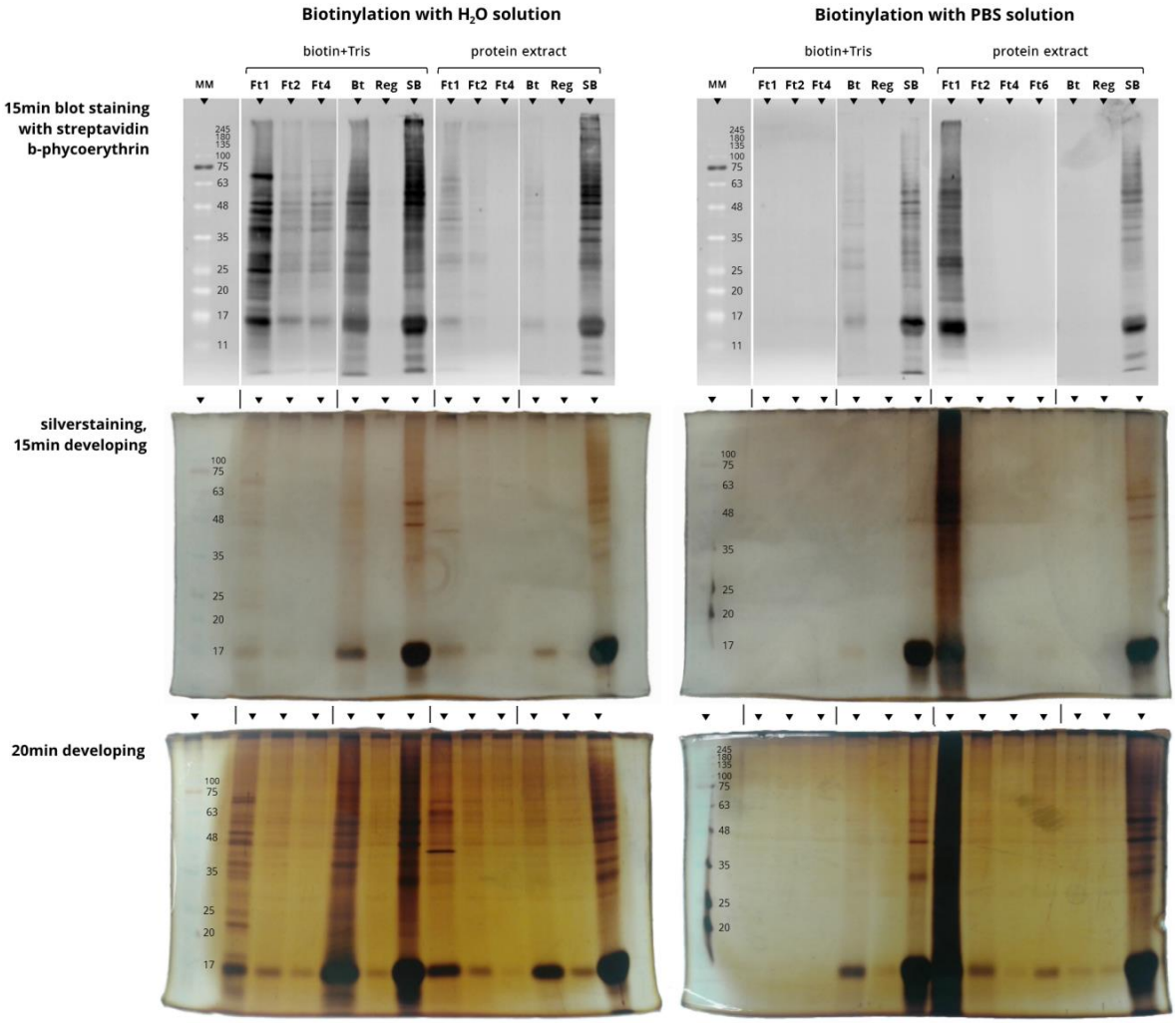

Figure 4.9 – Protein blotting and silver staining, after SDS-PAGE separation for the detection of biotinylated and total amount of proteins, respectively. Samples after the biotinylation process, using biotin solubilized in water (left images) or PBS (right). MM = molecular marker; Ft[x] = washing fractions collected for avidin resin washing, for removal of non-bound proteins; Bt = fraction of proteins eluted with Biotin Buffer; Reg = fraction of elution with Regeneration Buffer; SB = elution with addition of Sample Buffer and protein denaturation.

Comparing both biotinylation procedures, it is possible to see that its execution with biotin in PBS shows almost no amount of biotinylated or total proteins in the Tris+biotin fractions, with only some proteins present in the SB fraction. In the procedure performed with biotin in water, fractions of Tris+biotin pull-down contain much more biotinylated and total protein – even more than what can be observed in the respective protein extract. This demonstrates that incubation of biotin prepared in

water and quenching Tris-HCl may result in SH-SY5Y cells suffer lysis or detachment - though some cells remain attached to the culture plate. Hence, it is preferred the use of biotin solubilized in PBS and TBS quenching to maintain cell integrity and attachment to plate, and allowing only the labelling of cell surface proteins.

Furthermore, and regarding washing fractions of the pull-down from all samples, it is noted two characteristics: a large amount of total proteins in FT1 fraction, and a large decrease in later FT fractions, confirming a satisfactory removal of proteins not bound to avidin resin; there is also a considerable amount of biotinylated protein detected in almost all FT1 fractions, pointing out the necessity of increasing the amount of avidin resin for total capture of labelled proteins, or performance of a second pull-down with incubation of FT1 with avidin resin aliquot and collection of the remaining biotinylated proteins.

Regarding the elution fractions, western blot and silver staining indicates that biotinylated proteins are mostly captured from resin with SB addition; almost any total or biotinylated protein is observed in BT or Reg fractions. This states that the use of Sample Buffer is the best method to effectively collect the biotinylated proteins captured in avidin resin – though there is the risk of also eluting proteins that were nonspecifically bound to avidin, it would still occur an enrichment of biotinylated cell surface proteins.

A key observation is the unanimous presence of a protein band at around 17 kDa, in both protein detection techniques: this may correspond to avidin, which monomeric form has a similar molecular weight, pointing out the difficulty of handling the avidin resin and perform the pull-down without a gradual loss of resin and protein.

Both gel-based procedures allowed a comprehensive study of the biotinylation process and gave valuable data for the optimization of the proposed protocol, such as: the use of isotonic buffers (PBS for preparation of the biotin solution, TBS for biotin quenching); unnecessary pull-down of Tris+biotin; increase of the amount of avidin resin used for the pull-down of each protein extract; use of Sample Buffer and denaturation for elution of biotinylated proteins.

4.2.1.2. Fluorescence microscopy observation of cell surface biotinylation

After the indication of an overall biotinylated protein enrichment efficiency, it was necessary to know whether Sulfo-NHS-LC-biotin labels specifically cell surface proteins: the proposed procedure may still result in cell lysis or disruption of the plasma membrane integrity, allowing the permeation of Sulfo-NHS-LC-biotin and protein labelling of intracellular proteins. The use of microscopy techniques, using SAPE as a fluorophore, is crucial for an *in situ* observation of the cell surface biotinylation.

For the fluorescence microscopy observation, HeLa cells were plated, subjected to the designed biotinylation procedure (with Sulfo-NHS-LC-biotin solubilization in PBS, or sole use of PBS in control condition), fixed and stained with SAPE (Figure 4.10). Visualizing the cells at bright-field, it was possible to see that cells do not alter its morphology throughout the procedure, but it was apparent a decrease of the attached cell density, when compared to microscopy observation before biotinylation, which may be related to the various culture washes and incubation steps performed. Furthermore, it was confirmed a successful cell biotinylation: using a red filter for observation of the HeLa cultures, only cells subjected to incubation with biotin presented fluorescence emission. It was not evident the labelling of intracellular proteins or in extracellular areas, but the low resolution of this method did not allow to clearly stipulate that cells were labelled exclusively at its surface.

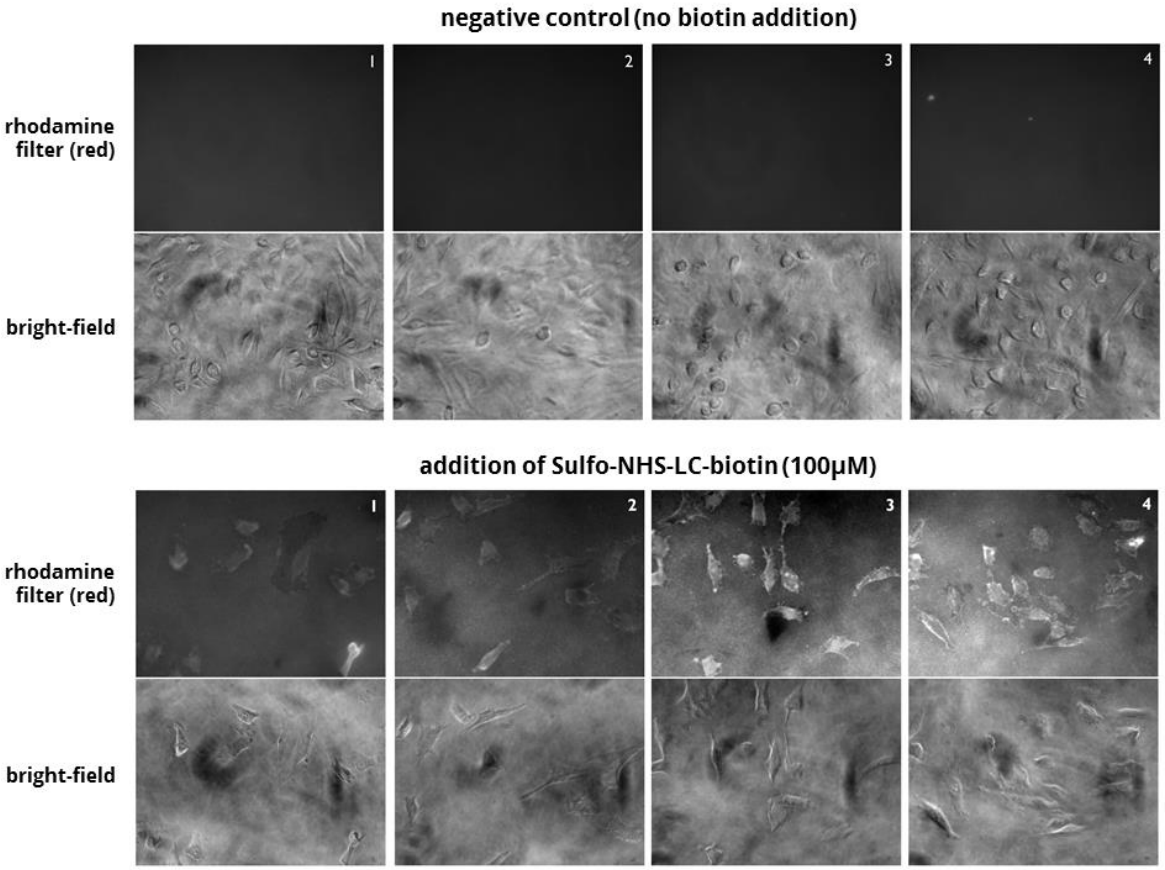

Figure 4.10 – Fluorescence microscopy of HeLa cells after 24h incubation, biotinylation (or incubation with PBS in negative control), TBS wash for biotin quenching, fixation and SAPE staining of biotinylated proteins. 1 to 4 correspond to each replicate condition, with photographs taken at 40× magnification and using bright-field (light transmission) for cell observation, or rhodamine filter (550/25 bandpass emission filter, 570 nm dichroic filter, 605/70 bandpass excitation filter) for observation of SAPE fluorescence signaling of biotinylated proteins.

A similar HeLa biotinylation, fixation and SAPE procedure (and control procedure, with no biotin addition) was applied for the preparation of microscope slides, for confocal microscopy observation. Comparing both procedures, it is possible to see again the SAPE staining of HeLa cells only after its biotinylation (Figure 4.11). Increasing the resolution of this condition (Figure 4.12), it is notorious the presence of SAPE fluorescence only at the surface of HeLa cells, without any signaling of intracellular proteins, demonstrating Sulfo-NHS-LC-biotin impermeability to the plasma membrane and exclusive labelling of cell surface proteins, with the used procedure.

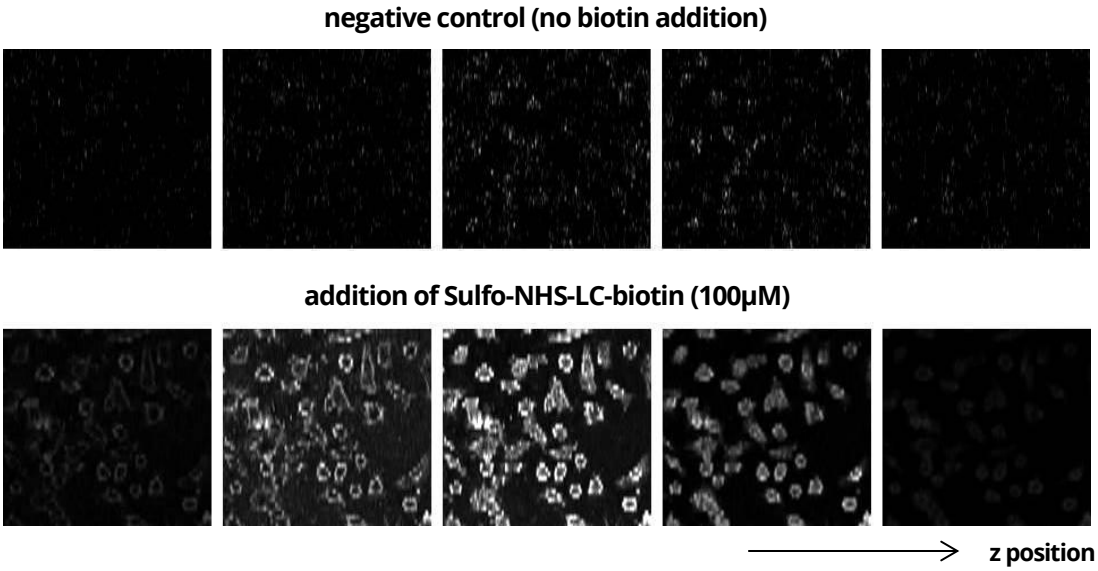

Figure 4.11 – Low resolution confocal microscope Z-stack imaging of HeLa cells, after 24 incubation, cell biotinylation (or PBS incubation in negative control), quenching, fixation, SAPE labelling and preparations of microscope sides. Observation using BPE Smart Setup, with 488nm excitation laser. Images from left to right correspond to different z positions registered for the same sample, in down-up direction.

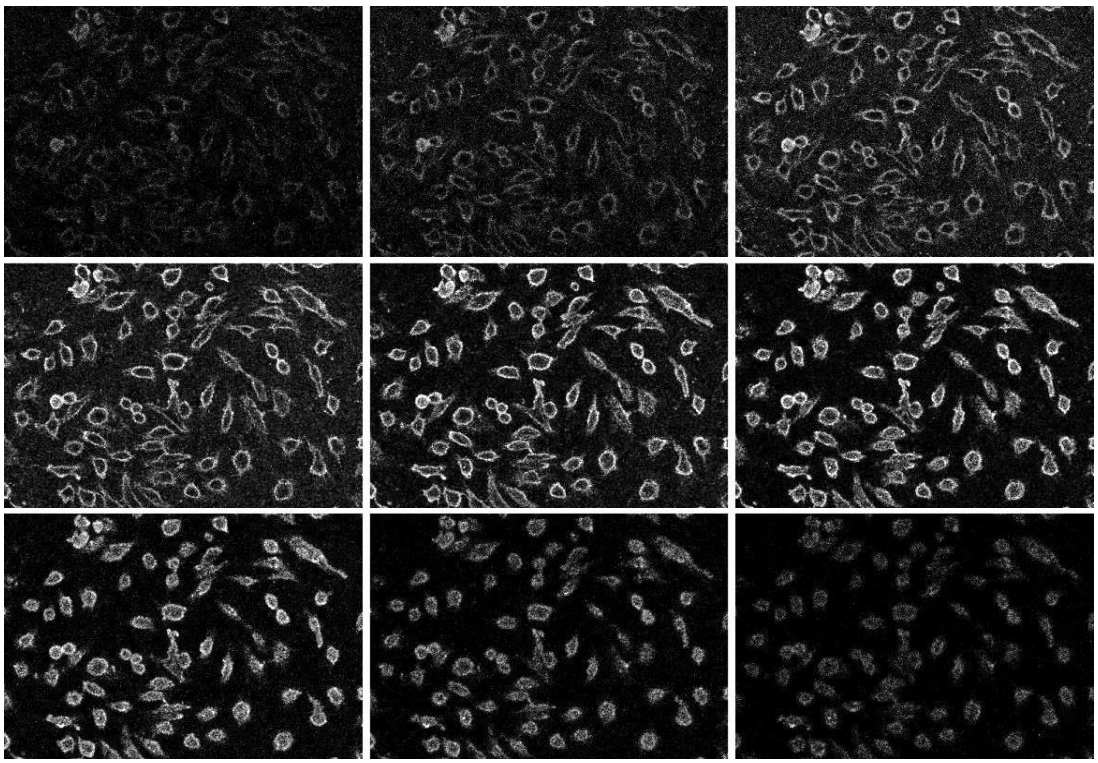

Figure 4.12 – High resolution confocal microscope Z-stack imaging of HeLa cells, biotinylation condition. Observation with BPE Smart Setup, 488nm laser. Several images from the same biotinylated HeLa cells, taken in successive z positions (from left to right and up to bottom)

Overall, the procedures used for SAPE signalling of biotinylated proteins, in blotting and microscopy procedures, allowed to demonstrate the efficiency of the used procedure for biotinylation of cell surface and pull-down of biotinylated proteins, providing the possibility of the MS analysis of an enriched fraction of cell surface subcellular proteome.

4.2.2. MS analysis of SH-SY5Y surface biotinylation and H_2O_2 proteome modulation

The techniques involved in the monitoring of biotinylated proteins, using SAPE staining of protein extracts or in vitro cells, helped to demonstrate biotin specificity and efficiency of its pull-down, but the adequacy of the proposed procedure for an MS analysis has still to be assessed. The amount of biotinylated protein, and the removal efficiency of non-biotinylated proteins, must be high enough to allow an extensive identification and accurate quantification of cell surface proteins, a small fraction of the cell proteome, in order to be possible the discovery of SH-SY5Y surface biomarkers of oxidative stress or DJ-1 intake.

Since cell surface proteins are located in the plasma membrane, on the extracellular side or integral to the structure, they can be characterized with hydrophobic regions, which have less exposure in hydrophilic environments and less trypsin digestion sites. In order to see whether the MS analysis of cell surface proteins is compromised by the standard sample preparation procedure, an enriched membrane protein extract was subjected to liquid digestion using trypsin or trypsin with chymotrypsin, for IDA and SWATH acquisition analysis. Actually trypsin demonstrated a higher number of total proteins, higher protein reproducibility and peptide hydrophobicity, and number and percentage of membrane proteins, hence was the enzyme used for the digestion of membrane proteins (Supplementary Data 8.5).

Furthermore, it was performed an MS analysis of the biotinylation and avidin pull-down procedure, similar to the one executed for western blotting, in condition of biotin preparation in water. It was also used the three elution methods (biotin buffer,

regeneration buffer, SB denaturation of resin) for collection of labelled proteins in Tris+biotin and protein extract collected from biotinylation; then also executed a second avidin pull-down of first washing fraction (FT1) collected on each pull-down. Selected washing and elution pull-down samples were subjected to IDA and SWATH acquisition, and SWATH was additionally used for analysis of samples from pull-down of a non-biotinylated SH-SY5Y extract. Though western blotting and MS analysis demonstrated that the use of biotin in water induces cell detach and lysis, making it inadequate for cell surface labelling (observed with the presence of a high protein amount in Tris+biotin derived samples), this MS analysis still aided on the establishment of some criteria for the cell surface enrichment procedure: use of approximately 100 µg of resin for each pull-down (double of what was used), and not needed a second pull-down of FT1, to have all biotinylated proteins in one array; elution with biotin or regeneration buffers not efficient, since there was an increase of number of identified proteins and quantification values in SB fraction (resin denaturation). Furthermore, MS data also confirms the cell disruption and biotinylation of all protein categories, since Tris+biotin samples presented a higher protein number, and comparing elution with washing fractions, there is not a percentage increase of cell surface proteins or related subcellular location ontologies (Supplementary Data 8.6).

After all SAPE and MS based studies have been performed, the labelling of SH-SY5Y cell surface proteins, for preparation of the enriched subcellular extract, the procedure similar to the one used for confocal microscopy was then applied with the following steps: removal of culture medium and PBS washing of plated SH-SY5Y cells; 15 min incubation with Sulfo-NHS-LC-biotin prepared in PBS; TBS plate wash for biotin quenching; and avidin pull-down with elution of captured proteins in denaturing conditions.

This procedure would be then used, to see whether the MS analysis of the enriched fraction of biotinylated proteins allow an increased identification and quantification of cell surface and related proteins. Since the protocol aims for the *in vitro* study of Parkinson's disease and the assessment of any related cell surface profile alterations, the protocol and MS analysis was applied for the study of normal and

oxidative stress conditions (induced 24 hours after cell plating and 24 h before biotinylation). Viability assays demonstrated a clear decrease of SH-SY5Y cell culture viability in the presence of hydrogen peroxide, already demonstrated to be a cytological model for the study of Parkinson's disease, so the discovery of proteome variation associated with oxidative stress would be relevant to broaden the study over the pathological modulation of cell surface proteins, mainly regarding the intake of wild-type or mutant forms of DJ-1.

Moreover, it was also tested the use of ultracentrifugation for sample processing of protein extract, after cell biotinylation and before avidin pull-down: the removal of soluble proteins (associated with the cytosol) and preparation of subfraction of membrane proteins could aid on the enrichment of cell surface proteins associated with the plasma membrane. Hence, it was performed the IDA and SWATH acquisition for each of three different conditions, with four replicates each: (i) control membrane, with no SH-SY5Y oxidative stress induction and with ultracentrifugation of protein extract; (ii) H_2O_2 membrane, with oxidative stress induction and ultracentrifugation; (iii) control extract, with no hydrogen peroxide addition, (iv) and direct use of protein extract for avidin pull-down, without ultracentrifugation for extraction of membrane fraction. It was followed by the identification of proteins collected from avidin resin, with combination of IDA files of replicates for ProteinPilot processing of each condition, and the quantification of proteins from a library created from the combination of all IDA acquisition files.

4.2.2.1. IDA acquisition analysis

When comparing control extract and control membrane samples, it was demonstrated that, though it is a process used for protein removal, ultracentrifugation before avidin pull-down allowed the identification of a higher number of peptides and proteins (Table 4.4). Furthermore, regarding the list of identified proteins on both conditions, it was observed that control membrane condition presented a higher number and percentage of proteins attributed to membrane, plasma membrane and

cell surface, or with predicted of α-transmembrane regions. Comparing lists from both conditions, 70% of control extract and 61% of control membrane are common to each other (Figure 4.15). These results are indicative that future assays should include an ultracentrifugation step for enrichment of membrane proteins before pull-down, to increase the number and percentage of proteins of interest.

Table 4.4 – Comparison of IDA acquisition data processing, from pull-down protein extract samples of biotinylated cultures after H_2O_2 or control stimulation (H2O2, C-, respectively), and with or without ultracentrifugation (membrane, extract, respectively). Data of total identified peptides and proteins was compared in total number and percentage (related to total number) of proteins with gene ontology attributed to membrane (GO:0044425), plasma membrane (GO:0005886), extracellular region (GO:0005576) and cell surface (GO:0009986), and proteins with predicted α-transmembrane region (TMHMM Server v.20 online tool).

	total peptides	total number of proteins	proteins with nr peptides >= 3	proteins with nr peptides < 3	membrane proteins		plasma membrane		α-trans-membrane prediction (TMHMM)		extracellular region		cell surface proteins	
					nr	%	nr	%	nr	%	nr	%	nr	%
C- extract	2661	544	336	208	358	65.8	80	14.7	50	9.2	256	47.1	22	4.0
C- membrane	2756	629	351	278	444	70.6	111	17.6	100	15.9	303	48.2	23	3.7
H2O2 membrane	2218	531	280	251	372	70.1	94	17.7	79	14.9	266	50.1	22	4.1

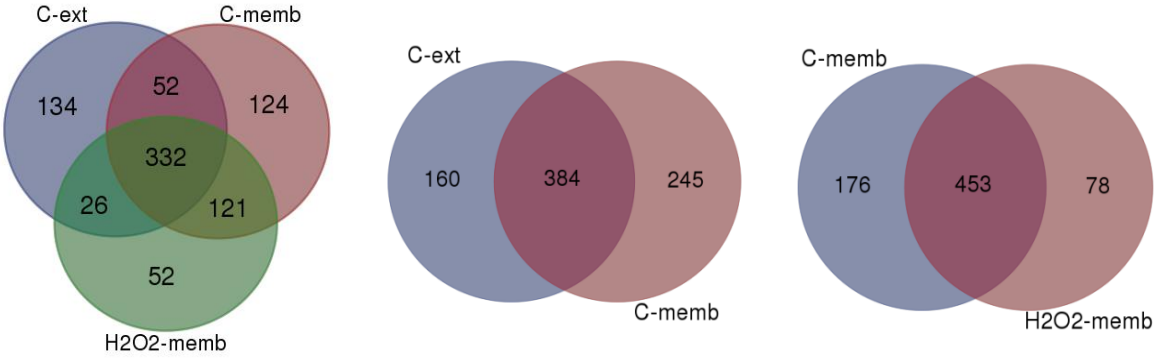

Figure 4.15 – Venn diagrams for total identified proteins in replicates of each condition, control extract (C-ext), control membrane (C-memb) and H_2O_2 membrane (H2O2 membrane) conditions, after biotinylation of SH-SY5Y cell surface.

When comparing the conditions with absence and presence of hydrogen peroxide during SH-SY5Y incubation, both subjected to ultracentrifugation (control and H_2O_2 membrane conditions), it is possible to see a decrease over the number of identified total proteins, as well in the number of membrane, plasma membrane, cell

surface and α-transmembrane predicted proteins (Table 4.4). In this case, the number of proteins common to both conditions increases to 72% in control membrane and 85% of H_2O_2 membrane (Figure 4.13). Although results from protein identification are not conclusive, the differences in the protein identification suggest a variation in proteome as a result of oxidative stress induction.

Nevertheless, and regarding all conditions, the biotinylation and pull-down procedure permitted the identification of a considerable amount of proteins, most of them with three or more attributed peptides. Of all identified 841 unique proteins identified in the three conditions, 332 proteins (almost 40%) were common to all three conditions. Also, it is seen a slight increase of membrane and cell surface proteins, but decrease of plasma membrane and α-transmembrane proteins. In the case of the H_2O_2 membrane condition, it presented the fewer amount of proteins exclusive to its condition (Figure 4.15).

4.2.2.2. SWATH acquisition analysis

SWATH acquisition data of twelve replicates was processed using a library resulted from the combined IDA acquisition files of all samples; quantification data was analysed regarding the enrichment of cell surface proteins, the detection of oxidative stress induced variations of the cell surface proteome, and a complementary analysis of the process with and without separation of membrane part of protein extract, for optimization of the cell surface enrichment processing.

Though IDA acquisition allowed the identification of 841 unique and 332 common proteins to the three conditions, SWATH acquisition processing resulted in the quantification of 80 proteins, almost all of them identified in IDA of three conditions (Table 4.5 and 4.6). Among these, 14 proteins were found to be associated to the plasma membrane, 5 associated to the cell surface, and 5 proteins were predicted as having α-transmembrane regions. Comparing common IDA and SWATH proteins, the later presented a minor increase of membrane and cell surface proteins (Table 4.5).

Table 4.5 - Comparison of selected proteins for identification and quantification: total distinct proteins = identified with at least one peptide in IDA acquisition processing of three conditions (control extract, control membrane, H_2O_2 membrane); proteins common to all conditions = identified with at least one peptide in IDA acquisition processing of all three conditions; SWATH acquisition = protein selected for quantification (with at least one peptide identified in all replicates). Annotation of total number proteins, and percentage of proteins with attributed gene ontology [membrane proteins (GO:0044425), plasma membrane (GO:0005886), cell surface (GO:0009986)], and with predicted α-transmembrane region (TMHMM Server).

			Total nr of proteins	Membrane proteins	Plasma membrane	α-trans-membrane prediction	Cell surface	Extracellular region
IDA acquisition	total distinct proteins	nr	841	567	144	125	29	381
		%	100.0	67.42	17.12	14.86	3.45	45.30
	proteins common to all conditions	nr	332	231	53	31	17	180
		%	100.0	69.58	15.96	9.34	5.12	54.22
SWATH acquisition		nr	80	61	14	5	5	58
		%	100.0	76.25	17.50	6.25	6.25	72.50

After selection of quantifiable proteins identified in SWATH acquisition, it was determined intensity values attributed to each protein (addition of identified peptides intensity, itself the sum of all attributed ion areas), which was then normalized in two possible methods: normalization to total intensity of each replicate (combination of all proteins intensity values); normalization to internal standard (added to all replicates after pull-down). Comparing both normalization methods, normalization to total intensity appears to provide more reproducible data, giving the fact that in all conditions was found a lower average of %CV values. This normalization method also presents lower average of mean proteins values. In addition, both normalizations in three conditions present a median lower than the average, meaning that most proteins present values under the average – except in H_2O_2 condition, with normalization to total intensity, where average and median have similar results (Table 4.6). The main goal of SWATH quantification is to compare conditions with and without ultracentrifugation, and with/without oxidative stress induction. Therefore, after normalization of protein values on each condition, it was determined the variation of "control extract" and "H_2O_2 membrane" conditions in comparison to "control membrane" (considered assay's control condition). Firstly, it was performed an independent t-test for each protein

Table 4.6 – Comparison of the average and median of proteins intensity (mean intensity values in the four condition replicates of each condition) and average of between-replicates standard deviation (st dev) and coefficient variation (%CV) of all SWATH quantified proteins, after protein intensity normalization to total intensity or internal standard (IS) of each replicate.

	Ctrl extract				Ctrl memb				H202 memb			
	average (mean replicates)	median (mean replicates)	average st dev	average %CV	average (mean replicates)	median (mean replicates)	average st dev	average %CV	average (mean replicates)	median (mean replicates)	average st dev	average %CV
protein normalisation to IS	2.83E-01	1.34E-01	7.62E-02	26.76	2.21E-01	9.45E-02	7.63E-02	39.31	1.87E-01	9.35E-02	8.52E-02	50.26
protein normalisation to total intensity	1.25E-02	5.84E-03	1.87E-03	16.43	1.25E-02	5.26E-03	2.33E-03	23.71	1.25E-02	1.25E-02	1.86E-03	17.76

(each with n=4), for the detection of statistically significant differences between values registered for each condition. Control condition was compared to "control extract" and to "H_2O_2 membrane", using protein values normalized to total standard or to total intensity, and was identified all tests with p-value under 0.05 or 0.01 (Table 4.7). It was demonstrated a significant variation of several proteins from "control extract" to control: 35 with normalization to total intensity, 32 with normalization to internal standard. But there was a decreased number of significantly different proteins when comparing "H_2O_2 membrane" to control: only normalization to total intensity permitted the identification of statistically different proteins, four with p-value under 0.05 and one under 0.01). Hence, t-tests reinforced the preferable use of normalization to total intensity for the quantification of proteins.

Secondly, it was calculated the fold variation for each protein in queried conditions, compared to control, with the division of "control extract" or "H_2O_2 membrane" protein values with "control membrane" values, normalized to total intensity. This would allow to access the increase (fold>1, positive variation $\log_{10}$) or decrease (fold<1, negative $\log_{10}$) of quantity regarding all proteins (Table 4.6). Comparing distribution of $\log_{10}$ variations of queried conditions ("control extract", "H_2O_2 membrane"), it is seen that "control extract" proteins vary more relatively to control condition values, though only about two thirds of proteins register higher quantity in "control extract", where ultracentrifugation was not executed (Figure 4.14).

Table 4.6 - Comparison of SWATH acquisition data quantitation of proteins with at least one quantified peptide in all twelve replicates, after pull-down of biotinylated SH-SY5Y after H_2O_2 or control stimulation (H_2O_2, Ctrl, respectively), with or without ultracentrifugation (memb, ext). Gene ontology protein attribution of selected proteins: memb = membrane (GO:0044425); plasma memb = plasma membrane (GO:0005886); cell surface (GO:0009986); transmemb = proteins with predicted α-transmembrane region (TMHMM Server). PARK7 (DJ1) STRING score = score attributed to proteins identified on STRING 10 online tool search for 500 PARK7 interactors (predicted with neighborhood, gene fusion, co-occurrence, co-expression, text-mining, databases and experiments). t-test = statistically significant difference of each protein between independent conditions (Ctrl ext or H_2O_2 memb against Ctrl memb), with p-value less than 0.05 or 0.01. norm to total int = protein intensity normalization to total intensity of each replicate; norm to IS = normalization to internal standard; var = condition variation, of each protein in Ctrl ext and H_2O_2 memb conditions normalized to control condition, Ctrl memb.

			identification in IDA acquisition			gene ontology				PARK7 (DJ-1) STRING score	Ctrl ext vs. memb t-test				H2O2 vs. Ctrl memb t-test				condition variation (var): values normalised to total int., ratios to control values (Ctrl memb)			
											norm total int.		norm IS		norm total int.		norm IS		Ctrl ext		H2O2 memb	
Entry	Entry name	Protein names	Ctrl ext	Ctrl memb	H2O2 memb	memb	plasma memb	cell surface	trans-memb		p < 0.05	p < 0.01	p < 0.05	p < 0.01	p < 0.05	p < 0.01	p < 0.05	p < 0.01	log10 (var)	fold (var)	log10 (var)	fold (var)
Q08211	DHX9	ATP-dependent RNA helicase A	x	x	x	x													0.081	1.21	0.156	1.43
P52272	HNRPM	Heterogeneous nuclear ribonucleoprotein M	x	x	x	x	x				x	x	x	x					0.319	2.08	0.131	1.35
P25705	ATPA	ATP synthase subunit alpha, mitochondrial	x	x	x	x	x				x								0.184	1.53	0.007	1.02
P19338	NUCL	Nucleolin	x	x	x	x		x			x	x	x						0.244	1.75	-0.050	0.89
Q71U36	TBA1A	Tubulin alpha-1A chain	x	x	x						x	x	x	x					0.380	2.40	0.023	1.06
P22626	ROA2	Heterogeneous nuclear ribonucleoproteins A2/B1	x	x	x	x													0.097	1.25	-0.044	0.90
O60506	HNRPQ	Heterogeneous nuclear ribonucleoprotein Q	x	x	x	x													0.136	1.37	0.013	1.03
P06576	ATPB	ATP synthase subunit beta, mitochondrial	x	x	x	x	x	x			x								0.137	1.37	0.026	1.06
P63261	ACTG	Actin, cytoplasmic 2	x	x	x	x	x												0.021	1.05	-0.067	0.86
Q9Y230	RUVB2	RuvB-like 2	x	x	x	x					x	x	x						0.173	1.49	-0.028	0.94
P11940	PABP1	Polyadenylate-binding protein 1	x	x	x	x					x	x	x						0.200	1.58	0.003	1.01
P14625	ENPL	Endoplasmin	x	x	x	x	x			0.25	x	x	x						0.349	2.23	0.096	1.25
P36578	RL4	60S ribosomal protein L4	x	x	x	x													-0.018	0.96	-0.091	0.81
P04264	K2C1	Keratin, type II cytoskeletal 1	x	x	x	x	x												0.064	1.16	0.095	1.25
P62805	H4	Histone H4	x	x	x	x					x	x	x						-0.622	0.24	0.033	1.08
Q99623	PHB2	Prohibitin-2	x	x	x	x		x											0.122	1.33	0.050	1.12
P62701	RS4X	40S ribosomal protein S4, X isoform	x	x	x	x					x	x							-0.225	0.60	-0.036	0.92
P35232	PHB	Prohibitin	x	x	x	x	x	x		0.397									0.003	1.01	0.000	1.00
Q02878	RL6	60S ribosomal protein L6	x	x	x	x									x				0.053	1.13	-0.096	0.80
P39023	RL3	60S ribosomal protein L3	x	x	x														0.063	1.16	-0.053	0.89
P23396	RS3	40S ribosomal protein S3	x	x	x	x	x			0.247									0.002	1.00	-0.009	0.98
P18124	RL7	60S ribosomal protein L7	x	x	x	x													-0.007	0.98	-0.014	0.97
P05388	RLA0	60S acidic ribosomal protein P0	x	x	x	x				0.271									0.027	1.06	0.015	1.04
P46781	RS9	40S ribosomal protein S9	x	x	x														-0.094	0.81	-0.040	0.91
P13010	XRCC5	X-ray repair cross-complementing protein 5	x	x	x		x												0.112	1.29	0.021	1.05
P07910	HNRPC	Heterogeneous nuclear ribonucleoproteins C1/C2	x	x	x	x													0.120	1.32	-0.001	1.00
Q00839	HNRPU	Heterogeneous nuclear ribonucleoprotein U	x	x	x	x		x			x	x							-0.161	0.69	0.016	1.04
P17987	TCPA	T-complex protein 1 subunit alpha	x	x	x					0.323	x		x						0.115	1.30	-0.038	0.92
Q5VTE0	EF1A3	Putative elongation factor 1-alpha-like 3	x	x	x						x		x	x					0.381	2.40	0.189	1.55
P40429	RL13A	60S ribosomal protein L13a	x	x	x	x				0.303									0.012	1.03	-0.041	0.91

P15880	RS2	40S ribosomal protein S2	x	x	x													-0.124	0.75	-0.025	0.94
P62249	RS16	40S ribosomal protein S16	x	x	x	x					x	x						-0.230	0.59	-0.005	0.99
P11142	HSP7C	Heat shock cognate 71 kDa protein	x	x	x	x	x			0.464								-0.126	0.75	0.019	1.05
Q92522	H1X	Histone H1x	x	x	x						x		x	x				0.178	1.51	0.004	1.01
P61313	RL15	60S ribosomal protein L15	x	x	x													-0.099	0.80	-0.055	0.88
P62906	RL10A	60S ribosomal protein L10a	x	x	x	x							x	x				0.119	1.32	0.103	1.27
P62424	RL7A	60S ribosomal protein L7a	x	x	x	x									x			0.061	1.15	-0.094	0.81
P61254	RL26	60S ribosomal protein L26	x	x	x	x												0.095	1.24	-0.052	0.89
P51991	ROA3	Heterogeneous nuclear ribonucleoprotein A3	x	x	x													-0.167	0.68	-0.130	0.74
P62917	RL8	60S ribosomal protein L8	x	x	x					0.278								-0.035	0.92	-0.038	0.92
P62269	RS18	40S ribosomal protein S18	x	x	x													0.023	1.05	0.104	1.27
P45880	VDAC2	Voltage-dependent anion-selective channel protein 2	x	x	x					0.282	x	x	x	x				-0.510	0.31	0.035	1.08
P61353	RL27	60S ribosomal protein L27	x	x	x	x												0.029	1.07	0.032	1.08
Q00325	MPCP	Phosphate carrier protein, mitochondrial	x	x	x	x	x		x		x	x	x	x				0.235	1.72	0.085	1.22
P26373	RL13	60S ribosomal protein L13	x	x	x	x												-0.079	0.83	-0.048	0.90
Q71DI3	H32	Histone H3.2	x	x	x						x	x	x					-0.699	0.20	0.137	1.37
P18077	RL35A	60S ribosomal protein L35a	x	x	x													0.036	1.09	-0.023	0.95
P62241	RS8	40S ribosomal protein S8	x	x	x													0.029	1.07	-0.050	0.89
Q9BPW8	NIPS1	Protein NipSnap homolog 1	x	x	x	x	x											0.025	1.06	0.080	1.20
P62244	RS15A	40S ribosomal protein S15a	x	x	x					0.291	x	x						-0.228	0.59	0.011	1.02
Q07020	RL18	60S ribosomal protein L18	x	x	x													0.010	1.02	-0.040	0.91
P62277	RS13	40S ribosomal protein S13	x	x	x					0.237								-0.008	0.98	0.017	1.04
Q14103	HNRPD	Heterogeneous nuclear ribonucleoprotein D0	x	x	x						x	x	x	x				0.441	2.76	0.113	1.30
P62899	RL31	60S ribosomal protein L31	x	x	x													0.020	1.05	-0.072	0.85
P62987	RL40	Ubiquitin-60S ribosomal protein L40	x	x	x		x				x	x	x					-0.662	0.22	0.044	1.11
Q16629	SRSF7	Serine/arginine-rich splicing factor 7	x	x	x													0.001	1.00	-0.054	0.88
P18621	RL17	60S ribosomal protein L17	x	x	x						x	x						-0.326	0.47	-0.129	0.74
P67809	YBOX1	Nuclease-sensitive element-binding protein 1	x	x	x						x		x	x				0.171	1.48	-0.037	0.92
P62873	GBB1	Guanine nucleotide-binding protein G(I)/G(S)/G(T) subunit beta-1		x		x	x				x	x	x					-0.576	0.27	-0.077	0.84
P62753	RS6	40S ribosomal protein S6	x	x	x													0.089	1.23	-0.246	0.57
P62913	RL11	60S ribosomal protein L11	x	x	x					0.365	x	x						-0.256	0.55	-0.017	0.96
P62841	RS15	40S ribosomal protein S15	x	x	x					0.328								-0.154	0.70	-0.071	0.85
P50914	RL14	60S ribosomal protein L14	x	x	x													0.024	1.06	0.129	1.35
P62847	RS24	40S ribosomal protein S24	x	x	x						x	x	x	x				0.300	2.00	-0.041	0.91
P83731	RL24	60S ribosomal protein L24	x	x	x								x					0.090	1.23	0.031	1.07
P63162	RSMN	Small nuclear ribonucleoprotein-associated protein N	x		x													0.149	1.41	0.156	1.43
P57088	TMM33	Transmembrane protein 33	x	x	x				x		x		x		x			0.197	1.57	0.217	1.65
P00403	COX2	Cytochrome c oxidase subunit 2	x	x	x	x			x				x					0.094	1.24	-0.024	0.95
P42766	RL35	60S ribosomal protein L35	x	x	x						x		x	x				0.233	1.71	-0.072	0.85
O14979	HNRDL	Heterogeneous nuclear ribonucleoprotein D-like	x	x	x													-0.090	0.81	-0.067	0.86
Q99880	H2B1L	Histone H2B type 1-L		x	x						x		x					-0.605	0.25	0.110	1.29
P61619	S61A1	Protein transport protein Sec61 subunit alpha isoform	x	x	x				x									-0.127	0.75	-0.015	0.97
Q01130	SRSF2	Serine/arginine-rich splicing factor 2	x	x	x						x	x	x	x				0.387	2.44	-0.046	0.90
P62266	RS23	40S ribosomal protein S23	x	x	x					0.349	x	x	x					0.146	1.40	0.026	1.06
Q71UI9	H2AV	Histone H2A.V	x	x	x						x	x	x	x				-0.656	0.22	0.053	1.13
P60866	RS20	40S ribosomal protein S20	x	x	x					0.438	x	x						-0.212	0.61	0.054	1.13
P02768	ALBU	Serum albumin	x	x	x					0.396			x		x	x		0.160	1.44	0.212	1.63
P68366	TBA4A	Tubulin alpha-4A chain	x	x	x						x	x	x	x				0.581	3.81	0.215	1.64
P62318	SMD3	Small nuclear ribonucleoprotein Sm D3	x	x	x													-0.079	0.83	-0.047	0.90
P12236	ADT3	ADP/ATP translocase 3	x	x	x				x				x					0.175	1.49	0.041	1.10

About two thirds of SWATH quantified proteins appear increased in this condition, and list of increased proteins include 4 of 5 SWATH queried cell surface proteins and all proteins where t-test found a significant difference between control and "H_2O_2 membrane" conditions. Analysing "H_2O_2 membrane" variation (Figure 4.15), it is observed that there is an equal quantity of proteins with increased and decreased values, though variation is very slim: there is not a protein having a 2 fold increase or decrease ($\log_{10} = \pm 0.301$); only three proteins present a 1.5-fold increase ($\log_{10} = 0.176$), and one protein presents a 1.5-fold decrease.

Furthermore, it was used the STRING 10 online tool for searching of PARK7 interactors: 16 of the proteins used for SWATH quantification are found among the 500 highest scoring PARK7 interactors; nine proteins registered a confidence score above 0.3 (being 1 the upper limit), and two of them were related to PARK7 with medium confidence, of score above 0.4 (Table 4.7). Also, protein IDA lists of each condition and SWATH protein list were subjected to identification of enriched gene ontology terms using GOrilla tool: contrary to what was expected, in almost all queries was observed a feeble enrichment of cell surface proteins, no increase regarding plasma membrane proteins, and a significant increase of intracellular proteins. It is implausible that insufficient washing of avidin resin during pull-down, since protein concentration of washing fractions was monitored using Nanodrop, and it could also be due to non-specific protein binding to avidin resin.

It can be consulted in Supplementary Data 8.7 detailed information regarding protein values normalised total intensity or internal standard and respective comparison over t-test and fold variation, distribution of proteins intensity values and %CV, comparison with IDA protein lists and Gorilla component enrichment diagrams.

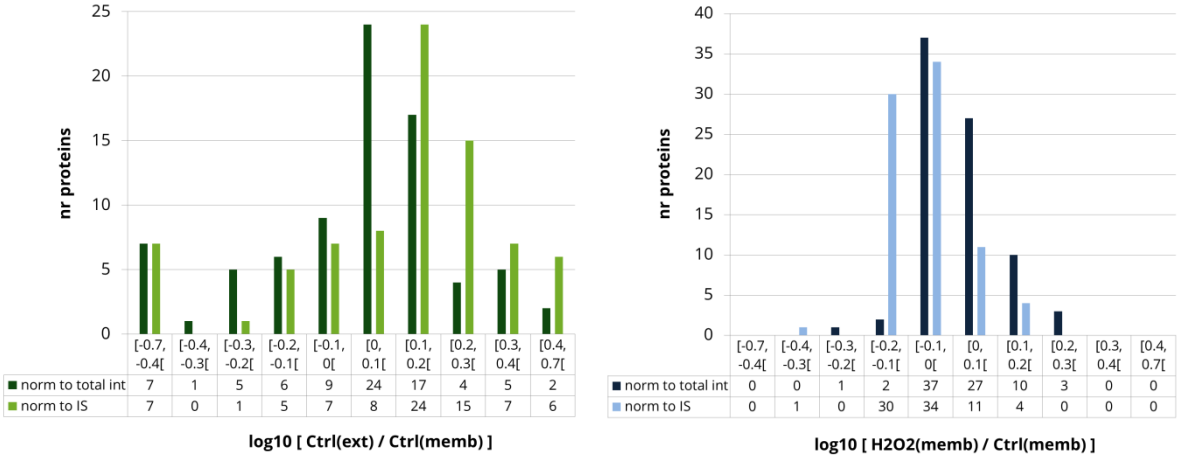

	[-0.7, -0.4[	[-0.4, -0.3[	[-0.3, -0.2[	[-0.2, -0.1[	[-0.1, 0[	[0, 0.1[	[0.1, 0.2[	[0.2, 0.3[	[0.3, 0.4[	[0.4, 0.7[
norm to total int	7	1	5	6	9	24	17	4	5	2
norm to IS	7	0	1	5	7	8	24	15	7	6

	[-0.7, -0.4[	[-0.4, -0.3[	[-0.3, -0.2[	[-0.2, -0.1[	[-0.1, 0[	[0, 0.1[	[0.1, 0.2[	[0.2, 0.3[	[0.3, 0.4[	[0.4, 0.7[
norm to total int	0	0	1	2	37	27	10	3	0	0
norm to IS	0	1	0	30	34	11	4	0	0	0

Figure 4.14 - Distribution of number of proteins according to logarithmic value of variation ratio of each quantified protein: at the left, variation of control extract against values of control membrane; at the right, variation of H_2O_2 membrane. Variation ratios determined from protein values previously normalized to total intensity (norm to total int) or to internal standard (IS).

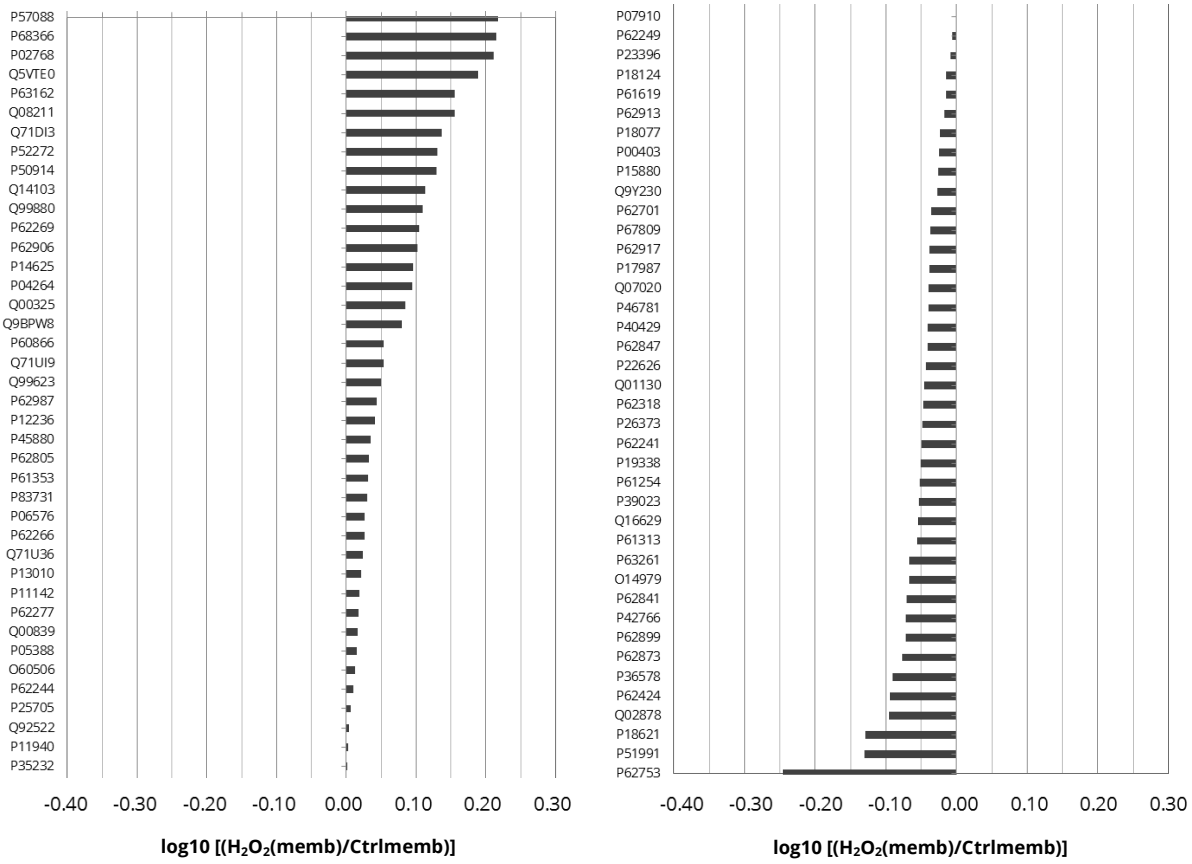

Figure 4.15 – Logarithmic value of the variation of quantified proteins in H_2O_2 membrane condition, by division of each mean protein value by respective values of control condition (control membrane). Protein intensity values of both conditions previously normalized to total intensity. Positive logarithmic values denote increased protein value from control to H_2O_2 condition, negative values a decreased protein value.

Table 4.8 – Description and characterization of proteins of interest, selected according to: protein values normalized to total intensity, with statistically significant difference, or above 1.5 fold decrease or increase, between H_2O_2 and control conditions; gene ontology attribution to cell surface (GO:0009986); PARK7 interactors with STRING score over 0.3. * = t-test with p-value under 0.01 between H_2O_2 and control; ** = p-value under 0.05.

		gene ontology				PARK7 STRING score	+1.5-fold increase	+1.5-fold decrease
		memb	plasma memb	cell surf	trans-memb			
* Serum albumin	P02768					0.396	x	
** Transmembrane protein 33	P57088				x		x	
** 60S ribosomal protein L6	Q02878	x						
** 60S ribosomal protein L7a	P62424	x						
Tubulin alpha-4A chain	P68366						x	
Putative elongation factor 1-alpha-like 3	Q5VTE0						x	
40S ribosomal protein S6	P62753							x
Nucleolin	P19338	x		x				
ATP synthase subunit beta, mitochondrial	P06576	x	x	x				
Heterogeneous nuclear ribonucleoprotein U	Q00839	x		x				
Prohibitin-2	Q99623	x		x				
Prohibitin	P35232	x	x	x		0.397		
60S ribosomal protein L13a	P40429	x				0.303		
T-complex protein 1 subunit alpha	P17987					0.323		
40S ribosomal protein S15	P62841					0.328		
40S ribosomal protein S23	P62266					0.349		
60S ribosomal protein L11	P62913					0.365		
40S ribosomal protein S20	P60866					0.438		
Heat shock cognate 71 kDa protein	P11142	x	x			0.464		

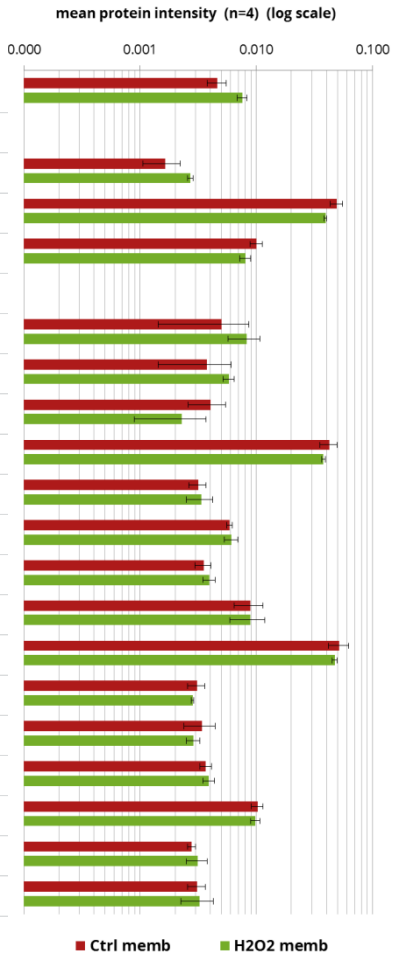

Figure 4.16 – Comparison of mean intensity values, normalized to total intensity, of replicates of control membrane (Ctrl memb) and H_2O_2 membrane (H2O2 memb), regarding proteins of interest of table 4. Negative and positive error bars of each condition corresponding to respective standard deviation (n=4)

Lastly, and taking in account all approaches performed for the analysis of protein variation between cultures stimulated in absence or presence of hydrogen peroxide, with ultracentrifugation of protein extract, it was selected a small group of proteins taking in account normalization to total intensity and the following criteria: statistical significance between conditions, with p-value lower than 0.05; 1.5-fold

increase or decrease of protein; attribution of cell surface ontology; predicted PARK7 interactors with confidence score over 0.3 (Table 4.8 and Figure 4.16). After the study of stress oxidative induced proteome variations in a Parkinson's disease *in vitro* model, these proteins would be of the utmost interest for further analysis of the effects regarding the extracellular addition and intake of native and mutant DJ-1 forms.

Overall, though MS analysis didn't demonstrate a competent enrichment of cell surface proteins using the current biotinylation and avidin pull-down protocol, contradicting previous performed blotting and fluorohistochemistry assays that assure the labelling of cell surface proteins, it still permitted the detection of some proteome variations as a result of oxidative stress SH-SY5Y induction.

5. Discussion

Parkinson's disease is a neurodegenerative disorder of idiopathic origins, with two histological hallmarks: the selective decrease reduction of the dopaminergic neurons at the *substancia nigra pars compacta*, associated with the depletion of dopamine levels, and the appearance of Lewy structures resulting from the deposition of insoluble proteins [6]. There are some protective and risk environmental factors attributed to the onset of the pathology, but several key mechanisms by which these affect the neurons remain largely unknown [2]. Nevertheless, there are two main histological events correlated to neurodegeneration: protein aggregation; and oxidative stress related mitochondria impairment [3]. Also, recent studies have been contributing for the association of a growing number of several genes to PD onset - one of which is DJ-1. This protein has a multiprotective role, which includes protection from oxidative insults, maintenance of mitochondria integrity and prevention of protein aggregation [29], [49].

DJ-1 gene can present several mutations that lead to the expression of a protein with structural and/or biological impairments, associated to the onset of some cases of familial PD – including missense mutations M26I, present in a conservative region of the protein core and resulting in decreased dimer stability, and E163K, which also affects dimerization due to disruption of salt bridge and has an additional impairment of mitochondria translocation for oxidative stress protection [55], [86]

For the study of these mutations in the context of Parkinson's disease, it was firstly produced and purified protein solutions of M26I and E163K mutant forms of human DJ-1 protein, for its use on future application in studies based on *in vitro* models of the pathology. SH-SY5Y neuroblastoma cell line has been often used in Parkinson's disease related research, since they possess several dopaminergic neuron features, and demonstrate decreased cell viability after induction of oxidative stress with hydrogen

peroxide or PD related oxidants, among other cytological features correlated with *in vivo* PD onset [145], [146], [153].

The production of DJ-1 mutant forms was based on the construction of a previously prepared recombinant plasmids, for the expression of the included human WT DJ-1 protein recombined with a N-terminal hexahistidine affinity tag; this plasmid was then modified with site-directed mutagenesis, based on PCR replication with mutation containing primers, for expression of M26I or E163K DJ-1 recombinant protein; plasmids were then transformed onto an *E. coli* culture for the high-throughput expression of the recombinant protein, based on an IPTG induction system; protein was then separated from cell extract using immobilized metal-affinity chromatography for the capture of his-tagged M26I/E163K DJ-1, then subjected to size-exclusion chromatography for the exclusion of other oligomerization modes besides the homodimer, characteristic of DJ-1 (Figure 4.1 and 4.3). These techniques have all been applied previously for the a large scale production of proteins, particularly of wild-type and mutant forms of DJ-1 [86], [114], [116], [154], [155].

Analysis of the expression and purification process, using SDS-PAGE monitorization of the 20-25 kDa band, attributed to DJ-1 monomer [84], in collected samples, revealed that the production and purification procedure was performed with success (Figure 4.2 and 4.4). Either in M26I or E163K DJ-1 production, it is seen an increased expression after IPTG addition to culture medium, and an effective loading of HisTrap column for affinity chromatography. Though the collected analyzed chromatography elution fractions detected the presence of DJ-1 protein, the following size-exclusion chromatography demonstrated a proper purification of the protein. Furthermore, coomassie and silver staining of prepared stock solutions, compared also to already existent stock solution of WT-DJ1 (Figure 4.5), demonstrated an almost exclusive presence of DJ-1, with presence of a minor fraction of contaminants.

It followed an MS analysis of all three forms of DJ-1 protein, WT, M26I and E163K (stored in protein vehicle, PBS with 5% glycerol) with IDA acquisition, for identification of DJ-1 and contaminants presents in stock solutions (Table 4.1, Supplementary Data 8.2). Besides the use of a holistic Swissprot database as a protein library, it was

used a customized protein library, with the addition of FASTA entries describing several synthetic and natural DJ-1 mutations. Also, the section containing DJ-1 attributed band was analyzed separately from the rest of the gel lane in any of the samples, where DJ-1 was the most identified protein, having the highest MS protein summary values (unused score, number of identified peptides, percentage of sequence coverage) and trypsin was the only detected contaminant (Supplementary Table 8.2 and 8.3, Supplementary Figure 8.2). Furthermore, the use of the customized database allowed the direct identification of mutant DJ-1: with standard protein database, WT DJ-1 registered almost 98% of protein coverage, and M26I and E163K DJ-1 showed decreased values in; using database with DJ-1mutations, both produced forms were identified with 100% protein coverage. In other sections of the gel lane of any sample, DJ-1 was still the second most identified protein (though with decrease of MS protein summary values), and it was identified several other contaminants: human keratin, 8 different *E. coli* proteins (most of which ribosomal) and 18 eukaryotic proteins, 14 of which attributed to *Bos taurus* or *Rattus norvegicus*. Trypsin and keratine are inherent to sample processing for MS analysis, and the others can be associated to the host and culture medium used for protein production. Since contaminants represent a minor, and innocuous, fraction of the identified proteins, and given the efficient identification of DJ-1 protein sequences, all three stock solutions of WT, M26I and E163K DJ-1 were all considered adequate for further characterization.

DJ-1 native form is mainly found in a solution or in a cellular milieu with a homodimeric form, which is essential for the protein to exert its protective role; though M26I and E163K mutations result in a destabilization of DJ-1 quaternary structure, it does not cause major structural changes or loss of the dimeric form in solution [86], [113], [114], [116]. Since it is a determinant feature expected to be found in WT, M26I and E163K forms, all DJ-1 protein samples were then subjected to SEC-HPLC analysis, in non-denaturant conditions, for the determination of the molecular weight of the quaternary structure (Figure 4.6 and Table 4.2). WT and M26I solutions registered a MW of aproximatelly 60 kDa and 59 kDa, respectively, which was considered to be translation as the presence of both forms in a dimeric form; E163K solutions presented

34 kDa, which is closer to the expected DJ-1 dimer MW, but much lower than other DJ-1 forms. A second chromatography was performed for comparison of produced E163K with previously produced protein, already demonstrated to be in solution as a dimer: since it actually registered a slightly larger MW, produced E163K was considered to exist in solution as a dimer (Figure 4.7 and Table 4.3). Overall, it was assured that the native and both mutant forms are still able of homodimerization, which is essential for the maintenance of several structural and biological features of the protein. These proteins can then be used in the future to study DJ-1 mediated neuroprotection against oxidative stress induced cell death and *in vitro* proteome studies.

There are several *in vitro* assays that already reported the protective effects of DJ-1 in a cellular milieu, in a model of Parkinson's disease: DJ-1 downregulation or knockdown in neuron cells resulted in its susceptibility to death induced by hydrogen peroxide, and overexpression of WT DJ-1 confers oxidative stress protection [102], [145], [146], [156], [157]; besides, it has also been demonstrated neuroprotection from oxidative stress with the extracellular presence of WT DJ-1 [146], [147], [156], [158], [159]. In addition, M26I and E163K DJ-1 mutations have been related to an increased cell death after exposure to oxidative insults, as a result of a compromised biological role [92], [116]. Regarding this, it was evaluated the viability of SH-SY5Y cells in oxidative stress conditions, with exogenous addition of 50 μM hydrogen peroxide, and in the extracellular presence of WT, M26I or E163K DJ-1 proteins, to address the biological features of the produced protein in such conditions (Figure 4.8). It was added 1μM of each DJ-1 form to the culture medium of SH-SY5Y cultures, and proteins were concentrated previously to 1.2 mg/mL to be used equal volumes of DJ-1 protein solutions and to nullify any protective effect that could arise from the presence of glycerol from the protein vehicle [160], [161]. The presence of equal amount of recombined WT, M26I and E163K also nulls effects from histidine tag. In absence of added DJ-1 protein, there is a significant decrease of SH-SY5Y viability from normal to oxidative stress conditions, of almost 30%. But in the extracellular presence of WT DJ-1, cell viability is maintained, with a significant difference between viability of control and WT DJ-1 in oxidative stress. Considering DJ-1 mutations, M26I and E163K register a

significant cell decrease viability in oxidative stress, when compared to the respective condition of hydrogen peroxide absence, or to the viability registered in the condition of oxidative stress and WT DJ-1 addition. These results demonstrate the expected neuroprotection provided by WT DJ-1, and the possibility to use 50 μM hydrogen peroxide in further studies for replication of oxidative stress. Also, it was possible to observe a decrease cell viability as a result of the extracellular addition of M26I and E163K mutant forms of DJ-1 when compared to the wild-type form, being related with an impaired provision of self-oxidation for ROS scavenging, mitochondria integrity maintenance and apoptosis inhibition, which results in higher oxidative sensitivity associated with Parkinson's disease [109], [158], [159]. Particularly, in oxidative stress conditions, M26I DJ-1 also presents significantly higher cell viability when compared to protein absence.

All of these characterization assays were then very valuable to confirm the adequacy of the structure of produced proteins M26I and E163K DJ-1, with confirmation of the primary and quaternary structure of WT, M26I and E163K DJ-1, and also to differentiate the biological effects between mutants and DJ-1 native form, in order to be able to use M26I and E163K DJ-1 solutions in future *in vitro* studies to analyze the Parkinson's disease associated mutations.

There are studies suggesting an astrocyte mediated protection of neurons from oxidative stress: DJ-1 is largely expressed in astrocytes, more than in neurons, and oxidative stress can lead to a modulation for increased release of DJ-1 to exert its neuroprotective role [147], [158], [162]. But it is still not known the mechanisms by which DJ-1 is assimilated by neurons, how oxidative stress increases DJ-1 intake, or whether DJ-1 mutations could affect this process and lead to the neurodegeneration associated with PD. Therefore, in a second phase of this study it was developed a protocol based on biotinylation and avidin affinity chromatography, to allow the enrichment of the cell surface proteome and its MS analysis in sample of reduced complexity. This would be applied for a comparison of normal and pathological conditions in a SH-SY5Y Parkinon's disease model, which could lead to the identification of cell surface proteins modulated by the existence of oxidative stress or

intake of DJ-1 native or mutant forms, providing new data over the pathological and DJ-1 protective mechanisms in dopaminergic neurons.

The use of biotin for labelling of antibodies, proteins, nucleic acids or other biomolecules, companied with a downstream use of avidin (labelled with a detectable molecule or immobilized for the capture of biotinylated compounds in a complex mixture) has been extensively used for a large variety of bioanalytical purposes, such as immunological or immunohystochemical assays, and nucleic acid hybridization assays [142], [163]. The use of Sulfo-NHS-LC-biotin, soluble in water and impermeable to the membrane, has also proven to deliver an effective *in vitro* labelling of cell surface proteins and downstream avidin pull-down for a collection of an enriched fraction to be analyzed using mass spectrometry, for example, which can aid on the identification of surface markers or signaling proteins [139], [164]–[166]. The biotinylation and pull-down procedure has inclusively been applied in SH-SY5Y cell line for the MS analysis; though the technique was not used for the study of dynamic proteomics, particularly resulted from oxidative stress or DJ-1 induced variations related to Parkinson's disease [151], [152].

In order to achieve a high-yield enrichment of cell surface proteins, it is necessary to guarantee: the application of a biotinylation procedure that labels proteins located exclusively at the cell surface, and with the least cell detachment or lysis; performance of an avidin pull-down with low non-specific binding capacity, with an effective elution technique for the capture of biotinylated proteins, for MS analysis. The execution of such demonstrative assays require the use of compounds capable of biotin detection, which are generally based on the binding capacity of biotinylated proteins to avidin: use of the direct spectrophotometry analysis of competition of biotin with other avidin ligand, such as the often used 4'-hydroxyazobenzene-2-carboxylic acid (HABA)-avidin complex [167]; or direct detection of avidin binding to biotin, such as streptavidin b-phycoerythrin (SAPE) conjugate. Due to its availability, it was used SAPE for the performance of the demonstrating assays: it is commonly used in microarrays, immunohistological microscopy and flow cytometry, and though its application is usually based on binding of biotinylated antibodies for protein indirect detection, other

similar staining probes such as streptavidin conjugated with horseradish peroxidase are described for the direct labelling of proteins in blotting assays [168]–[173]. Due to the use of SAPE in techniques not often reported for its use, several steps were performed to assure the in-gel and in vivo direct detection of biotinylated proteins.

A dot blot analysis confirmed a successful detection of biotinylated proteins with SAPE detection, with direct SAPE staining and fluorescence observation in samples of biotinylated WT DJ-1 and its absence in non-biotinylated protein (Supplementary Data 8.4). This could then be used to detect biotinylated proteins in complex samples, which was then applied for blotting methods, in order to make several assessments regarding the cell surface enrichment process. After SH-SY5Y cell plating, biotinylation was performed with Sulfo-NHS-LC-biotin prepared in PBS, an isotonic buffer of intended use, or prepared in water, in order to have a comparative analysis of the procedure when having an extensive cell lysis - which results in a non-specific biotinylation and great loss of proteins onto biotin and quenching solutions. It was then performed an avidin pull-down for collection biotinylated proteins present in protein extract and solutions of biotinylation incubations, named Tris+biotin. It was used three different capture techniques - elution with d-biotin solution, glycine solution, and resin denaturation - since the use of monomeric avidin allows the release of biotinylated proteins without using denaturing conditions [133], [152]. It was then performed silver and SAPE staining of samples collected throughout all pull-downs, for the detection of total and biotinylated proteins, respectively (Figure 4.9). It was then inferred that direct resin denaturation is the most effective method to gather biotinylated proteins, since other elution fractions of any pull-down showed residual detection of SAPE signaling. Also, it was confirmed the use of PBS as the solvent for preparation of Sulfo-NHS-LC-biotin solution, due to the absence of biotinylated or total proteins in any sample of respective Tris+biotin pull down, on the contrary to biotinylation with water where it is noticed an approximately equal quantity of proteins in collected Tris+biotin and protein extract. In addition, the presence of biotinylated protein in the first washing fraction of several pull-downs implies the necessity of increasing resin quantity on each

pull-down, or the performance of a separated pull-down for this fraction, to collect remaining biotinylated proteins.

Afterwards, biotinylation was observed in microscope based assays, for the localization of the Sulfo-NHS-LC-biotin reaction sites in biotinylated *in vitro* HeLa culture. Firstly, microscope fluorescence observation of HeLa cultures incubated with Sulfo-NHS-LC-biotin, or solely with its used biotin solvent, PBS, proved the biotin reactivity and binding to HeLa proteins, given the detection of fluorescence in biotinylated cultures – opposed to the absence of SAPE fluorescence in the negative control (Figure 4.10). Also, dot blot analysis and fluorescence microscope denoted SAPE reduced photostability, given the rapid loss of fluorescence signal in both procedures. Since image quality was insufficient to discern an exclusive labelling of HeLa cell surface, it used confocal microscopy to reduce the background noise of fluorescence emission in other planes below and above the focal point [174]. As expected, it was possible to observe the sole fluorescence emission in biotinylated HeLa cells (Figure 4.13), and a z-stack imaging confirmed the sole fluorescence emission of the surface of HeLa cells, with absence in the intracellular milieu, demonstrating Sulfo-NHS-LC-biotin lack of membrane permeability and reaction to cell surface proteins (Figure 4.14).

Having in consideration previous SH-SY5Y cell surface biotinylation assays [151], [152] and data obtained from previous assays, it was established the following protocol for cell surface enrichment: after SH-SY5Y plating and 24 hour incubation, culture medium exchange to stimulating medium containing reduced serum amount and addition of hydrogen peroxide, for oxidative stress, and/or different forms of DJ-1; after 24 hour starvation, removal of culture medium and plate PBS washing; 15 min incubation with 10 mL 0.5 mM Sulfo-NHS-LC-biotin solubilized in PBS; plate washing with TBS; cell scraping with 2 mL RIPA buffer, removal of cell debris and protein extract subjection to Vivaspin tubes for biotin removal and buffer exchange to PBS; 16 hour incubation with 100 µL Monomeric Avidin Resin, with centrifugation for supernatant discard and about 5 resin washes with 1 mL PBS; elution of biotinylated proteins with Sample Buffer addition and 5 min incubation in 95 ºC; SDS-PAGE separation of resin

supernatant, and in-gel digestion with trypsin; LC-MS/MS analysis of obtained peptides, with IDA and SWATH acquisition, for the identification and quantification of cell surface protein profiles attributed to different SH-SY5Y incubation conditions. It was also yet to be defined the inclusion of an ultracentrifugation process as an alternative for Vivaspin centrifugal concentration before pull-down, since this step would allow a removal of soluble fraction and collection of a crude membrane fraction, to reduce sample complexity and increase MS identification of membrane proteins [120], [135].

To access the capacity of this procedure for the detection of proteome variations in SH-SY5Y cell surface related to Parkinson's disease pathological conditions (oxidative stress, extracellular presence of WT, E163K or M26I DJ-1), it was experimented for the comparison of control and oxidative stress conditions, without the addition of DJ-1 protein. It was also included the ultracentrifugation of protein extract for both conditions (Ctrl membrane, H_2O_2 membrane), and performed a third control condition without subjection of biotinylated protein extract to ultracentrifugation (Ctrl extract). Four replicates of each condition were processed and analyzed in LC-MS/MS, with IDA and SWATH acquisition. IDA acquisition processing of samples (Table 4.4, Figure 4.13) resulted in the identification of 629 proteins in "Ctrl membrane" condition, 531 proteins in "H_2O_2 membrane" condition and 544 in "Ctrl extract", having 332 proteins in common to all conditions. Comparing the ultracentrifugation procedure, with "Ctrl extract" and "Ctrl membrane" analysis, more proteins were identified in the later and registered a slight increase in the number and percentage of proteins with ontologies attributed to membrane, plasma membrane, cell surface and with α-transmembrane prediction. Furthermore, "H_2O_2 membrane" registered 98 less proteins than "Ctrl membrane", but both conditions had similar percentage of gene ontology attribution: 70% of membrane proteins, 18% of plasma membrane, 4% of cell surface proteins and 15% of proteins with α-transmembrane prediction. SWATH acquisition processing resulted in the quantification of a total of 80 proteins, almost all of them identified in all three conditions in IDA acquisition (Table 4.6). Of those, 61 are attributed to the membrane, 14 to plasma membrane and 5 to cell surface proteins Comparing SWATH quantification list with IDA protein lists, it is observed a tenuous increase of the

percentage of such ontologies (Table 4.5). Five proteins with α-transmembrane prediction were identified, and 16 proteins were found to be predicted interactors with PARK7, two of them having a medium confidence score (Table 4.7). To study protein variations, “Ctrl membrane” was considered the control condition for the analysis of “Ctrl extract” and “H_2O_2 membrane”. The total intensity normalization option was used for each replicate, since protein average registered a lower coefficient of variation between replicates, in three conditions (Table 4.6), and t-test for inter-condition comparison of protein values presented more relevant results (Table 4.7). Four proteins were found with statistically significant difference from control to oxidative stress condition: increase of serum albumin and transmembrane protein 33, and decrease of 60S ribosomal protein L6 and L7a. All registered a p-value under 0.05, and serum albumin registered a p-value of under 0.01 (Table 4.7 and 4.8). Considering fold variations between such conditions, there was no protein with over 2-fold increase or decrease; four proteins registered a 1.5-fold increase, and one protein a 1.5-fold decrease (Figure 4.15). After the combination of such proteins with to identified cell surface proteins and proteins with PARK7 interaction prediction score above 0.3, it was concluded a subset of 20 proteins of interest (Table 4.8 and Figure 4.16), which could be relevant targets when proteomics studies advance for comparison of conditions with WT/mutant DJ-1 addition and oxidative stress induction.

The DJ-1 protective activity against glyoxal or methylglyoxal induced death has been shown, converting it to glycolic or lactic acid derivatives, respectively, and was also reported the contribution of oxidative stress to the glyoxal cytotoxic mechanism [101], [175]. Besides being the only with p-value under 0.01, though not attributed to the plasma membrane or cell surface, serum albumin becomes all the more relevant due to the recent report of DJ-1 capacity to deglycate and repair methylglyoxal- and glyoxal-glycated amino acids in three major glycated residues (cysteines, arginines and lysines) of certain proteins including serum albumin, being able to repair such proteins and restore cell viability [176].

Comparing data from “Ctrl extract” and membrane conditions, it becomes debatable the use of ultracentrifugation before pull-down. IDA acquisition identified

less proteins in control extract condition, and had more unfavorable gene ontology attributions (Table 4.4). On the other hand, about two thirds of SWATH quantified proteins appear increased from “Ctrl membrane” to “Ctrl extract” condition, which includes four of five quantified cell surface proteins and all proteins where t-test found a significant difference between control and “H_2O_2 membrane” conditions (Table 4.6). Among the 20 proteins designated as of interest after SWATH quantification (Table 4.8), t-test between “Ctrl extract” and membrane conditions indicated that the absence of ultracentrifugation contributed to a statistically significant increase of seven of those proteins, and decrease of three proteins (Table 4.6). The discordance of such data compels for the repetition of the study of oxidative stress induced proteome variations with absence of ultracentrifugation processing of protein extract, in order to see if it provides MS data capable of a better distinction between normal and PD related conditions, to advance for the detection of cell surface variations modulated by wild-type and mutant forms of DJ-1.

In addition, the analysis of protein lists from IDA identification and SWATH quantification with GOrilla gene ontology enrichment (Supplementary Data 8.31 to 8.34), added to the comparison to previous MS studies regarding SH-SY5Y cell surface biotinylation [151], [152], lead to the conclusion that the used protocol for biotinylation and avidin pull-down did not permit a considerable enrichment for identification of a high number of cell surface or plasma membrane proteins. Since the executed assays confirmed a competent biotin reaction with cell surface proteins, problems may arise from avidin pull-down step, with inability of the removal of non-biotinylated proteins or complete removal of biotinylated proteins retained in monomeric avidin. This is often the limiting step of separation procedures based on avidin-biotin interaction, which could be remediated with the use of alternative biotinylating compounds, for example biotin derivatives with a cleavable spacer arm, or pull-down with other resins such as tetrameric avidin, streptavidin or neutravidin [134], [139], [177], [178].

Nevertheless, the designed procedure permitted the identification of some protein variations between normal and oxidative stress, with the use of ultracentrifugation: though such variations were not found for most proteins, it was still

found a significant difference in four proteins, and other 16 proteins may provide relevant data for the study of cell surface variations resulted from the extracellular presence of WT/mutant DJ-1 in an *in vitro* PD related model. This proteomic study, to be performed in the future, may then be executed with the current designed procedure, but it is more prudent the execution of more assays to assure the use of an optimized protocol that allows the maximum enrichment of cell surface proteins and high-yield detection of proteome variations that grant the identification of surface signal proteins related to oxidative stress feedback, DJ-1 intake and mutant impairment, and thereby Parkinson's disease molecular mechanisms.

6. Conclusion

This study had two main objectives: the production of recombinant mutant forms of DJ-1, M22I and E163K, natural occurring and associated with PD; and the development of a biotinylation process, coupled with avidin pull-down, for the enrichment of cell surface proteins. The designed enrichment protocol was then used on an *in vitro* model of the disease for the analysis of the subcellular proteome outcome resulted from oxidative stress, a histological hallmark of PD physiology and a main pathological feature to which DJ-1 has a protective role.

In the first part of the project, the production of stock solutions of M26I and E163K DJ-1 was performed with success, according to the SDS-PAGE analysis of the protein expression and purification process. An LC-MS/MS characterization of the stock solutions also confirmed the primary structure of M26I and E163K DJ-1, with total sequence coverage and distinction of each DJ-1 mutations, and also demonstrated that stock solutions did not contain any relevant contaminant that could quench or interfere with DJ-1 activity. SEC-HPLC allowed the identification of the quaternary structure, with attribution of the dimeric forms for both produced DJ-1 mutants, similar to WT. Lastly, SH-SY5Y viability assays in oxidative stress conditions and after exogenous addition of WT, M26I and E163K forms of DJ-1 demonstrated that the mutations have an impaired protective role when compared to the native form.

On a second phase of the project, it was delineated a protocol for the enrichment of cell surface proteins using the biotinylation and avidin pull-down procedure, which was then verified using several assays: dot blot confirmed the fluorescence detection of biotinylated proteins with SAPE incubation; western blotting and experimental LC-MS/MS and viability assays permitted to confirm the use of PBS for solubilisation of Sulfo-NHS-LC-biotin, quenching with TBS, collection of proteins retained by monomeric avidin resin using denaturing conditions; protein in-gel digestion with trypsin;

fluorescence and confocal microscopy confirmed biotin low membrane permeability and specific labelling of proteins located in the cell surface. The use of ultracentrifugation as an alternative for centrifugal concentration of biotinylated protein extract, with the benefit of allowing the downstream pull-down of a simplified crude membrane subcellular part of the protein extract, provided some discordant results in regard of increased protein identification or quantification and cell surface enrichment. The outlined procedure, with inclusion of ultracentrifugation, was then expected to be able of a more thorough LC-MS/MS detection of alterations in the cell surface proteome in the used *in vitro* model caused by pathological conditions of oxidative stress. Such analysis allowed the IDA identification of about 600 proteins in assayed conditions and SWATH quantification of 80 proteins. From the latter, it was selected 20 proteins of special interest for PD studies, of which four proteins were found to be significantly varied from normal to oxidative stress condition: serum albumin, transmembrane protein 33, and 60S ribosomal protein L6 and L7a.

Despite the detection of some proteome variations, the procedure did not provide satisfactory results regarding the identification and quantification of cell surface proteins, requiring a future research for optimization of protocol, namely the use of biotin or avidin alternatives. Eventually, a biotin-avidin based protocol could allow a comprehensive analysis of the effect of exogenous addition of wild-type or mutant forms of DJ-1, in order to establish relations between the neuron intake of DJ-1 and the modulating effects of oxidative stress or DJ-1 mutation in this process, potentially leading to the discovery of any relation with the neurodegenerative process responsible to the development of Parkinson’s disease.

7. Bibliography

[1] J. Parkinson, *An Essay on the Shaking Palsy*. Whittingham and Rowland, 1817.

[2] L. de Lau and M. Breteler, “Epidemiology of Parkinson’s disease,” *Lancet Neurol.*, vol. 5, no. June, pp. 525–535, 2006.

[3] W. Dauer and S. Przedborski, “Parkinson’s disease: mechanisms and models,” *Neuron*, vol. 39, pp. 889–909, 2003.

[4] U. B. Muthane, H. S. Swamy, P. Satishchandra, M. N. Subhash, S. Rao, and D. Subbakrishna, “Early onset Parkinson’s disease: are juvenile- and young-onset different?,” *Mov. Disord.*, vol. 9, no. 5, pp. 539–44, Sep. 1994.

[5] A. Janca, “Parkinson’s disease from WHO perspective and a public health point of view,” *Parkinsonism Relat. Disord.*, vol. 9, no. 1, pp. 3–6, Oct. 2002.

[6] A. J. Lees, J. Hardy, and T. Revesz, “Parkinson’s disease.,” *Lancet*, vol. 373, no. 9680, pp. 2055–66, Jun. 2009.

[7] S.-Y. Chen and S.-T. Tsai, “The Epidemiology of Parkinson’s Disease,” *Tzu Chi Med. J.*, vol. 22, no. 2, pp. 73–81, Jun. 2010.

[8] S. Muzerengi, D. Contrafatto, and K. R. Chaudhuri, “Non-motor symptoms: identification and management.,” *Parkinsonism Relat. Disord.*, vol. 13 Suppl 3, pp. S450–6, Jan. 2007.

[9] D. Aarsland, J. Zaccai, and C. Brayne, “A systematic review of prevalence studies of dementia in Parkinson’s disease.,” *Mov. Disord.*, vol. 20, no. 10, pp. 1255–63, Oct. 2005.

[10] A. J. Hughes, S. E. Daniel, and A. J. Lees, “Improved accuracy of clinical diagnosis of Lewy body Parkinson’s disease,” *Neurology*, vol. 57, no. 8, pp. 1497–1499, Oct. 2001.

[11] L. . Shulman, R. . Taback, A. . Rabinstein, and W. . Weiner, “Non-recognition of depression and other non-motor symptoms in Parkinson’s disease,” *Parkinsonism Relat. Disord.*, vol. 8, no. 3, pp. 193–197, Jan. 2002.

[12] I. Litvan, K. P. Bhatia, D. J. Burn, C. G. Goetz, A. E. Lang, I. McKeith, N. Quinn, K. D. Sethi, C. Shults, and G. K. Wenning, “Movement Disorders Society Scientific Issues Committee report: SIC Task Force appraisal of clinical diagnostic criteria for Parkinsonian disorders.,” *Mov. Disord.*, vol. 18, no. 5, pp. 467–86, May 2003.

[13] P. Damier, “The substantia nigra of the human brain: II. Patterns of loss of dopamine-containing neurons in Parkinson’s disease,” *Brain*, vol. 122, no. 8, pp. 1437–1448, Aug. 1999.

[14] H. Bernheimer, W. Birkmayer, O. Hornykiewicz, K. Jellinger, and F. Seitelberger, “Brain dopamine and the syndromes of Parkinson and Huntington Clinical, morphological and neurochemical correlations,” *J. Neurol. Sci.*, vol. 20, no. 4, pp. 415–455, Dec. 1973.

[15] G. R. Uhl, D. Walther, D. Mash, B. Faucheux, and F. Javoy-Agid, “Dopamine transporter messenger RNA in Parkinson’s disease and control substantia nigra neurons.,” *Ann. Neurol.*, vol. 35, no. 4, pp. 494–8, Apr. 1994.

[16] P. L. McGeer and E. G. McGeer, “Inflammation and neurodegeneration in Parkinson’s disease.,” *Parkinsonism Relat. Disord.*, vol. 10 Suppl 1, pp. S3–7, May 2004.

[17] S. Greffard, M. Verny, A.-M. Bonnet, D. Seilhean, J.-J. Hauw, and C. Duyckaerts, “A stable proportion of Lewy body bearing neurons in the substantia nigra suggests a model in which the Lewy body causes neuronal death.,” *Neurobiol. Aging*, vol. 31, no. 1, pp. 99–103, Jan. 2010.

[18] H. Braak, D. Sandmann-Keil, W. Gai, and E. Braak, “Extensive axonal Lewy neurites in Parkinson’s disease: a novel pathological feature revealed by α-synuclein immunocytochemistry,” *Neurosci. Lett.*, vol. 265, no. 1, pp. 67–69, Apr. 1999.

[19] K. Wakabayashi, K. Tanji, F. Mori, and H. Takahashi, “The Lewy body in

Parkinson's disease: Molecules implicated in the formation and degradation of α-synuclein aggregates," *Neuropathology*, vol. 27, no. 5, pp. 494–506, Oct. 2007.

[20] T. P. Harrower, A. W. Michell, and R. A. Barker, "Lewy bodies in Parkinson's disease: protectors or perpetrators?," *Exp. Neurol.*, vol. 195, no. 1, pp. 1–6, Sep. 2005.

[21] B. I. Giasson, J. E. Duda, I. V Murray, Q. Chen, J. M. Souza, H. I. Hurtig, H. Ischiropoulos, J. Q. Trojanowski, and V. M. Lee, "Oxidative damage linked to neurodegeneration by selective alpha-synuclein nitration in synucleinopathy lesions.," *Science*, vol. 290, no. 5493, pp. 985–9, Nov. 2000.

[22] M. Y. Sherman and A. L. Goldberg, "Cellular defenses against unfolded proteins: a cell biologist thinks about neurodegenerative diseases.," *Neuron*, vol. 29, no. 1, pp. 15–32, Jan. 2001.

[23] P. M. Keeney, J. Xie, R. A. Capaldi, and J. P. Bennett, "Parkinson's disease brain mitochondrial complex I has oxidatively damaged subunits and is functionally impaired and misassembled.," *J. Neurosci.*, vol. 26, no. 19, pp. 5256–64, May 2006.

[24] J. Clark, Y. Dai, and D. Simon, "Do somatic mitochondrial DNA mutations contribute to Parkinson's disease?," *Parkinsons. Dis.*, 2011.

[25] G. COHEN, "Oxidative Stress, Mitochondrial Respiration, and Parkinson's Disease," *Ann. N. Y. Acad. Sci.*, vol. 899, no. 1, pp. 112–120, Jan. 2006.

[26] S. Pennathur, V. Jackson-Lewis, S. Przedborski, and J. W. Heinecke, "Mass Spectrometric Quantification of 3-Nitrotyrosine, ortho-Tyrosine, and o,o'-Dityrosine in Brain Tissue of 1-Methyl-4-phenyl-1,2,3,6-tetrahydropyridine-treated Mice, a Model of Oxidative Stress in Parkinson's Disease," *J. Biol. Chem.*, vol. 274, no. 49, pp. 34621–34628, Dec. 1999.

[27] M. C. Rodriguez-Oroz, M. Jahanshahi, P. Krack, I. Litvan, R. Macias, E. Bezard, and J. a Obeso, "Initial clinical manifestations of Parkinson's disease: features and pathophysiological mechanisms.," *Lancet. Neurol.*, vol. 8, no. 12, pp. 1128–39, Dec. 2009.

[28] J. A. Obeso, M. C. Rodríguez-Oroz, M. Rodríguez, J. L. Lanciego, J. Artieda, N.

Gonzalo, and C. W. Olanow, “Pathophysiology of the basal ganglia in Parkinson’s disease.,” *Trends Neurosci.*, vol. 23, no. 10 Suppl, pp. S8–19, Oct. 2000.

[29] a Wood-Kaczmar, S. Gandhi, and N. W. Wood, “Understanding the molecular causes of Parkinson’s disease.,” *Trends Mol. Med.*, vol. 12, no. 11, pp. 521–8, Nov. 2006.

[30] S. K. Van Den Eeden, “Incidence of Parkinson’s Disease: Variation by Age, Gender, and Race/Ethnicity,” *Am. J. Epidemiol.*, vol. 157, no. >11, pp. 1015–1022, Jun. 2003.

[31] S. von Campenhausen, B. Bornschein, R. Wick, K. Bötzel, C. Sampaio, W. Poewe, W. Oertel, U. Siebert, K. Berger, and R. Dodel, “Prevalence and incidence of Parkinson’s disease in Europe.,” *Eur. Neuropsychopharmacol.*, vol. 15, no. 4, pp. 473–90, Aug. 2005.

[32] R. L. Nussbaum and C. E. Ellis, “Alzheimer’s Disease and Parkinson's Disease,” *N. Engl. J. Med.*, vol. 348, no. 14, pp. 1356–1364, 2003.

[33] F. Raudino, “The Parkinson disease before James Parkinson.,” *Neurol. Sci.*, vol. 33, no. 4, pp. 945–8, Aug. 2012.

[34] D. Twelves, K. S. M. Perkins, and C. Counsell, “Systematic review of incidence studies of Parkinson’s disease.,” *Mov. Disord.*, vol. 18, no. 1, pp. 19–31, Jan. 2003.

[35] R. Saunders-Pullman, “Estrogens and Parkinson disease: neuroprotective, symptomatic, neither, or both?,” *Endocrine*, vol. 21, no. 1, pp. 81–7, Jun. 2003.

[36] K. Wirdefeldt, H.-O. Adami, P. Cole, D. Trichopoulos, and J. Mandel, “Epidemiology and etiology of Parkinson’s disease: a review of the evidence.,” *Eur. J. Epidemiol.*, vol. 26 Suppl 1, pp. S1–58, Jun. 2011.

[37] J. W. Langston, P. Ballard, J. W. Tetrud, and I. Irwin, “Chronic Parkinsonism in humans due to a product of meperidine-analog synthesis.,” *Science*, vol. 219, no. 4587, pp. 979–80, Feb. 1983.

[38] R. Betarbet, T. B. Sherer, G. MacKenzie, M. Garcia-Osuna, A. V Panov, and J. T. Greenamyre, “Chronic systemic pesticide exposure reproduces features of

Parkinson's disease.," *Nat. Neurosci.*, vol. 3, no. 12, pp. 1301–6, Dec. 2000.

[39] G. Van Maele-Fabry, P. Hoet, F. Vilain, and D. Lison, "Occupational exposure to pesticides and Parkinson's disease: a systematic review and meta-analysis of cohort studies.," *Environ. Int.*, vol. 46, pp. 30–43, Oct. 2012.

[40] A. Priyadarshi, S. A. Khuder, E. A. Schaub, and S. S. Priyadarshi, "Environmental risk factors and Parkinson's disease: a metaanalysis.," *Environ. Res.*, vol. 86, no. 2, pp. 122–7, Jun. 2001.

[41] M. A. Hernán, B. Takkouche, F. Caamaño-Isorna, and J. J. Gestal-Otero, "A meta-analysis of coffee drinking, cigarette smoking, and the risk of Parkinson's disease.," *Ann. Neurol.*, vol. 52, no. 3, pp. 276–84, Sep. 2002.

[42] G. Hu, S. Bidel, P. Jousilahti, R. Antikainen, and J. Tuomilehto, "Coffee and tea consumption and the risk of Parkinson's disease.," *Mov. Disord.*, vol. 22, no. 15, pp. 2242–8, Nov. 2007.

[43] J. F. Chen, K. Xu, J. P. Petzer, R. Staal, Y. H. Xu, M. Beilstein, P. K. Sonsalla, K. Castagnoli, N. Castagnoli, and M. A. Schwarzschild, "Neuroprotection by caffeine and A(2A) adenosine receptor inactivation in a model of Parkinson's disease.," *J. Neurosci.*, vol. 21, no. 10, 2001.

[44] M. Quik, "Smoking, nicotine and Parkinson's disease.," *Trends Neurosci.*, vol. 27, no. 9, pp. 561–8, Sep. 2004.

[45] S. Lemay, S. Chouinard, P. Blanchet, H. Masson, V. Soland, A. Beuter, and M.-A. Bédard, "Lack of efficacy of a nicotine transdermal treatment on motor and cognitive deficits in Parkinson's disease.," *Prog. Neuropsychopharmacol. Biol. Psychiatry*, vol. 28, no. 1, pp. 31–9, Jan. 2004.

[46] H. Chen, E. J. O'Reilly, M. A. Schwarzschild, and A. Ascherio, "Peripheral inflammatory biomarkers and risk of Parkinson's disease.," *Am. J. Epidemiol.*, vol. 167, no. 1, pp. 90–5, Jan. 2008.

[47] H. Chen, S. M. Zhang, M. A. Hernán, M. A. Schwarzschild, W. C. Willett, G. A. Colditz, F. E. Speizer, and A. Ascherio, "Nonsteroidal anti-inflammatory drugs and the risk of Parkinson disease.," *Arch. Neurol.*, vol. 60, no. 8, pp. 1059–64, Aug.

2003.

[48] T. Wang, Z. Pei, W. Zhang, B. Liu, R. Langenbach, C. Lee, B. Wilson, J. M. Reece, D. S. Miller, and J.-S. Hong, “MPP+-induced COX-2 activation and subsequent dopaminergic neurodegeneration.,” *FASEB J.*, vol. 19, no. 9, pp. 1134–6, Jul. 2005.

[49] I. Martin, V. L. Dawson, and T. M. Dawson, “Recent advances in the genetics of Parkinson’s disease.,” *Annu. Rev. Genomics Hum. Genet.*, vol. 12, pp. 301–25, Jan. 2011.

[50] V. Bonifati, “Genetics of Parkinson’s disease--state of the art, 2013.,” *Parkinsonism Relat. Disord.*, vol. 20 Suppl 1, pp. S23–8, Jan. 2014.

[51] K. Nuytemans, J. Theuns, M. Cruts, and C. Van Broeckhoven, “Genetic etiology of Parkinson disease associated with mutations in the SNCA, PARK2, PINK1, PARK7, and LRRK2 genes: a mutation update.,” *Hum. Mutat.*, vol. 31, no. 7, pp. 763–80, Jul. 2010.

[52] M. H. Polymeropoulos, C. Lavedan, E. Leroy, S. E. Ide, A. Dehejia, A. Dutra, B. Pike, H. Root, J. Rubenstein, R. Boyer, E. S. Stenroos, S. Chandrasekharappa, A. Athanassiadou, T. Papapetropoulos, W. G. Johnson, A. M. Lazzarini, R. C. Duvoisin, G. Di Iorio, L. I. Golbe, and R. L. Nussbaum, “Mutation in the alpha-synuclein gene identified in families with Parkinson’s disease.,” *Science*, vol. 276, no. 5321, pp. 2045–7, Jun. 1997.

[53] K. Nishioka, S. Hayashi, M. J. Farrer, A. B. Singleton, H. Yoshino, H. Imai, T. Kitami, K. Sato, R. Kuroda, H. Tomiyama, K. Mizoguchi, M. Murata, T. Toda, I. Imoto, J. Inazawa, Y. Mizuno, and N. Hattori, “Clinical heterogeneity of alpha-synuclein gene duplication in Parkinson’s disease.,” *Ann. Neurol.*, vol. 59, no. 2, pp. 298–309, Feb. 2006.

[54] D. M. Maraganore, M. de Andrade, A. Elbaz, M. J. Farrer, J. P. Ioannidis, R. Krüger, W. A. Rocca, N. K. Schneider, T. G. Lesnick, S. J. Lincoln, M. M. Hulihan, J. O. Aasly, T. Ashizawa, M.-C. Chartier-Harlin, H. Checkoway, C. Ferrarese, G. Hadjigeorgiou, N. Hattori, H. Kawakami, J.-C. Lambert, T. Lynch, G. D. Mellick, S. Papapetropoulos, A. Parsian, A. Quattrone, O. Riess, E.-K. Tan, and C. Van Broeckhoven, “Collaborative analysis of alpha-synuclein gene promoter variability and Parkinson disease.,” *JAMA*, vol. 296, no. 6, pp. 661–70, Aug. 2006.

[55] O. Corti, S. Lesage, and A. Brice, “What genetics tells us about the causes and mechanisms of Parkinson’s disease.,” *Physiol. Rev.*, vol. 91, no. 4, pp. 1161–218, Oct. 2011.

[56] F. Mori, K. Tanji, M. Yoshimoto, H. Takahashi, and K. Wakabayashi, “Demonstration of α-Synuclein Immunoreactivity in Neuronal and Glial Cytoplasm in Normal Human Brain Tissue Using Proteinase K and Formic Acid Pretreatment,” *Exp. Neurol.*, vol. 176, no. 1, pp. 98–104, Jul. 2002.

[57] C. E. Ellis, E. J. Murphy, D. C. Mitchell, M. Y. Golovko, F. Scaglia, G. C. Barceló-Coblijn, and R. L. Nussbaum, “Mitochondrial lipid abnormality and electron transport chain impairment in mice lacking alpha-synuclein.,” *Mol. Cell. Biol.*, vol. 25, no. 22, pp. 10190–201, Nov. 2005.

[58] D. E. Cabin, K. Shimazu, D. Murphy, N. B. Cole, W. Gottschalk, K. L. McIlwain, B. Orrison, A. Chen, C. E. Ellis, R. Paylor, B. Lu, and R. L. Nussbaum, “Synaptic vesicle depletion correlates with attenuated synaptic responses to prolonged repetitive stimulation in mice lacking α-synuclein,” *J. Neurosci.*, vol. 22, no. 20, pp. 8797–8807, 2002.

[59] J. E. Galvin, “Interaction of alpha-synuclein and dopamine metabolites in the pathogenesis of Parkinson’s disease: a case for the selective vulnerability of the substantia nigra.,” *Acta Neuropathol.*, vol. 112, no. 2, pp. 115–26, Aug. 2006.

[60] J. Hardy, P. Lewis, T. Revesz, A. Lees, and C. Paisan-Ruiz, “The genetics of Parkinson’s syndromes: a critical review.,” *Curr. Opin. Genet. Dev.*, vol. 19, no. 3, pp. 254–65, Jun. 2009.

[61] S. Lesage, A. Dürr, M. Tazir, E. Lohmann, A.-L. Leutenegger, S. Janin, P. Pollak, and A. Brice, “LRRK2 G2019S as a cause of Parkinson’s disease in North African Arabs.,” *N. Engl. J. Med.*, vol. 354, no. 4, pp. 422–3, Jan. 2006.

[62] A. Zimprich, S. Biskup, P. Leitner, P. Lichtner, M. Farrer, S. Lincoln, J. Kachergus, M. Hulihan, R. J. Uitti, D. B. Calne, A. J. Stoessl, R. F. Pfeiffer, N. Patenge, I. C. Carbajal, P. Vieregge, F. Asmus, B. Müller-Myhsok, D. W. Dickson, T. Meitinger, T. M. Strom, Z. K. Wszolek, and T. Gasser, “Mutations in LRRK2 cause autosomal-dominant parkinsonism with pleomorphic pathology.,” *Neuron*, vol. 44, no. 4, pp.

601–7, Nov. 2004.

[63] B. I. Giasson, J. P. Covy, N. M. Bonini, H. I. Hurtig, M. J. Farrer, J. Q. Trojanowski, and V. M. Van Deerlin, “Biochemical and pathological characterization of Lrrk2.,” *Ann. Neurol.*, vol. 59, no. 2, pp. 315–22, Feb. 2006.

[64] R. von Coelln, V. L. Dawson, and T. M. Dawson, “Parkin-associated Parkinson’s disease.,” *Cell Tissue Res.*, vol. 318, no. 1, pp. 175–84, Oct. 2004.

[65] C. B. Lücking, A. Dürr, V. Bonifati, J. Vaughan, G. De Michele, T. Gasser, B. S. Harhangi, G. Meco, P. Denèfle, N. W. Wood, Y. Agid, and A. Brice, “Association between early-onset Parkinson’s disease and mutations in the parkin gene.,” *N. Engl. J. Med.*, vol. 342, no. 21, pp. 1560–7, May 2000.

[66] A. B. West and N. T. Maidment, “Genetics of parkin-linked disease.,” *Hum. Genet.*, vol. 114, no. 4, pp. 327–36, Mar. 2004.

[67] M. S. Goldberg, S. M. Fleming, J. J. Palacino, C. Cepeda, H. A. Lam, A. Bhatnagar, E. G. Meloni, N. Wu, L. C. Ackerson, G. J. Klapstein, M. Gajendiran, B. L. Roth, M.-F. Chesselet, N. T. Maidment, M. S. Levine, and J. Shen, “Parkin-deficient mice exhibit nigrostriatal deficits but not loss of dopaminergic neurons.,” *J. Biol. Chem.*, vol. 278, no. 44, pp. 43628–35, Oct. 2003.

[68] J. J. Palacino, D. Sagi, M. S. Goldberg, S. Krauss, C. Motz, M. Wacker, J. Klose, and J. Shen, “Mitochondrial dysfunction and oxidative damage in parkin-deficient mice.,” *J. Biol. Chem.*, vol. 279, no. 18, pp. 18614–22, Apr. 2004.

[69] Y. Kuroda, T. Mitsui, M. Kunishige, M. Shono, M. Akaike, H. Azuma, and T. Matsumoto, “Parkin enhances mitochondrial biogenesis in proliferating cells.,” *Hum. Mol. Genet.*, vol. 15, no. 6, pp. 883–95, Mar. 2006.

[70] D. Yao, Z. Gu, T. Nakamura, Z.-Q. Shi, Y. Ma, B. Gaston, L. A. Palmer, E. M. Rockenstein, Z. Zhang, E. Masliah, T. Uehara, and S. A. Lipton, “Nitrosative stress linked to sporadic Parkinson’s disease: S-nitrosylation of parkin regulates its E3 ubiquitin ligase activity.,” *Proc. Natl. Acad. Sci. U. S. A.*, vol. 101, no. 29, pp. 10810–4, Jul. 2004.

[71] E. M. Valente, P. M. Abou-Sleiman, V. Caputo, M. M. K. Muqit, K. Harvey, S. Gispert,

Z. Ali, D. Del Turco, A. R. Bentivoglio, D. G. Healy, A. Albanese, R. Nussbaum, R. González-Maldonado, T. Deller, S. Salvi, P. Cortelli, W. P. Gilks, D. S. Latchman, R. J. Harvey, B. Dallapiccola, G. Auburger, and N. W. Wood, “Hereditary early-onset Parkinson’s disease caused by mutations in PINK1.,” *Science*, vol. 304, no. 5674, pp. 1158–60, May 2004.

[72] V. Bonifati, C. F. Rohé, G. J. Breedveld, E. Fabrizio, M. De Mari, C. Tassorelli, A. Tavella, R. Marconi, D. J. Nicholl, H. F. Chien, E. Fincati, G. Abbruzzese, P. Marini, A. De Gaetano, M. W. Horstink, J. A. Maat-Kievit, C. Sampaio, A. Antonini, F. Stocchi, P. Montagna, V. Toni, M. Guidi, A. Dalla Libera, M. Tinazzi, F. De Pandis, G. Fabbrini, S. Goldwurm, A. de Klein, E. Barbosa, L. Lopiano, E. Martignoni, P. Lamberti, N. Vanacore, G. Meco, and B. A. Oostra, “Early-onset parkinsonism associated with PINK1 mutations: frequency, genotypes, and phenotypes.,” *Neurology*, vol. 65, no. 1, pp. 87–95, Jul. 2005.

[73] L. Silvestri, V. Caputo, E. Bellacchio, L. Atorino, B. Dallapiccola, E. M. Valente, and G. Casari, “Mitochondrial import and enzymatic activity of PINK1 mutants associated to recessive parkinsonism.,” *Hum. Mol. Genet.*, vol. 14, no. 22, pp. 3477–92, Nov. 2005.

[74] I. E. Clark, M. W. Dodson, C. Jiang, J. H. Cao, J. R. Huh, J. H. Seol, S. J. Yoo, B. A. Hay, and M. Guo, “Drosophila pink1 is required for mitochondrial function and interacts genetically with parkin.,” *Nature*, vol. 441, no. 7097, pp. 1162–6, Jun. 2006.

[75] D. Nagakubo, T. Taira, H. Kitaura, M. Ikeda, K. Tamai, S. M. Iguchi-Ariga, and H. Ariga, “DJ-1, a novel oncogene which transforms mouse NIH3T3 cells in cooperation with ras.,” *Biochem. Biophys. Res. Commun.*, vol. 231, no. 2, pp. 509–13, Feb. 1997.

[76] C. M. van Duijn, M. C. Dekker, V. Bonifati, R. J. Galjaard, J. J. Houwing-Duistermaat, P. J. Snijders, L. Testers, G. J. Breedveld, M. Horstink, L. A. Sandkuijl, J. C. van Swieten, B. A. Oostra, and P. Heutink, “Park7, a novel locus for autosomal recessive early-onset parkinsonism, on chromosome 1p36.,” *Am. J. Hum. Genet.*, vol. 69, no. 3, pp. 629–34, Sep. 2001.

[77] L. Zhang, M. Shimoji, B. Thomas, D. J. Moore, S.-W. Yu, N. I. Marupudi, R. Torp, I. A. Torgner, O. P. Ottersen, T. M. Dawson, and V. L. Dawson, “Mitochondrial

localization of the Parkinson's disease related protein DJ-1: implications for pathogenesis.," *Hum. Mol. Genet.*, vol. 14, no. 14, pp. 2063–73, Jul. 2005.

[78] R. M. Canet-Avilés, M. A. Wilson, D. W. Miller, R. Ahmad, C. McLendon, S. Bandyopadhyay, M. J. Baptista, D. Ringe, G. A. Petsko, and M. R. Cookson, "The Parkinson's disease protein DJ-1 is neuroprotective due to cysteine-sulfinic acid-driven mitochondrial localization.," *Proc. Natl. Acad. Sci. U. S. A.*, vol. 101, no. 24, pp. 9103–8, Jun. 2004.

[79] M. P. van der Brug, J. Blackinton, J. Chandran, L.-Y. Hao, A. Lal, K. Mazan-Mamczarz, J. Martindale, C. Xie, R. Ahmad, K. J. Thomas, A. Beilina, J. R. Gibbs, J. Ding, A. J. Myers, M. Zhan, H. Cai, N. M. Bonini, M. Gorospe, and M. R. Cookson, "RNA binding activity of the recessive parkinsonism protein DJ-1 supports involvement in multiple cellular pathways.," *Proc. Natl. Acad. Sci. U. S. A.*, vol. 105, no. 29, pp. 10244–9, Jul. 2008.

[80] W. Zhou, M. Zhu, M. A. Wilson, G. A. Petsko, and A. L. Fink, "The oxidation state of DJ-1 regulates its chaperone activity toward alpha-synuclein.," *J. Mol. Biol.*, vol. 356, no. 4, pp. 1036–48, Mar. 2006.

[81] D. W. Miller, R. Ahmad, S. Hague, M. J. Baptista, R. Canet-Aviles, C. McLendon, D. M. Carter, P.-P. Zhu, J. Stadler, J. Chandran, G. R. Klinefelter, C. Blackstone, and M. R. Cookson, "L166P mutant DJ-1, causative for recessive Parkinson's disease, is degraded through the ubiquitin-proteasome system.," *J. Biol. Chem.*, vol. 278, no. 38, pp. 36588–95, Sep. 2003.

[82] M. S. Goldberg, A. Pisani, M. Haburcak, T. A. Vortherms, T. Kitada, C. Costa, Y. Tong, G. Martella, A. Tscherter, A. Martins, G. Bernardi, B. L. Roth, E. N. Pothos, P. Calabresi, and J. Shen, "Nigrostriatal dopaminergic deficits and hypokinesia caused by inactivation of the familial Parkinsonism-linked gene DJ-1.," *Neuron*, vol. 45, no. 4, pp. 489–96, Feb. 2005.

[83] J. T. Greenamyre and T. G. Hastings, "Biomedicine. Parkinson's--divergent causes, convergent mechanisms.," *Science*, vol. 304, no. 5674, pp. 1120–2, May 2004.

[84] V. Bonifati, P. Rizzu, M. J. van Baren, O. Schaap, G. J. Breedveld, E. Krieger, M. C. J. Dekker, F. Squitieri, P. Ibanez, M. Joosse, J. W. van Dongen, N. Vanacore, J. C.

van Swieten, A. Brice, G. Meco, C. M. van Duijn, B. A. Oostra, and P. Heutink, “Mutations in the DJ-1 gene associated with autosomal recessive early-onset parkinsonism.,” *Science*, vol. 299, no. 5604, pp. 256–9, Jan. 2003.

[85] D. J. Moore, V. L. Dawson, and T. M. Dawson, “Genetics of Parkinson’s disease: what do mutations in DJ-1 tell us?,” *Ann. Neurol.*, vol. 54, no. 3, pp. 281–2, Sep. 2003.

[86] M. Lakshminarasimhan, M. T. Maldonado, W. Zhou, A. L. Fink, and M. A. Wilson, “Structural impact of three Parkinsonism-associated missense mutations on human DJ-1.,” *Biochemistry*, vol. 47, no. 5, pp. 1381–92, Feb. 2008.

[87] P. J. Kahle, J. Waak, and T. Gasser, “DJ-1 and prevention of oxidative stress in Parkinson’s disease and other age-related disorders.,” *Free Radic. Biol. Med.*, vol. 47, no. 10, pp. 1354–61, Nov. 2009.

[88] M. A. Wilson, “The role of cysteine oxidation in DJ-1 function and dysfunction.,” *Antioxid. Redox Signal.*, vol. 15, no. 1, pp. 111–22, Jul. 2011.

[89] M. A. Wilson, J. L. Collins, Y. Hod, D. Ringe, and G. A. Petsko, “The 1.1-A resolution crystal structure of DJ-1, the protein mutated in autosomal recessive early onset Parkinson’s disease.,” *Proc. Natl. Acad. Sci. U. S. A.*, vol. 100, no. 16, pp. 9256–61, Aug. 2003.

[90] J.-F. Trempe and E. A. Fon, “Structure and Function of Parkin, PINK1, and DJ-1, the Three Musketeers of Neuroprotection.,” *Front. Neurol.*, vol. 4, p. 38, Jan. 2013.

[91] X. Tao and L. Tong, “Crystal structure of human DJ-1, a protein associated with early onset Parkinson’s disease.,” *J. Biol. Chem.*, vol. 278, no. 33, pp. 31372–9, Aug. 2003.

[92] J. D. Hulleman, H. Mirzaei, E. Guigard, K. L. Taylor, S. S. Ray, C. M. Kay, F. E. Regnier, and J.-C. Rochet, “Destabilization of DJ-1 by familial substitution and oxidative modifications: implications for Parkinson’s disease.,” *Biochemistry*, vol. 46, no. 19, pp. 5776–89, May 2007.

[93] Y. Yang, S. Gehrke, M. E. Haque, Y. Imai, J. Kosek, L. Yang, M. F. Beal, I. Nishimura, K. Wakamatsu, S. Ito, R. Takahashi, and B. Lu, “Inactivation of Drosophila DJ-1

leads to impairments of oxidative stress response and phosphatidylinositol 3-kinase/Akt signaling.," *Proc. Natl. Acad. Sci. U. S. A.*, vol. 102, no. 38, pp. 13670–5, Sep. 2005.

[94] J. Waak, S. S. Weber, K. Görner, C. Schall, H. Ichijo, T. Stehle, and P. J. Kahle, "Oxidizable residues mediating protein stability and cytoprotective interaction of DJ-1 with apoptosis signal-regulating kinase 1.," *J. Biol. Chem.*, vol. 284, no. 21, pp. 14245–57, May 2009.

[95] J. Blackinton, M. Lakshminarasimhan, K. J. Thomas, R. Ahmad, E. Greggio, A. S. Raza, M. R. Cookson, and M. A. Wilson, "Formation of a stabilized cysteine sulfinic acid is critical for the mitochondrial function of the parkinsonism protein DJ-1.," *J. Biol. Chem.*, vol. 284, no. 10, pp. 6476–85, Mar. 2009.

[96] S. Bandyopadhyay and M. R. Cookson, "Evolutionary and functional relationships within the DJ1 superfamily.," *BMC Evol. Biol.*, vol. 4, p. 6, Feb. 2004.

[97] T. G. Hastings, D. A. Lewis, and M. J. Zigmond, "Role of oxidation in the neurotoxic effects of intrastriatal dopamine injections.," *Proc. Natl. Acad. Sci. U. S. A.*, vol. 93, no. 5, pp. 1956–61, Mar. 1996.

[98] M. Asanuma, I. Miyazaki, and N. Ogawa, "Dopamine- or L-DOPA-induced neurotoxicity: The role of dopamine quinone formation and tyrosinase in a model of Parkinson's disease," *Neurotox. Res.*, vol. 5, no. 3, pp. 165–176, Jan. 2003.

[99] S. Girotto, M. Sturlese, M. Bellanda, I. Tessari, R. Cappellini, M. Bisaglia, L. Bubacco, and S. Mammi, "Dopamine-derived quinones affect the structure of the redox sensor DJ-1 through modifications at Cys-106 and Cys-53.," *J. Biol. Chem.*, vol. 287, no. 22, pp. 18738–49, May 2012.

[100] V. Gautier, H.-T. Le, A. Malki, N. Messaoudi, T. Caldas, F. Kthiri, A. Landoulsi, and G. Richarme, "YajL, the prokaryotic homolog of the Parkinsonism-associated protein DJ-1, protects cells against protein sulfenylation.," *J. Mol. Biol.*, vol. 421, no. 4–5, pp. 662–70, Aug. 2012.

[101] J. Lee, J. Song, K. Kwon, S. Jang, C. Kim, K. Baek, J. Kim, and C. Park, "Human DJ-1 and its homologs are novel glyoxalases.," *Hum. Mol. Genet.*, vol. 21, no. 14, pp.

3215–25, Jul. 2012.

[102] C. Martinat, S. Shendelman, A. Jonason, T. Leete, M. F. Beal, L. Yang, T. Floss, and A. Abeliovich, “Sensitivity to oxidative stress in DJ-1-deficient dopamine neurons: an ES- derived cell model of primary Parkinsonism.,” *PLoS Biol.*, vol. 2, no. 11, p. e327, Nov. 2004.

[103] J. Chen, L. Li, and L.-S. Chin, “Parkinson disease protein DJ-1 converts from a zymogen to a protease by carboxyl-terminal cleavage.,” *Hum. Mol. Genet.*, vol. 19, no. 12, pp. 2395–408, Jun. 2010.

[104] K. Takahashi, T. Taira, T. Niki, C. Seino, S. M. Iguchi-Ariga, and H. Ariga, “DJ-1 positively regulates the androgen receptor by impairing the binding of PIASx alpha to the receptor.,” *J. Biol. Chem.*, vol. 276, no. 40, pp. 37556–63, Oct. 2001.

[105] J. Blackinton, R. Kumaran, M. P. van der Brug, R. Ahmad, L. Olson, D. Galter, A. Lees, R. Bandopadhyay, and M. R. Cookson, “Post-transcriptional regulation of mRNA associated with DJ-1 in sporadic Parkinson disease.,” *Neurosci. Lett.*, vol. 452, no. 1, pp. 8–11, Mar. 2009.

[106] P. M. Abou-Sleiman, D. G. Healy, N. Quinn, A. J. Lees, and N. W. Wood, “The role of pathogenic DJ-1 mutations in Parkinson’s disease.,” *Ann. Neurol.*, vol. 54, no. 3, pp. 283–6, Sep. 2003.

[107] M. Dekker, V. Bonifati, J. van Swieten, N. Leenders, R.-J. Galjaard, P. Snijders, M. Horstink, P. Heutink, B. Oostra, and C. van Duijn, “Clinical features and neuroimaging of PARK7-linked parkinsonism.,” *Mov. Disord.*, vol. 18, no. 7, pp. 751–7, Jul. 2003.

[108] R. Bandopadhyay, A. E. Kingsbury, M. R. Cookson, A. R. Reid, I. M. Evans, A. D. Hope, A. M. Pittman, T. Lashley, R. Canet-Aviles, D. W. Miller, C. McLendon, C. Strand, A. J. Leonard, P. M. Abou-Sleiman, D. G. Healy, H. Ariga, N. W. Wood, R. de Silva, T. Revesz, J. A. Hardy, and A. J. Lees, “The expression of DJ-1 (PARK7) in normal human CNS and idiopathic Parkinson’s disease.,” *Brain*, vol. 127, no. Pt 2, pp. 420–30, Feb. 2004.

[109] I. Irrcher, H. Aleyasin, E. L. Seifert, S. J. Hewitt, S. Chhabra, M. Phillips, A. K. Lutz, M. W. C. Rousseaux, L. Bevilacqua, A. Jahani-Asl, S. Callaghan, J. G. MacLaurin, K.

F. Winklhofer, P. Rizzu, P. Rippstein, R. H. Kim, C. X. Chen, E. A. Fon, R. S. Slack, M. E. Harper, H. M. McBride, T. W. Mak, and D. S. Park, “Loss of the Parkinson’s disease-linked gene DJ-1 perturbs mitochondrial dynamics.,” *Hum. Mol. Genet.*, vol. 19, no. 19, pp. 3734–46, Oct. 2010.

[110] F. Kamp, N. Exner, A. K. Lutz, N. Wender, J. Hegermann, B. Brunner, B. Nuscher, T. Bartels, A. Giese, K. Beyer, S. Eimer, K. F. Winklhofer, and C. Haass, “Inhibition of mitochondrial fusion by α-synuclein is rescued by PINK1, Parkin and DJ-1.,” *EMBO J.*, vol. 29, no. 20, pp. 3571–89, Oct. 2010.

[111] K. J. Thomas, M. K. McCoy, J. Blackinton, A. Beilina, M. van der Brug, A. Sandebring, D. Miller, D. Maric, A. Cedazo-Minguez, and M. R. Cookson, “DJ-1 acts in parallel to the PINK1/parkin pathway to control mitochondrial function and autophagy.,” *Hum. Mol. Genet.*, vol. 20, no. 1, pp. 40–50, Jan. 2011.

[112] A. P. Joselin, S. J. Hewitt, S. M. Callaghan, R. H. Kim, Y.-H. Chung, T. W. Mak, J. Shen, R. S. Slack, and D. S. Park, “ROS-dependent regulation of Parkin and DJ-1 localization during oxidative stress in neurons.,” *Hum. Mol. Genet.*, vol. 21, no. 22, pp. 4888–903, Nov. 2012.

[113] J. Blackinton, R. Ahmad, D. W. Miller, M. P. van der Brug, R. M. Canet-Avilés, S. M. Hague, M. Kaleem, and M. R. Cookson, “Effects of DJ-1 mutations and polymorphisms on protein stability and subcellular localization.,” *Brain Res. Mol. Brain Res.*, vol. 134, no. 1, pp. 76–83, Mar. 2005.

[114] T. Logan, L. Clark, and S. S. Ray, “Engineered disulfide bonds restore chaperone-like function of DJ-1 mutants linked to familial Parkinson’s disease.,” *Biochemistry*, vol. 49, no. 27, pp. 5624–33, Jul. 2010.

[115] G. Annesi, G. Savettieri, P. Pugliese, M. D’Amelio, P. Tarantino, P. Ragonese, V. La Bella, T. Piccoli, D. Civitelli, F. Annesi, B. Fierro, F. Piccoli, G. Arabia, M. Caracciolo, I. C. Cirò Candiano, and A. Quattrone, “DJ-1 mutations and parkinsonism-dementia-amyotrophic lateral sclerosis complex.,” *Ann. Neurol.*, vol. 58, no. 5, pp. 803–7, Nov. 2005.

[116] C. P. Ramsey and B. I. Giasson, “The E163K DJ-1 mutant shows specific antioxidant deficiency.,” *Brain Res.*, vol. 1239, pp. 1–11, Nov. 2008.

[117] M. Monti, S. Orrù, D. Pagnozzi, and P. Pucci, “Interaction Proteomics,” *Biosci. Rep.*, vol. 25, pp. 45–56, Feb. 2005.

[118] J. C. Smith and D. Figeys, “Proteomics technology in systems biology.,” *Mol. Biosyst.*, vol. 2, no. 8, pp. 364–70, Aug. 2006.

[119] M. Abu-Farha, F. Elisma, and D. Figeys, “Identification of protein-protein interactions by mass spectrometry coupled techniques.,” *Adv. Biochem. Eng. Biotechnol.*, vol. 110, pp. 67–80, Jan. 2008.

[120] W. Zhang, G. Zhou, Y. Zhao, M. A. White, and Y. Zhao, “Affinity enrichment of plasma membrane for proteomics analysis.,” *Electrophoresis*, vol. 24, no. 16, pp. 2855–63, Aug. 2003.

[121] T. S. Lewis, J. B. Hunt, L. D. Aveline, K. R. Jonscher, D. F. Louie, J. M. Yeh, T. S. Nahreini, K. A. Resing, and N. G. Ahn, “Identification of Novel MAP Kinase Pathway Signaling Targets by Functional Proteomics and Mass Spectrometry,” *Mol. Cell*, vol. 6, no. 6, pp. 1343–1354, Dec. 2000.

[122] R. Aebersold and D. R. Goodlett, “Mass Spectrometry in Proteomics,” *Chem. Rev.*, vol. 101, no. 2, pp. 269–296, Feb. 2001.

[123] R. Aebersold and M. Mann, “Mass spectrometry-based proteomics.,” *Nature*, vol. 422, no. 6928, pp. 198–207, Mar. 2003.

[124] L. C. Gillet, P. Navarro, S. Tate, H. Röst, N. Selevsek, L. Reiter, R. Bonner, and R. Aebersold, “Targeted data extraction of the MS/MS spectra generated by data-independent acquisition: a new concept for consistent and accurate proteome analysis.,” *Mol. Cell. Proteomics*, vol. 11, no. 6, p. O111.016717, Jun. 2012.

[125] T. N. Decaestecker, S. R. Vande Casteele, P. E. Wallemacq, C. H. Van Peteghem, D. L. Defore, and J. F. Van Bocxlaer, “Information-dependent acquisition-mediated LC-MS/MS screening procedure with semiquantitative potential.,” *Anal. Chem.*, vol. 76, no. 21, pp. 6365–73, Nov. 2004.

[126] X. Zhu, Y. Chen, and R. Subramanian, “Comparison of information-dependent acquisition, SWATH, and MS(All) techniques in metabolite identification study employing ultrahigh-performance liquid chromatography-quadrupole time-of-

flight mass spectrometry.," *Anal. Chem.*, vol. 86, no. 2, pp. 1202–9, Jan. 2014.

[127] J. D. Egertson, A. Kuehn, G. E. Merrihew, N. W. Bateman, B. X. MacLean, Y. S. Ting, J. D. Canterbury, D. M. Marsh, M. Kellmann, V. Zabrouskov, C. C. Wu, and M. J. MacCoss, "Multiplexed MS/MS for improved data-independent acquisition.," *Nat. Methods*, vol. 10, no. 8, pp. 744–6, Aug. 2013.

[128] A. T. Roemmelt, A. E. Steuer, M. Poetzsch, and T. Kraemer, "Liquid chromatography, in combination with a quadrupole time-of-flight instrument (LC QTOF), with sequential window acquisition of all theoretical fragment-ion spectra (SWATH) acquisition: systematic studies on its use for screenings in clinical and foren," *Anal. Chem.*, vol. 86, no. 23, pp. 11742–9, Dec. 2014.

[129] T. Basak, A. Bhat, D. Malakar, M. Pillai, and S. Sengupta, "In-depth comparative proteomic analysis of yeast proteome using iTRAQ and SWATH based MS.," *Mol. Biosyst.*, vol. 11, no. 8, pp. 2135–43, Aug. 2015.

[130] R. Y. K. Chang, N. Etheridge, A. S. Nouwens, and P. R. Dodd, "SWATH analysis of the synaptic proteome in Alzheimer's disease.," *Neurochem. Int.*, vol. 87, pp. 1–12, Aug. 2015.

[131] S.-E. Ong and M. Mann, "Mass spectrometry-based proteomics turns quantitative.," *Nat. Chem. Biol.*, vol. 1, no. 5, pp. 252–62, Oct. 2005.

[132] G. E. Craft, A. Chen, and A. C. Nairn, "Recent advances in quantitative neuroproteomics.," *Methods*, vol. 61, no. 3, pp. 186–218, Jun. 2013.

[133] J. H. Jang and S. Hanash, "Profiling of the cell surface proteome.," *Proteomics*, vol. 3, no. 10, pp. 1947–54, Oct. 2003.

[134] K. Smolders, N. Lombaert, D. Valkenborg, G. Baggerman, and L. Arckens, "An effective plasma membrane proteomics approach for small tissue samples.," *Sci. Rep.*, vol. 5, p. 10917, Jan. 2015.

[135] M. P. Weekes, R. Antrobus, J. R. Lill, L. M. Duncan, S. Hör, and P. J. Lehner, "Comparative analysis of techniques to purify plasma membrane proteins.," *J. Biomol. Tech.*, vol. 21, no. 3, pp. 108–15, Sep. 2010.

[136] S. J. Cordwell and T. E. Thingholm, “Technologies for plasma membrane proteomics.,” *Proteomics*, vol. 10, no. 4, pp. 611–27, Feb. 2010.

[137] Y. Kim, S. Elschenbroich, P. Sharma, L. Sepiashvili, A. O. Gramolini, and T. Kislinger, “Use of colloidal silica-beads for the isolation of cell-surface proteins for mass spectrometry-based proteomics.,” *Methods Mol. Biol.*, vol. 748, pp. 227–41, Jan. 2011.

[138] W. Choksawangkarn, S.-K. Kim, J. R. Cannon, N. J. Edwards, S. B. Lee, and C. Fenselau, “Enrichment of plasma membrane proteins using nanoparticle pellicles: comparison between silica and higher density nanoparticles.,” *J. Proteome Res.*, vol. 12, no. 3, pp. 1134–41, Mar. 2013.

[139] G. Elia, “Biotinylation reagents for the study of cell surface proteins.,” *Proteomics*, vol. 8, no. 19, pp. 4012–24, Oct. 2008.

[140] Y. Zhao, W. Zhang, Y. Kho, and Y. Zhao, “Proteomic Analysis of Integral Plasma Membrane Proteins,” *Anal. Chem.*, vol. 76, no. 7, pp. 1817–1823, Apr. 2004.

[141] O. Livnah, E. A. Bayer, M. Wilchek, and J. L. Sussman, “Three-dimensional structures of avidin and the avidin-biotin complex.,” *Proc. Natl. Acad. Sci. U. S. A.*, vol. 90, no. 11, pp. 5076–80, Jun. 1993.

[142] L. M. Schiapparelli, D. B. McClatchy, H.-H. Liu, P. Sharma, J. R. Yates, and H. T. Cline, “Direct Detection of Biotinylated Proteins by Mass Spectrometry,” *J. Proteome Res.*, vol. 13, no. 9, pp. 3966–3978, Sep. 2014.

[143] M. H. Qureshi and S.-L. Wong, *Design, production, and characterization of a monomeric streptavidin and its application for affinity purification of biotinylated proteins*, vol. 25, no. 3. 2002, pp. 409–415.

[144] H. Xie, L. Hu, and G. Li, “SH-SY5Y human neuroblastoma cell line: in vitro cell model of dopaminergic neurons in Parkinson’s disease.,” *Chin. Med. J. (Engl).*, vol. 123, no. 8, pp. 1086–92, Apr. 2010.

[145] T. Taira, Y. Saito, T. Niki, S. M. M. Iguchi-Ariga, K. Takahashi, and H. Ariga, “DJ-1 has a role in antioxidative stress to prevent cell death.,” *EMBO Rep.*, vol. 5, no. 2, pp. 213–8, Feb. 2004.

[146] M. Inden, T. Taira, Y. Kitamura, T. Yanagida, D. Tsuchiya, K. Takata, D. Yanagisawa, K. Nishimura, T. Taniguchi, Y. Kiso, K. Yoshimoto, T. Agatsuma, S. Koide-Yoshida, S. M. M. Iguchi-Ariga, S. Shimohama, and H. Ariga, “PARK7 DJ-1 protects against degeneration of nigral dopaminergic neurons in Parkinson’s disease rat model.,” *Neurobiol. Dis.*, vol. 24, no. 1, pp. 144–58, Oct. 2006.

[147] S. J. Mullett and D. A. Hinkle, “DJ-1 knock-down in astrocytes impairs astrocyte-mediated neuroprotection against rotenone.,” *Neurobiol. Dis.*, vol. 33, no. 1, pp. 28–36, Jan. 2009.

[148] M. Parsanejad, N. Bourquard, D. Qu, Y. Zhang, E. Huang, M. W. C. Rousseaux, H. Aleyasin, I. Irrcher, S. Callaghan, D. C. Vaillant, R. H. Kim, R. S. Slack, T. W. Mak, S. T. Reddy, D. Figeys, and D. S. Park, “DJ-1 interacts with and regulates paraoxonase-2, an enzyme critical for neuronal survival in response to oxidative stress.,” *PLoS One*, vol. 9, no. 9, p. e106601, Jan. 2014.

[149] S. Ishikawa, T. Taira, T. Niki, K. Takahashi-Niki, C. Maita, H. Maita, H. Ariga, and S. M. M. Iguchi-Ariga, “Oxidative status of DJ-1-dependent activation of dopamine synthesis through interaction of tyrosine hydroxylase and 4-dihydroxy-L-phenylalanine (L-DOPA) decarboxylase with DJ-1.,” *J. Biol. Chem.*, vol. 284, no. 42, pp. 28832–44, Oct. 2009.

[150] R. Chen, J. Wei, S. C. Fowler, and J.-Y. Wu, “Demonstration of functional coupling between dopamine synthesis and its packaging into synaptic vesicles,” *J. Biomed. Sci.*, vol. 10, no. 6, pp. 774–781, Oct. 2003.

[151] J. Garcia, V. Faca, J. Jarzembowski, Q. Zhang, J. Park, and S. Hanash, “Comprehensive profiling of the cell surface proteome of Sy5Y neuroblastoma cells yields a subset of proteins associated with tumor differentiation.,” *J. Proteome Res.*, vol. 8, no. 8, pp. 3791–6, Aug. 2009.

[152] B. K. Shin, H. Wang, A. M. Yim, F. Le Naour, F. Brichory, J. H. Jang, R. Zhao, E. Puravs, J. Tra, C. W. Michael, D. E. Misek, and S. M. Hanash, “Global profiling of the cell surface proteome of cancer cells uncovers an abundance of proteins with chaperone function.,” *J. Biol. Chem.*, vol. 278, no. 9, pp. 7607–16, Feb. 2003.

[153] H. Büeler, “Impaired mitochondrial dynamics and function in the pathogenesis of

Parkinson's disease.," *Exp. Neurol.*, vol. 218, no. 2, pp. 235–46, Aug. 2009.

[154] R. C. Stevens, "Design of high-throughput methods of protein production for structural biology," *Structure*, vol. 8, no. 9, pp. R177–R185, Sep. 2000.

[155] H. J. Jung, S. Kim, Y. J. Kim, M.-K. Kim, S. G. Kang, J.-H. Lee, W. Kim, and S.-S. Cha, "Dissection of the dimerization modes in the DJ-1 superfamily.," *Mol. Cells*, vol. 33, no. 2, pp. 163–71, Feb. 2012.

[156] T. Yokota, K. Sugawara, K. Ito, R. Takahashi, H. Ariga, and H. Mizusawa, "Down regulation of DJ-1 enhances cell death by oxidative stress, ER stress, and proteasome inhibition," *Biochem. Biophys. Res. Commun.*, vol. 312, no. 4, pp. 1342–1348, Dec. 2003.

[157] N. Lev, D. Ickowicz, E. Melamed, and D. Offen, "Oxidative insults induce DJ-1 upregulation and redistribution: implications for neuroprotection.," *Neurotoxicology*, vol. 29, no. 3, pp. 397–405, May 2008.

[158] T. Yanagida, J. Tsushima, Y. Kitamura, D. Yanagisawa, K. Takata, T. Shibaike, A. Yamamoto, T. Taniguchi, H. Yasui, T. Taira, S. Morikawa, T. Inubushi, I. Tooyama, and H. Ariga, "Oxidative stress induction of DJ-1 protein in reactive astrocytes scavenges free radicals and reduces cell injury.," *Oxid. Med. Cell. Longev.*, vol. 2, no. 1, pp. 36–42, Jan. .

[159] D. Yanagisawa, Y. Kitamura, M. Inden, K. Takata, T. Taniguchi, S. Morikawa, M. Morita, T. Inubushi, I. Tooyama, T. Taira, S. M. M. Iguchi-Ariga, A. Akaike, and H. Ariga, "DJ-1 protects against neurodegeneration caused by focal cerebral ischemia and reperfusion in rats.," *J. Cereb. Blood Flow Metab.*, vol. 28, no. 3, pp. 563–78, Mar. 2008.

[160] W. I. Rosenblum and F. El-Sabban, "Dimethyl sulfoxide (DMSO) and glycerol, hydroxyl radical scavengers, impair platelet aggregation within and eliminate the accompanying vasodilation of, injured mouse pial arterioles.," *Stroke.*, vol. 13, no. 1, pp. 35–9, Jan. .

[161] C. Limoli, "Attenuation of radiation-induced genomic instability by free radical scavengers and cellular proliferation," *Free Radic. Biol. Med.*, vol. 31, no. 1, pp. 10–19, Jul. 2001.

[162] S. J. Mullett, R. Di Maio, J. T. Greenamyre, and D. A. Hinkle, “DJ-1 expression modulates astrocyte-mediated protection against neuronal oxidative stress.,” *J. Mol. Neurosci.*, vol. 49, no. 3, pp. 507–11, Mar. 2013.

[163] E. P. Diamandis and T. K. Christopoulos, “The biotin-(strept)avidin system: principles and applications in biotechnology.,” *Clin. Chem.*, vol. 37, no. 5, pp. 625–36, May 1991.

[164] T. M. Dawson, H. S. Ko, and V. L. Dawson, “Genetic animal models of Parkinson’s disease.,” *Neuron*, vol. 66, no. 5, pp. 646–61, Jun. 2010.

[165] A. Deora, S. Chatterjee, A. D. Marmorstein, C. Zurzolo, A. Le Bivic, and E. Rodriguez-Boulan, *Cell Biology*, vol. 2. Elsevier, 2006.

[166] K. Nunomura, K. Nagano, C. Itagaki, M. Taoka, N. Okamura, Y. Yamauchi, S. Sugano, N. Takahashi, T. Izumi, and T. Isobe, “Cell surface labeling and mass spectrometry reveal diversity of cell surface markers and signaling molecules expressed in undifferentiated mouse embryonic stem cells.,” *Mol. Cell. Proteomics*, vol. 4, no. 12, pp. 1968–76, Dec. 2005.

[167] H. Hofstetter, M. Morpurgo, O. Hofstetter, E. A. Bayer, and M. Wilchek, “A labeling, detection, and purification system based on 4-hydroxyazobenzene-2-carboxylic acid: an extension of the avidin-biotin system.,” *Anal. Biochem.*, vol. 284, no. 2, pp. 354–66, Sep. 2000.

[168] G. Elia, “Cell surface protein biotinylation for SDS-PAGE analysis.,” *Methods Mol. Biol.*, vol. 869, pp. 361–72, Jan. 2012.

[169] T. Zell, A. Khoruts, E. Ingulli, J. L. Bonnevier, D. L. Mueller, and M. K. Jenkins, “Single-cell analysis of signal transduction in CD4 T cells stimulated by antigen in vivo.,” *Proc. Natl. Acad. Sci. U. S. A.*, vol. 98, no. 19, pp. 10805–10, Sep. 2001.

[170] C. Z. Michaylira, G. S. Wong, C. G. Miller, C. M. Gutierrez, H. Nakagawa, R. Hammond, A. J. Klein-Szanto, J.-S. Lee, S. B. Kim, M. Herlyn, J. A. Diehl, P. Gimotty, and A. K. Rustgi, “Periostin, a cell adhesion molecule, facilitates invasion in the tumor microenvironment and annotates a novel tumor-invasive signature in esophageal cancer.,” *Cancer Res.*, vol. 70, no. 13, pp. 5281–92, Jul.

2010.

[171] U. B. Nielsen and B. H. Geierstanger, “Multiplexed sandwich assays in microarray format.,” *J. Immunol. Methods*, vol. 290, no. 1–2, pp. 107–20, Jul. 2004.

[172] X. Jin, X. Jin, J.-E. Jung, S. Beck, and H. Kim, “Cell surface Nestin is a biomarker for glioma stem cells.,” *Biochem. Biophys. Res. Commun.*, vol. 433, no. 4, pp. 496–501, Apr. 2013.

[173] I. Sekiya, J. T. Vuoristo, B. L. Larson, and D. J. Prockop, “In vitro cartilage formation by human adult stem cells from bone marrow stroma defines the sequence of cellular and molecular events during chondrogenesis.,” *Proc. Natl. Acad. Sci. U. S. A.*, vol. 99, no. 7, pp. 4397–402, Apr. 2002.

[174] A. Nwaneshiudu, C. Kuschal, F. H. Sakamoto, R. R. Anderson, K. Schwarzenberger, and R. C. Young, “Introduction to confocal microscopy.,” *J. Invest. Dermatol.*, vol. 132, no. 12, p. e3, Dec. 2012.

[175] N. Shangari and P. J. O’Brien, “The cytotoxic mechanism of glyoxal involves oxidative stress.,” *Biochem. Pharmacol.*, vol. 68, no. 7, pp. 1433–42, Oct. 2004.

[176] G. Richarme, M. Mihoub, J. Dairou, L. C. Bui, T. Leger, and A. Lamouri, “Parkinsonism-associated protein DJ-1/Park7 is a major protein deglycase that repairs methylglyoxal- and glyoxal-glycated cysteine, arginine, and lysine residues.,” *J. Biol. Chem.*, vol. 290, no. 3, pp. 1885–97, Jan. 2015.

[177] T. Khare and C. S. Giometti, “Differential recovery of biotinylated microbial proteins using monomeric or polymeric avidin.,” *Biotechniques*, vol. 40, no. 5, pp. 584, 586, 588, May 2006.

[178] S. Healy, B. Perez-Cadahia, D. Jia, M. K. McDonald, J. R. Davie, and R. A. Gravel, “Biotin is not a natural histone modification.,” *Biochim. Biophys. Acta*, vol. 1789, no. 11–12, pp. 719–33, Jan. 2009.

8. Supplementary data

8.1. Protein quantification with 2D-Quant

After protein purification with affinity and size-exclusion chromatography, M26I and E163K DJ-1 solutions were concentrated with Nanodrop monitorization of concentration, to store proteins in PBS or PBS with 5% glycerol, at about 2 mg/mL.

Later the protein concentrations of the stock solutions and previous stock of WT DJ-1 in equal buffers, were determined using the 2D-Quant protein determination assay. After definition of the calibration curve (Figure 8.1), it was calculated concentrations of stock solutions (Table 8.1): produced M26I and E163K solutions registered concentrations of around 2mg/mL, but WT DJ-1 in PBS registered an absorbance beyond the allowed by standard solutions. Therefore, concentrations determined for M26I and E163K were used for future assays, and it would be used WT concentration values previously measured by Matilde, of 4.1 mg/mL for PBS and 2.2185 mg/mL for PBS with 5% glycerol.

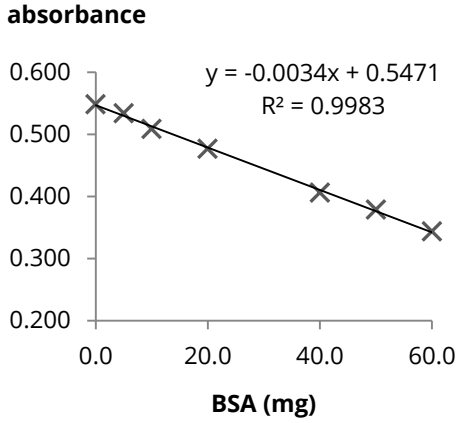

Figure 8.1 – Calibration curve measured for bovine serum albumin (BSA) standard solutions. PBS as blank.

Table 8.1 – Calculated values for concentration of WT, M26I and E163K DJ-1 stock solutions (n=3), using 2D-Quant assay.

sample	mean of [ ]	st dev	% CV
WT DJ-1 in PBS	3.995	0.143	3.58
WT DJ-1 in PBS + 5% glycerol	2.489	0.110	4.43
M26I DJ-1 in PBS	2.718	0.325	11.96
M26I DJ-1 in PBS + 5% glycerol	2.571	0.034	1.32
E163K DJ-1 in PBS	2.231	0.235	10.55
E163K DJ-1 in PBS + 5% glycerol	1.865	0.586	31.43

8.2. Protein identification with LC-MS/MS

WT, M26I and E163K DJ-1 stock solutions, stored in PBS with 5% glycerol, were processed for MS identification of DJ-1 and the corresponding mutation, and contaminants. After separating stock solution with SDS-PAGE, each gel lane was divided in four sections that were separately subjected for LC-MS/MS for best discrimination of protein contaminants: the upper and lower section (1 and 4, respectively) were processed together, due to low protein detection on silver staining (Figure 4.5); section 3 included DJ-1 band. Secondly, MS data was processed in ProteinPilot using two different protein databases: one including every protein on Uniprot (Table 8.2), and another where the protein sequence of recombinant WT DJ-1 (with hexahistidine tag sequence) and several synthetic and natural mutant forms, including M26I and E163K were added to the FASTA files, designated as Protein+Mutation database (Table 8.3). Summary of results from each database can be found in Table 4.1.

After processing of peptide and protein summary, it was observed the sequence coverage of the DJ-1 form correspondent to the sample in question, identified in section 3 with protein + mutation database, using ProteinPilot software (Figure 8.2). It was observed a full coverage of M26I and E163K DJ-1 protein sequence over 95% confidence; in identified WT DJ-1, initial methionine and nine residues of DJ-1 sequence presented a confidence under 95% but over 50%, being sufficient for a valid identification of WT DJ-1 in the analysed stock solution.

Table 8.2 – Values of protein identification provided by ProteinPilot processing of LC-MS/MS IDA data, using protein database (no added DJ-1 entry). nr pepts = number of peptides; %cov (95%) = percentage of protein coverage with attributed peptides with over 95% confidence

		solution	WT									M26I									E163K								
		gel section	1+4			2			3			1+4			2			3			1+4			2			3		
accession code	protein name	species	nr pepts	unused score	%cov (95%)	nr pepts	unused score	%cov (95%)	nr pepts	unused score	%cov (95%)	nr pepts	unused score	%cov (95%)	nr pepts	unused score	%cov (95%)	nr pepts	unused score	%cov (95%)	nr pepts	unused score	%cov (95%)	nr pepts	unused score	%cov (95%)	nr pepts	unused score	%cov (95%)
sp|P00761|TRYP_PIG	Trypsin	*Sus scrofa*	90	67.81	57.58	78	52.78	55.84	22	7.52	36.36	111	64.04	57.14	62	50.95	49.78	32	46.03	41.99	100	####	58.44	52	60.00	53.68	21	17.64	35.93
sp|Q99497|PARK7_HUMAN	Protein DJ-1	*Homo sapiens*	37	29.91	68.25	37	25.52	62.96	504	80.86	97.88	70	42.73	89.42	33	29.50	60.32	326	160.55	97.35	68	48.15	87.30	75	40.57	67.20	225	122.21	89.42
sp|Q8UW59|PARK7_CHICK	Protein DJ-1	*Gallus gallus*																16	6.00	42.33									
sp|P35527|K1C9_HUMAN	Keratin, type I cytoskeletal 9	*Homo sapiens*	22	30.20	29.86	6	7.87	8.35				16	22.34	21.51							14	18.00	14.77	3	6.23	5.78			
sp|P13645|K1C10_HUMAN	Keratin, type I cytoskeletal 10	*Homo sapiens*	13	19.93	22.60							20	31.40	28.94							15	26.24	21.40	7	12.65	11.64			
sp|P02533|K1C14_HUMAN	Keratin, type I cytoskeletal 14	*Homo sapiens*	4	6.57	8.26																7	10.00	16.10						
sp|P08779|K1C16_HUMAN	Keratin, type I cytoskeletal 16	*Homo sapiens*										6	5.06	10.15															
sp|P04264|K2C1_HUMAN	Keratin, type II cytoskeletal 1	*Homo sapiens*	25	39.19	32.92	10	18.00	16.15				25	38.96	29.97	8	14.24	12.42				25	40.00	33.54	10	20.00	15.37			
sp|P35908|K22E_HUMAN	Keratin, type II cytoskeletal 2 epidermal	*Homo sapiens*	10	15.58	16.28							13	19.80	21.28							16	24.00	24.26						
sp|P13647|K2C5_HUMAN	Keratin, type II cytoskeletal 5	*Homo sapiens*	4	5.09	7.12																								
sp|P0A7W1|RS5_ECOLI	30S ribosomal protein S5	*Escherichia coli*	7	12.13	61.15							4	6.24	32.34							5	10.00	38.92						
sp|P0A7X3|RS9_ECOLI	30S ribosomal protein S9	*Escherichia coli*	3	5.07	22.31																								
sp|P0A7W1|RS5_ECOLI	30S ribosomal protein S13	*Escherichia coli*	7	12.13	61.15							4	6.24	32.34							5	10.00	38.92						
sp|P60723|RL4_ECOLI	50S ribosomal protein L4	*Escherichia coli*	4	7.95	22.89							4	8.00	31.54							7	12.00	37.73						
sp|P02413|RL15_ECOLI	50S ribosomal protein L15	*Escherichia coli*	3	6.00	26.39																								
sp|P0A9A9|FUR_ECOLI	Ferric uptake regulation protein	*Escherichia coli*	5	8.00	40.54							4	6.00	40.54															
sp|P0ABB0|ATPA_ECOLI	ATP synthase subunit alpha	*Escherichia coli*																						4	8.00	8.38			
sp|P60712|ACTB_BOVIN	Actin, cytoplasmic 1	*Bos taurus*	7	14.06	32.00	5	10.00	29.33													3	6.00	13.60						
sp|P41340|ACT3_LIMPO	Actin-3	*Limulus polyphemus*										5	6.00	21.54	6	8.10	30.59												
sp|O17320|ACT_CRAGI	Actin	*Crassostrea gigas*																						4	6.05	17.82			
sp|P04764|ENOA_RAT	Alpha-enolase	*Rattus norvegicus*	5	10.00	21.20	11	14.00	26.96																					
sp|P02662|CASA1_BOVIN	Alpha-S1-casein	*Bos taurus*	3	6.00	17.29																								
sp|P02663|CASA2_BOVIN	Alpha-S2-casein	*Bos taurus*										3	6.00	13.51															
sp|P07335|KCRB_RAT	Creatine kinase B-type	*Rattus norvegicus*				6	6.09	18.37																					
sp|O02675|DPYL2_BOVIN	Dihydropyrimidinase-related protein 2	*Bos taurus*				5	10.00	17.48																					
sp|P04797|G3P_RAT	Glyceraldehyde-3-phosphate dehydrogenase	*Rattus norvegicus*	4	6.87	22.22	7	8.01	32.73																					
sp|P19120|HSP7C_BOVIN	Heat shock cognate 71 kDa protein	*Bos taurus*				4	5.85	13.62																					
sp|P01946|HBA_RAT	Hemoglobin subunit alpha-1/2	*Rattus norvegicus*	4	6.00	33.10	4	8.00	35.92				3	6.00	33.10	4	6.00	33.10												
sp|P02091|HBB1_RAT	Hemoglobin subunit beta-1	*Rattus norvegicus*				4	5.85	28.57																					
sp|Q2HJ86|TBA1D_BOVIN	Tubulin alpha-1D chain	*Bos taurus*				4	8.00	14.41																					
sp|P62261|1433E_BOVIN	14-3-3 protein epsilon	*Bos taurus*																			3	6.00	10.81						
sp|P63102|1433Z_RAT	14-3-3 protein zeta/delta	*Rattus norvegicus*				4	5.64	22.04																					

Table 8.3 - Values of protein identification using Protein+Mutation database (protein database with added FASTA entries, categorized in light green). nr pepts = number of peptides; %cov (95%) = percentage of protein coverage with attributed peptides with over 95% confidence.

		solution	WT									M26I									E163K								
		gel section	1+4			2			3			1+4			2			3			1+4			2			3		
accession code	protein name	species	nr pepts	unused score	%cov (95%)	nr pepts	unused score	%cov (95%)	nr pepts	unused score	%cov (95%)	nr pepts	unused score	%cov (95%)	nr pepts	unused score	%cov (95%)	nr pepts	unused score	%cov (95%)	nr pepts	unused score	%cov (95%)	nr pepts	unused score	%cov (95%)	nr pepts	unused score	%cov (95%)
sp|P00761|TRYP_PIG	Trypsin	*Sus scrofa*	81	64.47	57.58	64	42.22	54.55	18	16.23	32.03	88	61.96	52.38	57	59.45	49.78	40	38.22	48.05	85	100.06	55.84	50	56.97	53.68	30	28.09	39.83
sp|Q99497|PARK7_HUMAN	Protein DJ-1	*Homo sapiens*	30	29.52	64.02	27	24.52	59.26																					
sp|Q8UW59|PARK7_CHICK	Protein DJ-1	*Gallus gallus*																19	8.01	34.92							18	5.96	30.69
D00000|Protein	DJ-1 WT	*Homo sapiens*							169	132.83	95.33																		
D00001|Protein	DJ-1 M26I	*Homo sapiens*										55	43.50	68.22	26	32.86	53.27	320	222.96	100.00				34	41.31	59.35			
D00002|Protein	DJ-1 E163K	*Homo sapiens*																									292	178.36	100.00
D00003|Protein	DJ-1 C106A	*Homo sapiens*							154	10.00	95.33																		
D00004|Protein	DJ-1 C106DD	*Homo sapiens*							169	10.00	95.35							253	12.00	99.53									
sp|Q99497|PARK7_HUMAN; D00004|Protein; D00003|Protein; D00000|Protein	Protein DJ-1; DJ-1 C106DD; DJ-1 C106A; DJ-1 WT	*Homo sapiens*																			50	50.01	75.66						
sp|P35527|K1C9_HUMAN	Keratin, type I cytoskeletal 9	*Homo sapiens*	22	29.98	29.86	5	7.00	8.35				16	21.42	21.51							15	18.00	15.89	3	6.37	5.78			
sp|P13645|K1C10_HUMAN	Keratin, type I cytoskeletal 10	*Homo sapiens*	13	19.80	22.60							19	29.60	27.74							16	28.00	22.60	7	12.88	11.64			
sp|P02533|K1C14_HUMAN	Keratin, type I cytoskeletal 14	*Homo sapiens*	4	6.38	8.26																8	10.00	17.58						
sp|P04264|K2C1_HUMAN	Keratin, type II cytoskeletal 1	*Homo sapiens*	24	39.02	31.06	9	17.80	16.15				24	37.22	28.11	8	15.17	12.42				25	40.00	33.54	10	20.00	15.37			
sp|P35908|K22E_HUMAN	Keratin, type II cytoskeletal 2 epidermal	*Homo sapiens*	10	15.36	16.28							13	20.00	21.28							16	24.00	24.26						
sp|P13647|K2C5_HUMAN	Keratin, type II cytoskeletal 5	*Homo sapiens*	4	5.01	7.12																								
sp|P0A7W1|RS5_ECOLI	30S ribosomal protein S5	*Escherichia coli*	3	5.94	21.56							3	5.16	21.56							4	8.00	28.14						
sp|P0A7X3|RS9_ECOLI	30S ribosomal protein S9	*Escherichia coli*										4	8.00	31.54															
sp|P0A7W1|RS5_ECOLI	30S ribosomal protein S13	*Escherichia coli*	3	5.94	21.56							3	5.16	21.56							4	8.00	28.14						
sp|P60723|RL4_ECOLI	50S ribosomal protein L4	*Escherichia coli*	4	7.79	22.89																4	6.00	22.31						
sp|P02413|RL15_ECOLI	50S ribosomal protein L15	*Escherichia coli*	3	6.00	26.39																4	8.00	34.03						
sp|P0A9A9|FUR_ECOLI	Ferric uptake regulation protein	*Escherichia coli*	5	8.00	40.54							3	6.00	30.41															
sp|P0ABB0|ATPA_ECOLI	ATP synthase subunit alpha	*Escherichia coli*																						4	7.96	8.38			
sp|P0ACJ8|CRP_ECOLI	cAMP-activated global transcriptional regulator CRP	*Escherichia coli*							5	6.55	22.38																		
sp|P60712|ACTB_BOVIN	Actin, cytoplasmic 1	*Bos taurus*	6	12.15	25.87										5	10.00	24.53												
sp|Q7ZVI7|ACTB1_DANRE	Actin, cytoplasmic 1	*Danio rerio*				4	8.00	29.33																					
sp|P29751|ACTB_RABIT	Actin, cytoplasmic 1	*Oryctolagus cuniculus*										5	6.01	21.60															
sp|O17320|ACT_CRAGI	Actin	*Crassostrea gigas*																			3	6.00	13.56	4	6.07	17.82			
sp|P04764|ENOA_RAT	Alpha-enolase	*Rattus norvegicus*	4	8.00	17.74	6	10.00	23.04																					
sp|P02662|CASA1_BOVIN	Alpha-S1-casein	*Bos taurus*	3	6.00	17.29																								
sp|P02663|CASA2_BOVIN	Alpha-S2-casein	*Bos taurus*										3	6.00	13.51															
sp|P07335|KCRB_RAT	Creatine kinase B-type	*Rattus norvegicus*				5	6.03	14.96																					
sp|O02675|DPYL2_BOVIN	Dihydropyrimidinase-related protein 2	*Bos taurus*				5	10.00	17.48																					
sp|P04797|G3P_RAT	Glyceraldehyde-3-phosphate dehydrogenase	*Rattus norvegicus*	3	6.09	18.02	4	6.00	17.12																					
sp|P19120|HSP7C_BOVIN	Heat shock cognate 71 kDa protein	*Bos taurus*				3	5.50	10.22																					
sp|P01946|HBA_RAT	Hemoglobin subunit alpha-1/2	*Rattus norvegicus*	4	6.00	33.10	4	8.00	35.92				3	6.00	33.10	4	6.00	33.10												
sp|P02091|HBB1_RAT	Hemoglobin subunit beta-1	*Rattus norvegicus*				4	5.40	28.57																					
sp|P81947|TBA1B_BOVIN	Tubulin alpha-1B chain	*Bos taurus*				4	8.00	14.48																					
sp|P62261|1433E_BOVIN	14-3-3 protein epsilon	*Bos taurus*				3	5.24	16.86																					

Figure 8.2 - Sequence coverage of identification of recombinant WT, M26I and E163K DJ-1, after SDS-PAGE and gel processing of each stock solution in PBS with 5% glycerol, IDA acquisition of section 3 of gel lanes and IDA processing with protein + mutation database. Colour of residues: green = residue identification over 95% confidence; yellow = over 50% and under 95% confidence. 6His = hexahistidine; TEV site = N-terminal cleavage site; apostrophe = peptidic bond cut by TEV protease; triangular arrow = mutation site; vertical bar = DJ-1 N-terminus (DJ-1protein sequence to the right of vertical bar); middle point = marker for 25 and multiple residue length of protein

8.3. SH-SY5Y viability assays

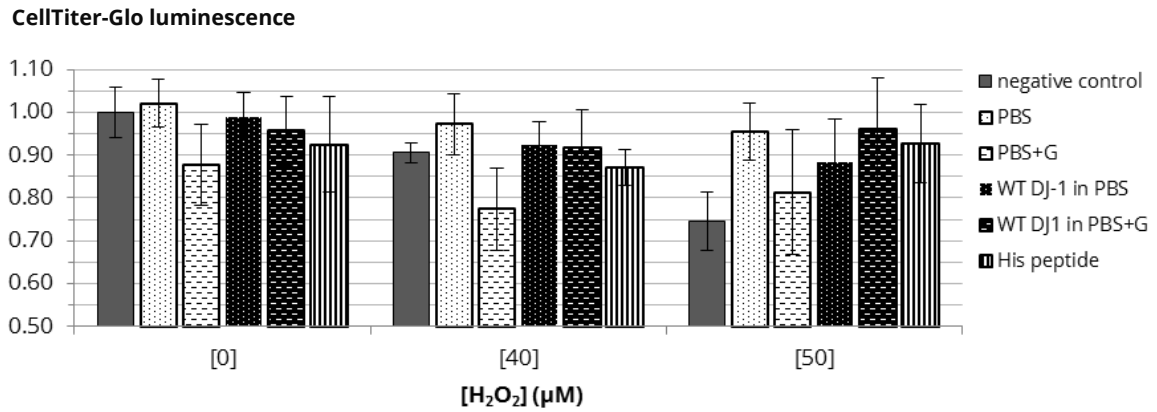

Figure 8.3 –SH-SY5Y viability CellTiter-Glo assay, after MW-96 plating and 24h incubation in absence or presence of oxidative stress (40, 50 μM hydrogen peroxide), and addition of 1 μM WT DJ-1 in PBS or PBS with 5% glycerol (PBS+G) or addition of PBS or PBS+G with equal volume of correspondent added protein (PBS = 2.24 μL; PBS+G = 4.18 μL). n=2

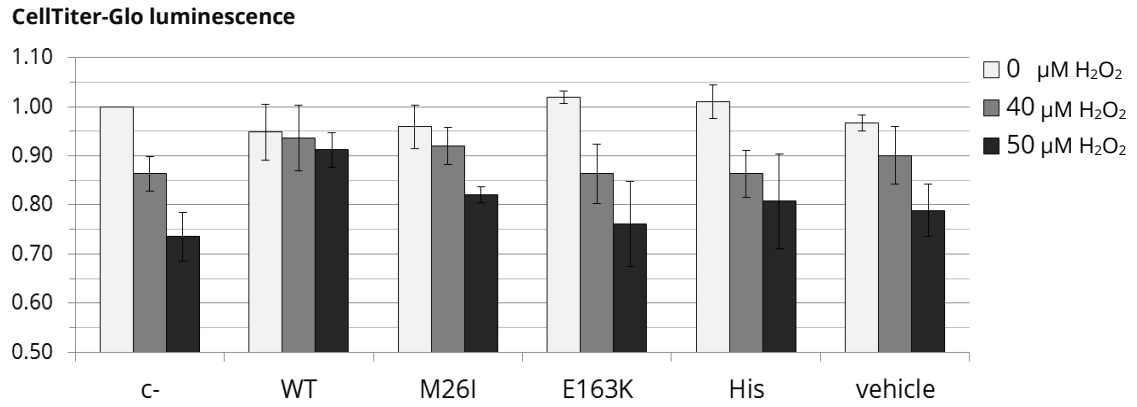

Figure 8.4 - SH-SY5Y viability CellTiter-Glo assay, after MW-96 plating and 24h incubation in absence or presence of oxidative stress (40, 50 μM hydrogen peroxide), and addition of 1 μM WT, M26I or E163K DJ-1 in equal volumes of PBS with 5% glycerol or addition of vehicle (PBS with 5% glycerol) in equal volume to added of all DJ-1 protein forms (5.11 μL), or absence of protein addition (c-). n=3. Selected conditions (WT, M26I and E163K, in 0 and 50 μM hydrogen peroxide) subsequently submitted to t-test and construction of figure 4.8. n=3

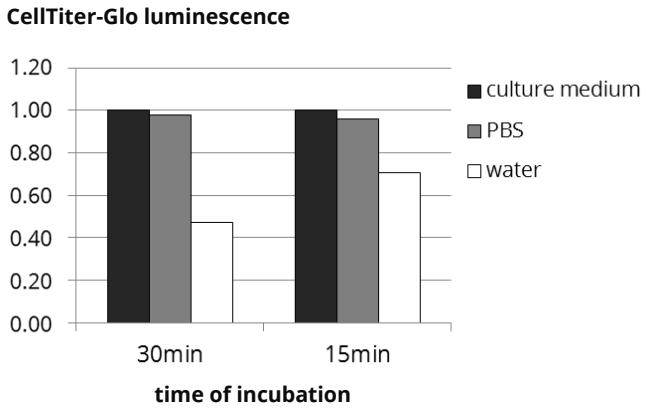

Figure 8.5 – SH-SY5Y cell viability after 48h plating, culture medium removal and incubation with new culture medium (MEM-F12 with 10% FBS), PBS or water, at room temperature, for 15 or 30 minutes.

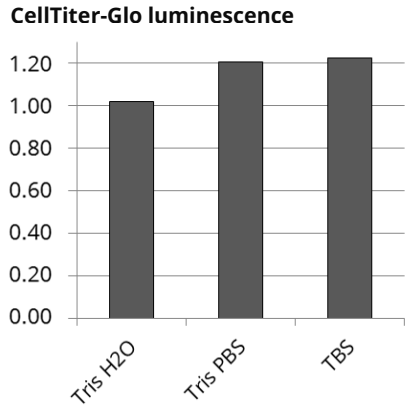

Figure 8.6 – SH-SY5Y viability after 48h plating, culture medium removal and incubation for 5 minutes in 50mM Tris prepared in water (Tris H_2O) or in PBS (Tris PBS) or incubation in Tris-buffered Saline isotonic buffer (TBS).

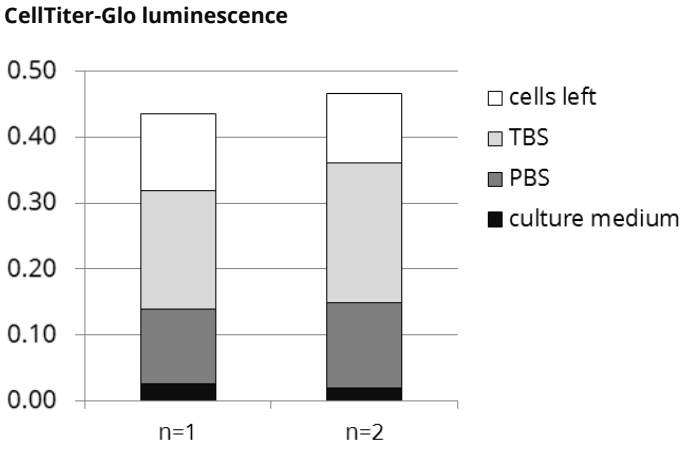

Figure 8.7 – SH-SY5Y cell viability assay, with culture medium exchange 24 h after plating, and simulation of biotinylation protocol 48h after plating. Viability quantified in solutions used over SH-SY5Y in equal conditions to delineated biotinylation control: removed culture medium, 15 min incubation with the Sulfo-NHS-LC-biotin solvent PBS, quenching washes with TBS) and cells left adhered to well bottom. Values normalized to control condition, with medium exchange 24 h after plating and absence of simulated biotinylation.

8.4. SAPE dot blot assay

It was performed a dot blot to confirm the biotinylation of proteins and its detection using SAPE fluorophore. The used protocol was adapted from the recurrent dot blot procedure, with membrane incubation in SAPE containing Solution after sample addition and membrane blocking (Figure 8.8). This procedure served to access the efficiency of SAPE fluorescence emission and specific binding to biotin-containing compounds, examining the fluorescence emitted by several samples: biotinylated WT DJ-1; non-biotinylated DJ-1, as negative control; SAPE fluorophore added directly to membrane, before blocking, as positive control.

Biotinylation of WT DJ-1 was previously performed, and besides dot blot analysis it was used for liquid digestion and MS IDA acquisition analysis: the MS run of biotinylated WT DJ-1 served for the modification of the ProteinPilot processing parameters, in order to recognize the biotin modification (addition of Sulfo-NHS-LC-biotin residue to lysine and N termination of proteins) and allow the detection of biotinylated proteins in samples processed in LC-MS/MS – as used in section 8.6.

Figure 8.8 – Dot blot assay for detection of biotinylated protein with SAPE staining. biot-DJ1 = biotinylated WT DJ-1; DJ1 = non-biotinylated DJ-1; SAPE = streptavidin b-phycoerythrin conjugate.

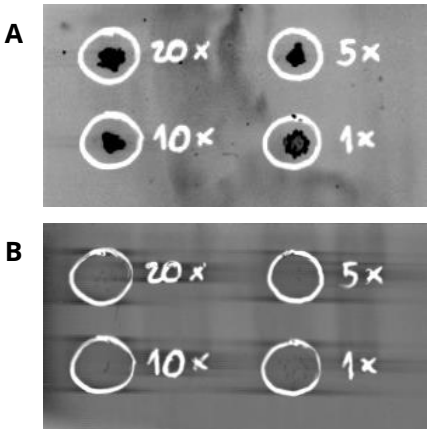

Figure 8.9 – Dot blot assay of positive control (SAPE) added in several concentrations (20×, 10×, 5×, 1×). A = fluorescence emission after SAPE addition; B = fluorescence after membrane blocking and wash.

As expected, it was possible to observe fluorescence emission with biotinylated DJ-1, absence regarding the non-biotinylated protein, confirming a successful biotinylation of protein and its direct detection using SAPE. Since streptavidin is a protein, it was expected to be retained in the PVDF membrane along the dot blot processing. But SAPE condition didn't show fluorescence, which could be attributed to: lack of fluorescence emission when SAPE is not bound to proteins; low concentration of added SAPE; low photostability, insufficient for SAPE to endure blocking and later steps of the procedure; lack of SAPE binding capacity to the PVDF membrane.

A second dot blot with the use of several concentrations of SAPE was executed to clarify this issue and attest SAPE as the origin of fluorescence observation (Figure 8.9). Any used SAPE concentration emitted fluorescence after its addition to membrane, but the signal disappeared after 2h membrane blocking and washing. This indicates that the lack of signal seen in first dot blot assay may be due to a low binding capacity of SAPE to the PVDF membrane, being removed during blotting process. Nevertheless, it is demonstrated that fluorescence emission in the biot-DJ1 condition resulted from its SAPE binding capacity, and the fluorophore is able to emit signal either in free form (though the protocol used removes efficiently SAPE membrane staining solution) or when interacting with biotinylated proteins.

8.5. Experimental digestion of membrane proteins with trypsin or trypsin + chymotrypsin

Trypsin, the digestion enzyme most often used in MS analysis, hydrolyzes proteins in lysine and arginine residues. These correspond to polar amino acids, more often found in hydrophilic regions of proteins. Cell surface proteins, on the other hand, will include membrane proteins, with hydrophobic regions and also transmembrane regions. Hence, it is of great value an MS analysis using other digestion enzyme, with a digestion more prone to hydrophobic regions of proteins, such as chymotrypsin.

It was performed an MS analysis of four biological replicates, consisting of an enriched fraction of membrane proteins, for a qualitative and quantitative analysis of the digestion efficiency with trypsin or with trypsin and chymotrypsin, for the detection of hydrophobic proteins. The resulted data was analyzed in regards of reproducibility of digestion, number of identified and quantified proteins, and increased identification of hydrophobicity associated proteins.

8.5.1. IDA analysis

Overall, trypsin digestion provided the best results (table 8.4 and 8.5), since its use allowed the MS identification of more total and membrane proteins, and also total number of distinct proteins between replicates. Also, trypsin digestion provided higher number and percentage of proteins common to all replicates, and also a higher number of distinct proteins. On the other hand, digestion with trypsin and chymotrypsin had lower coefficient of variation (%CV) and a higher percentage of membrane proteins.

Between both conditions (Figure 8.10), it was identified overall 717 unique proteins (36.3% of which only found in trypsin digested samples, and 4.0% only in samples of trypsin with chymotrypsin). Also, 233 proteins were common to all eight samples: 153 were membrane proteins and 40 had a predicted α-transmembrane region.

Table 8.4 – Number of identified proteins for each biological replicate of proteins digested with trypsin (Tx) or trypsin with chymotrypsin (TCx). Membrane proteins identification from total of proteins made through Uniprot attribution of gene ontology regarding the corresponding cellular component (GO:0044425).

	T1	T2	T3	T4	TC1	TC2	TC3	TC4
nr pept >2	265	324	347	350	227	257	234	219
nr pept <3	221	220	228	213	98	116	109	133
total nr proteins	**486**	**544**	**575**	**563**	**325**	**373**	**343**	**352**
nr membrane proteins	295	326	339	337	202	230	213	212
% membrane proteins	60.70	59.93	58.96	59.86	62.15	61.66	62.10	60.23

Table 8.5 – Data processing of protein identification lists acquired for each replicate. Average GRAVY score calculated from the hydropathy quantification of all peptides identified on the samples of each condition. st dev = standard deviation; %CV = coefficient of variation.

	total proteins			total distinct prots	nr common proteis in all replicates (n=4)	%common (in mean total proteins)	%common (in total distinct prots)	**membrane proteins**			average %memb	average GRAVY score
	mean	st dev	%CV					mean	st dev	%CV		
Trypsin (Tx)	542.00	39.45	7.28	688	409	75.46%	59.45%	324.25	20.32	6.27	59.86	-0.223
Trypsin + Chymotrypsin (TCx)	348.25	19.96	5.73	457	251	72.02%	54.92%	214.25	11.62	5.42	61.54	-0.266

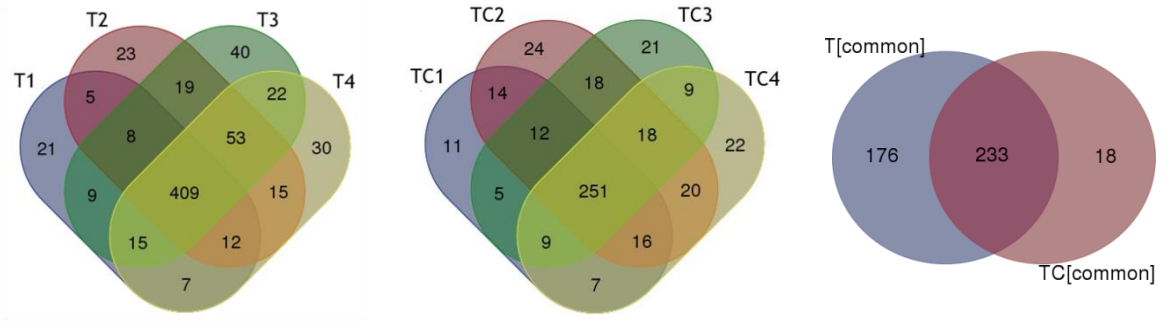

Figure 8.10 - Venn diagrams for total proteins identified on each sample digested with trypsin (left), digested with trypsin and chymotrypsin (middle) and for common proteins regarding the four samples of each of the two conditions (right).

To access hydropathy of the identified proteins, especially the efficient and total coverage of hydrophobic and hydrophilic regions of the protein sequence, it was calculated the GRAVY score for each peptide, using Kyte and Doolithle parameters for

score attribution of peptide sequence (Figure 8.11 and 8.12): contrary to what expected, samples digested only with trypsin demonstrate a lower average GRAVY score. Considering a distribution of GRAVY score values of total and relative number of proteins identified for each digestion condition, it is possible to see that, in all GRAVY score subclasses, trypsin registered higher number of peptides. Furthermore, regarding its percentage against total number of peptides, it is seen that in higher GRAVY scores, attributed to more hydrophobic sequences, trypsin registers higher percentage than trypsin with chymotrypsin, contrary to what can be observed in lower GRAVY scores.

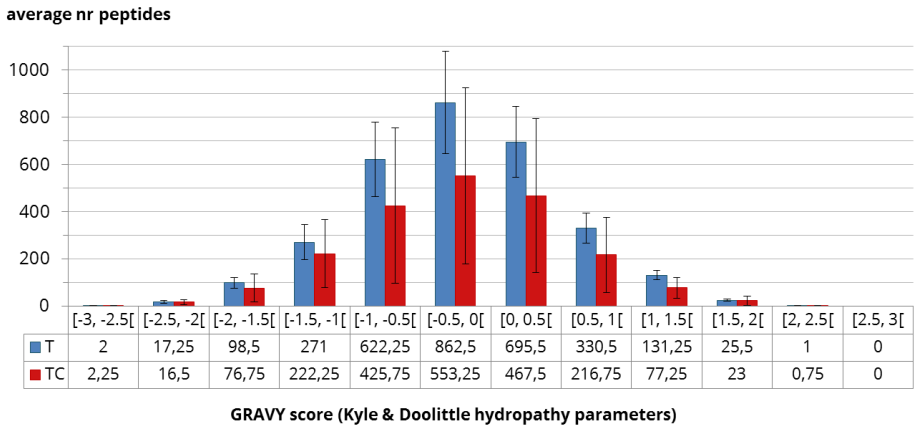

	[-3, -2.5[	[-2.5, -2[	[-2, -1.5[	[-1.5, -1[	[-1, -0.5[	[-0.5, 0[	[0, 0.5[	[0.5, 1[	[1, 1.5[	[1.5, 2[	[2, 2.5[	[2.5, 3[
T	2	17,25	98,5	271	622,25	862,5	695,5	330,5	131,25	25,5	1	0
TC	2,25	16,5	76,75	222,25	425,75	553,25	467,5	216,75	77,25	23	0,75	0

Figure 8.11 – Distribution of identified peptides according to GRAVY score, for replicates of each digestion condition.

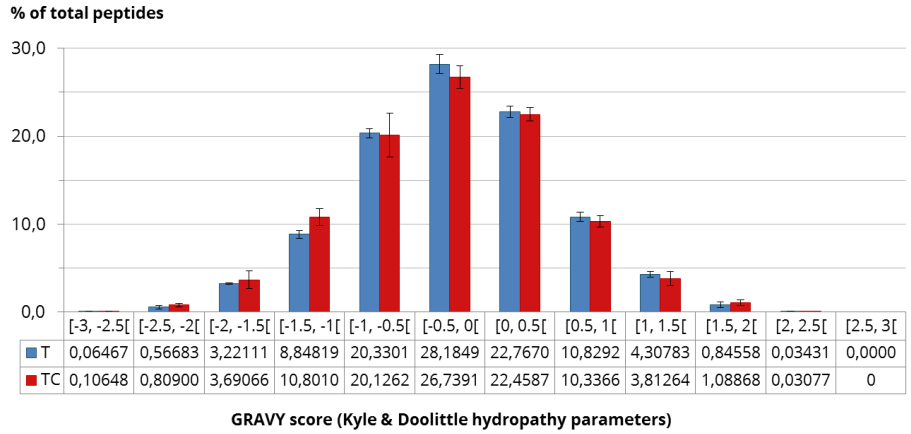

	[-3, -2.5[	[-2.5, -2[	[-2, -1.5[	[-1.5, -1[	[-1, -0.5[	[-0.5, 0[	[0, 0.5[	[0.5, 1[	[1, 1.5[	[1.5, 2[	[2, 2.5[	[2.5, 3[
T	0,06467	0,56683	3,22111	8,84819	20,3301	28,1849	22,7670	10,8292	4,30783	0,84558	0,03431	0,0000
TC	0,10648	0,80900	3,69066	10,8010	20,1262	26,7391	22,4587	10,3366	3,81264	1,08868	0,03077	0

Figure 8.12 – Distribution of identified peptides according to GRAVY score, with values translated to its percentage from total identified peptides.

8.5.2. SWATH analysis

Regarding a SWATH acquisition of T or TC samples, for quantification of identified proteins, IDA processing results of each biological replicate was used as a library for the SWATH analysis of each condition, then it was analyzed proteins quantified in all replicates (Table 8.6 and Figure 8.13). As in IDA acquisition, trypsin digested samples had more quantified peptides, total proteins and membrane proteins, and almost 87% of the quantified total proteins were also present in the IDA analysis of all four replicates of the corresponding condition. In digestion with trypsin and chymotrypsin, it was registered a higher percentage of membrane proteins. Of the 218 proteins common to samples digested in trypsin (T) or trypsin with chymotrypsin (TC), gene ontology attributed 148 proteins to the membrane and 43 were integral to membrane.

Table 8.6 –SWATH acquisition data of samples with trypsin or trypsin and chymotrypsin digestions. Membrane and integral to membrane identification made through Uniprot attribution of gene ontology regarding the cellular components membrane (GO:0044425) and integral component of membrane (GO:0016021). Average GRAVY score calculated from the hydropathy quantification of all peptides identified on the samples of each condition.

					common proteins			
	nr of peptides	**nr of proteins**	**nr membrane proteins**	**nr proteins on SWATH common to all IDA replicates**	**total number**	**membrane proteins**	**integral to membrane**	**average peptide GRAVY score**
T	1021	329	210 (63.83%)	286 (86.93%)	218	148	43	-0.1145
TC	860	259	173 (66.80%)	203 (78.38%)				-0.2123

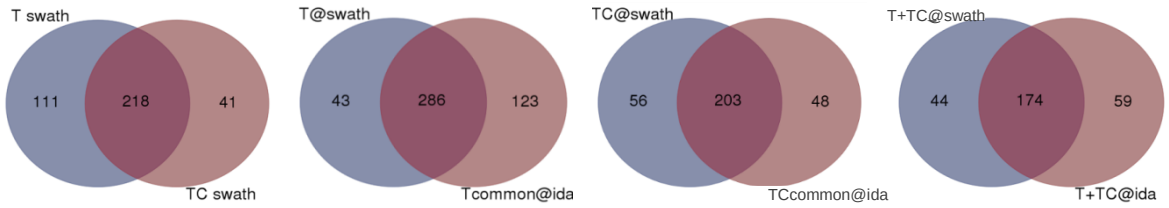

Figure 8.13 – Venn diagrams for convergence analysis of protein list acquired in IDA or SWATH analysis, from left to right: quantified proteins in T or TC digestion; quantified proteins of T digestion against proteins found in IDA analysis of all four replicates; quantified proteins of TC digestion against proteins found in IDA analysis of all four replicates; 218 proteins quantified on SWATH analysis common for T and TC against 233 proteins common to all T and TC replicates identified with IDA acquisition.

Furthermore, and similarly to IDA analysis, a distribution of peptides considered in SWATH analysis according to their hydropathy, translated on its GRAVY score (Figure 8.14 and 8.15), it is identified more peptides using trypsin digestion in almost all subclasses of GRAVY score, and if the value is relativized against total number of peptides of each digestion, trypsin register a higher percentage in GRAVY subclasses of higher value, attributed to hydrophobic peptides.

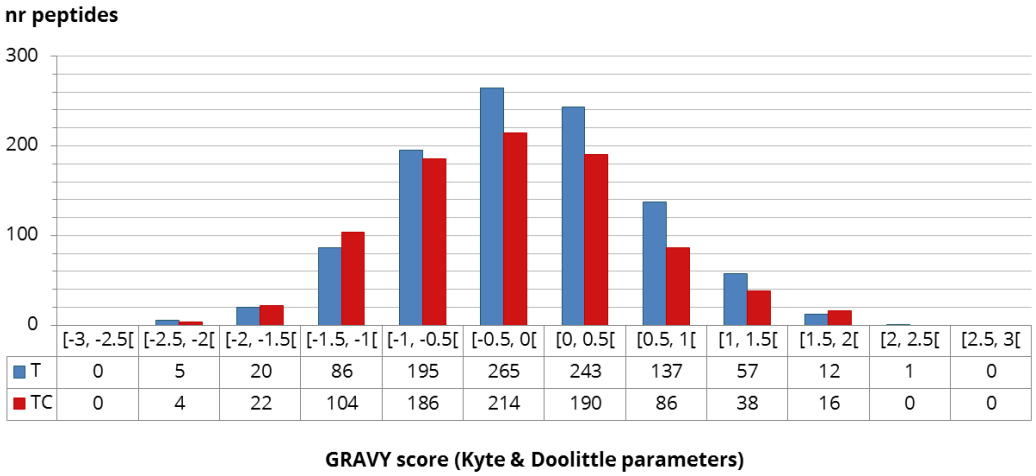

	[-3, -2.5[	[-2.5, -2[	[-2, -1.5[	[-1.5, -1[	[-1, -0.5[	[-0.5, 0[	[0, 0.5[	[0.5, 1[	[1, 1.5[	[1.5, 2[	[2, 2.5[	[2.5, 3[
T	0	5	20	86	195	265	243	137	57	12	1	0
TC	0	4	22	104	186	214	190	86	38	16	0	0

Figure 8.14 - Distribution of peptides, attributed to all samples of each condition in SWATH quantification, according to GRAVY score,

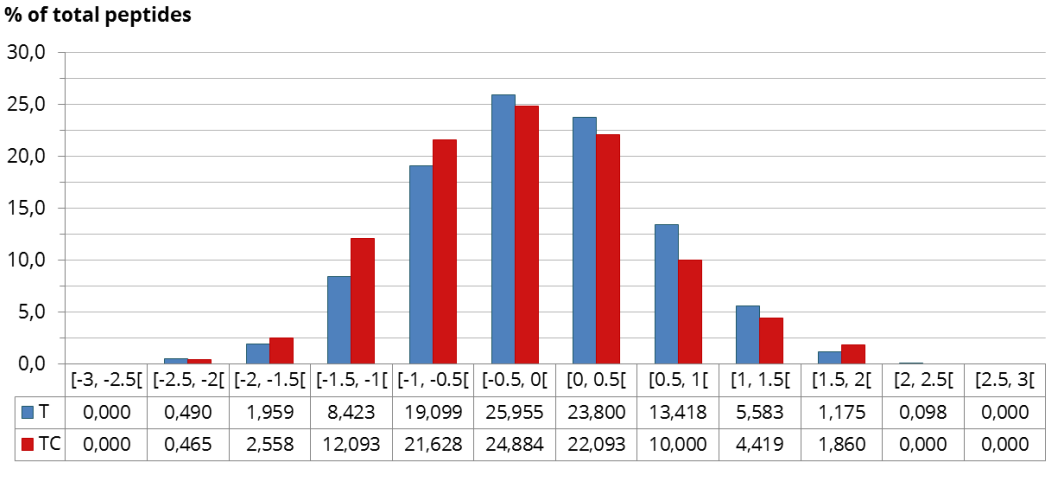

	[-3, -2.5[	[-2.5, -2[	[-2, -1.5[	[-1.5, -1[	[-1, -0.5[	[-0.5, 0[	[0, 0.5[	[0.5, 1[	[1, 1.5[	[1.5, 2[	[2, 2.5[	[2.5, 3[
T	0,000	0,490	1,959	8,423	19,099	25,955	23,800	13,418	5,583	1,175	0,098	0,000
TC	0,000	0,465	2,558	12,093	21,628	24,884	22,093	10,000	4,419	1,860	0,000	0,000

Figure 8.15 - Distribution of percentage of identified peptides according to GRAVY score, against total number of peptides attributed to SWATH acquisition on each digestion condition.

After data processing and selection of quantifiable proteins in T and TC digestion, the protein peak intensity values correspondent to each protein, different between replicates of each condition were processed in two ways: normalization to total intensity, or normalization to internal standard (added peak intensities of GFP and MALE), added to each replicate before liquid digestion (Table 8.7). Analyzing the between-replicate variation of relative quantification of proteins, and after calculation of the mean, standard deviation and %CV for each protein among the four replicates, it is noticeable that normalization to total intensity provided a lower average of %CV measured among all proteins.

Table 8.7 – Calculation of average of protein intensity values after calculation of the mean, standard deviation and %CV for each protein among the four replicates, comparing normalization of peak intensities with total intensity or internal standard,

	normalisation to total intensity			**normalisation to internal standard (IS)**		
	mean average	st dev average	%CV average	mean average	st dev average	%CV average
T	0.00304	0.00016	7.069	0.01091	0.00089	12.370
TC	0.00386	0.00055	11.792	0.02125	0.00988	56.737

Taking in account the average of each protein value among the replicates, and normalization with internal standard, it was made a distribution for the normalized intensities and %CV of each protein (Figure 8.16 to 8.19): trypsin with chymotrypsin allowed the quantification of more proteins in higher intensity values, but trypsin demonstrated high sensitivity by having much more proteins quantified with lower intensities. Also, the distribution of %CV for each protein has much lower values regarding proteins digested only with trypsin.

Overall, it is concluded that digestion with trypsin is more effective for MS analysis of membrane-related proteins, despite chymotrypsin being more suitable for hydrophobic regions of proteins.

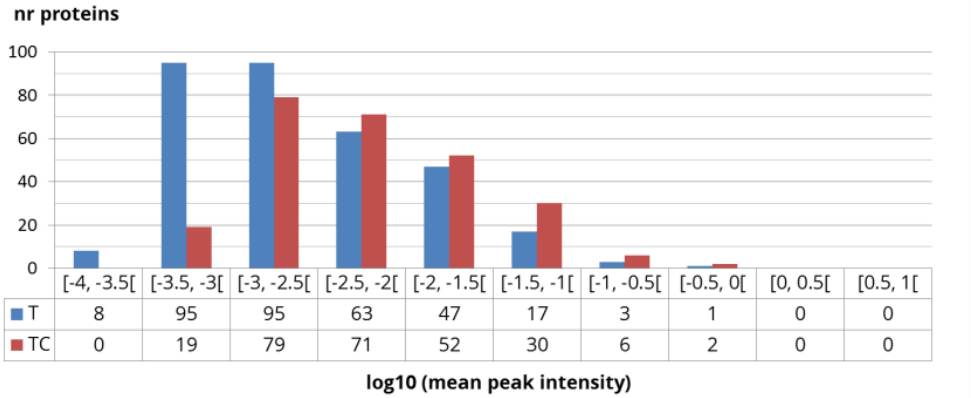

	[-4, -3.5[	[-3.5, -3[	[-3, -2.5[	[-2.5, -2[	[-2, -1.5[	[-1.5, -1[	[-1, -0.5[	[-0.5, 0[	[0, 0.5[	[0.5, 1[
T	8	95	95	63	47	17	3	1	0	0
TC	0	19	79	71	52	30	6	2	0	0

Figure 8.16 – Distribution of the number of proteins according to determined mean peak intensity.

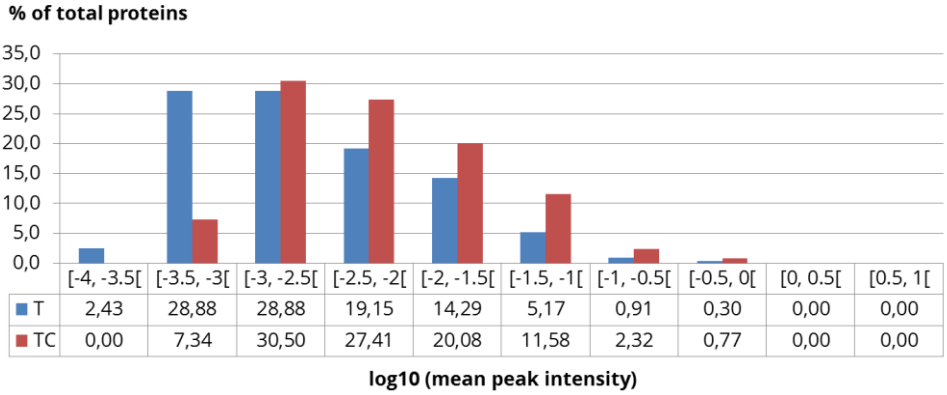

	[-4, -3.5[	[-3.5, -3[	[-3, -2.5[	[-2.5, -2[	[-2, -1.5[	[-1.5, -1[	[-1, -0.5[	[-0.5, 0[	[0, 0.5[	[0.5, 1[
T	2,43	28,88	28,88	19,15	14,29	5,17	0,91	0,30	0,00	0,00
TC	0,00	7,34	30,50	27,41	20,08	11,58	2,32	0,77	0,00	0,00

Figure 8.17 – Percentage of proteins according to determined mean peak intensity.

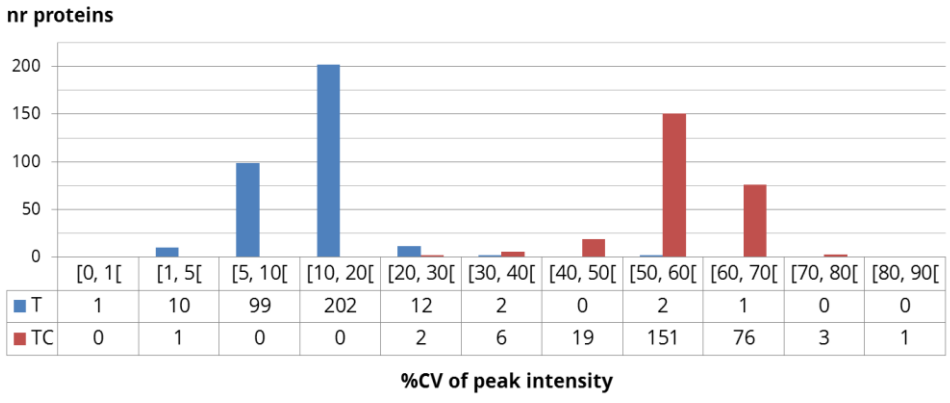

	[0, 1[	[1, 5[	[5, 10[	[10, 20[	[20, 30[	[30, 40[	[40, 50[	[50, 60[	[60, 70[	[70, 80[	[80, 90[
T	1	10	99	202	12	2	0	2	1	0	0
TC	0	1	0	0	2	6	19	151	76	3	1

Figure 8.18 - Distribution of %CV attributed to each quantified protein.

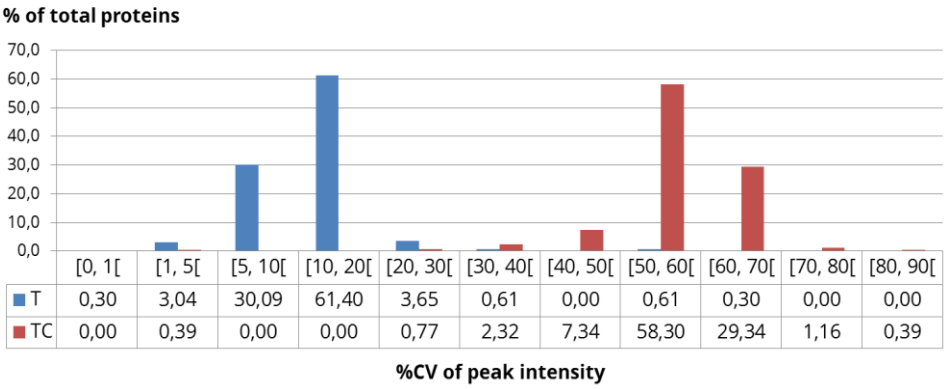

	[0, 1[	[1, 5[	[5, 10[	[10, 20[	[20, 30[	[30, 40[	[40, 50[	[50, 60[	[60, 70[	[70, 80[	[80, 90[
T	0,30	3,04	30,09	61,40	3,65	0,61	0,00	0,61	0,30	0,00	0,00
TC	0,00	0,39	0,00	0,00	0,77	2,32	7,34	58,30	29,34	1,16	0,39

Figure 8.19 – Percentage of proteins according to determined %CV values.

8.6. Experimental avidin pull-down

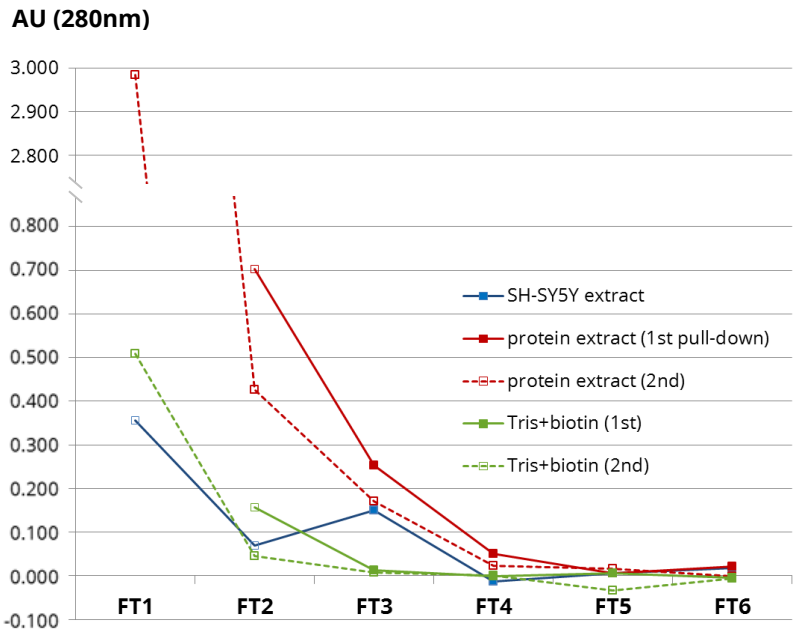

Figure 8.20 – Nanodrop measurement of fractions collected during washing steps of avidin pull-down, using PBS as blank. Full squares were measured after collection; squares with no filling were fractions measured after storage at -20ºC. AU = absorbance units

Table 8.8 – Comparison of total number of proteins identified in washing and eluting fractions collected during avidin pull-down of protein extract and Tris+biotin, and respective number and percentage of proteins with gene ontology attributed to membrane (GO:0044425), plasma membrane (GO:0005886), extracellular region (GO:0005576) and cell surface (GO:0009986), and proteins with predicted α-transmembrane region (using TMHMM Server v.20 online tool).

			total number of proteins	protein with nr peptides >= 3	proteins with nr peptides < 3	membrane proteins		plasma membrane		proteins with predicted α-transmembrane (TMHMM)		extracellular region		cell surface proteins	
						nr	%	nr	%	nr	%	nr	%	nr	%
protein extract	1st pull-down	bt	63	33	30	35	55.56	24	38.10	2	3.17	55	87.30	2	3.17
		reg	52	30	22	33	63.46	18	34.62	1	1.92	44	84.62	2	3.85
		sb	176	83	93	115	65.34	48	27.27	9	5.11	127	72.16	9	5.11
	2nd pull-down	ft1	545	284	261	325	59.63	110	20.18	72	13.21	354	64.95	32	5.87
		bt	39	22	17	18	46.15	11	28.21	1	2.56	32	82.05	1	2.56
Tris+biotin solution	1st pull-down	bt	813	524	289	415	51.05	129	15.87	15	1.85	442	54.37	22	2.71
	2nd pull-down	bt	245	153	92	102	41.63	53	21.63	7	2.86	193	78.78	15	6.12

Table 8.9 – Determination of number of proteins with cellular component attributions of interest (membrane, plasma membrane, cell surface) and with α-transmembrane prediction, aong list of proteins common to all fractions, and total distinct proteins found among all washing and eluting fractions.

	total distinct proteins	proteins common to all samples
Total proteins	1093	17
Membrane proteins	580	11
Plasma membrane proteins	193	8
Cell surface proteins	41	1
Proteins with predicted α-transmembrane	83	0

Table 8.10 – Comparison of identified peptides and proteins among fractions collected after pull-down of protein extract and Tris+biotin solution, using ProteinPilot processing of IDA acquisition files with normal parameters and with modified parameters (where modification list includes coupling of Sulfo-NHS-LC-biotin with lysine and N-terminal residues). Number of proteins and peptides with biotin determined with its identification on protein and peptide summary files, acquired after ProteinPilot processing with modified parameters.

			protein extract					Tris+biotin	
			1st pull-down			2nd pull-down		1st pull-down	2nd pull-down
			bt	**reg**	**sb**	**ft1**	**bt**	**bt**	**bt**
PP with normal parameters		proteins	63	52	176	545	39	813	245
		peptides	398	314	693	2338	275	4910	1413
PP with modified parameters	total	proteins	61	53	170	545	39	818	247
		peptides	398	319	699	2344	274	4959	1433
	with biotin	proteins	0	0	0	2	0	21	11
		peptides	0	0	0	2	0	31	11

Table 8.11 – Comparison of identified proteins using normal and modified ProteinPilot parameters (the later detects increased mass of biotinylated residues), regarding total number, proteins with less and more than 3 peptides, and gene ontology attributions of interest (membrane, plasma membrane, extracellular region, cell surface)

	protein extract										Tris + biotin			
	1st pull-down						2nd pull-down				1st pull-down		2nd pull-down	
	bt		**reg**		**sb**		**ft1**		**bt**		**bt**		**bt**	
	normal parame-ters	*modified parame-ters*	normal	*modified*	normal	*modified*	normal	*modified*	normal	*modified*	normal	*modified*	normal	*modified*
nr proteins >= 3	33	*33*	30	*30*	83	*82*	284	*284*	22	*22*	524	*527*	153	*153*
nr proteins < 3	30	*28*	22	*23*	93	*88*	261	*261*	17	*17*	289	*291*	92	*94*
nr total	**63**	***61***	**52**	***53***	**176**	***170***	**545**	***545***	**39**	***39***	**813**	***818***	**245**	***247***
nr membrane proteins	35	*34*	33	*34*	115	*111*	325	*327*	18	*18*	415	*425*	102	*106*
nr plasma membrane	24	*23*	18	*20*	48	*48*	110	*113*	11	*11*	129	*133*	53	*56*
nr extracellular region	55	*55*	44	*44*	127	*123*	354	*353*	32	*32*	442	*443*	193	*193*
nr cell surface proteins	2	*2*	2	*4*	9	*13*	32	*32*	1	*1*	22	*24*	15	*16*

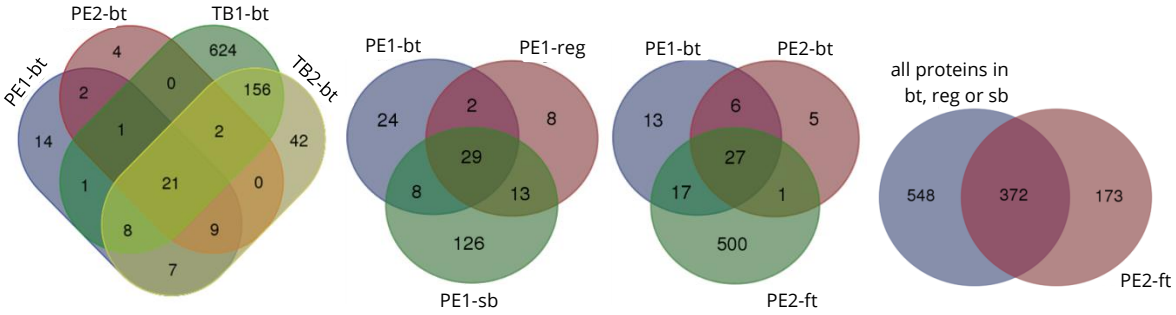

Figure 8.21 – Venn diagrams for convergence analysis of protein list acquired in IDA analysis in the various fractions collected after pull-down: PE1 = first pull-down of protein extract; PE2 = second elution of protein extract, using first washing fraction from PE1; TB1 = first pull-down of Trisand biotin solutions used in biotinylation; TB2 = second pull-down of Tris and biotin solutions. Collection of several fractions in each pull-down: ft = first washing fraction, with non-biotinylated proteins; bt = elution of biotinylated protein with biotin solution; reg = elution with glycine solution; sb = elution with addition of Sample Buffer and resin denaturation.

Table 8.12 - Comparison of SWATH libraries created after ProteinPilot processing of all fractions considered for IDA acquisition analysis, using normal or modified parameters.

	peptides	proteins						
		total	>=3	<3	membrane	plasma membrane	cell surface	extracellular region
PP normal parameters	6103	1059	661	398	576	191	43	595
PP modified parameters	6202	1055	662	393	574	190	43	592

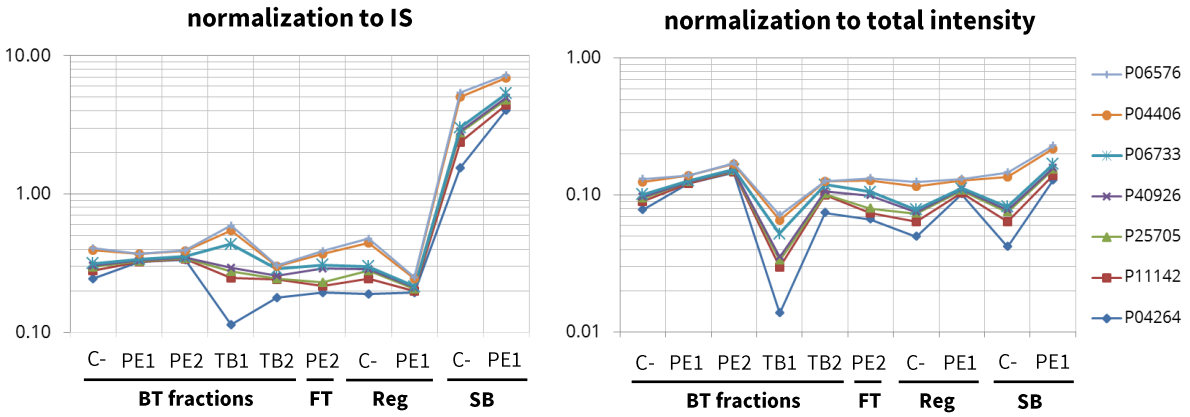

Figure 8.22 – Quantification of proteins after normalization to total intensity of each fraction or to internal standard (IS). Selection of proteins: common to all FT, BT, Reg and SB fractions subjected to IDA acquisition; plasma membrane or cell surface localization (not found proteins with α-transmembrane prediction common to all samples). Execution of several pull-downs: C- = pull-down of non-biotinylated protein extract (not subjected to IDA acquisition); PE1 = first pull-down of protein extract; PE2 = second elution of protein extract, using first washing fraction from PE1; TB1 = first pull-down of Tris and biotin solutions used in biotinylation; TB2 = second pull-down of Tris and biotin solutions. Collection of several fractions in each pull-down: FT = first washing fraction, with non-biotinylated proteins; Bt = elution of biotinylated protein with biotin solution; Reg = elution with glycine solution; SB = addition of Sample Buffer and resin denaturation.

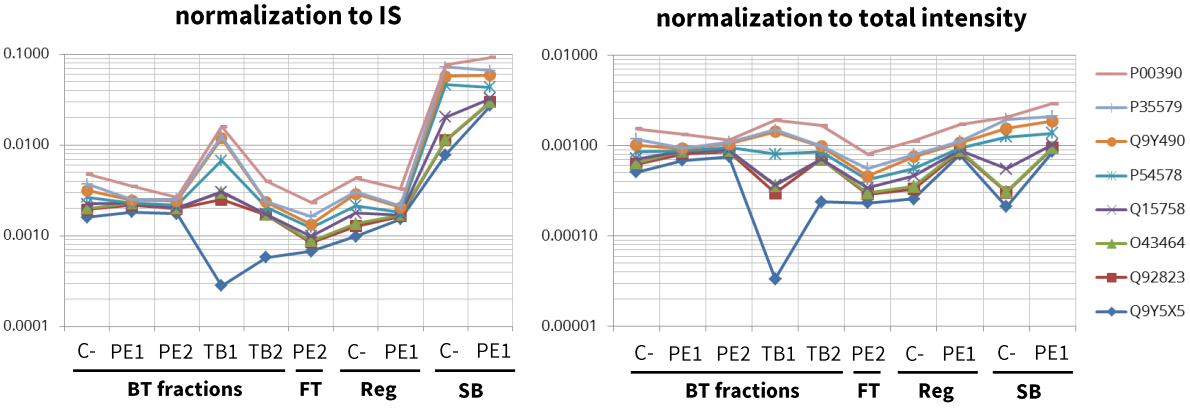

Figure 8.23 – Quantification of proteins after normalization to total intensity of each fraction or to internal standard (IS). Selection of proteins: identified in any BT, Reg and SB fractions subjected to IDA acquisition, and not identified in IDA acquisition of FT fraction of PE2 pull-down; at least two attributions regarding plasma membrane localization, cell surface localization or α-transmembrane prediction. Legend equal to figure 8.22.

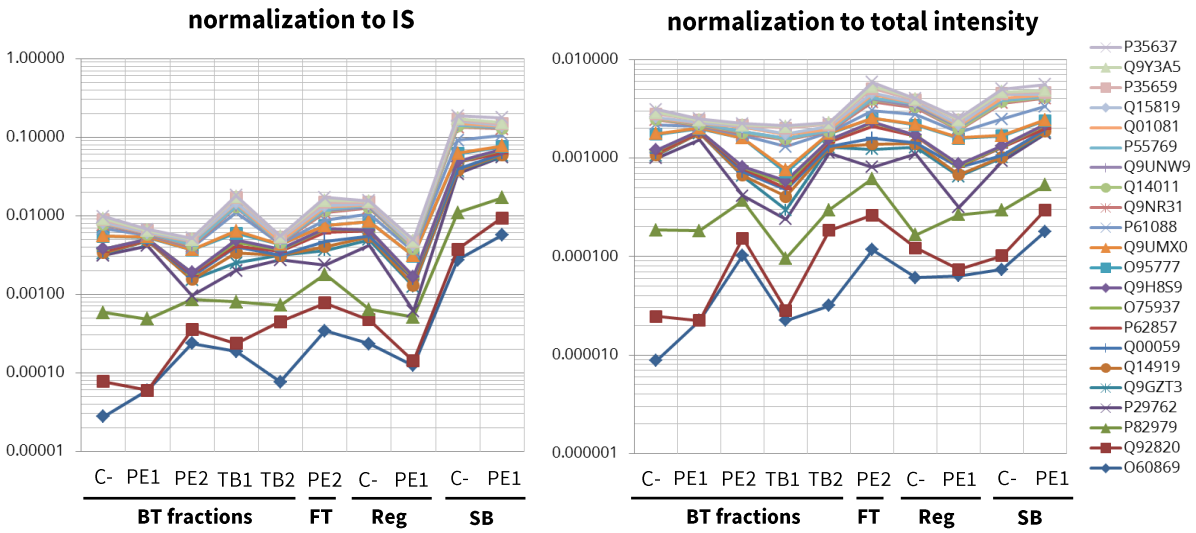

Figure 8.24 – Quantification of proteins after normalization to total intensity of each fraction or to internal standard (IS). Selection of proteins: only identified in identified in IDA acquisition of FT fraction of PE2 pull-down (not identified in any all BT, Reg or SB fractions); not attributed to plasma membrane localization, cell surface localization or α-transmembrane prediction. Legend equal to figure 8.22.

8.7. Complementary data from MS analysis of cell surface biotinylation

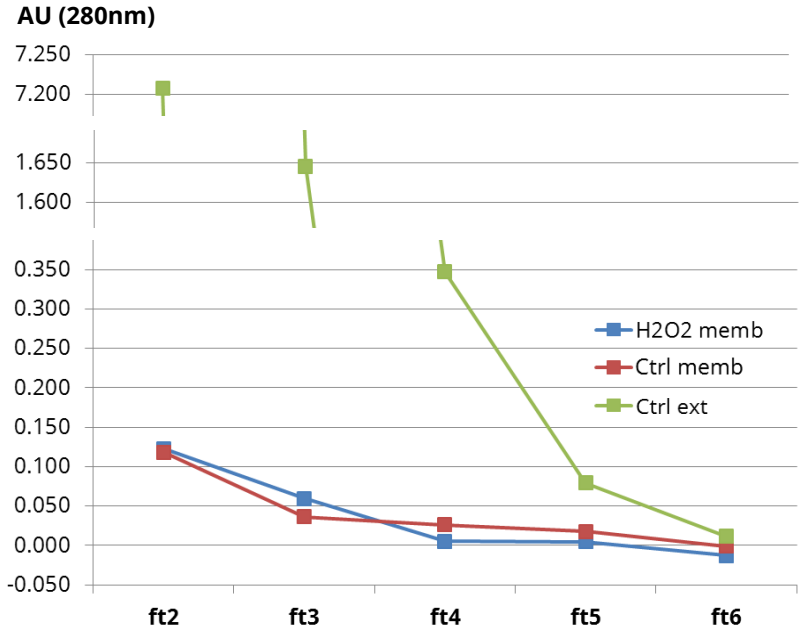

Figure 8.25 - Nanodrop measurement of fractions collected during washing steps (ft 2 to 6) of avidin pull-down (fractions ft 2 to 6) of the three pull-downs of SH-SY5Y protein extract: Ctrl ext = control conditions without ultracentrifugation; Ctrl memb = control condition, with ultracentrifugation and collection of crude membrane fraction; H2O2 memb = oxidative stress incubation conditions, with ultracentrifugation. Use of PBS as blank. AU = absorbance units.

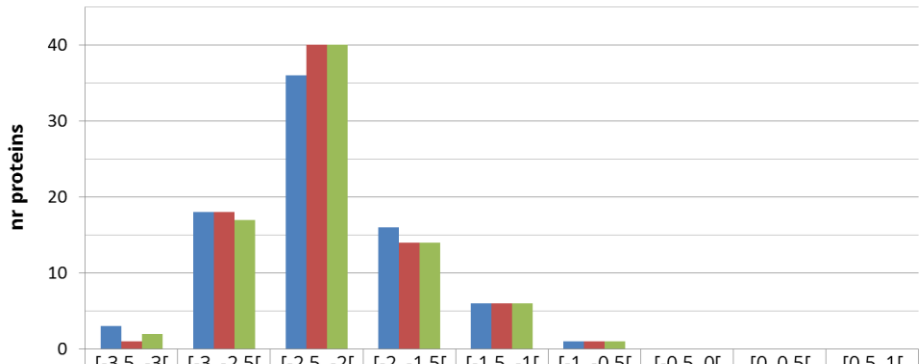

	[-3.5, -3[	[-3, -2.5[	[-2.5, -2[	[-2, -1.5[	[-1.5, -1[	[-1, -0.5[	[-0.5, 0[	[0, 0.5[	[0.5, 1[
Ctrl extract	3	18	36	16	6	1	0	0	0
Ctrl memb	1	18	40	14	6	1	0	0	0
H2O2 memb	2	17	40	14	6	1	0	0	0

Figure 8.26 - Distribution of number of proteins quantified in SWATH acquisition, according to logarithmic value determined for mean of protein intensity in four replicates of each pull-down (Ctrl extract, Ctrl memb, H_2O_2 memb), after values normalization to total intensity.

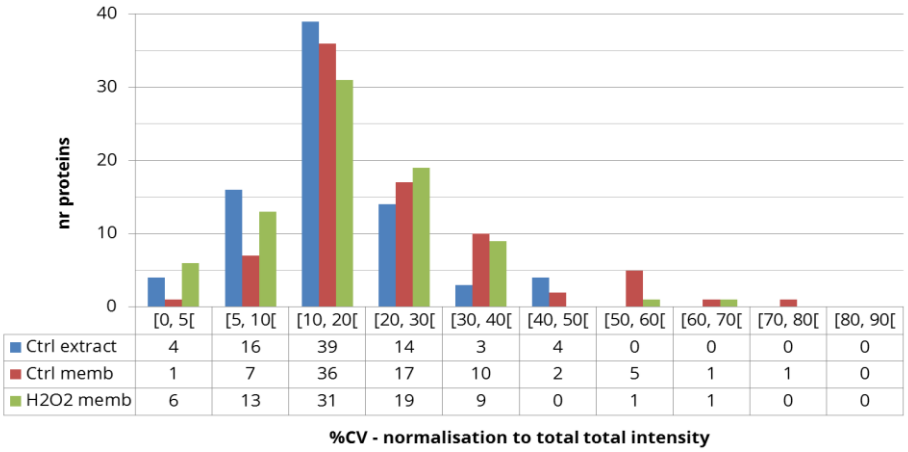

	[0, 5[	[5, 10[	[10, 20[	[20, 30[	[30, 40[	[40, 50[	[50, 60[	[60, 70[	[70, 80[	[80, 90[
Ctrl extract	4	16	39	14	3	4	0	0	0	0
Ctrl memb	1	7	36	17	10	2	5	1	1	0
H2O2 memb	6	13	31	19	9	0	1	1	0	0

Figure 8.27 - Distribution of number of quantified proteins according to coefficient of variation (%CV) of protein intensity between the four replicates of each pull-down (Ctrl extract, Ctrl memb, H_2O_2 memb), after intensity values normalization to total intensity of each replicate.

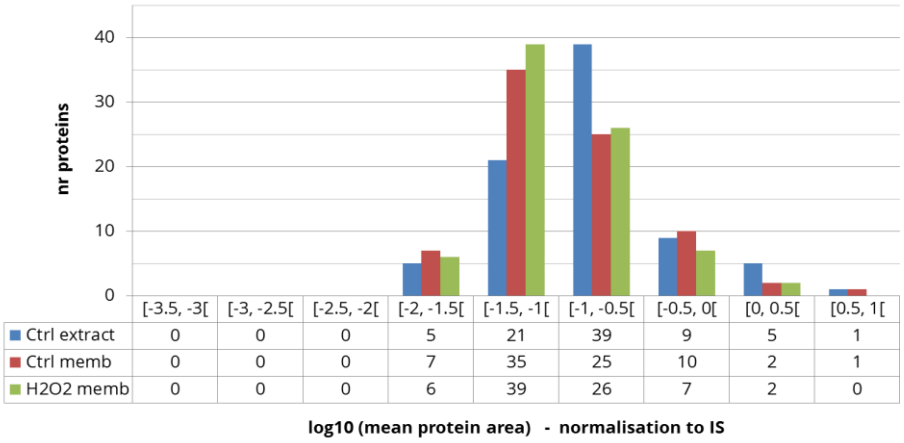

	[-3.5, -3[	[-3, -2.5[	[-2.5, -2[	[-2, -1.5[	[-1.5, -1[	[-1, -0.5[	[-0.5, 0[	[0, 0.5[	[0.5, 1[
Ctrl extract	0	0	0	5	21	39	9	5	1
Ctrl memb	0	0	0	7	35	25	10	2	1
H2O2 memb	0	0	0	6	39	26	7	2	0

Figure 8.28 - Distribution of number of quantified proteins according to logarithmic value for the mean of protein intensity, after values normalization to added internal standard (IS).

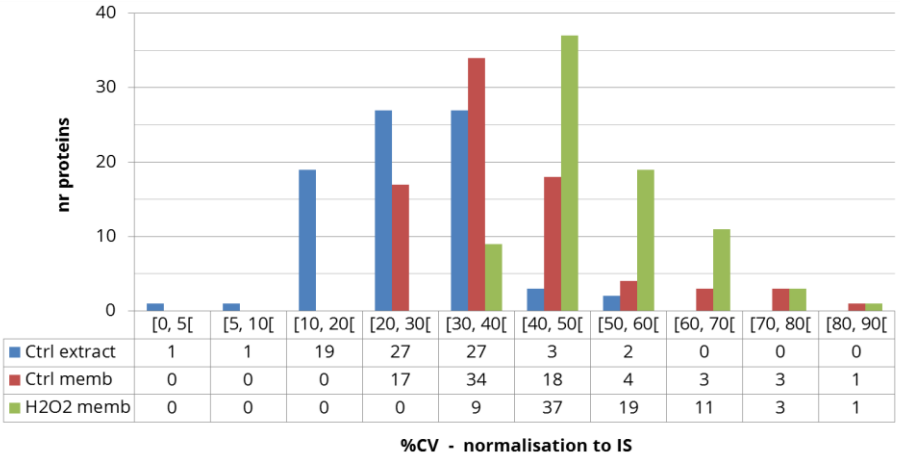

	[0, 5[	[5, 10[	[10, 20[	[20, 30[	[30, 40[	[40, 50[	[50, 60[	[60, 70[	[70, 80[	[80, 90[
Ctrl extract	1	1	19	27	27	3	2	0	0	0
Ctrl memb	0	0	0	17	34	18	4	3	3	1
H2O2 memb	0	0	0	0	9	37	19	11	3	1

Figure 8.29 - Distribution of number of quantified proteins according to coefficient of variation (%CV) between replicates, after values normalization to added internal standard (IS).

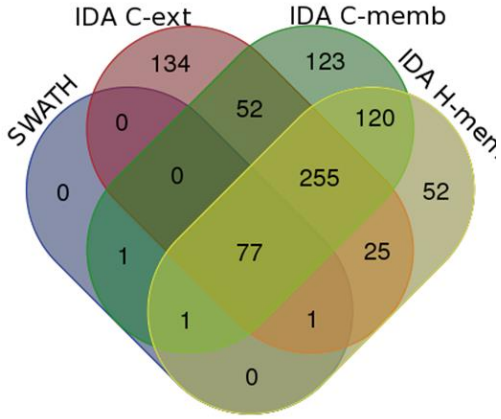

Figure 8.30 - Venn diagrams for convergence analysis of protein lists resulted from the acquisition and processing of samples: SWATH = selected proteins after SWATH acquisition and processing; IDA C-ext = proteins identified with IDA acquisition of pull-down of protein extract from control conditions, without ultracentrifugation processing; IDA C-memb = IDA acquisition of protein extract from control conditions, subjected to ultracentrifugation; IDA-H-memb = IDA acquisition of protein extract from oxidative stress conditions, subjected to ultracentrifugation.

Table 8.13 – Number and listing of proteins according to the convergence of protein lists obtained from SWATH acquisition and IDA acquisition of each condition (IDA C-ext, IDA C-memb, IDA H-memb), mentioned in Figure 8.30.

samples	nr	proteins (uniprot code)
IDA C-ext IDA C-memb IDA H-memb SWATH	77	P05388 Q00325 P12236 Q01130 P11142 P22626 P00403 P62424 Q71U36 Q07020 Q92522 P51991 P35232 O14979 P39023 Q9Y230 P67809 P25705 P62277 P61353 P62987 P62318 P02768 P62269 P18124 P68366 P18077 P36578 P57088 P06576 Q71DI3 Q14103 P62841 P04264 P23396 Q5VTE0 P45880 P19338 P62701 P63261 P62899 P17987 P14625 Q71UI9 P62249 P62917 O60506 P07910 P62753 P42766 P11940 P62847 P62266 Q99623 P61313 P52272 Q02878 P60866 P40429 P18621 P50914 P61254 P62805 P61619 Q9BPW8 P46781 P62913 P83731 P62906 Q00839 P15880 Q08211 P62244 P26373 Q16629 P13010 P62241
IDA C-ext IDA H-memb SWATH	1	P63162
IDA C-memb IDA H-memb SWATH	1	Q99880
IDA C-ext IDA C-memb IDA H-memb	255	Q9BSJ8 Q9NVI7 P09651 P30101 P13639 P62851 P41252 Q86U42 P62854 Q5JWF2 P14618 P50990 P14868 P53621 Q9Y224 P61513 A6NKG5 Q9NR30 Q8WXE9 P40939 Q07021 Q15029 O14980 Q9Y265 Q9P015 P39656 P78371 P61163 P19367 P40926 Q9NVJ2 O75533 Q9BUJ2 P51571 Q01813 P26378 P53618 P09874 P46778 P83881 Q99460 P62750 P61247 Q12905 Q9HD33 P22234 Q96CS3 P16615 Q9Y5B9 P49458 P55084 Q14839 P46977 P06493 Q5SSJ5 P37108 P62826 Q9UBF2 P42704 P18085 P84103 O14744 P27824 P04843 P22695 P62263 P13645 Q92499 P62333 P50416 P05141 P51532 O94906 P60842 Q16795 P17252 Q9Y3U8 Q7L2E3 Q14697 P14866 P07437 P04004 Q9UGP8 Q00610 P49411 P12956 Q9BZE4 P17844 Q6S8J3 P26583 Q7Z2W9 O75367 P23528 Q02978 P11021 Q9P2K5 Q13242 P31943 P16401 P84098 P36542 P10809 O75489 Q04837 P13667 Q9UBX3 Q71UM5 P49207 Q96DV4 Q9BYD1 Q01081 P27708 P48556 Q07955 Q9P035 P82650 O75643 Q1KMD3 P16403 Q14204 P56192 Q14974 P30050 Q8WXX5 P09661 P38646 Q14576 O75494 Q9H9B4 Q15046 P35527 O00425 Q92841 Q8N1F7 Q13838 P35580 Q9UKM9 P26599 O75352 P54136 P09172 Q6DRA6 P26641 P51659 P78527 O75964 Q99453 P62081 P08238 Q6ZMW2 P62304 O43143 P32119 Q9Y4L1 Q9BVA1 P48735 Q8N158 P07305 P62316 P35908 P04844 P22087 P08621 O43390 P62995 Q9BYD3 Q08945 P61978 Q13263 P12235 O60762 P02786 P62910 P43243 Q16555 P61026 Q96EY7 Q13740 P08237 Q9UHB9 P46783 Q16891 Q15717 P32969 Q9Y277 O43602 Q3KQU3 Q92552 P07477 Q13310 P62888 P30048 P31942 P20042 Q6P2Q9 P13591 P0AEY0 P31689 P62834 P62314 Q96CW1 Q08J23 Q9UJS0 P06748 P33992 Q9BQG0 P63244 P49406 Q9P2J5 Q99729 P05386 Q05639 P51398 Q13509 P62280 P46776 O76021 P10412 P42212 P23284 P62829 P38919 Q9BZE1 P48643 Q12860 P26368 O43242 P25205 P35579 Q16352 Q13595 Q96DH6 Q8N0U8 P05556 Q09161 Q15393 O00571 O60318 Q99714 P49721 Q02543 P47914 P04406 P27635 Q92900 P46779 O14880 Q15084 Q8TB36 O95347 P11387 P68371 P40227 P49368 P07900
IDA C-memb SWATH	1	P62873
IDA C-ext IDA C-memb	52	Q00577 P82914 Q9NYK5 O75306 O00422 P31040 Q7Z4S6 Q8N163 P82675 Q06830 P12268 Q8NBJ5 Q96A35 Q12789 Q92878 O75569 P40937 Q16540 P28331 Q9BWM7 P11182 P09012 P55209 P43246 Q9UQ80 Q9UJA5 P04792 P36957 Q14498 P53007 P82663 Q9BXJ4 O75140 Q13885 P62195 Q12906 Q13405 P46777 P67775 P52597 Q92673 Q03701 P33993 P02545 P04350 O15347 P00338 P82933 P08865 Q96SB4 O75477 P69905
IDA C-ext IDA H-memb	25	Q14739 Q5SY16 O00148 P54886 Q14194 P50454 P62879 Q16658 P84077 P37802 Q9NZ01 Q13243 Q8IVF1 P61158 P19404 P16402 P17858 P08670 P30876 P63173 Q9Y3D9 Q8WUD1 Q99943 Q9H936 Q9Y4W2

IDA C-memb **IDA H-memb**	120	P35268 Q53GQ0 Q9UJZ1 Q07666 P09001 P46087 P49327 Q13813 Q969V3 P50402 O43674 O75947 Q9H0S4 Q9NZB2 O43707 Q9UNM6 Q99832 Q92769 O14735 O60264 Q92616 Q8NBX0 Q8IUE6 P37235 P13073 P67812 Q9UQE7 Q9NXF1 P21796 Q15738 Q8IXI1 O60831 P05026 P61803 P08195 P68133 P61981 Q16850 Q9HD20 P05023 P62191 P46821 P19525 Q9UIG0 Q15019 O96008 O15260 P35998 P47897 O00232 O00154 P07237 P55072 Q9Y3E0 P69892 Q15758 O75531 P52701 O60313 P48047 Q15397 P55795 P51572 P56134 P07814 Q9BRX8 Q9H6V9 Q15008 Q9HDC9 P51665 Q96KA5 Q13155 Q9BV38 P50991 Q9UKX2 P31930 Q14152 Q9P0M6 P00387 P16104 P49748 Q99536 Q92945 Q8IZL8 P62308 Q8N766 Q96N67 Q96CW5 P46782 Q13724 Q6P2E9 P24539 O00217 Q16799 Q8N5K1 P57678 Q8IZ81 P11388 O43795 P68363 A5YKK6 Q9UHG3 Q8TEM1 Q15366 O00264 Q6FI13 Q13200 P49755 Q9NQC3 Q9NWU5 P14314 Q02880 P35659 Q5JPE7 A1L0T0 O00231 Q15233 Q9Y6C9 Q3ZCQ8 P13637
IDA C-ext	134	Q15287 Q9BQ75 Q86VP6 P07741 Q9Y3Y2 P09429 O60568 Q96QR8 Q9UBS4 Q13765 Q9H5Q4 Q07812 O75251 O60783 P62258 Q9BTW9 P21397 Q12931 Q15427 P32004 Q9H857 P29401 P82930 P49821 Q6SZW1 Q59GN2 P27694 Q92823 Q8TCJ2 P05455 O95071 Q13162 Q6PKG0 P26358 Q8IYB3 P19387 P12081 P38159 P62820 Q12849 P35606 O43633 P40222 Q9Y4C2 P78362 Q9BYD2 O95613 Q9NWB1 Q8NEV1 P61221 Q7Z6Z7 P61106 P11498 Q9NYU2 P61764 P07195 Q9Y2R9 P62136 P09622 Q96QV6 P15927 P55060 Q9UIA9 P33947 Q9BQ39 P36543 Q96ME7 O00541 Q96HS1 O60884 O43592 P35244 P06753 P07196 O95490 P12004 Q15274 Q6NUK1 P11586 Q13151 P30041 P20290 P60953 P22102 Q9HCC0 Q14566 P67870 O95793 P49448 Q9BYC9 Q9BVP2 A8MWD9 O75131 Q08170 Q15005 Q9H9J2 P23381 P14174 Q12769 Q9Y2Q9 O95747 P68871 P62140 P41250 P38606 Q93008 Q8N5N7 P17812 Q8IV08 P06733 O60832 P82673 Q9NSE4 Q96KR1 Q9HAV4 Q9UER7 Q9Y619 Q8IXM3 Q9NRG9 P33991 P82664 Q99873 P55786 Q01085 Q96P70 Q99879 O95433 Q9Y3B7 P11717 Q92665 Q92621 Q9UBU9 P19623 Q2NL82
IDA C-memb	123	Q5ZPR3 Q86UE4 Q8NF37 Q7L099 Q9H3N1 Q7Z5H4 Q9H3H5 Q9P0S9 Q13423 P08754 Q9Y315 Q15365 Q9C0H2 P27348 Q02809 P30153 Q92973 P51149 O75396 P55036 Q5BJF2 P05198 Q6ZVC0 Q14344 O75027 Q16576 P46459 B1AJZ9 P63010 P56537 Q29RF7 Q8IX01 O00303 P55265 Q9Y262 Q9BQB6 P20671 Q3SXM5 O95202 A6NHR9 O75323 Q9UMS4 O43776 Q15363 P21281 P17980 P14678 Q9BSJ2 Q9HCS7 P47985 O00560 Q16630 Q9BTV4 P51114 Q92542 Q15050 Q9ULC6 Q9UJY5 P23246 Q9Y3I0 Q9HB71 Q92643 P24534 Q8TCT9 P20674 Q9P258 Q9BRJ2 Q53H12 Q9NY12 P15311 O95197 P60468 P46940 P35249 O00471 Q07065 P25788 Q9UHD8 Q9Y394 Q99613 Q9H1A4 Q15907 Q9NVP1 P62937 P60228 Q9Y6Y8 P09471 O00487 P61006 P61019 Q5T653 P60660 Q9BVC6 Q8NHH9 P48444 Q8IZ83 P53396 Q96AG4 O94973 Q16643 P43307 O00567 P82921 O43913 Q14669 Q9Y3D6 Q9NTJ5 P17600 Q13247 P05387 O75431 P41091 P35613 P26640 Q96A72 P61081 P09543 P35030 Q16778 Q8TBY8 P53999 Q07866 O43681
IDA H-memb	52	Q14728 Q14108 Q01082 Q86XI2 O60306 P46100 P51148 P04899 Q9NTI5 Q9NS69 O15258 Q92974 Q14145 O43324 Q5T4S7 Q96G23 Q5VTL8 Q14683 Q9UNF1 O95299 P54920 O43809 Q9BTT0 Q7L014 Q96ST3 O15173 Q9Y2X3 P54289 Q9BW27 P28288 Q99575 Q9H7Z7 P08579 Q12836 Q9Y2R5 Q9Y2A7 P36776 O94925 Q12926 P35222 Q96F07 Q5JTH9 Q8TAE7 Q9Y5S9 O15240 Q96I24 P50148 Q9BYG3 P26196 Q9Y512 Q562R1 P26038

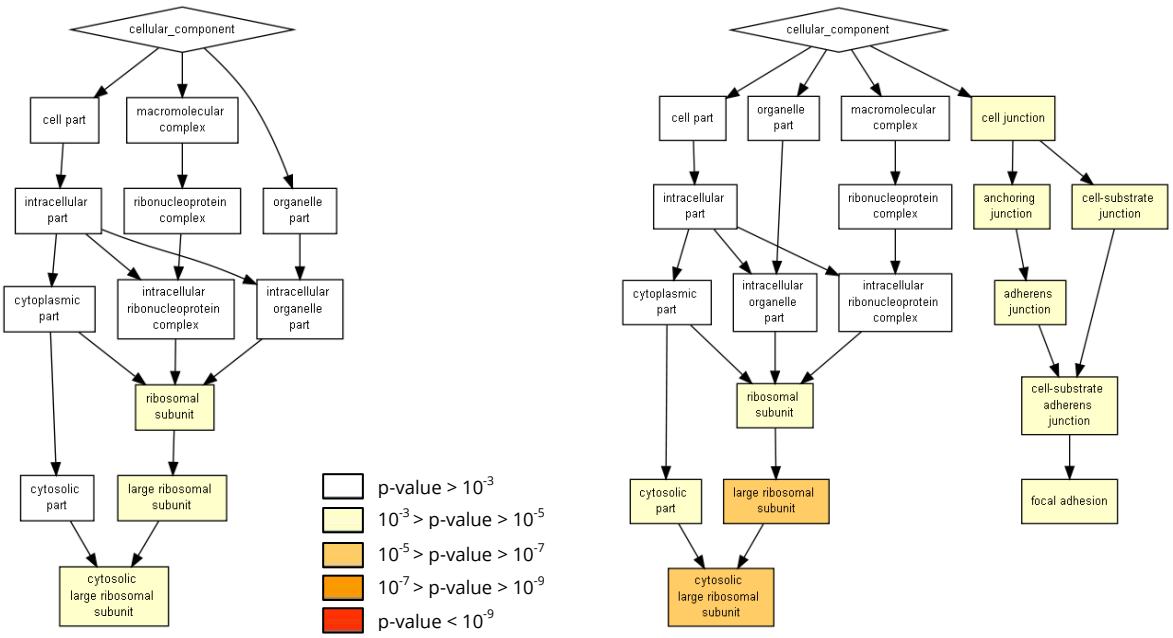

Figure 8.31 – Diagram for gene ontology enrichment, according to cellular component, after GOrilla online tool query of SWATH quantified proteins, with protein list ranked in decreasing order of mean protein value in the control condition (Ctrl memb): left diagram = ranking with values normalized to total intensity; right = values normalized to internal standard (IS).

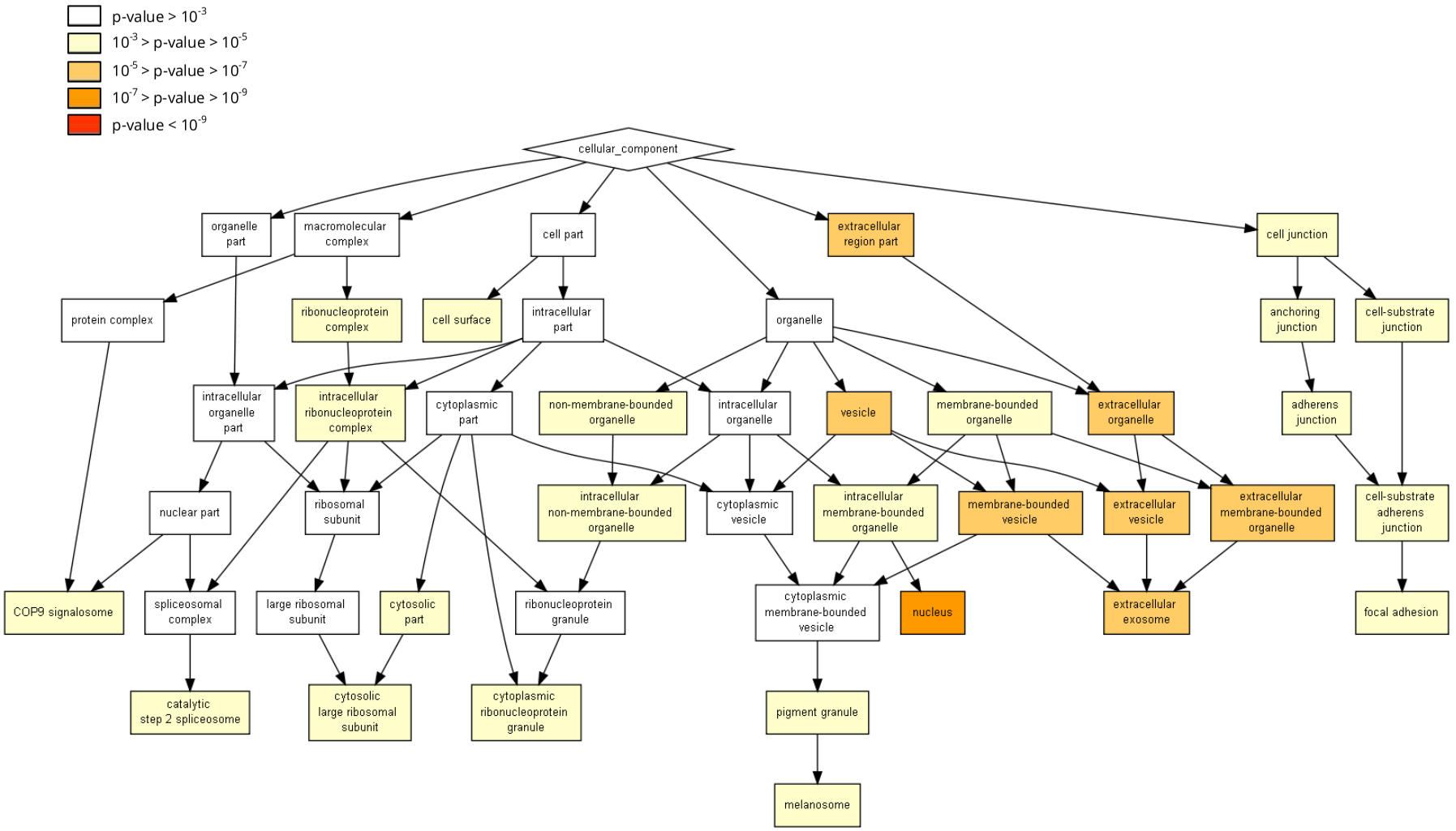

Figure 8.32 – Diagram for gene ontology sample enrichment, according to cellular component, after Gorilla online tool processing of list of proteins identified after IDA acquisition of Ctrl extract condition (normal SH-SY5Y incubation conditions, absence of ultracentrifugation).

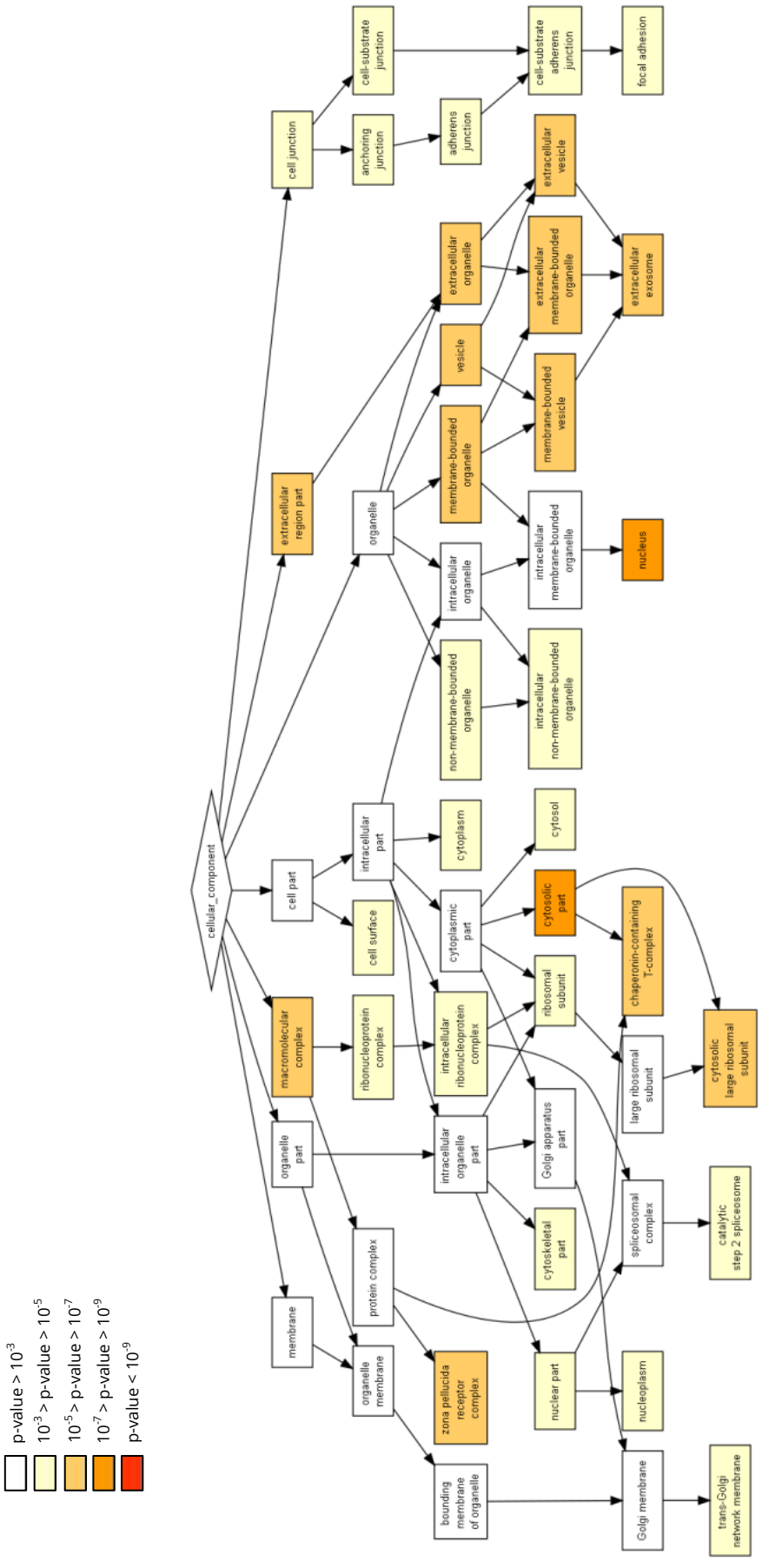

Figure 8.33 – Diagram for gene ontology sample enrichment, according to cellular component, after Gorilla online tool processing of list of proteins identified after IDA acquisition of Ctrl membane condition (normal SH-SY5Y incubation conditions, use of ultracentrifugation for collection and pull-down of crude membrane fraction).

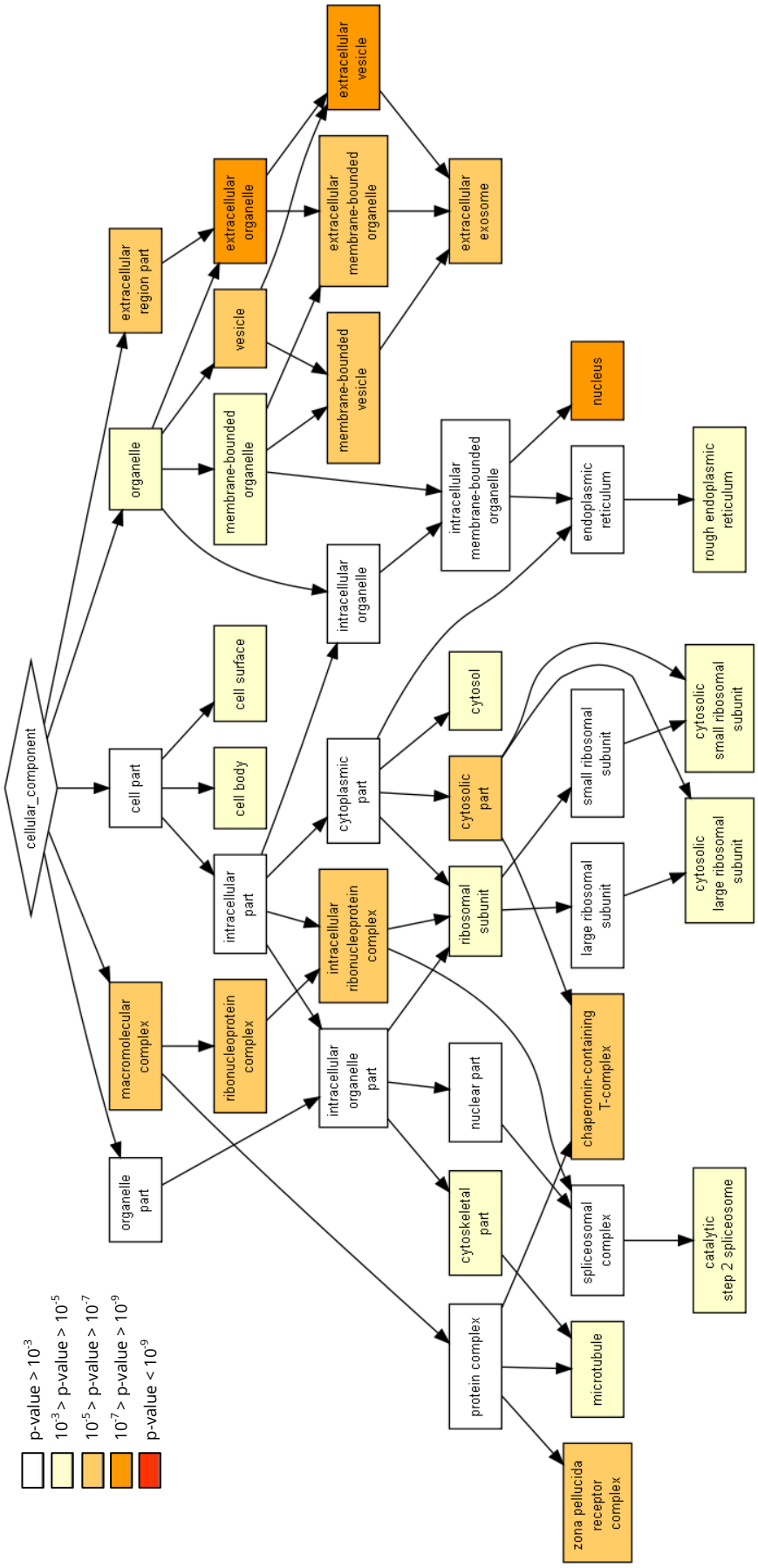

Figure 8.34 – Diagram for gene ontology sample enrichment, according to cellular component, after Gorilla online tool processing of list of proteins identified after IDA acquisition of H_2O_2 memb condition (SH-SY5Y oxidative stress induction, use of ultracentrifugation for pull-down crude membrane fraction).

Table 8.14 – List of intensity values of quantified proteins after SWATH acquisition and selection of proteins with at least one peptide detected with confidence in all samples: normalization to total intensity, or to added internal standard (IS), of each replicate. Four replicates for each condition: protein extract from control conditions and absence of ultracentrifugation (Ctrl extract); protein extract from control conditions and use of ultracentrifugation (Ctrl memb); protein extract from oxidative stress conditions and use of ultracentrifugation (Ctrl memb). Determination of logarithmic value from mean value [log(mean)], standard deviation (st dev) and coefficient of variation (%CV) between replicates of each condition. Comparison of Ctrl ext or H_2O_2 memb against control condition, considered Ctrl memb (Ctrl ext / Ctrl memb, H_2O_2 memb / Ctrl memb, respectively): determination of p-value from t-test between conditions for each protein (t-test p-value), and determination of fold variation between conditions [fold(var)] and respective logarithmic value [log10(var)].

		normalisation to total intensity																normalisation to IS															
		Ctrl ext			Ctrl memb			H202 memb			Ctrl ext / Ctrl memb			H2O2 memb / Ctrl memb				Ctrl ext			Ctrl memb			H202 memb			Ctrl ext / Ctrl memb			H2O2 memb / Ctrl memb		
Entry	Entry name	log(mean)	st dev	%CV	log(mean)	st dev	%CV	log(mean)	st dev	%CV	t-test p-value	log10 (var)	fold (var)	t-test p-value	log10 (var)	fold (var)		log(mean)	st dev	%CV	log(mean	st dev	%CV	log(mean)	st dev	%CV	t-test p-value	log10 (var)	fold (var)	t-test p-value	log10 (var)	fold (var)	
Q08211	DHX9	-2.744	4.33E-04	23.98	-2.825	7.74E-04	51.71	-2.669	6.26E-04	29.25	0.512	0.081	1.21	0.243	0.156	1.43		-1.378	1.73E-02	41.21	-1.562	1.91E-02	69.53	-1.464	2.49E-02	72.53	0.304	0.184	1.53	0.675	0.098	1.25	
P52272	HNRPM	-2.087	8.56E-04	10.47	-2.406	1.68E-03	42.75	-2.276	1.30E-03	24.50	0.004	0.319	2.08	0.242	0.131	1.35		-0.739	2.47E-02	13.54	-1.126	4.43E-02	59.26	-1.075	4.96E-02	58.95	0.005	0.387	2.44	0.788	0.051	1.12	
P25705	ATPA	-1.994	2.06E-03	20.36	-2.178	1.79E-03	26.91	-2.171	5.72E-04	8.48	0.043	0.184	1.53	0.917	0.007	1.02		-0.637	7.98E-02	34.59	-0.924	4.97E-02	41.76	-0.988	5.05E-02	49.20	0.055	0.288	1.94	0.662	-0.064	0.86	
P19338	NUCL	-1.129	1.34E-02	18.06	-1.373	7.15E-03	16.86	-1.423	1.25E-03	3.32	0.006	0.244	1.75	0.250	-0.050	0.89		0.238	6.57E-01	37.92	-0.124	2.51E-01	33.46	-0.251	2.31E-01	41.21	0.032	0.363	2.31	0.309	-0.126	0.75	
Q71U36	TBA1A	-0.816	3.58E-02	23.46	-1.196	7.06E-03	11.09	-1.173	1.54E-02	22.89	0.003	0.380	2.40	0.691	0.023	1.06		0.536	1.10E+00	32.14	0.045	2.86E-01	25.79	0.021	6.51E-01	61.94	0.007	0.491	3.10	0.875	-0.023	0.95	
P22626	ROA2	-2.076	2.34E-03	27.90	-2.173	5.52E-04	8.21	-2.216	2.02E-03	33.17	0.212	0.097	1.25	0.561	-0.044	0.90		-0.716	8.20E-02	42.67	-0.919	3.91E-02	32.49	-1.001	7.78E-02	77.90	0.165	0.203	1.60	0.653	-0.081	0.83	
O60506	HNRPQ	-2.282	5.93E-04	11.36	-2.418	1.43E-03	37.54	-2.406	4.75E-04	12.08	0.119	0.136	1.37	0.886	0.013	1.03		-0.920	3.77E-02	31.31	-1.166	3.73E-02	54.72	-1.221	3.24E-02	53.89	0.097	0.247	1.77	0.754	-0.055	0.88	
P06576	ATPB	-2.363	6.47E-04	14.94	-2.501	5.35E-04	16.94	-2.474	8.63E-04	25.72	0.031	0.137	1.37	0.710	0.026	1.06		-0.999	3.53E-02	35.23	-1.259	1.64E-02	29.81	-1.276	3.19E-02	60.21	0.059	0.260	1.82	0.911	-0.017	0.96	
P63261	ACTG	-1.611	1.35E-03	5.52	-1.633	6.91E-03	29.67	-1.699	6.94E-04	3.47	0.752	0.021	1.05	0.376	-0.067	0.86		-0.258	1.15E-01	20.78	-0.391	1.59E-01	39.27	-0.528	1.21E-01	40.77	0.187	0.134	1.36	0.317	-0.136	0.73	
Q9Y230	RUVB2	-2.124	7.06E-04	9.39	-2.297	7.81E-04	15.47	-2.324	4.94E-04	10.43	0.003	0.173	1.49	0.526	-0.028	0.94		-0.763	5.21E-02	30.20	-1.046	3.03E-02	33.74	-1.139	3.69E-02	50.82	0.034	0.283	1.92	0.496	-0.093	0.81	
P11940	PABP1	-2.295	7.00E-04	13.80	-2.494	4.73E-04	14.76	-2.492	3.64E-04	11.29	0.004	0.200	1.58	0.946	0.003	1.01		-0.932	3.93E-02	33.58	-1.250	1.68E-02	29.84	-1.321	2.07E-02	43.41	0.029	0.318	2.08	0.547	-0.071	0.85	
P14625	ENPL	-2.192	1.18E-03	18.36	-2.541	2.88E-04	10.00	-2.444	5.14E-04	14.31	0.001	0.349	2.23	0.051	0.096	1.25		-0.826	5.27E-02	35.33	-1.285	1.77E-02	34.06	-1.265	2.58E-02	47.49	0.013	0.459	2.88	0.880	0.020	1.05	
P36578	RL4	-1.610	3.97E-03	16.15	-1.592	4.52E-03	17.64	-1.683	4.67E-03	22.49	0.742	-0.018	0.96	0.186	-0.091	0.81		-0.246	1.99E-01	35.15	-0.347	1.41E-01	31.42	-0.519	1.30E-01	42.91	0.372	0.101	1.26	0.177	-0.172	0.67	
P04264	K2C1	-2.915	2.87E-04	23.57	-2.979	5.45E-04	51.96	-2.884	4.55E-04	34.81	0.607	0.064	1.16	0.496	0.095	1.25		-1.554	1.08E-02	38.51	-1.740	1.12E-02	61.55	-1.740	6.20E-03	34.08	0.257	0.186	1.53	0.998	0.000	1.00	
P62805	H4	-1.353	8.46E-03	19.08	-0.731	2.71E-02	14.60	-0.699	4.26E-02	21.30	0.000	-0.622	0.24	0.588	0.033	1.08		0.003	2.75E-01	27.28	0.525	1.24E+00	37.07	0.464	9.87E-01	33.94	0.010	-0.522	0.30	0.595	-0.062	0.87	
Q99623	PHB2	-2.331	1.24E-03	26.58	-2.453	5.47E-04	15.54	-2.403	4.79E-04	12.13	0.142	0.122	1.33	0.284	0.050	1.12		-0.983	3.22E-02	30.98	-1.207	2.01E-02	32.33	-1.234	2.22E-02	38.06	0.070	0.223	1.67	0.807	-0.028	0.94	
P62701	RS4X	-2.055	1.15E-03	13.01	-1.830	2.73E-03	18.45	-1.867	2.26E-03	16.62	0.007	-0.225	0.60	0.528	-0.036	0.92		-0.692	6.69E-02	32.90	-0.585	8.43E-02	32.44	-0.690	1.02E-01	50.19	0.336	-0.106	0.78	0.433	-0.105	0.79	
P35232	PHB	-2.047	2.08E-03	23.21	-2.051	2.43E-03	27.27	-2.050	2.96E-03	33.25	0.969	0.003	1.01	0.996	0.000	1.00		-0.697	6.19E-02	30.82	-0.791	6.94E-02	42.90	-0.868	7.51E-02	55.50	0.431	0.094	1.24	0.625	-0.077	0.84	
Q02878	RL6	-1.257	4.03E-03	7.28	-1.310	5.94E-03	12.12	-1.406	9.88E-04	2.51	0.129	0.053	1.13	0.018	-0.096	0.80		0.094	2.20E-01	17.76	-0.062	2.82E-01	32.58	-0.230	2.56E-01	43.44	0.081	0.156	1.43	0.195	-0.168	0.68	
P39023	RL3	-1.961	1.46E-03	13.34	-2.024	9.67E-04	10.21	-2.076	5.64E-04	6.73	0.144	0.063	1.16	0.101	-0.053	0.89		-0.599	8.08E-02	32.12	-0.781	4.27E-02	25.80	-0.899	5.92E-02	46.89	0.109	0.182	1.52	0.323	-0.118	0.76	
P23396	RS3	-2.004	8.52E-04	8.60	-2.006	1.52E-03	15.42	-2.014	1.85E-03	19.10	0.966	0.002	1.00	0.877	-0.009	0.98		-0.648	5.67E-02	25.24	-0.754	6.44E-02	36.56	-0.825	9.03E-02	60.37	0.301	0.106	1.28	0.648	-0.071	0.85	
P18124	RL7	-1.201	6.70E-03	10.65	-1.194	9.48E-03	14.83	-1.209	3.67E-03	5.94	0.874	-0.007	0.98	0.696	-0.014	0.97		0.151	2.93E-01	20.71	0.042	2.47E-01	22.45	-0.033	4.18E-01	45.17	0.153	0.109	1.28	0.498	-0.075	0.84	
P05388	RLA0	-1.969	1.21E-03	11.25	-1.997	1.91E-03	18.97	-1.982	1.00E-03	9.61	0.584	0.027	1.06	0.754	0.015	1.04		-0.615	5.94E-02	24.49	-0.763	3.88E-02	22.50	-0.816	5.65E-02	37.03	0.096	0.148	1.41	0.582	-0.053	0.88	
P46781	RS9	-2.017	1.32E-03	13.79	-1.924	3.07E-03	25.72	-1.964	1.22E-03	11.22	0.215	-0.094	0.81	0.550	-0.040	0.91		-0.657	7.12E-02	32.32	-0.682	7.53E-02	36.18	-0.785	8.18E-02	49.89	0.822	0.025	1.06	0.458	-0.103	0.79	
P13010	XRCC5	-2.325	2.01E-03	42.45	-2.437	6.18E-04	16.90	-2.416	8.99E-04	23.44	0.346	0.112	1.29	0.754	0.021	1.05		-0.947	6.50E-02	57.61	-1.184	2.49E-02	37.97	-1.229	3.07E-02	52.08	0.222	0.237	1.72	0.755	-0.045	0.90	
P07910	HNRPC	-2.498	1.41E-03	44.49	-2.618	4.76E-04	19.77	-2.620	5.33E-04	22.22	0.342	0.120	1.32	0.983	-0.001	1.00		-1.162	2.87E-02	41.62	-1.361	1.75E-02	40.16	-1.427	1.95E-02	52.07	0.181	0.200	1.58	0.658	-0.065	0.86	
Q00839	HNRPU	-2.391	7.27E-04	17.90	-2.230	3.23E-04	5.49	-2.214	8.09E-04	13.24	0.004	-0.161	0.69	0.624	0.016	1.04		-1.037	2.67E-02	29.03	-0.980	3.23E-02	30.83	-1.024	5.43E-02	57.36	0.564	-0.056	0.88	0.764	-0.043	0.91	
P17987	TCPA	-2.396	5.16E-04	12.84	-2.511	5.15E-04	16.72	-2.550	8.10E-05	2.87	0.042	0.115	1.30	0.356	-0.038	0.92		-1.041	2.36E-02	25.95	-1.266	1.72E-02	31.77	-1.375	1.78E-02	42.31	0.045	0.225	1.68	0.369	-0.109	0.78	
Q5VTE0	EF1A3	-2.045	2.33E-03	25.85	-2.426	2.32E-03	61.97	-2.237	6.52E-04	11.25	0.019	0.381	2.40	0.140	0.189	1.55		-0.707	2.55E-02	13.00	-1.184	4.89E-02	74.63	-1.068	3.46E-02	40.41	0.003	0.477	3.00	0.529	0.116	1.31	
P40429	RL13A	-1.274	3.78E-03	7.11	-1.286	1.02E-02	19.74	-1.327	2.44E-03	5.18	0.799	0.012	1.03	0.409	-0.041	0.91		0.082	3.05E-01	25.21	-0.048	2.56E-01	28.59	-0.152	3.17E-01	44.91	0.165	0.131	1.35	0.388	-0.103	0.79	
P15880	RS2	-1.742	2.34E-03	12.92	-1.618	6.84E-03	28.34	-1.643	6.80E-04	2.99	0.147	-0.124	0.75	0.705	-0.025	0.94		-0.391	8.62E-02	21.21	-0.364	1.89E-01	43.55	-0.467	1.52E-01	44.47	0.807	-0.027	0.94	0.477	-0.104	0.79	
P62249	RS16	-2.239	1.50E-04	2.61	-2.009	8.28E-04	8.46	-2.015	1.54E-03	15.95	0.000	-0.230	0.59	0.893	-0.005	0.99		-0.883	3.13E-02	23.93	-0.769	3.88E-02	22.80	-0.818	9.09E-02	59.79	0.167	-0.114	0.77	0.727	-0.049	0.89	
P11142	HSP7C	-2.635	3.86E-04	16.63	-2.508	5.32E-04	17.16	-2.489	1.00E-03	30.98	0.055	-0.126	0.75	0.813	0.019	1.05		-1.282	1.18E-02	22.61	-1.257	1.92E-02	34.75	-1.306	2.41E-02	48.71	0.795	-0.025	0.94	0.715	-0.049	0.89	
Q92522	H1X	-2.355	9.92E-04	22.47	-2.533	6.23E-04	21.24	-2.529	6.17E-04	20.85	0.044	0.178	1.51	0.953	0.004	1.01		-1.016	1.62E-03	1.68	-1.285	1.85E-02	35.63	-1.331	2.72E-02	58.24	0.003	0.269	1.86	0.765	-0.045	0.90	

		normalisation to total intensity																normalisation to IS													
		Ctrl ext			Ctrl memb			H202 memb			Ctrl ext / Ctrl memb			H2O2 memb / Ctrl memb			Ctrl ext			Ctrl memb			H202 memb			Ctrl ext / Ctrl memb			H2O2 memb / Ctrl memb		
Entry	Entry name	log(mean)	st dev	%CV	log(mean)	st dev	%CV	log(mean)	st dev	%CV	t-test p-value	log10 (var)	fold (var)	t-test p-value	log10 (var)	fold (var)	log(mean)	st dev	%CV	log(mean)	st dev	%CV	log(mean)	st dev	%CV	t-test p-value	log10 (var)	fold (var)	t-test p-value	log10 (var)	fold (var)
P61313	RL15	-2.240	4.42E-04	7.69	-2.141	1.38E-03	19.13	-2.197	1.49E-03	23.48	0.089	-0.099	0.80	0.427	-0.055	0.88	-0.882	3.45E-02	26.27	-0.895	4.27E-02	33.53	-1.028	4.53E-02	48.35	0.891	0.013	1.03	0.322	-0.133	0.74
P62906	RL10A	-2.022	1.88E-03	19.83	-2.142	7.01E-04	9.72	-2.039	1.63E-03	17.85	0.064	0.119	1.32	0.073	0.103	1.27	-0.681	1.23E-02	5.91	-0.893	4.05E-02	31.63	-0.860	6.03E-02	43.71	0.009	0.212	1.63	0.794	0.032	1.08
P62424	RL7A	-1.937	1.39E-03	12.07	-1.998	1.20E-03	11.97	-2.092	8.81E-04	10.89	0.153	0.061	1.15	0.040	-0.094	0.81	-0.576	8.35E-02	31.49	-0.757	4.44E-02	25.38	-0.921	5.23E-02	43.62	0.105	0.181	1.52	0.159	-0.164	0.69
P61254	RL26	-1.952	1.85E-03	16.53	-2.047	1.91E-03	21.24	-2.098	6.57E-04	8.24	0.151	0.095	1.24	0.357	-0.052	0.89	-0.608	2.64E-02	10.69	-0.790	6.56E-02	40.48	-0.923	5.34E-02	44.69	0.054	0.182	1.52	0.352	-0.133	0.74
P51991	ROA3	-3.167	2.15E-04	31.50	-3.000	2.18E-04	21.83	-3.131	3.89E-04	52.50	0.083	-0.167	0.68	0.289	-0.130	0.74	-1.817	4.78E-03	31.36	-1.749	6.65E-03	37.33	-1.939	9.68E-03	84.17	0.554	-0.068	0.86	0.324	-0.190	0.65
P62917	RL8	-1.761	2.37E-03	13.65	-1.726	2.67E-03	14.22	-1.764	3.01E-03	17.48	0.443	-0.035	0.92	0.461	-0.038	0.92	-0.402	1.21E-01	30.58	-0.481	9.81E-02	29.70	-0.605	8.76E-02	35.30	0.431	0.079	1.20	0.258	-0.124	0.75
P62269	RS18	-2.532	3.82E-04	13.01	-2.555	1.02E-03	36.56	-2.450	8.53E-04	24.05	0.792	0.023	1.05	0.299	0.104	1.27	-1.180	1.49E-02	22.59	-1.302	2.64E-02	52.91	-1.251	3.54E-02	63.01	0.329	0.121	1.32	0.788	0.051	1.12
P45880	VDAC2	-2.801	6.03E-04	38.15	-2.291	5.70E-04	11.14	-2.256	1.22E-03	22.10	0.000	-0.510	0.31	0.553	0.035	1.08	-1.466	1.17E-02	34.08	-1.042	2.80E-02	30.81	-1.066	4.49E-02	52.32	0.010	-0.424	0.38	0.860	-0.024	0.95
P61353	RL27	-1.431	4.17E-03	11.25	-1.460	6.89E-03	19.88	-1.428	4.03E-03	10.80	0.571	0.029	1.07	0.534	0.032	1.08	-0.077	1.91E-01	22.87	-0.223	1.68E-01	27.99	-0.260	2.25E-01	40.99	0.110	0.145	1.40	0.737	-0.037	0.92
Q00325	MPCP	-2.144	7.82E-04	10.89	-2.379	1.35E-03	32.37	-2.294	4.34E-04	8.53	0.009	0.235	1.72	0.252	0.085	1.22	-0.794	2.84E-02	17.63	-1.140	3.07E-02	42.40	-1.114	3.40E-02	44.21	0.006	0.346	2.22	0.856	0.025	1.06
P26373	RL13	-2.227	1.23E-03	20.82	-2.148	1.28E-03	18.00	-2.196	5.25E-04	8.25	0.230	-0.079	0.83	0.322	-0.048	0.90	-0.863	5.29E-02	38.57	-0.898	4.41E-02	34.84	-1.012	4.97E-02	51.17	0.769	0.035	1.08	0.411	-0.115	0.77
Q71DI3	H32	-2.776	2.90E-04	17.32	-2.077	2.85E-03	34.01	-1.941	1.71E-03	14.95	0.003	-0.699	0.20	0.111	0.137	1.37	-1.419	1.14E-02	29.97	-0.840	6.16E-02	42.64	-0.749	1.04E-01	58.31	0.015	-0.579	0.26	0.596	0.091	1.23
P18077	RL35A	-1.715	5.87E-04	3.05	-1.751	3.28E-03	18.51	-1.774	1.68E-03	10.01	0.390	0.036	1.09	0.634	-0.023	0.95	-0.359	9.94E-02	22.75	-0.512	8.74E-02	28.40	-0.604	1.07E-01	42.92	0.099	0.152	1.42	0.428	-0.092	0.81
P62241	RS8	-1.993	7.77E-04	7.65	-2.022	2.09E-03	22.03	-2.072	9.90E-04	11.68	0.579	0.029	1.07	0.409	-0.050	0.89	-0.640	4.75E-02	20.73	-0.769	6.54E-02	38.43	-0.900	5.70E-02	45.27	0.196	0.129	1.34	0.347	-0.131	0.74
Q9BPW8	NIPS1	-2.760	4.57E-04	26.29	-2.785	2.60E-04	15.85	-2.704	3.62E-04	18.34	0.726	0.025	1.06	0.185	0.080	1.20	-1.420	6.23E-03	16.39	-1.526	1.11E-02	37.32	-1.533	1.32E-02	45.09	0.242	0.106	1.28	0.957	-0.007	0.98
P62244	RS15A	-1.836	9.86E-04	6.75	-1.608	2.96E-03	11.98	-1.597	1.25E-03	4.96	0.001	-0.228	0.59	0.718	0.011	1.02	-0.476	9.35E-02	28.00	-0.352	1.58E-01	35.50	-0.418	1.80E-01	47.06	0.272	-0.125	0.75	0.616	-0.066	0.86
Q07020	RL18	-1.657	1.68E-03	7.63	-1.666	3.94E-03	18.26	-1.706	5.01E-03	25.47	0.825	0.010	1.02	0.577	-0.040	0.91	-0.299	1.33E-01	26.54	-0.425	1.11E-01	29.54	-0.539	1.37E-01	47.44	0.194	0.126	1.34	0.366	-0.113	0.77
P62277	RS13	-2.294	2.68E-04	5.28	-2.286	1.35E-03	26.04	-2.269	9.52E-04	17.67	0.897	-0.008	0.98	0.805	0.017	1.04	-0.941	2.25E-02	19.69	-1.022	4.35E-02	45.78	-1.089	3.88E-02	47.63	0.455	0.081	1.21	0.660	-0.066	0.86
Q14103	HNRPD	-2.240	8.41E-04	14.62	-2.681	1.21E-03	57.84	-2.568	5.17E-04	19.09	0.002	0.441	2.76	0.380	0.113	1.30	-0.893	1.83E-02	14.33	-1.430	2.72E-02	73.18	-1.370	2.68E-02	62.97	0.001	0.536	3.44	0.785	0.059	1.15
P62899	RL31	-2.079	8.69E-04	10.42	-2.099	2.44E-03	30.68	-2.171	9.73E-04	14.43	0.781	0.020	1.05	0.388	-0.072	0.85	-0.716	6.00E-02	31.25	-0.855	5.76E-02	41.27	-1.004	4.13E-02	41.65	0.253	0.139	1.38	0.297	-0.149	0.71
P62987	RL40	-2.524	6.17E-04	20.61	-1.862	3.87E-03	28.14	-1.818	1.49E-03	9.83	0.002	-0.662	0.22	0.509	0.044	1.11	-1.156	2.72E-02	38.90	-0.610	1.05E-01	42.83	-0.654	7.98E-02	36.03	0.018	-0.546	0.28	0.728	-0.045	0.90
Q16629	SRSF7	-2.455	6.32E-04	18.03	-2.457	1.75E-04	5.01	-2.511	6.04E-04	19.57	0.976	0.001	1.00	0.241	-0.054	0.88	-1.090	3.07E-02	37.75	-1.212	1.61E-02	26.28	-1.313	3.10E-02	63.77	0.294	0.122	1.32	0.495	-0.101	0.79
P18621	RL17	-2.778	2.53E-04	15.18	-2.452	9.47E-04	26.78	-2.581	6.17E-04	23.51	0.009	-0.326	0.47	0.159	-0.129	0.74	-1.421	1.10E-02	28.96	-1.206	2.44E-02	39.28	-1.375	2.88E-02	68.16	0.120	-0.215	0.61	0.329	-0.169	0.68
P67809	YBOX1	-2.004	1.51E-03	15.24	-2.176	1.10E-03	16.54	-2.212	8.27E-04	13.48	0.014	0.171	1.48	0.461	-0.037	0.92	-0.658	2.97E-02	13.52	-0.928	3.97E-02	33.70	-1.030	4.62E-02	49.55	0.006	0.270	1.86	0.450	-0.102	0.79
P62873	GBB1	-2.867	6.28E-05	4.62	-2.291	1.60E-03	31.19	-2.368	1.19E-03	27.86	0.003	-0.576	0.27	0.434	-0.077	0.84	-1.514	5.88E-03	19.20	-1.040	4.12E-02	45.09	-1.169	4.63E-02	68.19	0.027	-0.475	0.34	0.477	-0.129	0.74
P62753	RS6	-2.306	2.30E-04	4.66	-2.396	1.43E-03	35.45	-2.642	1.39E-03	60.86	0.250	0.089	1.23	0.131	-0.246	0.57	-0.952	2.42E-02	21.65	-1.146	3.39E-02	47.51	-1.478	2.41E-02	72.58	0.101	0.194	1.56	0.116	-0.332	0.47
P62913	RL11	-2.247	4.27E-04	7.55	-1.991	1.16E-03	11.37	-2.008	8.53E-04	8.69	0.000	-0.256	0.55	0.605	-0.017	0.96	-0.887	3.70E-02	28.58	-0.736	6.23E-02	33.96	-0.826	7.58E-02	50.78	0.188	-0.151	0.71	0.510	-0.090	0.81
P62841	RS15	-2.623	3.14E-04	13.17	-2.469	1.01E-03	29.74	-2.540	3.75E-04	13.01	0.103	-0.154	0.70	0.380	-0.071	0.85	-1.261	1.77E-02	32.31	-1.220	2.56E-02	42.53	-1.368	1.89E-02	44.18	0.742	-0.041	0.91	0.315	-0.148	0.71
P50914	RL14	-2.240	2.33E-03	40.59	-2.264	3.08E-03	56.62	-2.135	2.45E-03	33.46	0.880	0.024	1.06	0.376	0.129	1.35	-0.912	2.40E-02	19.55	-1.008	7.05E-02	71.80	-0.970	5.10E-02	47.56	0.539	0.096	1.25	0.843	0.038	1.09
P62847	RS24	-2.621	3.29E-04	13.75	-2.921	4.19E-04	34.97	-2.962	3.65E-04	33.47	0.004	0.300	2.00	0.710	-0.041	0.91	-1.269	1.28E-02	23.70	-1.668	1.10E-02	51.40	-1.770	1.05E-02	62.10	0.009	0.399	2.50	0.576	-0.102	0.79
P83731	RL24	-2.131	6.98E-04	9.44	-2.222	1.03E-03	17.08	-2.191	9.06E-04	14.07	0.066	0.090	1.23	0.547	0.031	1.07	-0.779	3.30E-02	19.89	-0.977	3.47E-02	32.90	-0.999	5.61E-02	55.94	0.045	0.197	1.57	0.877	-0.022	0.95
P63162	RSMN	-1.919	1.16E-03	9.61	-2.069	4.27E-03	50.04	-1.913	7.89E-04	6.46	0.164	0.149	1.41	0.141	0.156	1.43	-0.568	5.33E-02	19.72	-0.829	9.06E-02	61.04	-0.737	8.41E-02	45.93	0.059	0.260	1.82	0.594	0.091	1.23
P57088	TMM33	-2.589	2.34E-04	9.09	-2.786	5.82E-04	35.54	-2.569	1.48E-04	5.50	0.024	0.197	1.57	0.012	0.217	1.65	-1.237	1.14E-02	19.75	-1.543	1.37E-02	47.83	-1.398	1.61E-02	40.37	0.017	0.306	2.03	0.324	0.145	1.40
P00403	COX2	-2.508	5.33E-04	17.14	-2.602	8.62E-05	3.45	-2.626	7.58E-04	32.08	0.066	0.094	1.24	0.732	-0.024	0.95	-1.162	9.89E-03	14.36	-1.353	1.31E-02	29.52	-1.474	1.16E-02	34.56	0.024	0.191	1.55	0.264	-0.121	0.76
P42766	RL35	-2.127	1.26E-03	16.84	-2.360	1.30E-03	29.67	-2.432	4.07E-04	11.00	0.014	0.233	1.71	0.365	-0.072	0.85	-0.780	2.48E-02	14.92	-1.109	3.42E-02	43.90	-1.244	2.90E-02	50.85	0.006	0.329	2.13	0.390	-0.135	0.73
O14979	HNRDL	-3.029	1.16E-04	12.45	-2.939	2.58E-04	22.37	-3.006	1.54E-04	15.57	0.176	-0.090	0.81	0.315	-0.067	0.86	-1.679	3.94E-03	18.82	-1.686	7.92E-03	38.41	-1.818	8.35E-03	54.92	0.942	0.007	1.02	0.383	-0.132	0.74
Q99880	H2B1L	-3.082	3.39E-04	40.93	-2.477	1.55E-03	46.42	-2.367	1.51E-03	35.13	0.019	-0.605	0.25	0.409	0.110	1.29	-1.708	1.03E-02	52.75	-1.251	2.75E-02	48.97	-1.182	4.46E-02	67.85	0.047	-0.458	0.35	0.725	0.069	1.17
P61619	S61A1	-2.856	2.60E-04	18.65	-2.729	6.49E-04	34.80	-2.744	3.72E-04	20.64	0.225	-0.127	0.75	0.872	-0.015	0.97	-1.492	1.18E-02	36.78	-1.484	1.50E-02	45.75	-1.573	1.31E-02	49.13	0.951	-0.008	0.98	0.566	-0.089	0.82
Q01130	SRSF2	-1.884	1.06E-03	8.13	-2.271	3.58E-04	6.68	-2.317	6.52E-04	13.54	0.000	0.387	2.44	0.200	-0.046	0.90	-0.530	6.60E-02	22.38	-1.027	2.51E-02	26.64	-1.130	3.96E-02	53.44	0.001	0.496	3.13	0.427	-0.104	0.79
P62266	RS23	-2.288	5.36E-04	10.41	-2.434	4.10E-04	11.14	-2.408	4.46E-04	11.42	0.005	0.146	1.40	0.486	0.026	1.06	-0.937	2.14E-02	18.46	-1.180	2.31E-02	35.06	-1.232	2.46E-02	41.98	0.020	0.244	1.75	0.679	-0.051	0.89
Q71UI9	H2AV	-2.645	2.66E-04	11.76	-1.989	1.83E-03	17.88	-1.936	1.97E-03	17.05	0.000	-0.656	0.22	0.359	0.053	1.13	-1.284	1.60E-02	30.75	-0.732	6.93E-02	37.41	-0.752	8.55E-02	48.28	0.010	-0.552	0.28	0.885	-0.020	0.96
P60866	RS20	-2.769	1.27E-04	7.49	-2.557	2.27E-04	8.18	-2.503	6.49E-04	20.65	0.000	-0.212	0.61	0.327	0.054	1.13	-1.411	1.02E-02	26.18	-1.305	1.59E-02	32.07	-1.321	2.68E-02	56.11	0.297	-0.106	0.78	0.914	-0.016	0.96
P02768	ALBU	-2.175	1.78E-03	26.60	-2.334	8.50E-04	18.34	-2.122	7.22E-04	9.58	0.082	0.160	1.44	0.002	0.212	1.63	-0.825	4.74E-02	31.68	-1.098	1.99E-02	24.96	-0.960	3.68E-02	33.59	0.035	0.274	1.88	0.204	0.138	1.37
P68366	TBA4A	-1.718	2.77E-03	14.49	-2.300	3.59E-03	71.55	-2.085	2.52E-03	30.64	0.001	0.581	3.81	0.193	0.215	1.64	-0.364	1.13E-01	26.11	-1.050	7.79E-02	87.31	-0.877	8.59E-02	64.77	0.002	0.685	4.85	0.482	0.173	1.49
P62318	SMD3	-2.657	6.35E-04	28.82	-2.578	7.26E-04	27.51	-2.625	5.60E-04	23.61	0.399	-0.079	0.83	0.578	-0.047	0.90	-1.321	6.48E-03	13.58	-1.321	2.08E-02	43.54	-1.461	1.44E-02	41.59	0.996	-0.001	1.00	0.337	-0.140	0.72
P12236	ADT3	-2.321	1.69E-03	35.38	-2.495	9.27E-04	28.99	-2.454	9.12E-04	25.94	0.152	0.175	1.49	0.642	0.041	1.10	-0.985	3.11E-02	30.00	-1.256	2.11E-02	38.00	-1.297	1.62E-02	32.23	0.043	0.272	1.87	0.720	-0.041	0.91

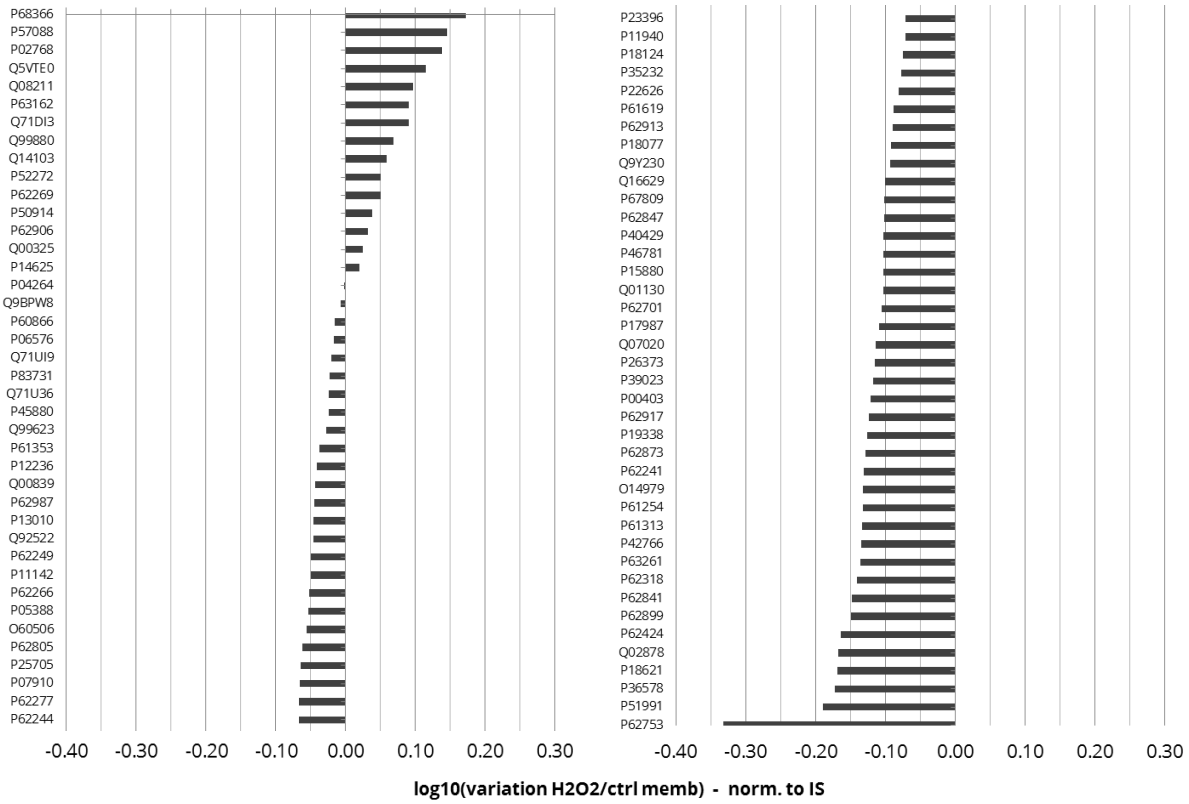

Figure 8.35 - Logarithmic value of the fold-variation of quantified proteins after oxidative stress incubation and use of ultracentrifugation (H_2O_2 memb condition), by division of each mean protein value by respective values determined for control condition (Ctrl memb condition). Protein intensity values of both conditions previously normalized to internal standard (IS). Positive logarithmic values denote increased protein value from control to H_2O_2.

8.8. Sulfo-NHS-LC-biotin reactivity assays

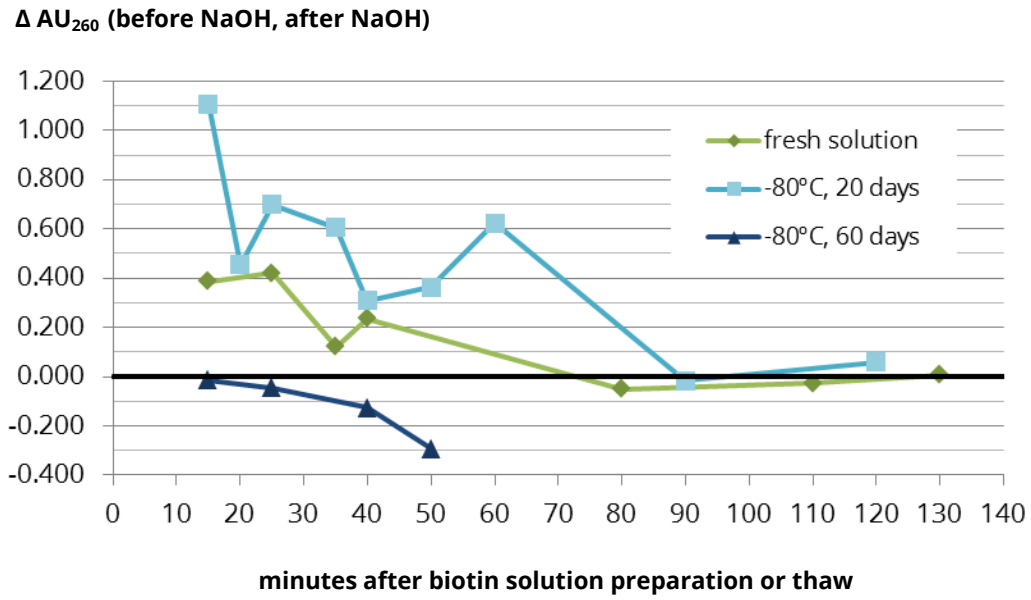

Figure 8.36 – Nanodrop measurement of absorbance at 260nm of concentrated Sulfo-NHS-LC-biotin solutions prepared in PBS, freshly prepared or stored at -80ºC for 20 or 60 days. After dilution of solution until an absorbance registry lower than 1, determination of absorbance difference before and after addition of 10% (v/v) of 1 M NaOH, in several aliquots measured at different time periods after Sulfo-NHS-LC-biotin solution preparation or thawing. A high increase of absorbance from before to after NaOH addition denotes NHS group reactivity.